

**ARC-100 Facility**  
**ARC20-NRC-FQ003 REV 0.0**  
**WHITE PAPER ON FUEL QUALIFICATION**

**SEPTEMBER 17, 2023**  
**REVISION 0.0**

**RESPONSIBLE ENGINEER:** \_\_\_\_\_ Robert C. Iotti

**RESPONSIBLE VERIFIER:** \_\_\_\_\_ Steve Marschke

**RESPONSIBLE MANAGER:** \_\_\_\_\_

## ARC NOTICES

### IMPORTANT NOTICE REGARDING AUTHORIZED USE OF THIS DOCUMENT

### PROPRIETARY INFORMATION NOTICE

### U.S. EXPORT CONTROLS NOTICE, RE-EXPORT AND TRANSFER LIMITATIONS

### PROTECTED INFORMATION

## REVISION CONTROL SHEET

Revision	Date	Description
0	September 2023	First issue

## TABLE OF CONTENTS

EXECUTIVE SUMMARY.....	11
1 PURPOSE .....	14
2 BACKGROUND INFORMATION .....	15
2.1 Design Background .....	15
2.2 Regulatory Background .....	17
2.2.1 NUREG 2246 Conformance Matrix.....	18
2.2.2 NUREG/CR 7305 Compliance Matrix.....	35
3 FUEL DESIGN CRITERIA .....	44
3.1 Analysis and Design of Fuel Elements (pins) .....	45
3.2 Analysis and Design of Fuel Assembly (Ductwork and Fittings) .....	53
3.2.1 Allowable stress and strains.....	54
3.2.2 Creep-Fatigue Damage.....	55
3.2.3 Non ductile Failure Protection .....	55
3.2.4 Special Requirements for Weldments.....	56
4 FUEL DESIGN DESCRIPTION .....	57
4.1 Fuel Design of the ARC-100 Reactor .....	57
4.2 Driver Fuel Assembly Design .....	64
4.2.1 Fuel slug design .....	66
4.2.2 Fuel Cladding Design .....	66
4.2.3 Assembly Design .....	68
4.2.3.1 Assembly Hardware Description .....	69
4.2.3.2 Completing the assembly.....	69
4.2.3.3 Interfaces with Fuel Assembly.....	70
4.3 Control Assemblies.....	70
4.4 Core Restraint System .....	73
4.5 Materials .....	75
4.6 Fuel System Design Basis.....	75
4.7 Fuel Fabrication .....	76
4.7.1 U-10Zr metal fuel production .....	76
4.7.2 Material supply and procurement .....	77
4.7.3 Recommended fabrication method and impact of ARC100 fuel pin dimensions on fabrication equipment design .....	79
4.7.4 Improvement of fabrication operations for the reduction of manual operations and minimization of fissile material waste. ....	81
4.7.5 Steps to ensure fuel fabrication will meet all requirements of its design during the commercial production .....	83
4.7.5.1 Manufacturing Specifications .....	83
4.7.5.2 Present status and schedule forward.....	86

4.7.6 Phase 1 - Preparatory work that is necessary to proceed to the subsequent phases. .... 86

4.7.7 Phase 2 - Procurement, installation, and testing of the equipment and the training of the CNL (or GNF) personnel in its use (Establishment of pin fabrication line). .... 87

**5 FUEL SYSTEM DESIGN EVALUATION..... 88**

5.1 Important Phenomena ..... 88

5.1.1 Formation of fission gas bubbles as function of burnup..... 88

5.1.2 Radial and axial expansion of the fuel matrix. .... 89

5.1.3 Potential fuel Slug Ratcheting ..... 91

5.1.4 Fuel Constituents Redistribution..... 93

5.1.5 Fuel Cladding Chemical Interaction..... 95

    5.1.5.1 Eutectic formation for planned fuel as function of temperature, and fuel composition ..... 96

    5.1.5.2 Fission products (Lanthanides) migration as a function of temperature and concentration gradients ..... 96

5.1.6 Other Phenomena ..... 103

5.2 Operating Experience ..... 103

5.3 Analytical predictions ..... 103

5.3.1 BISON Predictions ..... 103

5.3.2 SAS4A/SASSYS-1 MFUEL Module Predictions (Confirmations) ..... 116

5.3.3 SAS4A/SASSYS-1 Deterministic Analyses Predictions ..... 117

5.4 Design Gaps ..... 125

5.4.1 Swelling data for HT-9 ..... 126

5.4.2 Flow caused phenomena. .... 127

5.4.3 Seismic design ..... 127

5.4.4 Cladding wastage due to solid state interdiffusion..... 127

5.4.5 Eutectic formation/Liquefaction. .... 128

5.4.6 Reactivity feedback and Ratcheting ..... 128

5.4.7 Blockages..... 129

5.4.8 Loss of heat transfer (gas blanketing) ..... 129

5.4.9 Fission product transport ..... 130

5.5 Testing and Inspection ..... 130

**6 FUEL SYSTEM MONITORING FOR FUEL PIN FAILURES ..... 132**

6.1 Radionuclide Release Limit..... 132

6.2 Detection Methods ..... 137

**7 FUEL SURVEILLANCE ..... 138**

**8 CONCLUSION ..... 139**

**9 REFERENCES..... 140**

**10 APPENDICES ..... 146**

A Appendix A. PRIMAVERA (GANTT CHART) Notional Schedule for ARC 100 Fuel Qualification..... 146

B Appendix B Correlations for determination of Eutectic formation as function of temperature, and fuel composition ..... 149

C Appendix C. Experimental and Operational Data (EBR II/FFTF) ..... 151

D Appendix D: Duty Cycle Events for the ARC 100 Fuel (and Reactor Internals)..... 157

E Appendix E – Procedure for measuring the values of the quasi-static reactivity balance equation coefficients A, B, and C..... 169

F Appendix F Verification and Validation ..... 170

F.1 Legacy Data Qualification (Verification and Validation) ..... 170

F.2 Main Codes verification and Validation ..... 171

G Annex A Conservatism of Cumulative Damage Function (CDF) ..... 173

## LIST OF TABLES

Table E-1 Enveloping Design Parameters for Metal Fuel from Existing Database .....	11
Table 2-1 Conformance Matrix of ARC-100 Fuel Qualification Program and NUREG-2246	18
Table 2-2 Compliance of ARC 100 to NUREG/CR-7305.....	35
Table 3-1 Design Criteria for ARC-100 Fuel.....	47
Table 4-1 ARC 100 major operating parameters and limits compared with EBR II and FFTF fuel .....	60
Table 4-2 Comparison of ARC-100 fuel to HT-9 clad fuel tested in EBR II and FFTF.....	61
Table 4-3 Dimensions of Fuel Slugs and Pins of EBR II, FFTF, VTR and ARC-100 .....	79
Table 4-4 Isotopic Composition of Uranium in Core Enrichment Regions .....	85
Table 5-1 Quantity of Lanthanides in ARC 100 core at End (EOL) and Middle of Life (MOL)	98
Table 5-2 Summary of FCCI Data from X447, MFF-3, MFF-5	102
Table 5-3. Reference fuel pin design, operating parameters and BISON nodalization.....	104
Table 5-4. Axial power profile normalized to the length of the fuel slug.....	104
Table 5-5. ARC-100 design criteria for steady state fuel service .....	105
Table 5-6. End-of-life design criteria characteristics for ARC-100 peak fuel pin.....	106
Table 5-7 Fuel performance results with a two sigma uncertainty .....	115
Table 5-8 MFUEL Simulation results at 5256 and 6570 equivalent full power days (16 and 20 calendar years at 90% capacity factor - 2 $\sigma$ temperatures).....	116
Table 5-9 Comparison between BISON and MFUEL Results .....	117
Table 5.10 a: Summary of Protected SBO Event Analysis Results .....	121
Table 5.10 b: Summary of Unprotected SBO Event Analysis Results .....	122
Table 5.10 c: Summary of Protected TOP Event Analysis Results .....	122
Table 5.10 d: Summary of Unprotected TOP Event Analysis Results .....	123
Table 5.10 e: Summary of Protected LOHS Event Analysis Results .....	123
Table 5.10 f: Summary of Unprotected LOHS Event Analysis Results .....	123
Table 5.10.g: Summary of Analysis Results for Instantaneous Loss of 1 Primary EM Pump Event BOL/MOL/EOL .....	124
Table 5.10.h: Summary of Analysis Results for Instantaneous Loss of Loss of One Electrical Bus Event- BOL/MOL/EOL .....	124
Table 5.10 i: Steady State Temperatures .....	124
Table 6-1: Migration Fraction for Radionuclide Groups as Function of Burnup .....	135
Table C-1 Metal Fuel Irradiation Experiments in EBR-II and FFTF .....	151
Table C-2 Summary of Run-Beyond-Cladding Breach Tests with Metal Fuel at the EBR II	155
Table C-3 Summary of Selected TREAT Experiments (From Table 3 of Reference [41]) ....	155

## LIST OF FIGURES

Figure 2.1 ARC-100 Reactor and Safety Features .....	16
Figure 2.2 ARC 100 Reactor In Vessel Spent Fuel Storage .....	17
Figure 3.1 Fuel Qualification Program Elements .....	44
Figure 3.2 Summary of HT9 Pressurized Tube Failure Strain Data .....	49
Figure 3.3 Comparison of the unirradiated and irradiated Charpy curves for one third size specimen of 12Cr-1MoVW (HT9) and 9Cr-2WVTa steels in FFTF at 365°C .....	56
Figure 4.1 ARC-100 Bolted Fuel Assembly .....	58
Figure 4.2 ARC-100 Fuel Pin .....	59
Figure 4.3 Fractional gas release as a function of Burnup for EBR II and FFTF Metallic Fuel	62
Figure 4.4 Axial Elongation of Metal Fuel (References [51,52,53]) .....	63
Figure 4.5 Peak Cladding Diameter Increase and Gas Release Fraction for HT9 Clad U-19-Pu-10Zr Fuel of Various As-built Smeared Densities, at 12.5 at% Burnup. ....	64
Figure 4.6 Primary (Control) Assembly .....	71
Figure 4.7 Secondary (safety) control assembly .....	72
Figure 4.8 Elevation of core showing core and assemblies restraints.....	73
Figure 5.1 Phenomena Involved in Metal Fuel Irradiation [61].....	89
Figure 5.2. Optical micrography and measured constituent redistributions of U-19 wt% Pu-10 wt% Zr fuel at 1.9 at.% burnup. Reproduced from Ref. [65] .....	93
Figure 5.3 U-10Zr at 10at% burnup (DP-11 from X447 at different axial locations. Reproduced from reference [66] .....	94
Figure 5.4 Cladding Wastage Mechanisms .....	95
5.5 Fuel-Cladding Interdiffusion of U-10Zr and HT9 , in Pile, after ~6 at burnup at ~620°C [66].....	96
Figure 5.6 Data from Table 5-2 and projections with equation 2 .....	101
Figure 5.7. Fuel centerline temperature as a function of elevation.....	106
Figure 5.8. Cladding inner surface temperature as a function of elevation. ....	107
Figure 5.9. Fuel burnup as a function of elevation. ....	107
Figure 5.10. Fast neutron fluence as a function of axial elevation.....	108
Figure 5.11 Fuel-cladding chemical interaction as a function of elevation.....	108
Figure 5.12. Cladding hoop stress as a function of elevation .....	109
Figure 5.13 Cladding thermal creep strain as a function of elevation. ....	110
Figure 5.14. Cladding total hoop strain as a function of elevation .....	110
Figure 5.15. Cladding total hoop strain as a function of elevation for a hypothetical case featuring zero solid fission product swelling in the fuel.....	111
Figure 5.16. Cladding total hoop strain as a function of elevation for a hypothetical case featuring zero irradiation creep of the cladding.....	112
Figure 5.17. Cladding total hoop strain as a function of elevation for a hypothetical case featuring EOL FCCI of 100 micrometers. A prominent double-peak is evident. ....	113
Figure 5.18. Profilometry analysis of MFF-3-193045 pin.....	113
Figure 5.19. Porosity at the fuel centerline as a function of axial elevation.....	114
Figure 5.20. Cumulative damage index as a function of elevation. ....	114
Figure 6.1 ARC-100 Fuel Performance Envelope. ....	133

Figure 6.2 Maximum Activity Levels (MBq/kg) Measured in Primary Sodium ..... 133

Figure 6.3 Offsite Dose (TEDE) from failure of all the pins in the ARC-100 Core ..... 137

Figure 6.4 Radar plot of ARC-100 Fuel Design and Safety Limits..... 138

Figure B.1 Rates of cladding penetration by uranium-based melts as compiled from various sources. The correlation shown is a fit to laboratory measurements of iron dipped into melts and supported by data from a wide range of actual fuel pins [35]. ..... 149

Figure F.1 Measured vs. BISON Predicted FCCI thickness versus Fuel Centerline Temperature [86] ..... 172

Figure F.2 Measured vs. BISON Predicted FCCI thickness vs. Inner Cladding Temperature[86] ..... 172

Figure An.1 Statistical Distribution of Log<sub>10</sub> CDF ..... 173

Figure An.2 Temperature dependent Rupture Strength of HT9 (from Reference [6] ..... 174

Figure An.3 Comparison of Predicted and Measured Time to Rupture for HT9 Tubes in Ramp-and-Hold tests. Blue and Red are MCF and CDF Predictions, respectively(from Reference [13]). ..... 174

## ACRONYM AND TERMS/DEFINITIONS

Acronym	Term/Definition
316 SS	316 Stainless Steel
ACCI	Absorber-Cladding Chemical Interaction. Chemical reaction between the cladding and absorber that degrades the cladding mechanical properties. The thickness of the impacted region contributes to cladding wastage.
ACLP	Above Core Load Pad
AOO	Anticipated Operational Occurrences
ASME BPVC	American Society of Mechanical Engineers Boiler and Pressure Vessel Code. Standards for the safe design, manufacture and maintenance of boiler and pressure vessels, power-producing machines, and nuclear power plant components.
BISON	A computer code designed for fuel performance assessment
CRD	Control Rod Drive
CRDM	Control Rod Drive Mechanism
CRS	Core Restraint System
CSS	Core Support Structure
CTE	Coefficient of Thermal Expansion
DBTT	Ductile to Brittle Transition Temperature
DC	Design Criteria
DE	Destructive Exams
DOE	Department of Energy
dpa	Displacement per atom – a measure of the radiation damage caused by fast (>0.1 Mev) neutrons. 1 dpa equals $\sim 2 \times 10^{21}$ n/cm <sup>2</sup>
DSC	Differential Scanning Calorimetry
EBR-II	Experimental Breeder Reactor-II. Sodium-cooled fast reactor known for a series of experiments demonstrating passive safety features such as natural convection cooling after a simulated cooling pump failure.
EM	Evaluation Model
FCCI	Fuel-Cladding Chemical Interaction. Chemical reaction between the fuel and cladding that degrades the cladding mechanical properties in the interacted zone. The thickness of the impacted region contributes to cladding wastage.
FCRD	Fuel Cycle Research and Development. DOE research program on advanced fuels. They issued a Materials Handbook with relevant materials properties data for the Sodium fuel design.
FEA	Finite Element Analysis
FEM	Finite Element Model
FFTF	Fast Flux Test Facility. 400 MW thermal, liquid sodium cooled fast test reactor that operated from 1982 to 1992
FGR	Fission Gas Release
FIV	Flow Induced Vibration
FM	Ferritic Martensitic



Acronym	Term/Definition
FQAF	Fuel Qualification Assessment Framework.
Fuel	Fissile material used to sustain a nuclear chain reaction in a reactor.
Fuel Pin	Structural component of sodium-cooled fast reactor that consists of a steel tube housing a fuel column and an extra volume above it (gas plenum) to contain fission gases.
FUM	Fuel Unloading Machine- historical name for a machine which loads new fuel into the reactor vessel and unloads spent fuel from the reactor vessel and transfers to a transportation cask. More properly it should be called a Fuel Handling machine.
IAEA	International Atomic Energy Agency
IFR	Integral Fast Reactor. DOE research program to support advancing metallic fuels for closed fuel cycle applications.
IVTM	In-Vessel Transfer Machine
LBE	Licensing Basis Events
LDA	Lead Demonstration Assembly. Fuel assemblies with the ability to readily remove fuel pins from the assemblies after irradiation. Used in the ARC-100 Reactor as part of the fuel surveillance program to provide data on fuel at high burnup ahead of the rest of the core, as well as to irradiate test pins which contain micrometer barriers to between the fuel and the cladding to minimize or eliminate FCCI.
LHGR	Linear Heat Generation Rate. Local power generated per unit of length of fuel/absorber.
LMFBR	Liquid Metal Fast Breeder Reactor. Reactor that is cooled by a liquid metal and produces more fissionable material than it consumes to generate energy.
MFF	A series of fuel assemblies with metallic fuel that were irradiated in the FFTF to support conversion of the reactor from mixed oxide fuel to metallic fuel.
MFUEL	A computer code designed for fuel performance assessment interfacing with the system analysis code SAS.
NDE	Non-Destructive Exams
NRC	U.S. Nuclear Regulatory Commission
NSMH	Nuclear Systems Materials Handbook
PICT	Peak Inner Cladding Temperature
PIRT	Phenomena Identification and Ranking Tables
PRISM	Power Reactor Innovative Small Module. PRISM is a pool-type, metal-fueled, small modular sodium fast reactor designed by GE-Hitachi.
PSAR	Preliminary Safety Analysis Report
RAC	Regulatory Acceptance Criteria. Acceptance criteria derived from regulatory requirements and guidance.
RCP	Regulatory Compliance Plan
RES	Reactor Enclosure System
RG	Regulatory Guide
SAS	SAS4A/SASSYS-1 system analysis code

<b>Acronym</b>	<b>Term/Definition</b>
SFR	Sodium Fast Reactor/Sodium-cooled Fast Reactor. Nuclear reactor with a fast neutron spectrum and liquid sodium coolant
SQA	Software Quality Assurance
SSC	Structure, System, and Component
TLP	Top Load Pad
TREAT	Transient Reactor Test Facility. Test reactor facility at Idaho National Laboratory that can perform extreme transient tests on fuel to assess fuel failure limits and post-failure behavior.
ULOF	Unprotected Loss of Flow
USBO	Unprotected Station Blackout
UTOP	Unprotected Transient Over Power
UTS	Ultimate Tensile Strength
V&V	Verification and Validation
YS	Yield Strength

## EXECUTIVE SUMMARY

As a preface to the summary of the ARC proposed Fuel Qualification Program, it is useful to compare the position put forth by NUREG/CR 7305 experts that had reviewed this topic for the US Nuclear Regulatory Commission. Although that review took place in the very recent past, the experts have reached conclusions which are quite similar to those reached in 2012 by a different group of experts [88]. This is not surprising since no significant additional experimental or operational work has been done on metal fuels since that time. ...The experts conclusions (documented in References [24 and 88]) are presented in Table E-1 I where the Italicized are from reference [88]

Table E-1, which provides the NUREG/CR 7305 assessment of what are “acceptable” enveloping design parameters for Metal Fuel from the existing database, (in italics are those of Ref [88]) and compares them to the planned parameter of the ARC-100 fuel. This Table sets the basis for the proposed ARC 100 Fuel Qualification Assessment Framework (FQAF) documented in this White Paper.

**Table E-1 Enveloping Design Parameters for Metal Fuel from Existing Database**

Parameter	NUREG/CR 7305 and Reference [88] Value	ARC Value
Nominal Composition	U-10Zr ( <i>U-10Zr, U-20Pu-10Zr</i> )	U-10Zr
Pu/(U+Pu) range	N/P ( <i>17-28%</i> )	N/A
Smear Density (% of TD)	75 ( <i>75</i> )	
Plenum -to -fuel -volume	1.5 ( <i>1.4-1.5</i> )	
Fuel height (cm)	91.4 ( <i>91</i> )	
Fuel outer diameter (cm)	0.499 ( <i>0.5</i> )	
Fuel-clad bond	Na ( <i>Na</i> )	Na
Clad Material	HT9 ( <i>HT-9 or 20% cw 316SS D9 if burnup is limited to &lt;10 at%</i> )	HT-9
Cladding outer diameter	0.584-0.686 ( <i>0.6</i> )	
Cladding inner diameter	N/P ( <i>0.57</i> )	
Peal Linear Heat Rate (kW/m)	44-55 ( <i>49-52</i> )	
Peak Inner Clad Wall Temperature (°C)*	650 ( <i>620 for D9, 560 for HT9</i> )	)
Total radial strain and deformation	2% ( <i>N/P</i> )	
Radial deformation from thermal creep	1% ( <i>N/P</i> )	
Duct Material	HT9 ( <i>HT-9 or 20% cold worked 316SS</i> )	HT-9
Peak Clad Fast Fluence (n/cm <sup>2</sup> )	N/A ( <i>4 x10<sup>23</sup></i> )	
Maximum Burnup (at%) *	10 at% ( <i>10 if D9, 20 if HT-9</i> )	
Peak Clad Exposure (dpa)*	N/P ( <i>100 if D9, ~200 if HT-9</i> )	
*Reference [88] provides constraints on D9 and HT9 with respect to maximum burnup, peak clad exposure, and maximum temperatures		<b>Bold denotes Out of the Envelope Range</b>

N/P - not provided.

In addition, NUREG/CR-7305 and/or reference [88] provide recommendations that can be summarized as follows:

- In some cases, in-reactor testing of a new fuel assembly design, or a new design feature cannot be accomplished before operation of the design's full core. The inability to perform in-reactor testing may result from an incompatibility of the new design with the previous design. In such cases, special attention should be given to the surveillance plans.
- A post irradiation fuel surveillance program should be described for each plant to detect anomalies or confirm expected fuel performance. The extent of an acceptable program will depend on the history of the fuel design being considered (i.e., whether the proposed fuel design is the same as current operating fuel or incorporates new design features).
- For a fuel design similar to that in other operating plants, a minimum acceptable program should include a qualitative visual examination of some discharged fuel assemblies from each refueling. Such a program should be sufficient to identify gross problems of structural integrity, fuel rod failure, rod bowing, dimension changes, or crud deposition. The program should also commit to perform additional surveillance if unusual behavior is noticed in the visual examination or if plant instrumentation indicates gross fuel failures. The surveillance program should address the disposition of failed fuel.
- **When prototype testing cannot be performed, a special detailed surveillance program should be planned for the first irradiation of a new design.**

The bold signifies ARC's recognition that ARC-100 fuel can be considered to fall in this latter category. The proposed program specifically addresses the recommendation to carry out qualitative and quantitative inspection at interim points in the refueling period.

The schematic of Figure 3.1 and the timetable shown in Appendix A summarize the proposed ARC-100 Fuel Qualification Assessment Framework (program), which is a combination of qualification by design and surveillance/testing.

During the analysis/preliminary design phase (the phase covered by the ARC 20 program), the analysis and design activities described in Sections 3.1 and 3.2 will be done. During a subsequent period (licensing and detailed design), if necessary, out-of-pile tests could be conducted to determine the behavior of the core and individual assemblies to:

- flow as a function of different flow rates (pressure drop in the core, potential for flow induced vibrations, in order to validate the analytical modeling of the coupled hydraulic/structural behavior. and
- external loads, specifically seismic motions, by placing a scaled core and individual fuel and scaled assemblies on a shake table and comparing the measured vs the analytically predicted response to identical input motions that simulate an earthquake. This testing will validate the analytical modeling of the full-size core.

During the startup tests, the Power Reactivity Decrement (PRD) will be measured, and the coefficients A, B, and C of the quasistatic reactivity balance equation will be measured, and that will set the baseline PRD curve, and coefficient B against which future changes will be compared to provide indication of core deformations and overall behavior. The measurements of the coefficients A, B, and C of the Quasi-static Reactivity Balance equation also serve to confirm that they are within the range in which the ARC-100 has self-protecting characteristics.

Acceptance criteria for the fuel design are provided in section 3, and the fuel system design description is given in section 4, together with the fabrication methods employed to produce the

quality necessary for the fuel performance. Section 5 shows how fuel performance under the phenomena affecting its life can be predicted with verified and validated computer program. . Section 5.4 and Chapters 6 and 7 describe the surveillance, inspection and testing activities and methods that support the fuel qualification by providing early information that would indicate degrading performance and proof that the fuel is performing as intended.

Finally, section 5.4 lists where gaps in information from operation and experiments may affect the fuel design. The fuel dimensions of the ARC 100 are different from those of fuel elements that have been in operating reactors or tested in ex-core experiments. The operating environment of the ARC 100 generally falls within the fuel and cladding temperatures experienced in operating reactors. However, the radiation damage to which the cladding will be exposed during the planned 20 year of operation (equivalent to 18 Full Power years) is at or slightly exceeds the available operational and experimental data. Moreover, to achieve the desired 20 year between refueling, the core configuration has three enrichment zones, and the core region where peak burnup occurs changes over time. Since it is not practical to change the orifices of the assemblies during the operation, the selected "orificing" is not "optimal" for the individual assemblies, but optimal for the core overall for the time between refueling. . This does not allow all fuel assemblies to be run at low power to flow, as has been practiced by fast reactors (all with short refueling intervals). The relatively high power to flow ratio of the ARC-100 causes the location of high cladding strain, high gas plenum pressure and high cladding temperatures to occur in the peak burnup assemblies.

ARC Clean

Technology has identified a number of improvements/changes that could be made to increase the predicted life of the fuel. However, we believe that it is important to determine how conservative the present design limits are, and that can be established with the present design being placed in operation with an appropriate surveillance and test program. Those changes/improvements could then be implemented in future cores, if actually required.

The conclusion of the information presented in this white paper is that the ARC100 fuel cannot be completely qualified by design. Insufficient knowledge in the behavior of the HT9 material and the fuel matrix itself after the irradiation of the fuel over its long refueling interval of 20 years introduces uncertainties in the material properties and correlations used in the design

The testing program must be accompanied by a complementary program which compensates for the lack of knowledge by providing real time information on the condition of the fuel and can be used to stop operation at the moment its indication is that the behavior of the fuel may not be as expected.

## 1 PURPOSE

This report summarizes the ARC Clean Technology (hereinafter ARC) plan to qualify fuel to support operation of the ARC-100 Reactor. The overall fuel qualification approach (planning, testing, analysis, etc.) used to obtain qualified fuel is described. ARC's fuel qualification efforts have been informed by U.S. Nuclear Regulatory Commission (NRC) guidance, including Regulatory Guide (RG) 1.206, Section C.I.4, "Reactor" [91], NUREG-0800, Section 4.2, "Fuel System Design" [92], NUREG-2246, "Fuel Qualification for Advanced Reactors" [23], and NUREG/CR 7305 [24]. Additionally, principal design criteria (PDC) that are applicable to fuel performance and fuel qualification have been informed by RG 1.232, "Guidance for Developing Principal Design Criteria for Non-Light-Water Reactors" [93]. The information presented in this report will eventually apply to licensing efforts associated with the ARC-100 Reactor design.

This report identifies the acceptance criteria, derived from prior experience in fuels qualified for operation in similar reactors (EBR II and FFTF) and regulatory requirements. These criteria (also called limits) will be used for fuel qualification. ARC's fuel qualification results to date are shown.

Fuel qualification for the ARC-100 Reactor design includes the identification of key fuel manufacturing parameters, the specification of a fuel performance envelope to inform testing and operational requirements, the use of evaluation models in the fuel qualification process, and the assessment of experimental data used to develop and validate evaluation models, and empirical safety criteria.

ARC uses historic operating experience and data from EBR-II and FFTF, verifying the suitability of the historic data and qualifying the historic data for use in the fuel qualification methodology. The historic operating data which underpins and supports the ARC fuel qualification approach and specifically the limits established to ensure a satisfactory fuel performance, is not specifically included, but can be found in the much larger document of reference [6].

This white paper supports a finding that the fuel is qualified for use (i.e., reasonable assurance exists that the fuel, fabricated in accordance with its specification, will perform as described in the safety analysis).

Specifically, the fuel design criteria and associated limits are chosen to ensure that four key objectives (same objectives as used in fuel qualification of EBR II and FFTF) are achieved:

1. the fuel system is not damaged as a result of normal operation and AOOs,
2. core coolability is always maintained,
3. fuel system damage is never so severe during postulated accidents as to prevent reactivity control and control rod insertion when it is required and
4. The number of fuel pin failures is extremely low for normal operation, AOOs and DBAs, and not underestimated for postulated beyond design basis accidents.

NRC's review and comments are requested for the following:

- The use of legacy data and the planned testing is adequate to provide the necessary information to qualify the fuel.
- The identified acceptance criteria are adequate to support fuel qualification.
- The identified evaluation methods and models are adequate to support fuel qualification.
- The identified key fuel manufacturing parameters are adequate to support fuel qualification.

- The plans for inclusion of small subsets of fuel pins that can be extracted (whether by extracting a full assembly or removable pins), which are either: 1) different (e.g., have a protective layer between the fuel and the cladding intended to minimize or eliminate FCCI) or 2) operate outside the performance envelope of the bulk of the core, or 3) include advanced design features such as annular fuel.

## 2 BACKGROUND INFORMATION

### 2.1 Design Background

The ARC 100 reactor is a sodium cooled, pool type, metal fueled fast reactor designed to produce 286 MWt (100 MWe). It uses U-10Zr sodium bonded fuel pins (or elements), clad in HT9 stainless steel, adopting the basic design developed and very successfully used in the EBR II and FFTF reactors.

Unlike those reactors and others being presently designed, the ARC-100 reactor is designed for a 20-year refueling interval, by having a power density and liner heat rate substantially lower than those of EBR II and FFTF. The 20 yearlong refueling interval, with a 90% capacity factor, means the fuel will be irradiated for 18 equivalent full power years.

This is not necessarily an issue because what matter is the damage such fluence causes the cladding and ductwork. At the EBR II a  $4 \times 10^{23}$  n/cm<sup>2</sup> peak fast neutron fluence in EBR-II, corresponded to approximately 200 dpa peak dose to the cladding. At FFTF for the same peak fast neutron fluence corresponded to approximately 170 dpa [96]. EBR II, however, had a harder spectrum than that of FFTF and the ARC 100 reactor, and for the ARC100 reactor the fast neutron fluence would have to be near  $5 \times 10^{23}$  n/cm<sup>2</sup> in order to cause a damage of 200 dpa. Therefore, the ARC-100 fuel, in this respect, would operate at the edge of, or slightly exceed the available experimental data.

The qualification process adopted for the ARC100 fuel follows that used to qualify fuel for the EBR II and FFTF reactors. In those qualification efforts, the fuel behavior was determined with uncertainties at the  $2\sigma$  level, and acceptance criteria, (i.e., limits) were likewise developed conservatively based on the  $2\sigma$  temperatures. The ARC 100 has adopted the same approach and limits as that used for those reactors, because operation of the fuel, so qualified, demonstrated the validity of the approach, i.e., extremely low fuel pin failure.

For normal operation and many anticipated operational occurrences (AOOs), the relatively low fuel and cladding temperatures, and the small temperature difference between the two, result from the low power density and linear heat rate of the ARC 100 as compared to those of EBR II and FFTF. For some AOOs (e.g., loss of one or two primary pumps) and for protected and particularly unprotected transients, they stem from the behavior of the core which inherently stabilizes its power with increased temperatures to the level extracted from the system.

In summary the design of the ARC\_100 and in particular its fuel, is both innovative and evolutionary. Figures 2.1 and 2.2 provide an overview and principal safety features of the ARC-100 reactor. Some of the innovative ARC-100 features include: 1) the storage of all its used fuel within the reactor vessel, 2) the use of a supercritical carbon dioxide Brayton cycle as its power conversion system, and 3) the seismic isolation of the reactor building which provides its functional containment. It is evolutionary because for the majority of its planned operation, it has operating conditions (i.e., is subject to the same phenomena), driven by parameters such as temperatures, mechanical loads, burnup and irradiation, that are within the experience base. However, toward the end of the ARC-

100 refueling cycle it could exceed the EBR II and FFTF experience bases and requires confirmation that the behavior of the fuel under those phenomena continues to be predictable by the computer codes, which extend the operational data base to include long irradiation times.

As described within various sections of this white paper, the long refueling interval of the ARC 100 causes the limits established for its fuel qualification to be challenged after approximately 16 years of operation. The challenge occurs because while it is known that the established limits are conservative, the amount of their conservatism is not known, and varies among the limits.

Consequently, to confirm the appropriateness of the residence time, the fuel qualification program includes extraction of pins (either by extracting complete assemblies or selected central groups of pins that can be removed without removing the assembly), and nondestructive as well as destructive testing of the pins to confirm the fuel behavior. The testing of these lead demonstration assemblies or pins, are part of the fuel surveillance program. An initial testing at approximately 4 years of operation is planned to verify the fuel performance under the phenomena which are manifested early in the operation, i.e. fuel radial and axial expansion with fission gas evolution/ At approximately year 14 or 15 and every two or so years thereafter, additional pins will be extracted and tested to confirm the behavior under the longer-term phenomena (thermal and irradiation creep, FCCI and FCMI due to solid fission product fuel densification).

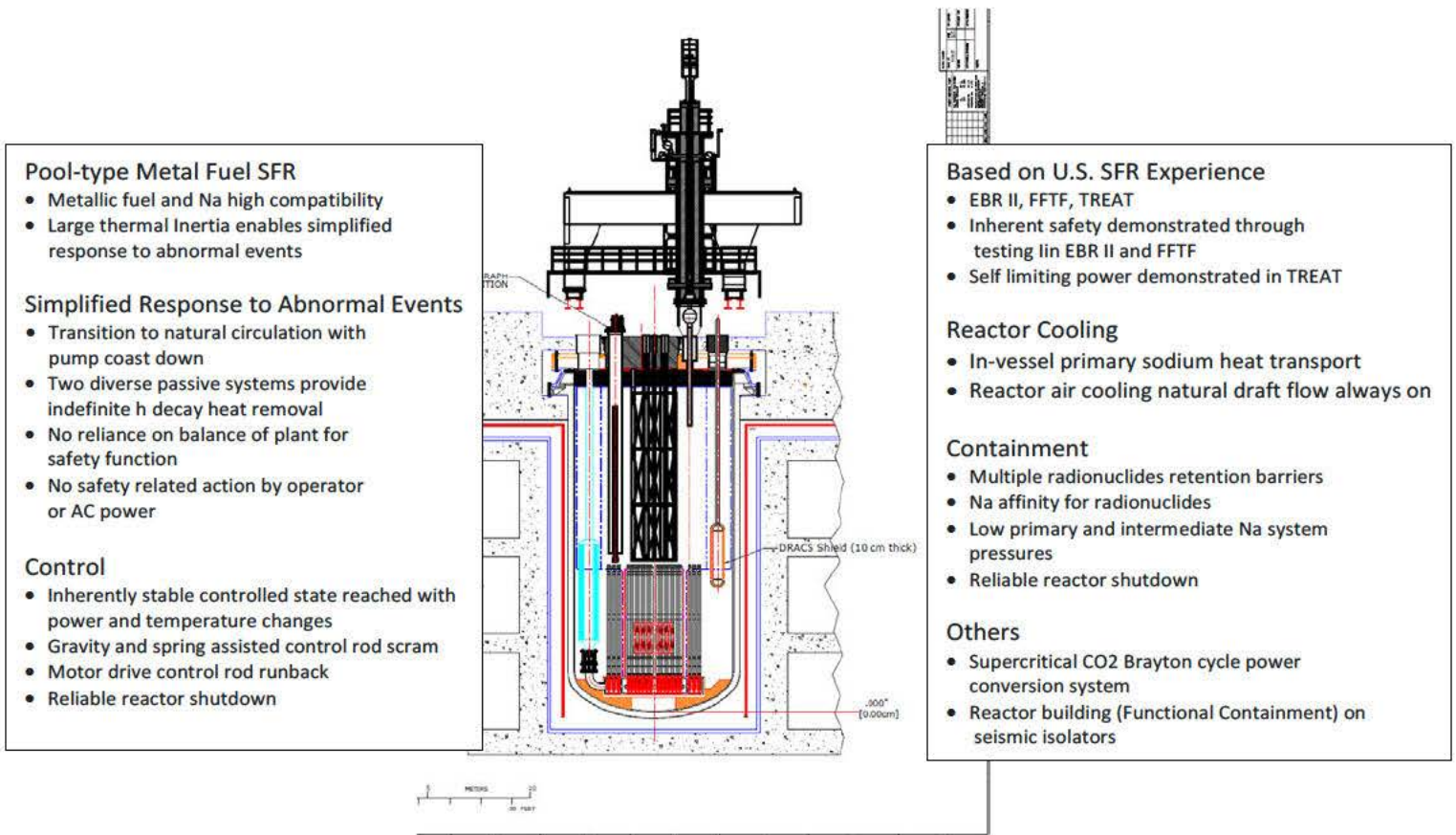


Figure 2.1 ARC-100 Reactor and Safety Features



Figure 2.2 ARC 100 Reactor In Vessel Spent Fuel Storage

## 2.2 Regulatory Background

ARC’s fuel qualification efforts began, in part, by identifying acceptance criteria that were developed using prior DOE fuel qualification effort, noting the differences between those and the requirements for light water reactor fuel. In March 2022, the NRC issued NUREG-2246, “Fuel Qualification for Advanced Reactors” [23], which includes fuel qualification assessment framework (FQAF) goals. Table 2-1 provides a cross-reference/conformance between the ARC developed/identified acceptance criteria and the possible Regulatory Acceptance Criteria (RAC) stemming from the goals of NUREG 2246, some of which are addressed by design specifications as identified in Table 2-1.

In August 2023, the NRC issued NUREG/CR 7305 [24], providing more specific guidance on how to apply NUREG 2246. Table 2-2 provides a comparison of the ARC 100 parameters/ acceptance limits, to those identified in NUREG/CR 7305.

**2.2.1 NUREG 2246 Conformance Matrix**

**Table 2-1 Conformance Matrix of ARC-100 Fuel Qualification Program and NUREG-2246**

*References denoted [xx] are at the end. References denoted [G....] are to NUREG-2246 sections.]*

Requirement/Guidance (from NUREG 2246)	ARC Clean Technology Approach	Comment
Section 1.3 Safety case - generally refers to the safety functions that the fuel is relied upon to perform. Principally among these safety-functions is the protection against the release of radionuclides.	Use of metal fuel clad with HT9 provide first (fuel itself) and second barrier (cladding) to release of radioactive material for normal operation and anticipated occurrence. Functional containment (combination of multiple barriers) helps the fuel preventing the release of radioactive material for accidents and beyond design basis events	When designed to operate within certain temperature limits, the metal fuel itself limits the release of many radionuclides. The cladding contains the radionuclides released by the fuel matrix. The small amount of fuel failures (0.1% of failed pin in the core) limit the amount of radioactivity that is released from the core for N.O, AOOs, DBAs and BDBAs
The regulation in 10 CFR 50.43(e)(1)(i) requires demonstration of the performance of each safety feature of the design, herein the fuel) through either analysis, appropriate test programs, experience, or a combination thereof.	Demonstrate performance by analysis, underpinned by experimental evidence, and supplemented by tests during operation if not FOAK, and nondestructive and destructive testing of assemblies testing if FOAK	Analyses and design approach given in section 3.1, and operational/experimental data supporting analysis and design approach provided in Appendix A
The regulation in 10 CFR 50.43(e)(1)(iii) requires that sufficient data exist on the safety features of the design to assess the analytical tools used for safety analyses over a sufficient range of normal operating conditions, transient conditions, and specified accident sequences, including equilibrium core conditions.	Analytical tools verified and validated for entire range of normal operating and transient conditions, with the exception of operation for which data on the material behavior of the fuel, under irradiation producing in excess of 208 dpa, is not available, and can only be inferred. In its 20 years of operation between refueling,	Present potential gap in knowledge Condition for which the radiation produces damage approaching 208 dpa are not reached until well after 15 -16 years in the core. Accelerated behavior confirming (or altering) inferred properties may be obtainable with dual heavy ion irradiation in a fraction of the time required if irradiated in a reactor (the latter is presently not available)
The regulations in 10 CFR 50.34(a)(1)(ii)(D), 10 CFR 52.47(a)(2)(iv), and 10 CFR 52.79(a)(1)(vi) require an evaluation of a postulated fission product release.	Conservatively determine postulated release, by employing mechanistic source terms, comparing them to operational experience and apply conservatism to those terms	Evaluation of postulated fission product release is provided in section 6.0

**ARC20-FQ-003 White Paper on ARC-100 Fuel Qualification Program**

<p>The regulations in 10 CFR 50.34(a)(3)(i), 10CFR52.47(a)(3)(i), 10 CFR 52.79(a)(4)(i), 10CF 52.137(a)(3)(i), and 10 CFR 52.157(a) require that the principal design criteria(PDC) be provided for a construction permit, design certification, combined license, standard design approval, or manufacturing license.</p>	<p>Design Criteria are provided in Sections 3.1 and 3.2</p>	
<p>GDC 2 and ARDC 2, “Design bases for protection against natural phenomena” requires that SSCs important to safety be designed to withstand the effects of natural phenomena such as earthquakes, tornadoes, hurricanes, floods, tsunami, and seiches without loss of capability to perform their safety functions.</p>	<p>Fully complies with requirement. What phenomena the fuel is designed to withstand is described in the Duty Cycle , Appendix D, Table D-1.</p>	<p>Loads resulting on the fuel from natural phenomena (to demonstrate compliance) are not described in this document. The natural phenomena design bases are described in detail in Table 5-1 of OPDD[22].</p>
<p>GDC 10 and ARDC 10, “Reactor Design,” require that specified acceptable fuel design limits (SAFDLs) or specified acceptable radionuclide release design limits (SARRDLs) not be exceeded during any condition of normal operation, including the effects of anticipated operational occurrences (AOOs).</p>	<p>Fully compliant. The design limits and the radionuclide limits are specified in sections 3.1, 3.2 and 6.0 respectively. For normal operation and AOOs the radionuclide releases are limited to the Ar41 from the RVACS, which is below the permissible release limits. Otherwise, the ARC 100 has essentially no releases. For accidents, analyses have established that even in case of involving the failures of all of the fuel pins, the radiation dose (TEDE) at the site boundary would meet the allowable limit. ( see Fig.6.3)</p>	<p>Figure 6.4 illustrates the various operational, design and safety limits for the fuel including its structural elements. Figure 6.4 also provides the information that will be utilized to establish Limited Conditions of Operations (LCOs).</p>
<p>GDC 27 and ARDC 26, “Combined Reactivity Control Systems Capability,” require, in part, the ability to achieve and maintain safe shutdown under postulated accident conditions and provide assurance that the capability to cool the core is maintained.</p>	<p>Design achieves safe controlled state inherently and maintains it indefinitely with two independent, diverse passive heat removal systems. Safe shutdown is achieved with independent control and safety rod systems , each one of which can take the reactor subcritical.</p>	

**ARC20-FQ-003 White Paper on ARC-100 Fuel Qualification Program**

<p>GDC 35 and ARDC 35, “Emergency Core Cooling,” require an emergency core cooling system that provides sufficient cooling under postulated accident conditions; they also require that fuel and clad damage that could interfere with continued effective core cooling is prevented.</p>	<p>Primary pump coast down is provided for loss of AC power to the pump. Natural circulation of the sodium in the pools cools the core while heat is removed by the passive heat removal systems. The fuel is designed to operate with limited failed fuel, and the core support and assemblies are designed to minimize the likelihood of blockage of flow to the assemblies.</p>	<p>Operational experience and analysis of the failure mechanism for cladding indicated failures do not cause significant impediment to flow. (See section 3) Flow blockage cannot be categorically excluded, and development program is being pursued intended to demonstrate that blockage of an assembly should not propagate extensively to neighboring assemblies, as the accident at Fermi 2 has shown. Progress in the simulation of the flow blockage does indeed confirm that damage of the affected assembly does not propagate to adjacent ones, in a manner that would significantly restrict their coolability.</p>
<p>Fuel manufacturing specification (G1)</p>	<p>The manufacturing process adopted is the same as that proven at the EBR II and FFTF. Fuel dimensions (and tolerances) are or will be provided.(See comment). Constituents (including allowed impurities) are provided. However, since dimensions are significantly different from those of the fuel for EBR II and FFTF, the scaling up of the manufacturing process will be necessary. The end state attributes of the material within fuel components therefore will have to be demonstrated to be the same as those of the EBR II and FFTF, by a prototype program for the fuel fabrication.</p>	<p>Figure 4.1 and 4.2 provide the fuel dimensions. Section 3.5 describes the fabrication approach and also the steps that will be taken to demonstrate in a prototype the ability to produce a fuel with performance comparable to that experienced in EBR II and FFTF. At this time The fuel design specification is not yet complete. moreover the overall design phase (including detailed design) involves the preparation of drawings that fully define the configuration of the fuel pin, the arrangement of the pins within the assembly with the necessary pin mounting and supports, the assembly parts (hexagonal duct, lower and support fitting), and how they are to be joined together (welded or bolted), and an accompanying design specification detailing the tolerances on material composition, dimensions etc. that the fuel slug, pin, and assembly are to meet. The initial part of this work has been</p>

		completed, i.e., high level drawing preparation, but the design specification is awaiting the determination of the tolerances which the prototype fuel slug, pin and assembly must meet.
Key dimensions and tolerances of fuel components are specified (G1.1).	As the design progresses, ARC will provide all of the necessary information. The comment column addresses the status at the conceptual design stage.	Some key dimensions of fuel rods (slugs and cladding) are specified throughout the report, although some dimensions are not yet determined (i.e., slug length since it is not known if they can be manufactured to the desired length). A summary of the tolerances is provided in section 3.5.1.1) and determining all key dimensions and tolerances is to be completed.
Key constituents are specified with allowance for impurities (G1.2).	See comment	Because a source of HALEU has not been identified, the form the uranium will take cannot be specified. For EBR-II, uranium was procured from the Oak Ridge Y-12 plant in the form of "buttons." The uranium enrichment and purity were specified in an ANL specific SPM-73-1. The total uranium content was required to be 99.8%, the sum of metallic impurities less than 2000 ppm, and the sum of nonmetallic impurities less than 1000 ppm. ARC Clean Technology expects that similar uranium content will be specified. For the cladding HT9 is specified, but HT (behavior above 208 dpa is not established) Section 3.5.1.1 provide a summary of the key constituents and the permissible content of impurities.
End state attributes for materials within fuel components are specified or otherwise justified (G1.3).	ARC will adopt the same manufacturing process proven at the EBR II and FFTF. Fuel dimensions (and tolerances) are or will be provided. Constituents (including allowed impurities) are or will be provided. However, since	At the end of the conceptual stage of design, the end state attributes are not yet fully specified (e.g., fuel slug roundness, straightness, length, flatness of ends, etc.).

	<p>dimensions are significantly different from those of the fuel for EBR II and FFFT, the scaling up of the manufacturing process will be necessary. The end state attributes of the material within fuel components therefore will have to be demonstrated to be the same as those of the EBR II and FFFT, by a prototype program for the fuel fabrication.</p>	
<p>Margins to Safety Limits can be demonstrated (G2).</p>	<p>Safety limits are essentially the margins above the design limits established for the ARC fuel. The latter are provided in Table 3-1 of section 3.1 for the fuel and the cladding, and in sections 3.2.1-3.2.5 for the structural materials of the fuel assemblies. The experimental and operational data supporting the establishment of the safety limits, radionuclides releases, and validation of the evaluation models are provided in Appendices referred to in the various chapters above. the determination of acceptance criteria, e.g., limits, for each of the requirements. These limits (operating and AOOs limits, and safety limits for design and beyond design basis accidents) are provided for each fuel component, (i.e., metallic slug, cladding, fuel assembly structural components) in sections 3.1 and 3.2 of this report.</p>	<p>Not all deterministic safety analyses have been completed during the conceptual design. Those complete to date, which are considered bounding, have shown that significant margins between the calculated parameters and the safety limits established for those parameters. The safety limits are provided in various sections of the report and are summarized in the radar plot of Figure 6.4.</p>
<p>Margin to design limits can be demonstrated under conditions of normal operation and AOOs (G2.1).</p>		
<p>G.2.1.1 the fuel performance envelop is defined.</p>	<p>Figure 6.1 defines the fuel performance envelop under normal operation, anticipated occurrences, design basis and beyond design basis events. Figure 6.4 is a radar chart indicating the safety limits and</p>	<p>The fuel performance envelope is indicated in Fig 6.1 “radar plot”. The envelope includes peak burnup, peak fluence, peak cladding temperature, peak fuel temperature. min. fuel melting margin. These parameters are</p>

**ARC20-FQ-003 White Paper on ARC-100 Fuel Qualification Program**

	<p>margins and the region of limited operational conditions.</p>	<p>based on, and conservative compared to, operational experience in EBR II and FFTF; but notably, the peak fluence is higher in ARC fuel. Maximum cladding penetration, coolant boiling margins and other design and safety parameters are shown in Figure 6.4.</p>
<p>G.2.1.2 Evaluation models are available to assess all the phenomena that can affect fuel performance against design limits to protect against fuel failure and degradation (i.e., life limiting) mechanisms.</p>	<p>Verified and validated evaluation models are available to assess all the phenomena that can affect the fuel performance and compare the results to the limits established in section 3.1. Potentially life limiting mechanisms are described in Section 5.1 with the evaluation model described in Section 5.3.</p>	<p>The models and codes used for the various phenomena that can affect the fuel are provided in section 5.3. The limits established for each phenomenon, as part of the overall limit, are described in section 3, and the phenomena are described in Section 5.1.</p>
<p>G.2.2 Margin to radionuclide release limits under accident conditions can be demonstrated.</p>	<p>As a bounding example. ARC Clean Technology has analyzed a postulated case in which all fuel pins were forced to fail and calculated the site boundary dose vs. time.</p>	<p>As a bounding assessment of the characteristics of the fuel matrix and the cladding which limit releases of radioactivity, ARC Clean Technology has analyzed a postulated case in which all fuel pins were forced to fail, by assuming incapacitation of both diverse passive heat removal system. After nearly 67 hours all pins failed and the high temperatures of the fuel caused a maximum amount of the radionuclides contained in the matrix to be released to the coolant, then the cover gas and then the reactor building spaces and ultimately the environment.</p> <p>The bounding analysis illustrated in Figure 6.3, shows the combination of the metal fuel ability to retain radionuclides within its matrix, even when the cladding fails, combined with the scrubbing action of the pools and the deposition of sodium aerosols in colder surfaces result in doses at an ARC 100 boundary</p> <p style="text-align: right;">which meet regulatory limits. (see also the identical</p>

		figure in section 3.5 of the Compliance with NUREG/CR 7305).
G.2.2.1 Radionuclide retention requirements of the fuel under accident conditions are specified.	<p>Section 6 provides retention requirement and information on accident condition releases.</p> <p>Retention requirements for Normal Operation and AOOs are that radionuclides should not be released and if released by anticipated occurrences they must meet allowable release limits.</p>	The Section 6 accident example used to demonstrate that the fuel and the functional containment provide adequate retention is a postulated accident in which both emergency heat removal system are assumed to fail, even though the two are diverse systems and both are passive.
G.2.2.2 Criteria for barrier degradation and failure under accident condition are suitably conservative.	<p>Section 3.1 provides criteria (limits) for the fuel and the cladding which if met would ensure failures do not occur. However, those limits for certain very unlikely accidents allow that degradation of the fuel and cladding barrier but no failure) can occur. The phenomena that can cause degradation of the fuel/cladding barrier are presented in Section 5.1.</p> <p>The established limits, however, implicitly assume the material properties of the fuel and cladding, i.e., tensile and creep strength, ductility are as inferred for irradiation past the currently available empirical data, and hence subject to uncertainty. This is a “gap” that is recognized, but not resolved., since the empirical data is lacking [G.2.2.2(b)].</p> <p>Limits on degradation of primary coolant boundary and functional containment are addressed in Section 2.</p>	<p>In addition to the conservative approach of assuming all cladding fails as a result of the simultaneous failures of both diverse emergency heat removal systems, the leakage of radionuclide through the barrier provide by the reactor top head is assumed to be 10 time greater than the leakage experienced in the comparable top heads at FFTF Furthermore, even though no significant pressure is built up in the reactor building, the building is assumed to leak at</p> <p>Resolution of the lacking empirical data may be obtainable by out of core testing of the material using heavy ions irradiation, which can produce results in a very short time compared to neutron irradiation. However, there is a question as to whether results obtained of a very limited layer of material are valid for the bulk material.</p> <p>Alternatively, a FOAK ARC 100 unit could serve as the test of the validity of the inferred behavior, by periodically</p>



		<p>extracting an assembly and both nondestructive and destructive testing of individual pins and the assembly. The first and second extraction would be conducted at times indicated in the schedule of Appendix A . Those tests would confirm the behavior of the fuel is as predicted prior to the irradiation exceeding the present empirical data, and subsequent extraction would add to the knowledge that is presently lacking.</p>
<p>G.2.2.3 Radionuclide retention and release behavior under accident conditions are modeled conservatively</p>	<p>ARC Clean Technology uses mechanistic source terms (best estimates) for the release of radionuclides under both normal and accident conditions. For design basis event (normal operation, AOOs and DBAs) the condition that can lead to releases are modelled conservatively, i.e., considering uncertainties (typically 3 sigma). And the upper limits of possible releases are used. . Whereas for beyond design basis events, the best estimate methods are used.</p> <p>Empirical data supports conservative estimates of the releases from the fuel, but transport of the fuel though the pool and subsequent behavior of the radionuclide chemical forms is not as extensive and in particular data on transport through the pool and aerosol deposition is scant (G.2.2.3 (b)).</p>	<p>Same as above</p> <p>The mechanistic source terms establish release percentages from the metal fuel for different groups of radioisotopes, e.g., halogens, alkali metals, noble metals, noble gases, Actinides, as function of temperatures of the fuel. The transport of the released radionuclides through the pools, the cover gas and the functional containment are modeled as documented in ANL-ART 49 [16].</p> <p>The radiological releases from the fuel, as underpinned from empirical data are documented in Section 2.0 and are subject to the following uncertainties:</p> <p>(1)Due to insufficient data regarding the migration of radionuclides within the fuel pin and subsequent release during fuel pin failure (as described in more detail in ANL-ART-38 [72], bounding radionuclide release fractions from failed fuel pins are necessary.</p> <p>(2)There are large uncertainties regarding the transport of radionuclides within bubbles in the sodium pool. This pathway could result in a bypass</p>

		<p>mechanism for radionuclides that would otherwise be largely retained within the sodium pool. Properly characterizing the bubble pathway is essential to a realistic source term assessment, but data and tools in this area are lacking. Gap closure in this area could be accomplished through experiments with nonradioactive elements.</p> <p>(3) The accurate modeling of radionuclide behavior within the cover gas region and containment can be problematic due to the unique chemical forms and interactions associated with SFR radionuclide (and sodium) release. Although conservative assumptions are straightforward to apply to selected gaps, such as aerosol deposition, other phenomena, such as chemical interactions, are more difficult to address through gross assumptions.</p>
<p>G.2.3 Ability to achieve and maintain safe shutdown can be assured</p>	<p>ARC Clean Technology approach is to rely on the reactor to respond to events by inherently reducing its power to the level that is removed by the heat removal system. This inherent response, however, produces a controlled, safe state, but the reactor is still critical. Each of two independent rod systems driven by two independent and diverse drive systems and actuated by a very reliable 4 channel reactor protection system, are used to shut down the reactor to a deeply subcritical state.</p> <p>Inherent negative reactivity insertion was demonstrated at during epochal test at the EBR II (the SHRT tests) and the test results have been very</p>	<p>In addition to the reactor protection system actuation of the control rods, and separate reactor protection system, using different sensors and a platform different from that of the control rods RPS, actuates the safety rod. Either system can independently shut down the reactor. Should both systems fail (the PRA has indicated such failure is of the order of <math>10^{-6}</math>) a rod run-in provides an alternate way to insert the rods in the core. The motor of the CRDM drive the rods into the core with a force sufficient to overcome possible deformations.</p>

	<p>successfully modeled by the main thermohydraulic code: SAS4A/SASSYS-1.[87] (G.2.3.2).</p> <p>The ability to insert the rods depends on the deformation of the core and the control elements themselves, and that is addressed below (G.2.3.1 and G.2.3.2).</p>	
<p>G.2.3.1 Maintenance of coolable geometry under accident conditions can be demonstrated.</p>	<p>Phenomena that can cause the loss of a coolable geometry include internal events, such as fuel swelling fuel melting, cladding failure resulting in blockage of flow channels or external events such as seismic causing very significant deformations of the core [G.2.3.1(a)].</p> <p>Fuel swelling is addressed and the support system and spacing between the pins by means of a spiral wound wire spacer as well as between the ducts is designed to prevent loss of coolability. Prevention of fuel melting is a criterion established for the design of the fuel (and the core) as shown in Section 3.1 All analyses for accidents have indicated significant margins to fuel melt [7].</p> <p>External loads, including seismic loads are used for the structural design of the fuel, and bot SSE and beyond design basis seismic evet will be considered in the design.</p>	<p>Seismic analysis of the fuel has not yet been performed, it will be done along with other mechanical and thermal loads to which the fuel will be subjected as identified in the fuel duty cycles of Appendix D</p> <p>The structural analysis code that will be used is ANSYS, which has been extensively verified and validated [G.2.3.1(b)].</p> <p>The computer codes used to determine the behavior of the fuel under internally caused conditions have been verified and validate as explained in Appendix F.</p> <p>Swelling behavior and tensile and creep properties of the material of the fuel and fuel assembly are established and underpinned by empirical date for a range of irradiation below 208 dpa.</p> <p>Either a separate FOAK for the ARC 100 or this reactor as its</p>

		FOAK could establish the behavior of the fuel beyond the 208 dpa. It is noted that the ARC 100 irradiation damage in 20 years is determined by MFUEL[90] to be 200 dpa,
(1) Criteria to ensure coolable geometry are specified.	Prevention of blockages is partially addressed by imposing criteria that prevent the cladding from melting, but other scenarios could result in blockage of flow have not yet been analyzed (e.g., seismic events), or performance of fuel and cladding at or beyond 208 dpa is subject to uncertainty .	Some criteria are specified but not all analyses have been completed.
Evaluation models are available (see EM Assessment Framework)	Mature codes for performing e.g., seismic analyses are available and planned to be used.	
G.2.3.2 Negative reactivity insertion can be demonstrated	<p>The inherent negative insertion of reactivity under transient conditions resulting in temperature increase within the core have been demonstrated by testing at the EBR II and FFTF and confirmed by analysis using SAS4A/SASSYS-1 code that has been verified and validated against those tests [G2.3.2(b)].</p> <p>The negative insertion of reactivity by the rods, require the geometry of the core and in particular the geometry of control element assembly ductwork, within which the rod bundle contained in its own internal duct, and their drivelines be maintained within limits, so the rod are able to insert . The allowable deformations have been and will be reconfirmed as the design progresses) and be</p>	<p>Prediction of core and individual assemblies’ deformations, including control assemblies and their drivelines use evaluation models in SAS4A/SASSYS-1 which has been verified and validated as described in Appendix F [G.2.3.2(b)].</p> <p>The further verify the adequacy of the evaluation model, ARC Clean Technology will utilize means of determining semi-quantitatively the extent of deformations during operation, by the following means briefly described in Section 5.5:                      (1)periodic exercising of the control rods, measuring the Power Reactivity Decrement (PRD- described in Reference [18], (2) periodic measurement of the pull-out forces of the assemblies.</p> <p>An additional parameter of interest is blockage in the core that prevents insertion of control</p>

	<p>maintained by the core support system.</p>	<p>and safety rods. ARC with ANL is developing the capability to determine the consequences of complete blockage of an assembly to adjacent assemblies. Progress of that work is reported in the separate ARC 20 R&amp;D program report [19], available upon request.</p>
<p>EM G1 The evaluation model contains appropriate modeling capabilities</p>	<p>There are three models employed to predict the behavior of the ARC100 fuel. The first is the SAS4/SASSYS-1 model used to assess the global behavior of the fuel during operation and transients. The geometry and material of the fuel is accurately captured and considers the fuel radial and axial expansion, as well as fuel cladding chemical interaction, to predict the performance of the fuel matrix and the cladding over time. The second is a detailed model of the fuel pin utilizing the BISON computer code. This code provides a detailed analysis of the fuel matrix and the cladding when subjected to the global performance of the fuel during N.O, AOOs and transients (from the SAS4A analysis) . This code model the geometry of the fuel and cladding as it is affected by fuel swelling, FCCI (both fission product migration induced fuel cladding brittle layer formation as well as eutectic formation, nickel and carbon depletion and sodium corrosion. EM G1.1, and EM G1.2 ) The third model assesses the transport of radiological releases from the fuel resulting from postulated fuel failures. This model is the SRT code [74] The important geometry modeled in this evaluation is not that of the fuel/cladding, but that of the surroundings, i.e., volume and height of the sodium pools</p>	<p>All three evaluation models contain the necessary physics, but also rely on correlations developed from empirical data, particularly when the physics is complex and perhaps not completely understood (as in the case of FCCI involving fission product migration , or the transport of radionuclide compounds through the sodium pool, and aerosol deposition.</p> <p>All three have been verified and validated against available empirical data. Documentation of for SAS4A/SASSYS-1 and BISON is provided in Appendix F and Reference [74] for SRT (EM G1.3).</p> <p>Various evaluation models exist and are largely validated for the operating domain of the ARC fuel; however, the models do not cover cladding (HT-9) performance above 208 dpa.</p>

	<p>above the core, volume and perimeter of the cover gas area above the pool, volume and perimeter of space in which the radionuclides can be dispersed. SRT evaluates transport of different radionuclides through the pool to the cover gas, from the cover gas to surrounding spaces, considering formation of possible chemical compounds of the radionuclides, and possible aerosol depositions.</p>	
EM G1.1 Evaluation model is capable of modeling the geometry of the fuel system.	Yes	Except not validated for HT-9 for 208 dpa and above. However, the ARC damage in 20 years of operation with a 90 % capacity factor is expected to be near 200 dpa [90],
EM G1.2 Evaluation model is capable of modeling the material properties of the fuel system.	Yes	Same as above
EM G1.3 Evaluation model is capable of modeling the physics relevant to fuel performance.	Yes	Same as above
EM G2 The evaluation model has been adequately assessed against experimental data.	<p>All three evaluation models described above have been assessed i.e., validated) against experimental data. Their validation is summarized in section 5.3 and Appendix F.</p> <p>Comparison of model prediction of fuel degradation (and failure) very experimental data has indicated that the evaluation model is adequate. Section 5.3 and Appendix F. provide the comparisons. (EM G2.2).</p> <p>Adequacy means that as used to determine the performance of the fuel over tis lifetime, the evaluation model suffices to provide information that enables establishing margins to fuel possible failures , which are</p>	<p>The experimental data ranges from out of core testing such as eutectic formation and creep rupture data, to in core operational data, and supporting out of core tests, such as the measurement of the FCCI layers in EBR II and FFTF . The data exists up to irradiation of 208 dpa, and for irradiation beyond that level of radiation damage, the codes presently assume a linear behavior. So, the experimental data used for assessment is appropriate for irradiation not exceeding 208 dpa but is generally nonexistent beyond that level (EM G2.1).</p>

**ARC20-FQ-003 White Paper on ARC-100 Fuel Qualification Program**

	sufficiently large to cover modeling underpredictions (i.e., errors) (EM G2.2.1 and G2.2.2).	In the regions of the fuel performance envelop, the region above 208 dpa contains either no data or sparse data. That data could become available if another reactor with the same fuel (material and dimensions) were to be a FOAK preceding the deployment of the ARC 20 program reactor. Alternatively, the ARC20 program reactor would be the FOAK, and its operation beyond 15 years could be subject to the results of nondestructive and destructive testing of fuel pins and assemblies. (EM G2.2.3 and section 5.5).
EM G2.1 Data used for assessment are appropriate (see ED Assessment Framework).	Mostly. Data from EBR-II and FFTF fuel operated in same operational envelope as that planned for ARC fuel, but there are some differences between ARC fuel and EBR-II/FFTF fuel so it should be clearly described how these differences are accounted for and how the available EBR-II/FFTF data covers the ARC fuel.	
EM G2.2 Evaluation model is demonstrably able to predict fuel failure and degradation mechanisms over the test envelope.	Yes, except not yet beyond 200 dpa.	ARC-100 fuel damage is expected to be limited to 200 dpa.
EM G2.2.1 Evaluation model error is quantified through assessment against experimental data.	The models are based on empirical data, but the quantified errors are not addressed in this report. See comment.	ARC developed a separate simplified Arrhenius equation, based on completely separate Japanese experiments, not utilizing the empirical data supported models, to determine whether the models properly reproduce the empirical results. Using core inventory data to determine the percentages of lanthanides present in the fuel of the empirical date, the simplified equation predicted rather accurately the thickness of the FCCI layers and confirmed that the adequate. employed in the models are generally good in
EM G2.2.2 Evaluation model error is determined throughout the fuel performance envelope.	The models are based on empirical data, but the quantified errors are not addressed in this report Throughout the main body of the report the cumulative damage fraction (CDF) is one of the methods of calculating fuel lifetime. The CDF method is determined by the thermal creep strain. The fraction of	

	<p>cladding life consumed within any period of operation is calculated by the amount of time at the relevant temperature, stress, neutron fluence divided by the total time to stress rupture. The thermal creep strain is a function of time, temperature, stress, and the neutron fluence. The hoop stress, in turn, depends upon cladding thickness, which is a function of FCCI, plenum pressure, and fuel slug FCMI. The temperature and neutron fluence depend upon reactor operating conditions. All the correlations that describe these phenomena have “considerable perhaps unquantifiable uncertainty” particularly when extrapolated to the ARC-100 long exposure irradiation time. This is why there is a need for a disciplined surveillance program where fuel is examined throughout the lifetime of the reactor operation.</p>	<p>their predictions. Section 5.3 of this report provides a summary of the use of the simplified equation and its results.</p>
<p>EM G2.2.3 Sparse data regions are justified.</p>	<p>Yes. Above 208 dpa.</p>	<p>As the irradiation period approaches the range of dpa beyond which no experimental /operational data exists, the uncertainties in the correlations employed for predicting fuel lifetime increase.</p>
<p>EM G2.2.4 Evaluation model is restricted to use within its test envelope.</p>	<p>No. ARC presently could extrapolate the models past 208 dpa, but perhaps does not need to (see note).</p>	<p>ARC-100 fuel damage is expected to be limited to 200 dpa [89,90].</p>
<p>ED G1 Assessment data is independent of data used to develop/train the evaluation model.</p>	<p>The experimental assessment data cannot be considered totally independent from the evaluation models, because the evaluation model utilized to different degrees the correlations developed from the assessment data, Since the correlation have been “tuned” to the assessment data, evaluation models should be expected to have small errors</p>	<p>For FCCI caused by migration of Fission products, the correlations used in and BISON and MFUEL were developed by operational data. A check on the ability of those correlation to accurately predict the behavior at times not covered by the empirical data used to develop the correlation , is the use of a different correlation developed for out- of core tests, as</p>



	<p>in predicting that data. Key is to use the evaluation methods to accurately predict outside the assessment data used to develop the correlations. The approach used by ARC Clean Technology whenever possible is to verify that "accuracy" by utilizing a different set of assessment data that was not directly used in developing the correlations. Examples are provided in the Notes.</p>	<p>modified for the actual condition in core. The comparison is satisfactory (section 5)</p> <p>The correlation of fission gas bubble formation and as release dependency on dimension of the fuel is shown to be independent of the dimension (section 5.1) and hence the specific evaluation model.</p> <p>Fuel and axial expansion under thermal and radiation induced effects is an example (Section 5.2). for which the assessment data from two different sources may insufficient since data on radiation damage is limited to 208 dpa,</p> <p>The assessment data for metal fuel ratcheting is not existent because fuel ratcheting has never been observed at either EBR II or FFTF. The ARC Clean Technology approach in this case is to demonstrate that if it were to occur, the consequences would be acceptable.</p> <p>Another example is the comparison between the correlation employed for Na corrosion of HT9 with data developed from different experiments conducted for different reasons.</p> <p>Finally, the comment on EM G221 and G.2.2.2 provide an example of using data that is independent of the data used to develop and train the evaluation models.</p>
<p>ED G2 The Experimental assessment data has been collected over a test envelope that covers the fuel performance envelope.</p>	<p>With the exception of slug ratcheting, for which experimental data on metal fuel (at smaller dimensions of the fuel lugs than those of the ARC 100) record no observations, (2)</p>	<p>Slug ratcheting and radiation damage are addressed in the notes of ED G1. Time of exposure deals with the time at temperature, and not of the data underpinning the</p>

**ARC20-FQ-003 White Paper on ARC-100 Fuel Qualification Program**

	<p>radiation damage in excess of 208 dpa, and (3) time of exposure all other data is within the fuel performance envelop.</p>	<p>correlation employed in the evaluation model , most if not all of which was generated at directly comparable burnups and temperatures, but during considerably shorter times. For FFCI where temperature and time at temperature are important parameters, the correlation used in BISON are validated by using a different correlation developed from out of core tests.</p>
<p>ED G3 Experimental data have been accurately measured.</p>	<p>ED G3.1) The experimental and operational facility used to develop much of the data that underpin the evaluation models did not have quality program that would now be considered appropriate, has been collected in data sets and subjected to an NRC approved quality program to verify (long after its collection) the adequacy and accuracy of the data. (Section 5.5).</p>	<p>Although the quality program at eh facilities where assessment data were developed would not be considered appropriate today, the data was collected using measurement techniques established at that time, and still acceptable today. (ED G3.2) The experimental data, as reported sometimes in scientific papers and mostly in technical reports (particularly in the latter) typically provides information regarding the source of experimental uncertainty (including instrumentation uncertainty) (ED 3.3).</p>
<p>ED G4 Tests represent prototypical conditions.</p>	<p>The dimensions of the ARC 100 fuel are different from the dimensions of eh fuel operated at EBR II and FFTF (or other metal fueled sodium cooled pool or loop fast reactors). As such the test cannot be considered entirely prototypical. However, the fabrication process used is entirely the same as that proposed of the ARC 100 fuel, and as described in section 4.7 fabrication of the ARC 100 fuel will be preceded by the fabrication and testing of its prototype (ED G4.1).</p>	<p>Because of the different dimension as well as the different performance envelope (25% greater fluence but dose (damage) limited to or slightly exceeding the experimentally measured damage of the ARC 100 fuel, the evaluation model used to predict the ARC 100 fuel performance. can only be relied upon to provide information that ultimately needs to be validate by performance in an actual reactor This is because unavoidably the evaluation models use extrapolation of the consequences of certain phenomena and material properties that are outside the range of the existing data (ED G4.2).</p>

**2.2.2 NUREG/CR 7305 Conformance Matrix**

<b>Table 2-2 Compliance of ARC 100 to NUREG/CR-7305</b>	
NUREG/CR 7305 Sections	ARC100 Compliance/Differences
2.1 Fuel Manufacturing	No difference from prior fabrication methods. -Fabrication of the ARC 100 zirconium-based fuel will be by injection casting used for EBR II [1] and FFTF fuel. ARC is presently awaiting requested FFTF information to examine the FFTF improvements made to the EBR II fuel fabrication.
2.1.1 Dimensions	ARC-100 fuel differs in dimensions from the EBR II and FFTF fuel. It uses longer and greater diameter fuel pins as shown in Table 1. The composition tolerances, are the same as those used in FFTF.
2.1.1 Tables 2-2 Dimensional Tolerances of the U-Zr Fuel System	Percentage wise the ARC 100 tolerances on fuel column height and width are generally smaller than those of EBR II and FFTF.
2.1.2 Constituents (Table 2-3 Composition Tolerances of the U-Zr Fuel System and Table 2-4 Composition Tolerances of the Na Bond	ARC-100 fuel and HT9 constituents and their tolerances are the same as those in EBR II.
2.1.2 End State Attributes	The only difference between the ARC 100 may be the height of the sodium bond above the fuel, which is justified to be at least , but can be greater because of the much longer fuel section.
2.2 Safety Criteria	The safety criteria for the ARC 100 are specified in the ARC 20 project Fuel Qualification Program [2] and summarized in this white paper.
2.2.1 Design Limits During Normal Operation and Anticipated Operational Occurrences	The limits established for the ARC 100 reactor fuel are based on the same operational data from EBR II and FFTF., as provided in Table 2-5 of NUREG/CR 7305 augmented by the details available in Reference [3] and numerous papers, one example of which is reference [4]. Safety analyses considered bounding have shown that for normal operation and anticipated operational occurrence the low temperatures experienced by the cladding (nominal peak temperature of ensure long life for the fuel pins and the absence of fuel failure. An indication of the limited fuel failures is provided by the Cumulative Damage Factor for steady state operation, which is considerably lower than the CDF value which with 95% confidence would imply that no more than 1 failure would occur in 100,000 pins. The ARC 100 core has a total of only 21,483 pins. Annex A of this provides the information for the CDF values

**ARC20-FQ-003 White Paper on ARC-100 Fuel Qualification Program**

<p>2.2.2 Design Limits During Anticipated and Accident Transients</p>	<p>Safety analysis of both protected and unprotected transients [7,8,9,10,11] considered to be bounding of the possible transients indicate that in all instance there is more than sufficient margins to fuel melting, and to coolant boiling. The maximum eutectic penetrations which could occur in an unprotected reactivity insertion or station blackout are limited to (significantly less than the 5% limit in EBR II). The combination of no fuel melting and large margin to coolant boiling ensure the core remain coolable including during beyond design basis accidents.</p>
<p>2.3 Fuel Performance Envelope</p> <ul style="list-style-type: none"> <li>• Peak Burnup</li> <li>• Peak Linear Heat Generation Rate</li> <li>• Peak fuel cladding interface Temperature</li> <li>• Peak fuel temperature</li> </ul>	<ul style="list-style-type: none"> <li>• The ARC 100 peak fuel rod burnup of exceeds the reference 10 at%. The average burnup for the ARC100 fuel is The peak burnup is achieved because of the very long life planned for the fuel in core (18 EFPY).</li> <li>• The Peak linear heat generation rate for the ARC 100 fuel at is much lower than the heat rates (40-55 kW/m) at which extensive testing has been performed and associated fuel evolution and kinetic are well characterized.</li> <li>• The nominal and peak cladding temperature are well below 650 °C.</li> <li>• The fuel temperature remains well below the local fuel composition solidus temperature</li> </ul>
<p>2.3 Fuel Performance Envelope</p> <ul style="list-style-type: none"> <li>• Radial Strain and Deformation</li> </ul>	<p>Cladding radial deformation from thermal creep has been determined well as irradiation creep caused strain at the nominal, <math>2\sigma</math> and <math>3\sigma</math> temperatures and irradiation exposure times. The correlations for thermal and irradiation creep were developed from operational and experimental data that did not cover the duration of time the ARC 100 fuel will experience (6570 equivalent full power days in the 20-year refueling interval at a 90% capacity factor) . The fuel thermal creep correlation used in the fuel performance codes has been developed from limited data and for temperature range in which the strain rate varies by order of magnitude, thereby introducing uncertainty in the predicted strains. The table below shown the predicted total, peak thermal creep and peak irradiation creep strains at <math>2\sigma</math> and <math>3\sigma</math> fuel and cladding temperatures for two different irradiation times equivalents to the 20-year refueling (6579 EFPD) and 16 years (5256 EFPD) [13].</p> <p>The verified and validated fuel performance codes BISON [12] and MFUEL [13] have been used to develop the information shown in the table below. Both codes consider FCCI and FCMI. The conservatism in determining the peak fuel and cladding temperatures and the conservatism employed in establishing the proposed design limits (see for instance Annex A), which are the same as have been used in past metal fuel qualification provide</p> <p>at 90% capacity factor. Thereafter confidence in its behavior decreases. The potential exceedance of the established limits does not signify that the fuel would experience a considerable number of failures. It does however indicate that the operation would take place beyond the period of time for which the behavior of the cladding under irradiation is underpinned by empirical data, hence it is inferred by extrapolation, and therefore subject to unquantifiable uncertainty. This is the reason ARC Clean Technology fuel qualification program relies on periodic extraction of fuel pins from</p>

	<p>the reactor with non-destructive and destructive testing of the pins to verify the fuel performance.</p>																												
	<table border="1"> <thead> <tr> <th rowspan="2">Parameter</th> <th colspan="2">6570 EFPD</th> <th>5256EFPD</th> <th rowspan="2">Proposed Design Limit</th> </tr> <tr> <th>2σ</th> <th>3σ</th> <th>2σ</th> </tr> </thead> <tbody> <tr> <td>Peak Cladding Total Permanent Strain %</td> <td></td> <td></td> <td></td> <td>2% Per NUREG 7305 and CEA findings</td> </tr> <tr> <td>Peak Cladding Thermal Creep Strain %</td> <td></td> <td></td> <td></td> <td>1% widely used in Fast Reactor design, for both steady state and transients</td> </tr> <tr> <td>Peak Cladding Irradiation Creep Strain %</td> <td></td> <td></td> <td></td> <td>2% Per NUREG 7305 and CEA findings</td> </tr> <tr> <td>Peak Cladding CDF</td> <td></td> <td></td> <td></td> <td>0.05 for steady state; 0.1 for transients</td> </tr> </tbody> </table>	Parameter	6570 EFPD		5256EFPD	Proposed Design Limit	2σ	3σ	2σ	Peak Cladding Total Permanent Strain %				2% Per NUREG 7305 and CEA findings	Peak Cladding Thermal Creep Strain %				1% widely used in Fast Reactor design, for both steady state and transients	Peak Cladding Irradiation Creep Strain %				2% Per NUREG 7305 and CEA findings	Peak Cladding CDF				0.05 for steady state; 0.1 for transients
Parameter	6570 EFPD		5256EFPD	Proposed Design Limit																									
	2σ	3σ	2σ																										
Peak Cladding Total Permanent Strain %				2% Per NUREG 7305 and CEA findings																									
Peak Cladding Thermal Creep Strain %				1% widely used in Fast Reactor design, for both steady state and transients																									
Peak Cladding Irradiation Creep Strain %				2% Per NUREG 7305 and CEA findings																									
Peak Cladding CDF				0.05 for steady state; 0.1 for transients																									
<p>2.3.1 Behaviors, Phenomena, and Properties</p>	<p>All of the phenomena and properties listed in NUREG/CR 7305 are addressed in the ARC Fuel design and the behaviors are predicted by using verified and validated codes [12,13, 14]. The operational regime for which the ARC 100 fuel is being designed, however, introduces uncertainties in some of the properties of the fuel and the cladding, as well as uncertainty in the use of the correlations developed to describe the evolution of certain phenomena, e.g., FCCI, creep.</p> <p>Another example is the uncertainty introduced when the burnup exceeds the 10% mentioned in NUREG/CR 7305. At this point solid fission products could eliminate or significantly reduce the path of the fission gases to the gas plenum, causing an additional axial swelling of the fuel. Since this process is not yet fully understood mechanistically, the ARC100 Fuel Qualification program proposes to extract pins before the peak burnup reaches much above 10%. In year 16 of operation the peak burnup is , and it is noted that at the percentage burnup, for U-10Zr fuel employed by the ARC 100 data from FIPD [3] data base (plutonium content at that burnup is approximately ) indicate axial fuel growth entirely consistent with that calculated by the fuel performance code MFUEL (see Figure 3-2 of NUREG/CR 7305).</p>																												

**ARC20-FQ-003 White Paper on ARC-100 Fuel Qualification Program**

<p>3.1 Geometric Evolution</p>	<p>The geometry of the unirradiated ARC 100 fuel is different than the geometry of the fuels addressed in NUREG/CR 7305. The ARC 100 fuel pins have a greater diameter and are longer. The evolution of the fuel over time, however, is caused by the same phenomena described in NUREG/CR 7305, and the fuel performance codes (BISON, MFUEL) a used for design capture the changes of the fuel and pin geometry. The empirical data suggest that cladding strain should not exceed 2% in order to not become a limiting factor. The ARC 100 fuel meets that criterion during the first 16 years of operation but might exceed it in subsequent years. It is planned that the evolution of the geometry of the fuel (swelling and gas evolution resulting in radial contact with the cladding and axial expansion) will be confirmed (and set a baseline for subsequent measurements) by extraction of pin in year 4 of operation at which time burnup will be approximately 2%. Thereafter surveillance of the behavior of the fuel will be by periodic extraction and testing of pins commencing in year 14 and continuing at intervals established based on the results of the testing. The ARC-100 fuel is designed with a smear density of 75%. Adopting a lower smear density would in principle reduce strains in the cladding, but that would require a significant change in the core configuration by altering the fissile content of the present core. It is noted that in several instances the literature reported smear densities of 75% (see Appendix C) were in fact lower [3]. For instance, X419, X429, X42, X425 and X441 subassemblies had pins designed to be 75% but had as fabricated smear densities of 72%. Similarly, the TREAT M-5,6 and 7 pins had 72% smear densities [95]. Therefore, there is good experience with fuel behavior at lower smear densities.</p>
<p>3.2 Fuel Constituent Migration</p>	<p>The models employed for the fuel performance evaluation over time(BISON, MFUEL) include fuel constituent redistribution, porosity dependent thermal conductivity, swelling, thermal and irradiation creep, cladding wastage resulting from FCCI (or eutectic formations at the fuel cladding interface), external corrosion and buildup of solid fission product over time.</p>
<p>3.3 Fuel Properties</p>	<p>With the exception of beyond design basis transients (unprotected reactivity insertion caused by the accidental withdrawal of the highest worth control rod at the beginning of life, or unprotected station blackout, the fuel cladding interface temperatures during the operation of ARC-100 remain below the temperature at which eutectic formation occur. Even in those unprotected events the duration of time during which the interface temperatures exceed the threshold for eutectic formation is short, and the resulting amount if eutectic is less than of the cladding thickness. The effect on thermal conductivity of the fuel porosity over time I accounted for in the fuel performance codes (BISON and MFUEL)</p>
<p>3.4 Cladding Integrity and Barrier Degradation</p>	<p>Both fuel performance codes (BISON and MFUEL) employ first principle based, but ultimately empirically derived correlations that predict wastage in the cladding resulting from eutectic formation, fission product interaction (interdiffusion) and Na induced corrosion of the cladding. Both codes have been validated against the results of post irradiation examination of pins from EBRII and FFTF and shown to be sufficiently accurate in their predictions to assure confidence in their use, provided temperatures are conservatively established. For past fuel qualifications [14] temperatures of the fuel and cladding have employed considerations of uncertainties at the 2σ level. ARC 100 is also using that approach fuel qualification The differences in temperature between the fuel centerline and the cladding, is significantly lower in the ARC 100 fuel than that in the EBRII and FFTF fuel. The FCCI is a function of burnup, temperature, and time at temperature. The lower fuel and cladding temperatures, and specifically lower fuel-cladding delta-T for the ARC 100 fuel is an advantage over the EBR II and FFTF fuels, as it results in decreased the diffusion of fission product and reduced reaction rate. However, the much longer</p>

time to achieve comparable burnup offsets this advantage. The longer ARC 100 fuel ( vs 91cm in FFTF and 35cm in EBRII) causes the region of high cladding temperature (near the top of the fuel column) to be at a location distant from the region of peak burnup (and fluence) where the fission product concentration is highest, and this is another advantage as peak thermal creep and peak irradiation creep occur in different region of the fuel. On the other hand, the colder fuel (with respect to EBR II and FFTF) makes it less pliant, and as the solid fission product accumulate over time and fill some of the pores of the fuel, the fuel cladding mechanical interaction with the pliant cladding is greater for the ARC 100 fuel than in EBR II an FFTF. In addition to the pressure developed in the gas plenum contributes a hoop strain in a manner directly proportional to the wastage created in the cladding at different locations.

<p>3.5 Fission Product Behavior and Source Term</p>	<p>Reference [15] provides the analysis of a severe accident resulting in failure of all of the pins in the ARC 100. The radiological source terms that are released to the environment are those provided by referenced ( 83) in this section of the NUREG/CR 7305. The overall approach used in the analysis is the same as documented in reference [16]. The results of this analysis are dependent on the functional containment designed for the ARC 100 and its leakage</p> <p style="padding-left: 40px;">the height and volume of the sodium pool, the , volume and configuration of the cover gas region above the pool, and the design of the penetrations of the reactor top enclosure which are assumed to leak at ten times the value measured at FFTF). The results are presented in the chart below and indicate that the ARC-0 100 can be designed so that no evacuation is required beyond the site boundary if the latter is at least 100 meters from the functional containment boundary.</p>
<p>3.6 Ducting Integrity</p>	<p>ARC-100 employs HT9 for the fuel assembly duct material . The thickness of the duct is 3 mm. The major issue with the ducting of the ARC100 is the behavior of the HT9 material at fluences beyond those for which swelling data is available. The peak fluence for the ARC 100 duct is approximately</p> <p style="text-align: right;">the behavior of the duct material is expected to remain the same as that measured at FFTF. Afterward the same</p>



	<p>surveillance program proposed for the fuel pins will encompass the duct material. Deformation of the ductwork under loading conditions dependent on the chose core support design are addressed in the section on Coolability.</p>
<p>3.7 Coolability</p>	<p>Coolability of the ARC 100 core is established by design which meets the limits described above though year 16 of operation and subsequent surveillance. The maintenance of coilability is further assured by periodic measurements (using the In vessel transfer machine-IVTM) of the pull-out force required to extract fuel assemblies form the core. Excessive pull-out force is indicative of potentially excessive deformations primarily ducting). In addition, a predictive tool that a relies on comparison of real time measurements of power reactivity decrement curves or the coefficient B of the quasistatic reactivity equilibrium equation (Equation E.1) against precalculated shapes or that are a function of deformations, will be used to alert the operator of possible abnormalities in the core . Finally, an R&amp;D program on the effects of flow blockage ( internally or externally caused) has progress sufficiently to suggest that if such a blockage in or of an assembly were to occur, the damage caused to the assembly would not propagate to adjacent assemblies to the extent of causing additional blockage [19].</p>
<p>3.8 Transients</p>	<p>The ARC 100 fuel qualification uses the same data referenced in the NUREG/CR 7305 to establish limits for transients, and the same fuel performance codes (BISON and MFUEL) to assess the transient fuel behavior. It is noted that MFUEL interactively uses input directly from SAS4A/SASSYS-1 code [17], which is the code used for the deterministic safety analysis and simulates the behavior of the overall primary system over time for the postulated transient, whereas BISON uses information indirectly provided by SAS4A to verify the inputs for its analysis. Predictions from the two codes are in general in close agreement, which is a expected since fundamentally both codes rely on the same correlations to simulate the effect of the phenomena affecting fuel performance.</p>
<p>4.1 Target Behavior for Modeling Purposes</p>	<p>The fuel behavior modeled for the ARC 100 fuel is the same as that described in NUREG/CR 7305 but recognizes that the length of the ARC 100 planned irradiation of 18 equivalent full power years introduces significant uncertainty in the modeling of the fuel behavior in the time period between 16 and 20 calendar year , for which empirical data underpinning some of h phenomena (e.g., swelling, combined thermal and irradiation creep) is not available . Furthermore, the potential effect of different manufacturing methods on the behavior of the fuel in radial and axial expansion is recognized and avoided by employment of the same manufacturing method (casting) used in EBR II and FFTF metal fuel manufacturing.</p>
<p>4.2 Fuel Performance modeling 4.2.1 Introduction and 4.2.2 Problem Definition</p>	<p>ARC 100 utilizes BISON as the primary computer code for fuel performance assessment, and MFUEL as the computer code to check/confirm the results obtained from BISON. A simple correlation utilizing an Arrhenius equation developed in Reference [20] modified to account for the percentage of Lanthanides present as a function of burnup and temperature of the fuel cladding interface only is used to check the appropriateness of the thickness of the FCCI layer and for sensitivity analysis of the effects of varying interface temperature on the layer. The correlations for thermal and irradiation creep for the fuel and the cladding provided in Reference [21] are similarly used for sensitivity studies on the effect of temperatures and gas plenum pressure on the resulting strain and cumulative damage functions. The sensitivity studies are used to guide the design of the fuel and are used as guidance to the parameters in the detailed performance models .</p>

**ARC20-FQ-003 White Paper on ARC-100 Fuel Qualification Program**

<p>4.2.3 Nuclear Core Environment Models</p>	<p>The local conditions of fuel and cladding as modeled for the ARC 100 include neutronic (neutron flux, burnup, fluence (above 0.1 MeV) thermohydraulic (temperature and pressure) and physical (porosity , conductivity ). The fuel performance code BISON and MFUEL develop the local conditions in different ways. BISON relies on the “externally provided” radial and axial distribution of the neutron flux information developed from the ANL neutronic suite of codes, and in particular the fluence (&gt;0.1MeV), and the ANL thermohydraulic steady state (SE2) and transient analyses (SAS4A/SASSYS-1 [17]) codes information on the local temperatures, pressures and flow rates. MFUEL is coupled SAS4A/SASSYS-1 therefore it derives that information directly from SAS4A/SASSYS-1., e.g. MFUEL receives power per axial node as an input from SAS. Then to compute linear heat rate, it divides power with the current axial height.</p>
<p>4.2.4 Pressure boundary conditions</p>	<p>For the ARC -100 fuel the performance codes account for the time varying volume of the gas plenum , caused by the bond sodium not logged into the pores of the expanding fuel being forced into the plenum by the fuel radial expansion, the fuel axial expansion, the subsequent filling of pores by solid fission products and the different thermal expansion of the fuel, the cladding and the bond sodium. The moles of fission gas products migrating to the gas plenum and their temperature and the flow of sodium outside the pins are used to calculate the pressure within the pin as a function of time. BISON uses the ideal gas law and MFUEL the VanderWall’s equation to calculate the pressure.</p>
<p>4.2.5 U-xPu-yZr Specific models</p>	<p>ARC 100 fuel begins its irradiation as U-10Zr, and as irradiation progresses through 18 EPFY Pu replaces approximately half the U235 and the average percent by weight of Pu in the fuel is 4.1% , with the peak burnup pins having about 7 wt % of Pu present. Both BISON and MFUEL codes utilize the thermal, mechanical and thermal and irradiation strain rates of reference [21].</p>
<p>4.2.6 Cladding Specific Models</p>	<p>ARC-100 employs HT9 cladding material. This material exhibits very low swelling behavior until fluences of <math>4 \times 10^{23} \text{ n/cm}^2</math> (~208 dpa). However, the behavior at greater fluences is not underpinned by empirical data.</p> <p style="text-align: center;">The uncertainty in the swelling behavior of HT(beyond 200 dpa is one of the reasons for testing the ARC100 fuel when approaching and exceeding 16 years of operation at full power. It is noted the conversion factor from fluence to dpa varies with the hardness of the neutron spectrum and the material being irradiated For a hard spectrum like that of EBR II and the slightly softer spectrum of FFTF, the typical conversion factor is <math>5 \text{ dpa}/10^{22} \text{ n/cm}^2</math>. ARC-100 has a softer spectrum that FFTF, and the conversion factor is closer to <math>4.1 \text{ dpa}/10^{22} \text{ n/cm}^2</math>.</p>
<p>4.3 Discussion</p>	<p>As pointed out in NUREG/CR 7305 the absence of constituent redistribution and the relative uncertainty of the predicted growth and therefore impact of FCCY layers occurring at higher burnups contributes to uncertainty in the predictions of the fuel performance codes. To some extent the proposed program of testing the ARC-100 fuel: (1) early in its irradiation history to confirm the predictions of the models of the fuel behavior under the phenomena that manifest early in its life (radial and axial expansion, porosity formation and interlinking and cracking, and gas evolution, and (2) much later when high irradiation effect (solid fission product filling of porosity and swelling , FCCI layers) effects of irradiation on creep properties and strains may be limiting, will contribute to the goal of better quantifying the uncertainties of the fuel performance models.</p>

**ARC20-FQ-003 White Paper on ARC-100 Fuel Qualification Program**

<p>5 Conclusions</p>	<p>As explained above the ARC100 fuel deviates from the parameters which NUREG 7305 has identified as being reliable predictable by the fuel performance codes. Until the 16<sup>th</sup> year of operation. The ARC 100 fuel meets the parameters, with the exception of peak burnup being slightly in excess of the 10% . This is confirmed by the fuel performance codes which predict peak thermal and irradiation creep strains within the established limits of 1 and 2 percent respectively a total strain within the 2% limit, and CDFs well below 0.05 at steady state.</p> <p style="text-align: center;">Periodic testing of fuel extracted form the core will determine the actual fuel behavior (vs. predicted) and provide the information needed to determine whether the irradiation can continue or terminate. As FCCI is a life limiting phenomenon , a limited number of pins in the assemblies where the peak burnup will occur at the later stages of irradiation, could be modified by having a protective layer between the fuel and the cladding which has been demonstrated to be effective in suppressing the FCCI in out of core testing. If found to be equally effective under long term irradiation, future fuel pin fabrication would include such layer , and contribute to advanced metallic fuel qualification.</p>
<p>Appendix A Retrospective of NURE_2246 Application to U-ZR</p>	<p>The reader is referred to comments below and the cARC100 fuel qualification approach conformance matrix with NUREG 2246, which is also part of this White Paper, i.e., Table 2-1.</p>
<p>A.1 Comments on the Process of Applying the NUREG and Suggestions of Updates</p>	<p>The comment on “Safety Case” being vague or undefined is noted. However, ARC Clean Technology fuel Qualification program implicitly addresses the fission product retention by ensuring that fuel failures would be very limited (operational limits is planned to be set at no more than 0.1%), assessing the impact of postulated severe accident onsite and the environment and showing that impact to be limited and likely not requiring evacuation beyond the site boundary. All other comments are noted.</p>
<p>A-2 Comments specific to U-Zr Fuel</p>	<p>While ARC-100 has established a limit of 2% on cladding total strain, 1% of on peak thermal creep strain and 2% on peak irradiation creep strain, we concur with the comment that the empirical data supports an increase of these vales to 2-3%. We note that such an increase would mean that the ARC-100 would meet the increased limits throughout its planned 18 EFPY. In addition, we also comment that the steady state cumulative damage function “traditional limit of 0.0 can could be significantly increased. Annex A to this compliance matrix provides justification for the increase. ARC also agrees with the other comments, which can be summarized as “limits should be established based on the specific design of the systems and fuel”. For instance, given the normal spacing between pins of maintained by the diameter of the ARC-100 spacing wire, and a radial deformation (strain of 3%) for the ARC100 pin diameter of , would mean a 60 % reduction in flow area between two adjacent pins, and the pins would still be cooled. However, a design that would employ a 0.5 mm diameter spacing wise would have flow potentially blocked in the area where the deformation occurs.</p> <p>In the preceding we have identified where The ARC 100 fuel design’s main concerns are, and what the plan is to address them.</p>

### 3 FUEL DESIGN CRITERIA

The ARC-100 Fuel Qualification Program will consist of all the steps shown in Figure 3.1. Each of those steps is defined in detail in the following sections. The timetable during which each of the steps will occur is presented in Appendix A

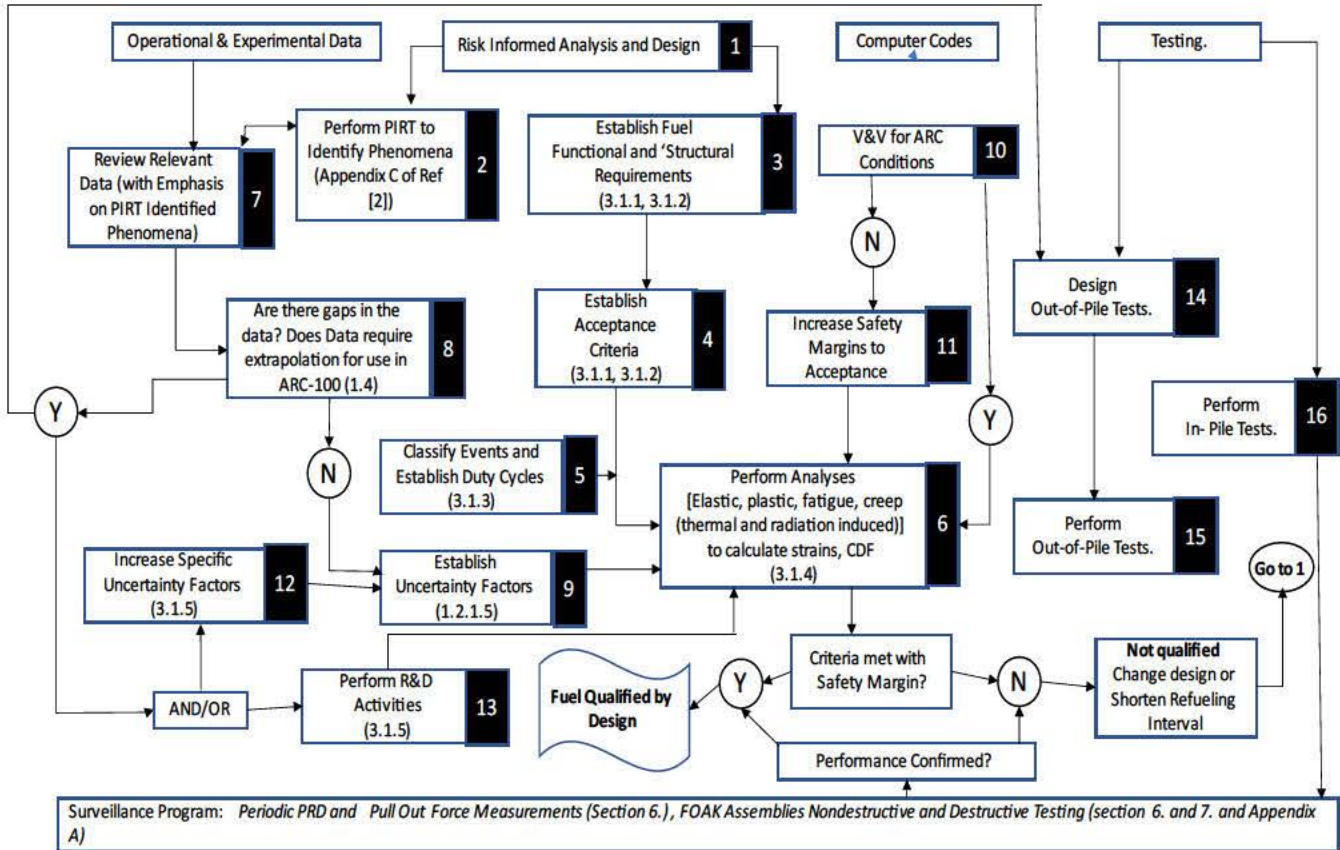


Figure 3.1 Fuel Qualification Program Elements

The numbers in Figure 3.1 are not intended to be used as an indication of the chronological order in which the fuel qualification activities are and will be conducted, but as a convenient reference to the activities, several of which are concurrent and the result of some of which may cause re-performance of certain other activities.

With regard to testing, there is a difference between out of pile and in pile tests. For the former (No. 14), it is necessary to design the tests that will be performed (No. 15). The prime motivator for conducting out of pile tests is to provide information on gaps found in the data used to the fuel design (Nos. 7 and 8) For instance the possible tests to obtain accelerated swelling and other mechanical properties data for the cladding material, by dual heavy ion irradiation will requires to design the manner in which testing will be conducted (test apparatus, tests samples etc.). Similarly tests that may be done to determine the reaction of fission products (lanthanides) with the cladding and the effect of introducing a protective layer .between the fuel and the cladding would require the design of the testing apparatus and the actual tests performance. For the in-pile tests, at present the only

available means to conduct the tests is by periodically extracting fuel assemblies irradiated in the first of a kind (FOAK) ARC 100 reactor (no. 16). Therefore, designing the tests is not necessary.

The results of out of pile tests may confirm the values of the properties assumed and used in the design of the fuel; or produce values which are at variance with some of them. If the latter, a re-examination of the design will be necessary to determine its acceptability (No. 6). If not acceptable, design changes will be required, and step No. 6 repeated until the revised design is acceptable. It is possible that, in order to revise the design, steps Nos 1, 3, 4 and 9 will have to be repeated prior to repeating Step 6.

The results of the in-pile tests (i.e., the results of the non-destructive and destructive tests conducted on assemblies extracted in a FOAK at the times indicated in Section 4 and Appendix A) will either confirm the fuel the performance is as predicted (i.e., the fuel qualified initially by design needs no modification) or indicate that it is not. If the latter, either the fuel will have to be modified (i.e., redesigned) or the refueling interval altered (shortened). Which of the two outcomes will occur depends on the timing at which the deviation from the expected performance occurs.

R&D activities may include the out of pile activities, but also include activities such as the pre-calculated Power Reactivity Decrement shapes as a function of core deformations, described in Section 6. The comparison of measure PRD to the precalculated shapes will provide indication of core deformations, anticipate potential for unacceptable deformations and call for either increased surveillance or immediate action to preclude them. The surveillance program is one that uses the precalculated and measured PRD, as well as periodic measurements of pull-out forces, as an indication of core deformations, and for a FOAK, the periodic extraction of fuel assemblies for both nondestructive and destructive tests.

Note that the surveillance program supplements the online monitoring program provided by the Reactivity Meter and the real time measurements of temperatures and flows at the exist of the individual fuel assemblies, both of which provide real time indication of any anomaly occurring in the core as a whole or in individual assemblies.

### 3.1 Analysis and Design of Fuel Elements (pins)

#### *Establishment of Design Basis*

The ARC-100 fuel assemblies are to be designed to perform their function in a safe and reliable manner over their design life of 20 years. The functional and operational requirements and design criteria to achieve this objective are described in the following subsections. Of course, in order to satisfy these requirements, other “derived” requirements are to be satisfied as well. Table 3-1 provides the list of requirements to be directly or indirectly satisfied by the fuel design and operation.

#### *Functional requirements*

The primary functions of the fuel assemblies in the ARC-100 are to provide, protect and position the nuclear fuel to produce heat for the reactor heat transport system. To do so safely and reliably, two design features are used: the fuel pin cladding acts as the primary fission product barrier and the hexagonal duct helps to protect the reactivity control system and the primary cooling system both during normal operation and during off-normal events. The design criteria and requirements that

have been established for the fuel ensure that these functions are fulfilled in accordance with the requirements of 10CFR50 Appendix A, 10CFR50.43(e)(1)(i), and guidance of NUREG 2246.

The principal requirements are:

- a. The fuel pin is designed so that statistically the number of fuel pin breaches during normal and off normal reactor operation (including unlikely events) is limited to a percentage of the pins which would not challenge the safe operations and performance goals of the ARC-100. Even though the reactor could continue to safely operate with a percentage approaching 1% (Table 1-5 indicates that operation can continue with failed fuel), in practice, extensive fuel failure (herein defined as more than very few pins) can result in increased personnel radiation exposures, difficulties in maintenance and repair and problems at decommissioning. Therefore, the design requirement is to ensure that no more than 0.1% of the fuel pins (21 pins in 21,433 driver pins) will fail during one core loading. The reason for the selection of 0.1% failed fuel as the limit to fulfill the regulations in 10CFR50.34(a)(1)(ii)(D), 10CFR52.47(a)(2)(iv) and 10CFR52.79(a)(1)(vi) is explained in Section 6. This reliability is to be demonstrated first through an analytical performance assessment described in Sections 3.3, following by a fuel surveillance program, briefly described at the end of Section 7 and in Appendix A.

The analytical performance acceptance criteria (i.e., what limits the calculations must meet) are shown in Table 3-1. These design criteria:

- Prevent stress-rupture of the cladding, utilizing materials for fuel (U-10 Zr) and clad (HT-9) which ensure the peak cladding temperature remains below the minimum fuel/cladding eutectic temperature for steady state operation, the peak fuel and cladding temperatures remain below the level at which substantial fuel cladding chemical interaction would occur for steady state operations, and a burnup limit at which point creep damage caused by fuel and fission product induced stress does not compromise cladding integrity. For this purpose, limits in steady state peak fuel and cladding  $2\sigma$  temperatures, have been established to be  $TBD^{\circ}C$  and  $600^{\circ}C$  respectively. This is consistent with past practices in fuel qualification which have resulted in operations with essentially no failures. It is noted that for deterministic safety analyses these temperatures have also been calculated with a  $3\sigma$  uncertainty.
  - The design and fabrication specifications eliminate manufacturing defects sufficiently to cause reduced reliability. This is evaluated initially by including assumptions regarding the extent of manufacturing defect (e.g., thinner than specified clad, scratches etc.) in the analytical method and calculations employed and then demonstrating it in the fuel surveillance program.
- b. The fuel pin and the assembly are designed so that their coolability is maintained during normal operation and all off normal events. During normal operation, anticipated events and unlikely events (DBEs), a low probability of pin failure assures that the fuel pin remains intact, and therefore the coolable pin bundle geometry will be maintained. For this purpose, limits have been established on:
    - Fuel/cladding eutectic liquid formation - maintain peak cladding temperature to less than  $715^{\circ}C$
    - Fuel melting – no melting
    - Maximum cladding stress checked against 150 MPa and limited to  $\frac{1}{2}$  of the yield strength at temperature

- Maximum cladding strain at 2%

For very low probability, extremely unlikely events [ Beyond Design basis Events called Design Extension Conditions (DECs)] more extensive pin failures could be justified. But for the ARC-100 those events are obviated by the limits imposed for no sodium boiling and maximum cladding penetration to control eutectic liquid formation to less than 5%.

**Table 3-1 Design Criteria for ARC-100 Fuel**

Design Criteria	Design Basis Events			
	Normal Operation	AOOs	Design Basis (unlikely)Events	Extremely Unlikely Events (DECs)
3.1.1	$\epsilon_{Th} < 1\%$ (see more details in <i>Criterion 3.1.1</i> )		N/A	N/A
3.1.2	$CDF_N < 0.05$ (see Annex A)	$CDF_A < 0.1$ see <i>criterion 3.1.7</i>		
3.1.3	No Fuel Melting			
3.1.4	No Eutectic liquefaction at the fuel cladding interface (Peak Clad $T_{Max} < 650^\circ C$ )  Limited Lanthanide enhanced FCCI (Peak Fuel $2\sigma T_{Max} < TBD^\circ C$ , Peak Clad $2\sigma T_{Max} < 600^\circ C$ )	N/A	N/A	N/A
3.1.5	$\sigma_H < 150MPa$ (see note)	N/A	N/A	N/A
3.1.6	N/A	$M \sum_{j=1}^{N_j} (\Delta r_{A_j} + \Delta r_U + \Delta r_{EU}) < 5\% \text{ of wall thickness}^{Note1}$		
3.1.7	N/A	$M \sum_{j=1}^{N_j} (CDF_{A_j}) + CDF_U < 0.1$		N/A
3.1.8	N/A	$M \sum_{j=1}^{N_j} (\epsilon_{A_j}) + \epsilon_U < 1\%$		N/A
3.1.9	Core remains coolable			
Note	The 150 MPa limit has been used in past fuel qualification. However, the properties of the material are very dependent on temperature and a more appropriate limit is ½ of the yield strength at temperature			

In Table 3-1 the various symbols are defined below, and the design criteria are explained in more detail hereinafter .

$\epsilon_{Th}$  is the thermal component of the plastic hoop strain during normal operation

$CDF_x$  is the Cumulative Damage Function during: N- normal operation; A - all M anticipated events and all N occurrences; U - during the single most damaging unlikely event.

$\sigma_H$  is the radially averaged primary hoop stress

$\Delta r_x$  is the cladding eutectic penetration for: A – all anticipated events; U – the single most damaging unlikely event; and EU – the extremely unlikely event.

$\epsilon_x$  is the total plastic hoop strain for : A – all anticipate occurrences; and U – for the single most damaging unlikely event

$M N_j$

$\Sigma$  signifies the summation of the penetration, CDFs and plastic hoop strains over M anticipated  $l=1$  events and N occurrences.

Note 1: *The reduction in cladding wall thickness must also considers fabrication imperfection , nickel/carbon depletion and fission product migration induced brittle layer formations, which are not directly determined by the thermo-hydraulic code, SAS4A/SASSYS-1, but are included when assessing the radial averaged primary hoop stress and plastic hoop strain*

*Criterion 3.1.1 During steady state (normal) operation, the thermal component of the plastic strain for HT9 cladding shall be less than 1%.*

Permanent strain consists of a volumetric swelling strain and in-reactor thermal creep and irradiation creep strain. Figure 3.1 shows data for HT9 for both out of reactor and in reactor pressurized tube tests [25, 26]. The lowest observed failure strain is 2%, so 1% is quite conservative. In addition, very few breaches have occurred in irradiated metallic fuel. Two breaches (out of fifteen ) occurred in U-10Zr/HT9 pins from EBR II assembly X447A at 10at% burnup. These fifteen pins were operated at a peak cladding temperature of 644°C. Measurement of the maximum strain in the un-failed pins reached 2% [27] which is above the limit established at 1%. For the long fuel section of the ARC-100, the cladding peak temperature occurs at or near the top of the fuel, whereas the peak irradiation creep occurs near the midpoint of the fuel. Although there is interaction between thermal and irradiation creep effects, limits are separately established for each , with the limit for thermal creep strain being 1% and the limit for irradiation creep 2%, and total permanent strain being 2%

Table 5-9 provides the result of the simulation for the ARC-100 peak pin during irradiation for 5256 days (16 EFPY) and 6570 (days)



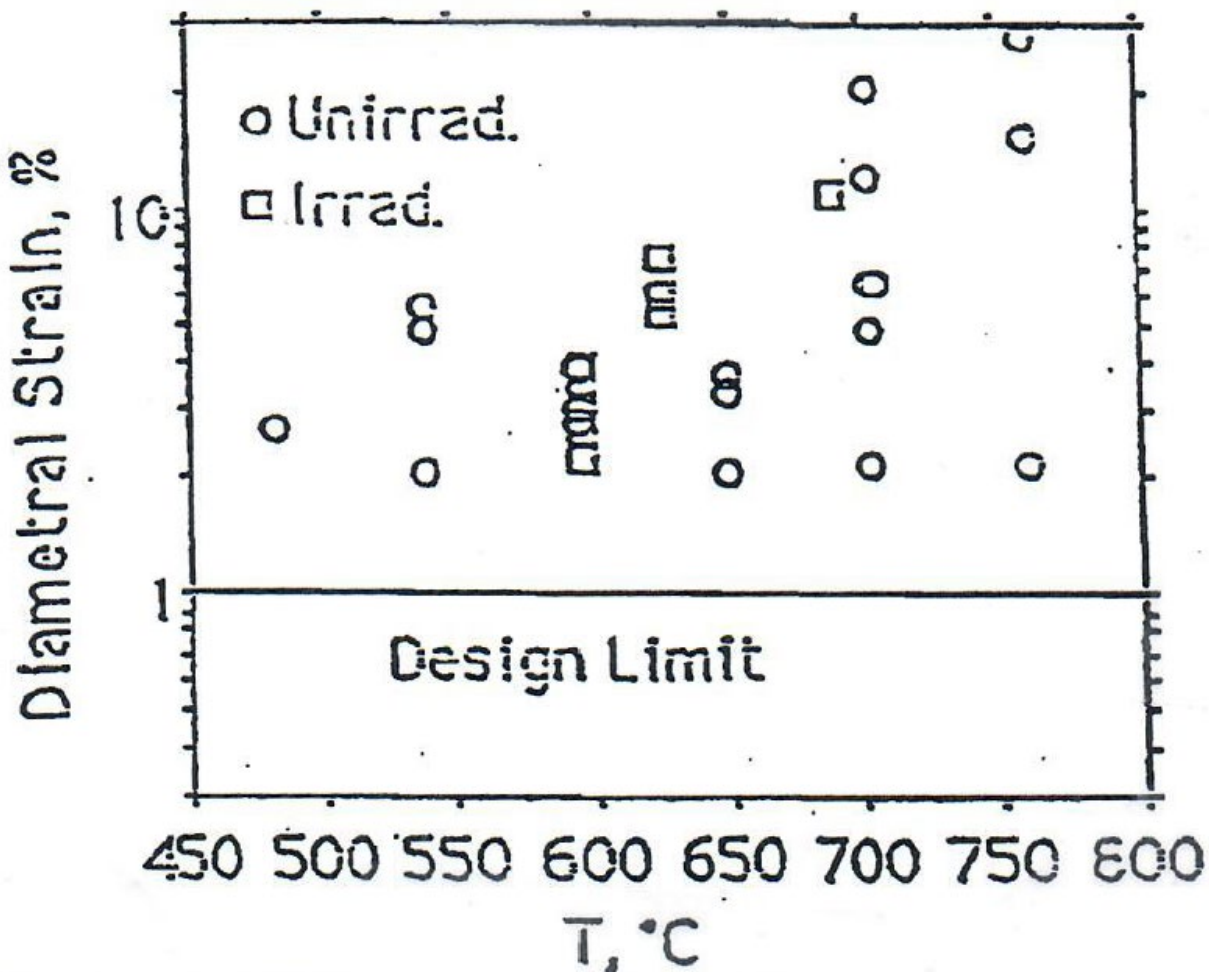


Figure 3.2 Summary of HT9 Pressurized Tube Failure Strain Data

*Criterion 3.1.2 During steady state operation, the cumulative damage function for HT9 cladding shall be limited to 0.05*

This requirement separates the steady state component of the CDF from the transient component. The steady state plus all of accumulated CDF for all transients (addressed by requirement 3.1.7) should of course be less than 1.0 less any uncertainty one wishes to associate with the CDF. Since in 3.1.7 the accumulated CDF for all transients is 0.1, the sum of the steady state and transient is less than 1, less any uncertainty, even if all transient were to occur at the end of life.

The common fuel failure mode of a metallic fuel is the cladding rupture with the stress largely provided by gaseous fission products along with the cladding wastage from the fuel and cladding chemical interaction (FCCI), and the cladding inner wall temperature and burnup are the major factors to determine the fuel failure mode. The cladding rupture can be predicted using the Cumulative Damage Function (CDF), which is defined by

(Eq. 3.1) 
$$CDF = \int_0^t \frac{dt}{t_r}$$

where  $t_r$  indicates the time to rupture, and the variable  $t$  is the irradiation time of a fuel. Unit CDF

value indicates that the fuel is irradiated till the fuel fails. The stress rupture has a different behavior between the steady-state operation condition and transient conditions. In the steady-state condition, the stress rupture occurs by the accumulation of temperature and stress creep strain, and the CDF in a steady-state condition was calculated using the time-to-rupture correlation of HT-9 cladding [14], where:

$$(Eq.3.2) \quad \log_{10} t_r = A + \frac{B}{T} + \frac{C}{T} \log_{10} \sigma$$

$\sigma$  = hoop stress, MPa,  $T$  = cladding temperature, °K.

The correlation coefficients (A, B, and C) are given in reference [14]. The CDF was estimated in a normal operation condition by assuming all gaseous fission products are released to the gas plenum at the pin which has the peak  $2\sigma$  cladding inner wall temperature. For steady state, reference [5] determined from statistical analysis of the data of time to rupture correlation used in the CDF formulation, that the logarithm (base10) of the CDF is distributed normally as shown in Annex A. Based on the total number of pins in the ARC-100 reactor, a goal to have no more than 1 pin fail out of the 21,483 pins, would justify use of a CDF =0.19. Therefore, the limit of 0.05 is very conservative.

Table 5.3-2 shows the resulting CDF, which is small. Table 5.3-2 indicates that the ARC-100 fuel has sufficient margin to fuel rupture in normal operating conditions. However, additional fuel performance calculations at various transients are required to ensure the fuel integrity in off-normal conditions.

For the transients, ARC plans to have ANL compute the CDFs using the stress-rupture correlations they have developed from the test data developed for the HT9. The CDF methodology has been used by ANL to qualify fuel for use in EBR II, and has been validated at ORNL [28] comparison of results of variable load and temperature tests (albeit for austenitic stainless steel not HT9 to predictions based on results of constant load and temperature test and the CDF law which basically assumes that creep damage is linearly additive, so that the damage over a given time interval,  $\Delta t$ , is proportional to the ratio of that time interval to the total time,  $t_r$ , that would cause failure at the instantaneous stress and temperature levels. Reference 28 found that a CDF (damage summation) of 0.65 was sufficient to prove a 95 % confidence that the observed life in variable load and temperature tests would be equal to or greater than the CDF predicted life.

*Criterion 3.1.3 During steady state operations, AOOs and all Unlikely Events (DBEs) the power in the hottest fuel pins shall be less than the minimum values for incipient bulk fuel melting. The redistribution of fuel alloying constituents shall be considered in satisfying this criterion.*

This criterion establishes sufficient margin approaching the over-power reactor trip points so that incipient melting is precluded. However, this does not mean that fuel melting in itself is detrimental. The melting point of ARC-100 fuel, is below the melting point of the cladding. Melt fuel remains within the cladding introduces a strong negative reactivity, which helps counteract the overpower condition.

The relatively benign effect of bulk melting was shown in EBR II Mark-IA where fuel pins were fabricated with bond sodium only in the lower part of the fuel region. The absence of the bond led to extensive melting, and the molten fuel simply relocated to close the gap and froze in place without

failing the clad. [29,30]. Only a small area of eutectic interaction was noted with a maximum wall penetration of 10% thickness.

This criterion, when met, will ensure no melting for power up to the 15% overpower trip set point. It also avoids the need to consider the consequences of molten fuel relocation on reactivity and the possibility that molten fuel may relocate in the coolant channels, thereby affecting core coolability. It also eliminates the need to consider the effect of molten fuel on the cladding failure analysis.

*Criterion 3.1.4 Within the bounds of reactor operation and maneuvering the power to flow ratio and the power to the hottest pin shall be less than the minimum values for macroscopic eutectic liquefaction at the fuel clad interface.*

Exceeding the eutectic liquefaction temperature during normal operation is not acceptable as it can lead to failures which would violate the first functional requirement in Section 3.1. It is however acceptable to exceed this temperature for short times during off-normal operation. Formation of a eutectic at the fuel-clad interface (and the data supporting the ability to tolerate short times beyond the eutectic) liquification temperature without excessively damaging the clad is presented in Appendix B

For the HT9 material used for the cladding (and the hexagonal ducts) the threshold temperature below which no macroscopic eutectic formation has ever been observed is 650°C. For temperatures above 715° but less than 1080°C, the Arrhenius equation given in Appendix B is used to predict the clad penetration depth, which depends on temperature and time at temperature. Above 1080°C the eutectic formation is rapid, and temperatures above this level must be avoided.

In addition, it is required that the lanthanide enhanced FCCI be minimized so that no more than an amount that when added to other wastage (from manufacturing imperfections and corrosion) causes 25-30% of the thickness of the cladding to be affected. In practice this means that the lanthanides caused by FCCI should be limited to 25% of the cladding thickness. For the ARC-100 clad thickness of 0.5 mm, this limits the peak  $2\sigma$  temperature of the fuel centerline and the clad inner wall during normal operation to 650°C and 605°C respectively. For the fuel cladding interface temperature limit refer to Table 5.3-1, which shows the calculated value of the depth of the FCCI layer for the 16 and 18 equivalent full power years at this temperature.

*Criterion 3.1.5 During normal operation the gas plenum pressure shall be less than that which would cause a peak, radially averaged hoop stress in the cladding of 150MPa in the hottest pin.*

The purpose of this limit is to preclude unstable plastic deformation. The value of 150MPa has been used in past fuel qualification and is therefore adopted as an acceptable value. However, if this limit is exceeded, it is recognized that one would meet the requirement to preclude unstable plastic deformation by keeping primary stresses below 50% of the yield strength. The HT9 yield strength at high temperature depends on the strain rate at which the tensile test is performed and the irradiation history. The primary loading due to internal gas pressure is most damaging since it can lead to plastic instability. Stresses caused by secondary loads (e.g., thermal stresses or FCMI) do not lead to instability since the plastic deformation relieves the stresses.

The value of 150Mpa limit for the hoop stress caused by the gas plenum pressure is derived from the level below which burst failures do not occur in pressurized cladding tubes. This was used to

argue that plastic instability would not occur if the cladding (tube) hoop stress remains below the high stress branch of the biaxial stress rupture curve. At the present stage of design, the conservatively calculated maximum value of the ARC-100 radially averaged hoop stress is less than 50% of yield strength at temperature

*Criterion 3.1.6 During all anticipated events, the single most damaging Unlikely Event (the DBE) and the Extremely Unlikely Event (DEC), the cumulative eutectic penetration of HT9 cladding shall be less than 5% of the wall thickness.*

This criterion implicitly includes the damage done to the cladding by Criteria 7 and 8. Criterion 7 includes the damage caused by cladding wastage (which includes eutectic formation and other FCCI) in the CDF for the anticipated occurrences and the DBE, and Criterion 8 includes the cumulative plastic strain for the same events. The purpose of these criteria is to limit the quantity of liquid formation, including that formed in DECs so that the clad would remain intact even during DEC. No transient CDF calculations have been done to date, but since the temperatures during anticipated occurrences and DBEs do not cause any eutectic penetrations and only limited lanthanides induced FCCI, and the amount of penetration calculated for the worst DEC is less than 1%, the ARC-100 is expected to meet this criterion.

*Criterion 3.1.7 During all Anticipated Events and the single most damaging Unlikely Event (DBE), the cumulative transient CDF for the HT9 cladding shall be less than 0.1. The effect of steady state and transient wastage due to metallurgical interaction between the fuel and the cladding shall be accounted for by assuming that any interaction zones are without strength.*

This required CDF analysis has not been done and will be performed by ANL/INL. The transient CDF correlation that ANL will utilize for the HT 9 is based on the results of the Westinghouse Hanford Company Fuel Cladding Transient Tester (FCTT) tests [31]. In these tests cladding tubes cut from irradiated fuel pins were pressurized and subjected to transient heating at various temperature ramp rates. The measured failure temperatures were used to estimate time-to rupture correlations as a function of stress and temperature. Transient failure strains were also measured [31]. For HT9 the data for time to rupture is provided in Reference [32].

The basis for the Transient CDF value of 0.1 is a statistical analysis of the FCTT data where it was shown that a transient CDF less than 0.103 is sufficient to assure with 95% confidence that the failure probability will be less than 1/3000. [For the ARC-100 reactor with 21,483 pin, satisfying a CDF of 0.1 means that at most 7 pins could fail, which is significantly less than the operational limit of 0.1% (21-22 pins).

*Criterion 3.1.8 During all Anticipated Events and the single most damaging Unlikely Event (DBE), the cumulative thermal component of the plastic diametral strain for the HT9 cladding shall be less than 1%. The effect of steady state and transient wastage due to metallurgical interaction between the fuel and the cladding shall be accounted for by assuming that any interaction zones are without strength.*

Just as above, this analysis has not been done and will be performed by ANL/INL. It is noted that the HT9 transient cladding deformation model that will be used to analyze the response of the ARC-100

fuel pin, has also been validated using the results of the FCTT tests. Those tests indicated that a strain-to failure of 6% would predict the failure temperature measured in the tests. This suggests that a design requirement of 1% is quite conservative to preclude cladding failure during accident conditions.

*Criterion 3.1.9 For all DBEs including DEC's, the core shall remain coolable.*

From an overall core standpoint, core coolability is challenged if blockages occur. From the fuel standpoint this equates to the cladding not melting or experiencing such large deformations that coolant channels are blocked. Meeting Criterion 1 assures that the clad will not melt, because melting is impossible so long as the sodium does not boil (the melting temperature HT9 is ~ 1400 °C). Blockages, however unlikely, could occur due to debris external to the core blocking the entrance. The latter is not considered part of the fuel design and qualification, but it is addressed by designing the inlet and outlets of the fuel in manner that blockage is extremely unlikely. Also, Criterion 3 assures that there will be no bulk fuel melting. For extremely unlikely events this and criterion 6 are the only functional requirement. An R&D program for the ARC100 is developing means to determine analytically whether a large failure of the cladding of one assembly, resulting from an assumed full blockage of flow to that assembly, would propagate to adjacent assemblies. This work is in progress and definitive results will not be available for some time. However initial results indicate that propagation would be limited and damage, if any to adjacent assemblies would be relatively minor [19].

Absent events such as full flow blockage, both in-pile and out of pile experiments have indicated that fuel pin cladding breaches are of the “pinhole” type, and therefore benign with respect to blockage formation [37, 38].

### **3.2 Analysis and Design of Fuel Assembly (Ductwork and Fittings)**

The functional requirements for the assemblies are very important because whole core phenomena associated with deformation of the assemblies have been the primary problems in sodium cooled pool type fast reactors. For the assembly as a whole, the functional requirements are:

- Provide support and protection for the fuel pin bundle and other components of the assembly.
- Provide a controlled path for the primary coolant.
- Provide a suitable structural unit that can be easily moved in and out of the reactor core by the in vessel transfer machine and in and out of the vessel by the fuel handling machine.
- Interact with the adjacent assemblies, retaining rings and core support plates in a manner that assures safe and predictable core geometry.
- Limit duct dilation to a maximum that can be accommodated within the tubes of the in-vessel fuel storage locations, the pantograph arm, and the fuel handling machine, whichever is more restrictive.

Limits on assembly bowing will be imposed indirectly in terms of the effect that assembly bowing has on the inter assembly forces during reactor operation and refueling.

The In Vessel Transfer Machine (IVTM) for the ARC-100 has not yet been designed, but it is expected that it will have gripper force limited to a “normal” push pull force of (set by the mass of a single driver assembly), and a hold down push force (holding the six neighboring assemblies) of 2,000 N. The IVTM will be designed so that the pull force can be increased to allow assemblies that may have considerable resistance to movement to The fuel assembly will be designed so that

it is structurally capable of withstanding (if "stuck") a pull without significant damage. Structural strength requirements will be determined, and by design it will have to be substantially above the

This precludes incidents of refueling where the assembly may come apart (as happened at BOR 60 and DNR).

Structural requirements can be defined once the service classification of the assembly is determined. Following the guidance of the ASME Code Section III, subsection NB, the assembly will be subjected to four service levels, A, B, C, and D. Service level A applies to normal operation and anticipated operational occurrences with frequencies greater than in every ten years. Level B is applied to occurrences with frequencies between 1 in ten years and 1 in a year. Level C is applied to unlikely events whose frequencies are greater than 10<sup>-6</sup>/year, and Level D is applied to DECs. In each service level associated with the categorization of events, the fuel assemblies and fuel bundles will experience a duty cycle. Appendix D provides the preliminary duty cycle for the ARC-100 fuel.

The structural evaluation criteria cover all parts of the fuel assembly, but not the fuel bundle, which is only considered in terms of its interaction with the hexagonal ducts. ***(Note: None of the analyses described in the following subsections have been performed at this time but will be performed during Preliminary and Final Design).***

### 3.2.1 Allowable stress and strains

To provide protection against ductile rupture from short term loadings and gross distortion from incremental deformation and ratcheting, a limit is imposed on either stress or inelastic strain. Stress is determined by elastic analysis in which mechanical loadings, thermal loading and interaction between assemblies are modeled [12.13]. The stress limits to be satisfied are:

- (1) Primary Membrane Stress Intensity Limit

$$P_m < \alpha S_F \quad (\text{Eq.3.3})$$

where  $S_F$  is the least of  $1.66 S_y$  or  $S_u$ , with  $S_y$ —Yield stress, and  $S_u$ —ultimate stress.

- (2) Primary Membrane plus Bending Stress Intensity Limit

$$P_L + P_b < \alpha K_t S_F \quad (\text{Eq. 3.4})$$

where  $P_L$  is the local primary stress,  $P_b$  is the bending stress, and  $K_t$  is the bending shape factor [39].

- (3) Primary plus Secondary Stress Intensity Limits

- (i) For axisymmetric structures subjected to axisymmetric loads and for material exhibiting a minimum uniform elongation of 1% at the time under consideration, the sum.

$$(P_L + (P_b/K_t))_{\text{Max}}/S_y + (Q)_{\text{Max}}/S_y \quad (\text{Eq. 3.5})$$

as a function of axial location is restricted to being within a modified shakedown boundary, defined in Figure 5 of reference [40], for all normal operation and anticipated faults. The  $S_y$  in this expression is the average yield stress at the maximum and minimum section temperatures during the period of time under consideration, and  $(Q)_{\text{Max}}$  is the maximum range of secondary stress intensity. The structure is considered unstable beyond the shakedown boundary.

(ii) For material with a minimum uniform elongation less than 1%

$$(P_L + P_b + Q)_{\text{Max}} < \chi S_u \quad (\text{Eq. 3.6})$$

In the formulas above  $\alpha = 0.55, 0.66, \text{ and } 0.75$ , and  $\chi = 0.60, 0.75 \text{ and } 0.95$  for service levels A, B, and C respectively.

(4) Maximum Primary Principal Stress Limit

$$S_{\text{Max}} < S_u \quad (\text{Eq. 3.7})$$

for  $RA/TF < 10\%$ , where RA is the reduction in area and TF is the stress triaxiality factor [40].

$S_{\text{Max}}$  is the largest principal stress, including the effect of stress concentration.

Higher stresses than the above limits are permissible but, in that case, an inelastic analysis must be performed which covers elastic, thermal, creep, plastic, thermal-creep, irradiation creep, and irradiation swelling strains. Limits are then imposed on two types of strains: (i) membrane plastic plus thermal creep strains at locations away from local structural discontinuities and (ii) peel plastic strains as any structural point.

### 3.2.2 Creep-Fatigue Damage

The cumulative Damage (D) is the sum of the creep damage ( $D_c$ ) and the fatigue damage ( $D_f$ ) and is to be maintained below a specified limit, which is 0.1, 0.5, and 0.9 for Service Levels A, B, and C respectively. Details for calculating  $D_c$  and  $D_f$  are given in reference [39].

### 3.2.3 Non ductile Failure Protection

HT9 undergoes a marked drop in ductility at low temperatures or high fluence as illustrated in Figure 1.10. Non-ductile fracture could lead to assembly failure at stresses well below those corresponding to ductile failure [41]. The two factors to consider are: (1) the operating temperature relative to the HT9 Ductile-Brittle Transition Temperature (DBTT) and (2) the amount of embrittlement induced by fast flux irradiation. The material embrittlement is manifested in the form of an increased DBTT and also in a lower upper shelf of fracture toughness at temperatures above the DBTT [42] as shown in Figure 3.2. Several studies have been conducted on the effect of irradiation on the fracture toughness of HT9. Figure 3.2 shows the greatest effect noted in these studies, which was an increase of the DBTT from  $0^\circ\text{C}$  (unirradiated) to  $180^\circ\text{C}$  for irradiation at  $360^\circ\text{C}$ . The same studies also showed among these samples above 3 dpa the DBTT shift to be insensitive to irradiation dose, suggesting a saturated behavior above that level, which is fortunate for the ARC-100 since the duct deposition during its lifetime in the core is 250 dpa vs the experimental data which is presently limited to 208 dpa. The greatest effect on the DBTT occurs for temperatures around  $360^\circ\text{C}$ .

Radiation hardening can be offset by softening when irradiation temperature is higher than  $425^\circ\text{C}$ . Irradiation embrittlement is recovered to some extent by a dislocation recovery process and precipitate coarsening. As a result, the shift in DBTT decreases with the increase of irradiation temperature. Byun et al. [43] showed a sharp decline in the DBTT between  $400^\circ$  and  $450^\circ\text{C}$ . However, the DBTT shift does not approach zero at high irradiation temperatures when irradiation hardening is completely absent.

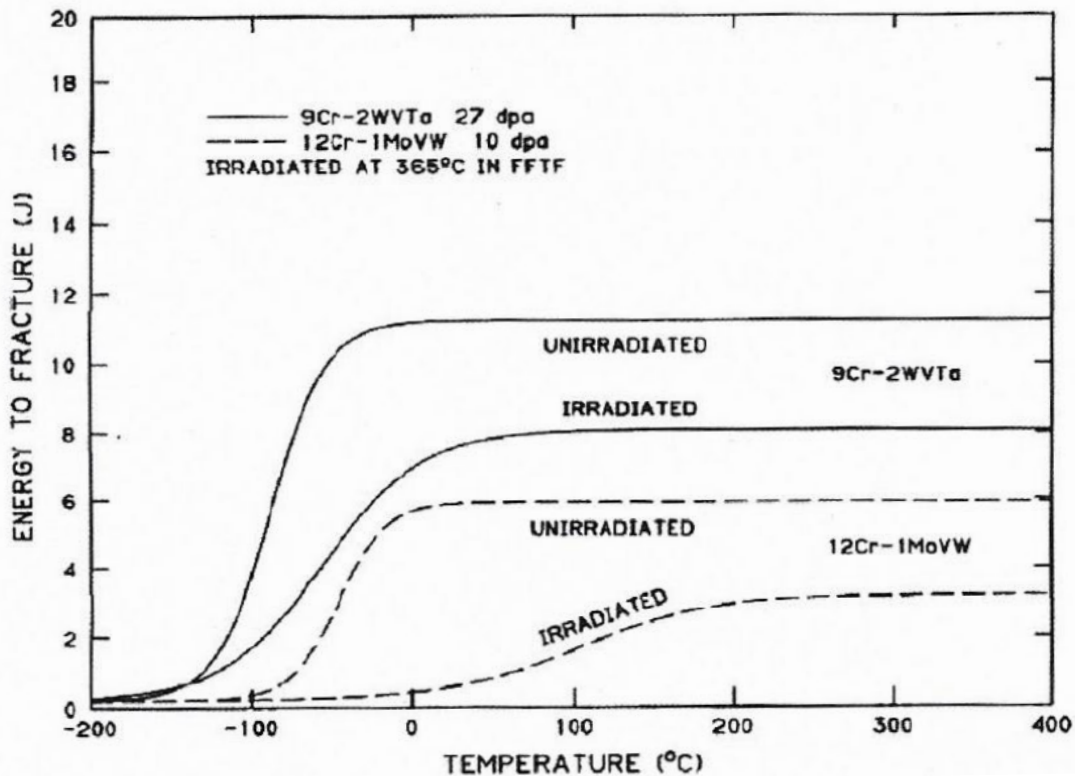


Figure 3.3 Comparison of the unirradiated and irradiated Charpy curves for one third size specimen of 12Cr-1MoVW (HT9) and 9Cr-2WVTa steels in FFTF at 365°C [42]

The evaluation of non-ductile failure protection for the HT9 hexagonal ducts will be as follows:

- Since the DBTT for irradiated HT9 is 180°C, and during operations (excluding refueling ) the duct will always be substantially above that temperature, the material is sufficiently ductile, so than no non-ductile evaluation is necessary.
- For refueling operations, the temperature of the pool is elevated to about 200°C, (but always above 185°C to avoid precipitation of impurities in the sodium). Moreover, during operation with the Fuel Unloading Machine (FUM) and the intra-building transportation cask, the duct temperature could be even lower. Therefore, a detailed fracture mechanics calculation will be performed as outlined in reference [44] to demonstrate that the duct can withstand the applied load. In this analysis the largest stress intensity factor shall be less than one half the fracture toughness of the HT9.

### 3.2.4 Special Requirements for Weldments

Special requirements must be specified for weldments to account for the potential high strain concentrations, particularly in the heat affected zone, and the limited ductility of weldments at elevated temperature and irradiation. The requirements specified in reference [44] will be followed. It is noted, regarding the ASME code, that Clinch River Breeder Reactor (CRBR) and the Power Reactor Innovative Small Module (PRISM) faced regulatory questions concerning compliance with the elevated temperature structural integrity criteria (at that time ASME Code Section III Subsection NH - ASME Section III Division 5 has replaced Subsection NH of Division 1 of Section III with the 2015



code). Currently Division 5 Subsection HB only permits 304SS, 316SS, Ni-Fe-Cr Alloy 800H, 2.25Cr-1Mo and Mod. 9Cr-1Mo (grade 91) structural materials and three bolting materials 304SS, 316SS and Ni-Cr-Fe-Mo-Cr Alloy 718.

Alloy HT-9 is used for cladding and duct applications in high temperature reactors and is not approved for pressure boundary applications. Efforts have r taken to add HT-9 as an approved material for Division 5 high temperature pressure boundary applications, and as described in the reference [44], HT-9 is being considered not only for fuel-cladding but for reactor vessel components and piping.

## 4 FUEL DESIGN DESCRIPTION

### 4.1 Fuel Design of the ARC-100 Reactor

Figures 4.1 and 4.2 illustrate the present design of the ARC-100 assembly and assembly pins, respectively. The major components of the driver fuel assembly are:

- the individual fuel pins, bundled together with a spacing wire separating the individual pins and the pin from the surrounding ductwork. Each pin
  - contains a number of fuel slugs in its lower region.
  - has a gas plenum above the fuel region, with a volume equal to 1.5 times that of the fuel region.
- a hexagonal ductwork to channel the coolant flow though the assembly.
- a monolithic upper fitting designed for grappling the assembly (in ARC 100 the assembly is grappled by a “male” gripper) which also provides the flow path out of the assembly.
- a monolithic lower fitting which has the nose piece for mating with the core support structure, acts as a lower reflector/shield, and houses the individualized orifices that provide different flows of the coolant to different driver assemblies.

The final design of the fuel assembly has not yet been decided upon. The features which have not yet been finalized are:

- the hexagonal ductwork may be either welded or bolted to the assemblies lower and upper fittings (at present the bolted approach is preferred)
- The pin bundle may contain pins that can be individually removed to facilitate testing of pins, or alternatively a removable much smaller bundle of pins within the bundle.

Several Considerations dictate that the pin be kept as short as practical within the requirements to be met by core physics considerations, and ARC had considered other configurations, some of which has much longer pins enclosed in an assembly with short lower and upper fittings, but limitations in the dimensions of the pin and the ability to extract it, nondestructively testing it and shipping it to a location where destructive testing could be performed, as well as its close similarity to previously employed fuel assembly (in EBR II those were referred to as subassemblies) have favored the present configuration.

**Figure 4.1**

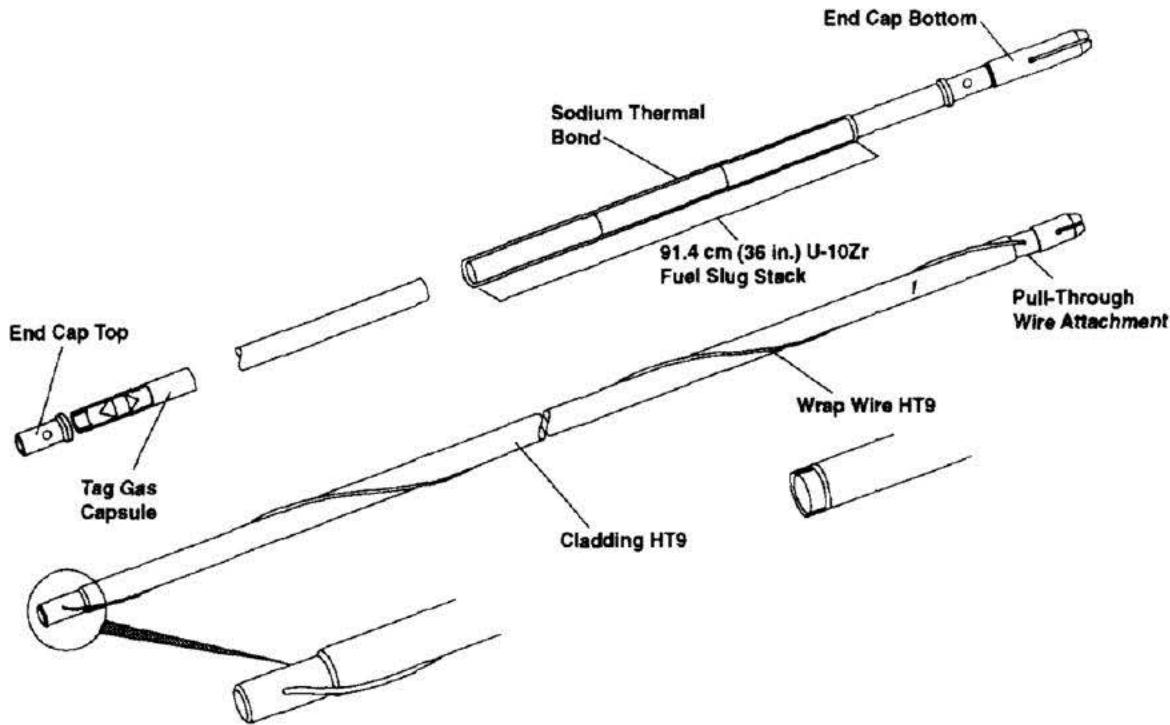


Figure 4.2 ARC-100 Fuel Pin

The basic configuration used of the ARC 100 fuel design is very similar to that employed at reactors worldwide that have used or plan to use metal fuel. Very few reactors have utilized metal fuel. Some have used both metal fuel and oxide fuel (e.g., FFTF). Different reactors have used a different fuel composition and different geometric arrangement. For instance, Fermi 1 [54] employed U-10Mo metal fuel in a square configuration. Their assemblies 6.72cm square by 242 cm long (about 7.94 ft), had both a lower and upper axial blanket section employing uranium rods, and the fuel section (only 84 cm long (about 2.76 ft)) contained 144 thin cylindrical pin fuel pins clad with zirconium. Suffice to state that almost every reactor had its own version of a fuel assembly. In fact, EBR II had several versions irradiated during its lifetime. The ARC 100 fuel assembly design configuration (but not the dimensions) is closest to the design of the EBR II MkIV-V fuel and the FFTF metal fuel designs.

Table 4-1 compares the major operating parameters established for the ARC 100 fuel to the EBR II and FFTF operating parameters. The comparison is made for steady state operation at full power, and fuel and cladding for the ARC-100 are nominal peak,  $2\sigma$  and  $3\sigma$ .

The ARC-100 fuel design is based on a binary U-10wt%Zr metal alloy that is clad with HT-9 steel. 16,811 binary U-10Zr fuel pins were irradiated at the EBR II, where, in addition, 660 U-xPU-Zr pins were also irradiated. More than 800 binary U-10Zr pins were irradiated at the Fast Flux Test Facility (FFTF).

The pins used in the EBR II Mark III fuel used the U-10Zr with either 316 stainless steel or D-9 cladding material. Later in the Mark IV and V fuels, HT-9 cladding was introduced. As shown in Table 4-2, all irradiated pins with HT-9 cladding completed their irradiation in the two reactors to high burnups up to 20 at% without cladding breach under normal operating conditions. There have been only four cases of cladding failure.

**Table 4-1 ARC 100 major operating parameters and limits compared with EBR II and FFTF fuel**

Parameter	ARC 100	EBR II	FFTF	Reason
Power Density (MW/ton)		171	311	20-year core life
Avg. Power Density (kW/liter)		390	735	20-year core life
Nominal Peak Cladding Inner wall Temp, (°C)	BOL EOL	623-660	667	Limit FCCI and longer term FCMI
2σ Peak Cladding Inner wall Temp, (°C)	BOL EOL			
3σ Peak Cladding Inner wall Temp, (°C)	BOL EOL			
Nominal Peak Centerline Fuel T (°C)	BOL EOL	720	736	Limit fission products migration gradient . Low fuel to cladding delta T ( compared to EBR II (50-110) and FFTF (60-150)
2σ Peak Centerline Fuel T (°C)	BOL EOL			
3σ Peak Centerline Fuel T (°C)	BOL EOL			

The failures in X429A and X429B assemblies occurred at 6.5 and 10 at.% burnup, respectively. The X429 assemblies contained fuel rods with a plenum-to-fuel-volume ratio of 1, and also contained rods with varying as-fabricated characteristics for the purpose of investigating sensitivity to deviation from fuel specifications. The two (2) failures in X447 occurred in at around 9.5 at.% burnup in assembly X447A, which was orificed to operate at a significantly higher-than nominal cladding temperature [45].

While Table 4.2 only shows the experiments conducted with HT-9 Cladding, the tables provided in Appendix C shows data obtained for different fuel types and different cladding. This data is very much relevant to the ARC-100 fuel since some of the early phenomena affecting fuel behavior are not dependent on fuel and cladding type. In addition to the data presented in the tables of Appendix C, more details on each of the experiments can be found by accessing the various data bases maintained by the Argonne National Laboratory [and the FFTF Metallic Fuel Irradiation Testing Database Pacific Northwest National Laboratory.

It is noted that during the 30 years of operation of EBR II, fuel pin failures occurred. For more than 13,000 U-Zr and U-Pu-Zr rods for the Mark III/IV fuel, 24 failures occurred. Of these the vast majority (16) were breached at defective welds (manufacturing defects), 3 breached for unknown causes in the gas plenum region, and only 5 breached in the fuel column region due to creep failure of the clad. One of these was with D-9 cladding. The four (4) with HT 9 cladding are described above.

**Table 4-2 Comparison of ARC-100 fuel to HT-9 clad fuel tested in EBR II and FFTF**

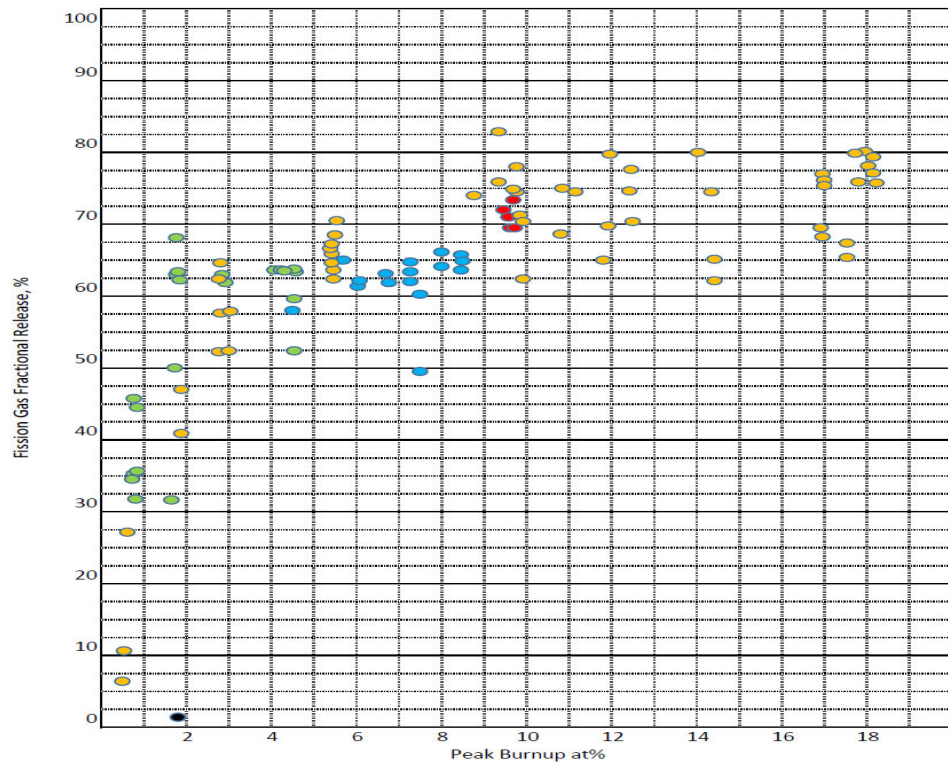
Reactor/ Test	# pins/ As'mbly	Smear Density (%)	Clad OD (cm)	Clad Thickn's (cm)	Plenu m /Fuel Ratio	Peak Power (kW/m ) BOL	Peak Clad Temp. (°C)	Peak Burnup (at%)	Fast Fluence (x10 <sup>22</sup> n/cm <sup>2</sup> )	Notes
ARC-100							(Nom 6 (3σ)			
Length of ARC-100 fuel is 150.0 cm										
EBR II	Length of EBR II fuel is 34.3 cm									
X425	61	75	0.584	0.038	1.0	48.2	590	3.0,11.0, 16.2, 19.3	20.6	
X429	61	75	0.584	0.038	1.0	42.7	600	7.7, 10.6, 14.4	13.8	2failures
X430	37	75	0.757	0.041	1.4	49.2	540	11.5	20.6	
X431 Blanket	19	85	0.940	0.038- 0.051	1.8	39.4	507	3.9	15.4	
X432 Blanket	19	85	0.940	0.038- 0.051	1.8	39.4	507	4.5	16.6	
X441*	61	70-85	0.584	0.038	1.1-2.1	45.9	600	12.7	10.1	
X447	49	75	0.584	0.046	1.4	36.1	660	10	9.17	2failures
X448	61	75	0.584	0.046	1.4	45.9	552	14.6	14.9	
X449	61	75	0.584	0.046	1.4	29.5	578	11.3	17.7	
X450	61	75	0.584	0.046	1.4	36.1	576	10.2	13.1	
X451	61	75	0.584	0.046	1.4	32.8	623	13.7	13.7	
X489**	61	75	0.584	0.041	1.4	36.1	606	5.4	4.83	
X492*+	61	75	0.584	0.038	1.4	41.0	551	10.5	11.1	
X496	37	59	0.636	0.056	3.0	63.3	536	8.3	6.9	
X501** *	2+57	75	0.584	0.046	1,4	44.9	540	7.6	6.4	
Length of FFTF fuel is 91.4 cm										
FFTF	Length of FFTF fuel is 91.4 cm									
M1A	8	75	0.686	0.056	1.2	42.7	577	~3.8	5.6	
M1	5	75	0.686	0.056	1.2	43.0	577	~9.5	17.3	
M2	169	75	0.686	0.056	1.3	54.1	618	~14.3	19.9	
M3	169	75	0.686	0.056	1.3	59.1	643	~13.8	19.2	
M4	169	75	0.686	0.056	1.5	56.8	618	~13.5	19.0	
M5	169	75	0.686	0.056	1.5	55.8	651	~10.1	14.0	

**ARC20-FQ-003 White Paper on ARC-100 Fuel Qualification Program**

M6	169	75	0.686	0.056	1.5	55.8	588	~14.1	12.8	
*Used U-19Pu-6Zr, U-19Pu-10Zr, and U-19Pu-12Zr					All other fuel is U-10Zr					
** Used U-19Pu-10Zr, and U-28Pu-10Zr										
*+ Used U-20.5Pu-10Zr										
*** Used U-10 Zr with minor actinides										

From Table 4-1 the parameters for which the ARC-100 fuel deviates considerably from the tested fuel are:

- Fast fluence, which is over two times greater than the fluences experienced by the test specimens,
- Cladding (and fuel slug) diameter, which is close to twice (                      times the diameters of most of the test specimens, except for the blanket specimens), and
- Length of fuel region which is roughly                      times that of EBR II fuel and                      times that of FFTF fuel.
- Time of exposure which is                      times longer for ARC-100.

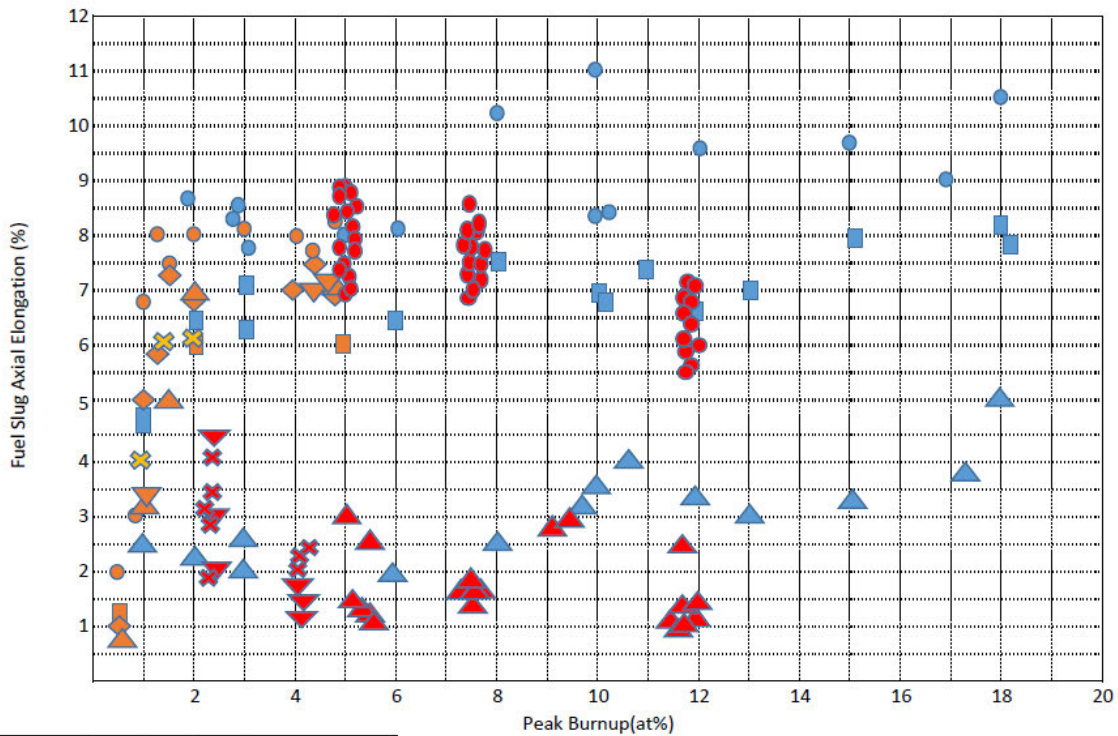


Legend				
Fuel Type		U-Fs,U-γZr and U-xPU-10Zr		
x	y		R (cm)	L (cm)
0, 8, 19		●	0.686	91.4
0, Fs		●	0.442	34.3
0, 3, 8, 19, 22, 26		●	0.737	34.3
0, 8, 19		●	0.584	34.3
	2, 6, 10	●	0.94	

**Figure 4.3 Fractional gas release as a function of Burnup for EBR II and FFTF Metallic Fuel**

FFTF tests demonstrated that the length of the fuel influences the locations of high burnup and fission product concentration and the highest cladding temperatures. For the short fuel region of EBR II the locations were almost coincident, whereas for the nearly three times longer FFTF fuel, the high cladding temperature occurred at or near the top of the fuel column, while the region with the highest fission product concentration (burnup) was near but above the midpoint of the fuel column. The same behavior is expected for the ARC-100 even longer fuel, and indeed simulation with the fuel performance codes [55] has so confirmed.

Analysis of the experimental data available for the early phenomena (radial and axial expansion and fission gas evolution) shown in Figures 4.3 and 4.4 indicate fuel length and diameter of cladding have little or no influence on those phenomena, but fuel composition does, with U-10Zr having the highest axial expansion. Smear density can have a lag effect on the radial and axial distribution and ultimately on strain experienced by the cladding, as shown in figure 4.5.



Experiment	X419-X421	X423	X430	Fuel Type
Legend	●	●	●	U-10Zr
	■	■		U-8Pu-10Zr
	▲	▲	▲	U-19Pu-10Zr
		◆		U-3Pu-10Zr
		▼	▼	U-22Pu-10Zr
		✕	✕	U-26Pu-10Zr
		4.32	5.66	5.66

Figure 4.4 Axial Elongation of Metal Fuel (References [51,52,53])

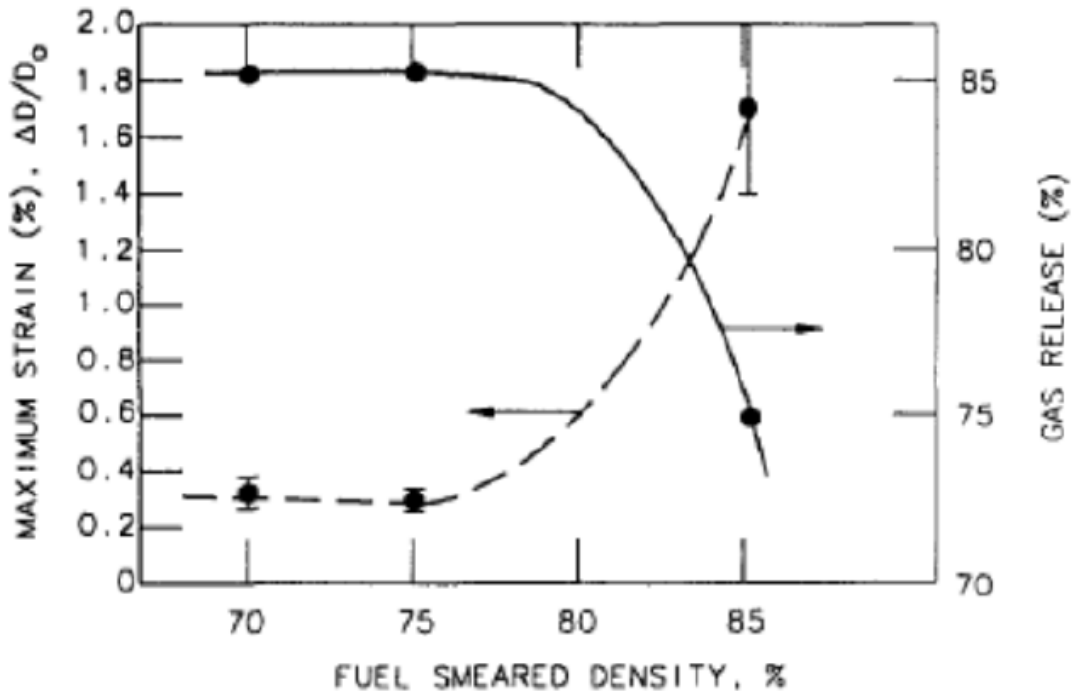


**Figure 4.5** Peak Cladding Diameter Increase and Gas Release Fraction for HT9 Clad U-19-Pu-10Zr Fuel of Various As-built Smear Densities, at 12.5 at% Burnup.

## 4.2 Driver Fuel Assembly Design

The design of the ARC 100 fuel is described component by component of the fuel assembly. To enable understanding of the reasons underpinning the design of each component, the behavior of the metallic fuel is provided in section 5, with section 5.1 describing the important phenomena affecting its behavior, and section 5.4 providing the analytical prediction of its behavior.

The fuel design must accomplish all of the functions that the fuels as a whole (fuel slug, cladding, pin, spacer wire, ductwork, assembly) must perform in order to have a safe design.

The primary functions of the driver fuel assemblies are to provide, protect and position the nuclear fuel in order to produce the heat for the reactor heat transport system.

The cladding's main function is to act as the primary fission product barrier both during normal operation and during off-normal events.

The primary function of the ductwork is to protect the flow of the primary cooling system and to protect the reactivity control system, both during normal operation and during off-normal events that will ensure meeting the requirements of insertion.

To satisfy these functions, design requirements are established to meet safety and reliability functions. The principal functional requirements are:

- Fuel pin performance reliability must be such as to statistically prevent a "significant" number of fuel pin failures during normal and off normal reactor operation (including unlikely events). Significant is not a precise number, but transport of radionuclides to auxiliary systems, and to



the environment dictates what percentage may be tolerable under normal operation and anticipated operational occurrences (from the ALARA standpoint of operability, inspection ability, and maintainability) and for unlikely events (design and beyond design basis accidents). Although traditionally the LWR industry has adopted 1% failed fuel as a limit, ARC believes that 0.1% is more appropriate, and has adopted it for the ARC 100 normal operation and anticipated occurrences. A detailed description of the reasons for this adoption is provided in section 5.2.

- Maintain a coolable geometry of both the fuel pin and the pin bundle for the life of the assembly. Maintenance of a coolable geometry means that despite stochastic failures of pins, the bundle geometry remains sufficiently intact. This in turn means minimizing or eliminating the causes of pin failures, and therefore establishing limits on maximum cladding stress and strain, minimizing the fuel cladding interaction, whether mechanical or chemical, avoiding the formation of fuel cladding eutectics or interactions that would cause significant weakening of the cladding, such a formation of brittle layers of cladding fuel material caused by fission product migration. In practice the FMCI is limited by (1) specifying a smear density for the fuel slug/cladding geometry, and (2) verifying that the fuel densification which occurs as a result of solid fission products build-up over time does not cause unacceptable interaction with the cladding. The FCCI is controlled by establishing limits for the fuel centerline and the fuel edge/inner cladding diameter temperatures under normal operations and AOOs, as well as for unlikely events.
- The deformation of the ductwork either caused by deformation in the fuel bundle or by flux/temperature gradients across the core, in combination with irradiation caused swelling must be such that the inner duct of the control elements and the elements themselves of the reactivity control system are not prevented from movement.

In addition to the functional requirements above, there are operational requirements stemming from the nature of the reactor operation that the assemblies have to endure during their lifetime. Operational requirements are developed based on limits on steady state power, duty cycles and use of uncertainty factors (and other worst-case conditions) to evaluate the fuel performance.

The duty cycles are provided in Appendix E. Their number have been derived based on operational experience, engineering judgment and probabilistic risk analyses performed for the EBR II (because the PRA for the ARC 100 has not yet been completed but is in progress – the duty cycles and their number will be revised after the ARC 100 PRA is completed). Included in the duty cycles are off normal events.

In the neutronic and thermo-hydraulic assessments of fuel performance, the analysis has generally been performed for nominal conditions and uncertainty factors of  $2\sigma$  and  $3\sigma$  applied to the nominal calculations. The  $2\sigma$  uncertainty has been used for the assessment of the performance of the pin. The reason is that prior fuel qualifications and acceptance criteria were established on this basis, and the fuel performed extremely well. Therefore, both the uncertainty and acceptance criteria adopted by the ARC100 are the same as those previously used. The  $3\sigma$  uncertainty was applied to the "global" safety analysis for the normal operation anticipated occurrence and design basis accidents to determine the possible behavior of the peak assemblies as well as the core overall and the heat removal system. For beyond design basis events, best estimates analyses are used (no uncertainties). For such deterministic analyses the use of  $3\sigma$  is considered more appropriate because the probability that the actual temperatures exceed the calculated temperature is less than 0.3%, and the temperature margins that ARC selects for the various conditions are generally at least 5 percent less than the threshold temperatures at which the phenomena become effective. For instance, while the eutectic formation threshold temperature is effectively 715 °C, ARC utilizes a

temperature limit of 650° C as an indicator of the possibility of eutectic formation . The difference between a nominal temperature and a 3 $\sigma$  temperatures for fuel and cladding is typically less than 65°C and 60°C respectively. For lanthanide migration induced significant weakening (>50 $\mu$ m) of the cladding, the threshold temperatures are about 610°C for the cladding and 680°C for fuel centerline and ARC uses a nominal 555 °C and 605 °C respectively.

#### 4.2.1 Fuel slug design

The design of the ARC 100 fuel slug will be prototyped prior to fabrication (as further detailed in section 4.7), in order to determine the length which can best be made using the casting technique developed at the EBR II and also used for the FFTF. Hopefully the length of the slug can be made to 50 cm. The diameter of the slug (within the Vicor molds, will be limited to so as to ensure a smear density of at most , and a residual bond sodium gap of 1 mil after the fuel radially expands during irradiation.

The fuel specification will be prepared, utilizing the experience gained at the EBR II and FFTF, so that the fuel slug size, weight, and chemical specification are combined in the manufacturing process. The important properties of the fuel slug are its :

- metallurgical composition which is U-10Zr by weight and having as uniform distribution of the uranium and zirconium matrix. For the nuclear standpoint, the fissile content of the fuel slug must consider the chemistry variations (deviation in nuclide masses) , that is uncertainties in fuel slug geometries and fissionable material concentration.
- initial thermal conductivity, how it is altered by the formation of pores and cracks during its radial and axial expansion, and the resulting filling of those by the sodium bond.
- the formation of a low melting eutectic between the uranium zirconium and the HT 9 cladding material as the temperature of the interface between the two (once contact is made) exceeds certain limits. The temperature at which macroscopic liquefaction does not occur has been shown to be 650°C for U-xPu-10Zr fuel and HT 9 cladding. Therefore, that is the limit set for the ARC 100 fuel cladding interface temperature during normal operation and anticipated operational occurrences.
- A threshold temperature of 610°C at 2 $\sigma$  for the cladding inner diameter is established to bound the effect of lanthanide migration and cladding wastage resulting from it.

#### 4.2.2 Fuel Cladding Design

The fuel pin cladding provides the primary barrier to the release of radioactive material. Therefore, the cladding strength must be sufficient to assure the probability of cladding failure is acceptably low during normal reactor operation and during off-normal reactor transients' events that occur or may occur over the life of the fuel. Very low probability, extremely unlikely events are also included in the design basis, although none are expected during the fuel lifetime. For these events, fuel failures may occur, but the pin geometry must remain intact, so the core remains coolable.

In addition to providing a barrier to the release of radioactive materials, the fuel system must provide a stable geometry, so that sodium coolant flow can always provide a path for heat removal. Moreover, the fuel slug itself within the cladding must maintain its geometry to the extent that fuel motion does not lead to unacceptable changes in reactivity or the regions of high smear density.

The reliability of the cladding as a barrier depends on the inherent strength of the cladding material in response to the applied loadings. The material chosen for the cladding (the duct and other structural elements of the entire assembly ) is a ferritic martensitic alloy HT 9.

The two properties that are used directly in the design criteria/requirements are: cladding plastic strain, and stress rupture, as shown in Table 3.1. Both are expressed as correlations established from experimental and operational data.

In the case of Stress Rupture correlations, the Cumulative Damage Function (CDF) method is used to apply the correlation to variable load and temperature conditions.

The other important factor determining cladding strength is cladding wastage, defined herein as that part of the original manufactured cladding wall that is assumed to no longer contribute to carrying the applied load. Mechanisms that have been identified as contributing to cladding wastage (see figure A.1.6.1) in the ARC 100 fuel and cladding systems are:

- scratches on the cladding surfaces introduced by manufacturing, transportation etc.
- solid state diffusion of fuel constituents, and fission products (especially lanthanides) into the cladding, creating a brittle region that weakens the cladding.
- eutectic liquefaction at the fuel cladding interfaces.
- sodium cladding interaction causing corrosion and carbon/nickel depletion at the cladding inner and outer diameter.

The standard ASTM specifications (A771-83) for fast reactor cladding call for external and internal surfaces to be free of scratches, dents, scuffs or pitting that exceed 25 microns in depth. The HT 9 material has sufficient ductility at operating temperatures that flaws of this type will not lead to brittle failure. However, some reduction in strength can be expected. Since, however, the computer codes used to assess the performance of the ARC 100 fuel [55] assume an axisymmetric geometry, they cannot model the three-dimensional nature of these imperfections. Assuming a uniform wastage of 25 micrometers would be too conservative, therefore an effective scratch depth of 12.5 micrometers is assumed as wastage.

A second reduction in cladding thickness may be due to Decarburization and Nickel depletion on both the external and internal surface. The internal surface reduction combined with the migration of fission products into the cladding is addressed below, because the two phenomena occur together. Incidentally decarburization has been noted to be insignificant in HT9 at the temperatures in which the ARC 100 will be operating [56]. The same reference also noted that the strength of the material and in particular its creep strength is not significantly altered by the depletion.

Solid state diffusion of fuel constituents and/or fission products into the cladding form a Fuel Cladding Chemical Interaction band on the inside of the cladding, which form during steady state irradiation and can grow larger during transients, The composition of the zone is complex, it is usually rich in lanthanides, and because the mechanical properties of the FCCI band are not known, and because it often contains cracks, it is assumed the band is strengthless and part of the wastage. The band's depth is a function of temperature, time at temperature and concentration of the fission products. Section 5.1 provides information on the depth of wastage to be assumed as a function of temperature of the fuel and the cladding.

Based on the nominal temperature limits established for steady state operation during the irradiation period, 605 for the fuel and 555 for the fuel/cladding interface, as well as the maximum steady state temperatures (with a  $2\sigma$  uncertainty of 605 and 635 respectively), and the peak temperatures determined by the safety analyses performed to date, the depth of this band is expected to be no greater than ).

During certain unprotected transients, the interface temperature between the fuel and the cladding exceeds the limits established by ARC for relatively brief interval of time, and some eutectic

liquefaction may occur. However, the depth of the liquefaction regions is predicted by the empirically derived Arrhenius equation (see Equation 1 of Appendix B) to be no more than of the cladding thickness, or microns. [7]

Finally, nickel and carbon depletion at both the inner and outer cladding surfaces can degrade the strength of the cladding material. The depletion at the inner surface is addressed by the determination of the strengthless layer caused by the combined depletion and migration of the fission products.

Carbon depletion of the outer is the primary concern for alloys other than the HT 9 alloy. It, and nickel depletion is caused by the interaction with the sodium coolant. The penetration depths on the outer surface are minor and determined on a preliminary basis by the correlation below.

$$D = F R_0 t \quad (\text{Eq.4.1})$$

where D is the penetration depth in  $\mu\text{m}$ ; F is the damage factor =  $0.021 \mu\text{m} \text{ dm}^2/\text{mg}$ ;  $R_0 = A \exp(-Q/RT)$  is the mass loss rate in  $\text{mg}/\text{dm}^2 \text{ yr}$ ;  $A = 1.76 \times 10^{11} \text{ mg}/\text{dm}^2 \text{ yr}$ ; Q is the activation energy, 36,000 cal/mole; R is the gas constant, 1.987 cal./mole $^\circ\text{K}$ ; T is the temperature in  $^\circ\text{K}$ , and t is the time in years. Thus, this could contribute another 12.85  $\mu\text{m}$  to the wastage. However, that may be masked in the overall corrosion rate for HT9 in flowing sodium, which at the operating temperatures of the ARC 100 has been determined to be about in 20 years [56]

The wastage in the interior surface of the cladding is neglected as having already been considered by the lanthanides caused FCCI above.

Preliminarily, and conservatively (because eutectic formation is not coincident with FCCI unless temperature exceed 715 C, which only occurs during unprotected transients) a total wastage of  $\sim 150 \mu\text{m}$  is considered wastage, and in the preliminary establishment of the hoop stress in the cladding, the effective cladding thickness would be reduced from .

The computer code used to as part of the design of the cladding (BISON[12,55] and MFUEL module [13,17] of SAS4A/SASSYS-1 etc.) employ correlations which allow consideration of all of the wastage stated above.

In summary the design features for the interface between the fuel slugs and the cladding are: a slug fabricated with a radial dimension to just fit within the cladding inner diameter after a radial and axial expansion with a smear density of 75%, and a cladding thickness which accounts for the reduction in its effective strength as a results of wastage from fabrication imperfections and FCCI and is still capable of withstanding internal pressure and external loadings with sufficient margins to minimize the possibility of cladding failure.

### 4.2.3 Assembly Design

The assembly design features are:

- Designed to place the position of the fuel slug of the pins at the same elevation in the reactor as those in all other driver assemblies.
- Designed to be compatible with the reactor handling equipment [In Vessel Transfer Machine (IVTM) and Fuel Handling Machine (FUM)]
- Designed with shielding sufficient to protect the reactor structures and help minimize activation of secondary sodium and NaK in the DRACS
- Provide drainage for all internal spaces designed to withstand a axial pull test at room and refueling temperatures without permanent deformation.

- Designed to ease disassembly of the upper and lower fittings to facilitate removal of pins for testing purposes.

#### **4.2.3.1 Assembly Hardware Description**

The fuel assembly is made up of three major components as shown in Figure 1.3: a central region containing the pins within a hexagonal duct; an upper preassembly; and a lower preassembly. The upper and lower preassemblies are described below.

##### ***4.2.3.1.1 Lower Preassembly***

The lower preassembly consists of a monolithic HT-9 piece that has a cylindrical adapter (the nose or pole piece portion) to insert and seat the assembly on the reactor grid plate at specific locations, by means of a key slot at its lower end. This portion and the key slot are designed to prevent inadvertent insertion of the assembly in other than the designated position. The upper portion is hexagonal in shape to accept the outer hexagonal can and lower shield/reflector for either welded or bolted attachments (both are presently being considered, but bolted is preferred).

The cylindrical portion of the lower preassembly includes the orifices designed to permit specific coolant flows through specific set of driver assemblies.

At the upper end of the lower preassembly, above a transition region where flow is distributed to the fuel pins, a set of plates are provided to seat the individual 217 pins and to hold the ends of the space wires. Just below that region, the hexagonal lower preassembly is designed with dimensions smaller than the hexagonal duct, providing a ledge is provided where the duct surrounding the central region can sit. Three of the flat faces of the hexagonal preassembly have threaded holes to accept three preinstalled screws. The hexagonal duct fits on the ledge and becomes affixed to the lower preassembly by backing the three internal screws (backed by rotation) into the duct.

##### ***4.2.3.1.2 Upper Preassembly***

The upper preassembly is also a monolithic piece mostly hexagonal in shape, which is used for gripping the fuel assembly. It directs the flow out of the assembly and is provided with openings on the side in case falling objects might obstruct flow out of the top. At its lower end, it is designed to mate with the central region, with the connection being either welded or bolted. The collar at its lower end has three threaded holes, into which screws are pre-inserted. The hexagonal collar's dimension allows it to be inserted into the hexagonal duct of the central region. How that connection is made is described in the complete assembly, section 4.2.3.2.

##### ***4.2.3.1.3 Central region***

The central region consists of the fuel pin bundle surrounded by the hexagonal duct. The design of the individual pin is described in section 3.5. The ductwork design is composed of HT 9 with a thickness of 0.3 cm and a flat-to-flat distance of cm. The design of the duct considers both the structural and thermo-hydraulic response of the duct to the duty cycles described in Appendix E. At the top of the central region a collar is provided with plates to which the spacing wires of the pins are fixed and into which the upper preassembly can be inserted.

#### **4.2.3.2 Completing the assembly**

The central region is coupled to the lower preassembly, with the duct sitting on the lower preassembly ledge. The three screws in the threaded holes and backed into the duct to retain it, and welding can then be made (if welding is the option chosen). The upper preassembly is then lowered to fit within the hexagonal duct and sit on the collar provided by the central region. The crews in the

threaded holes are then backed out to thread the ductwork. Welding (if chosen) can then be performed on the duct to the upper preassembly, completing the entire assembly.

The assembly is then load tested to a pull force of \_\_\_\_\_ Newton.

The total length of the assembly including the nose piece is 5.895 meters.

#### **4.2.3.3 Interfaces with Fuel Assembly**

The fuel assembly is subjected to thermal loads due to the fission's events in the fuel, thermohydraulic loads caused by the coolant flow, internal structural loads (flow induced vibrations) and external structural loads transmitted to the fuel via the reactor vessel supports, the core support and acting at the lower end of the fuel in the grid plate, the core barrel and the load pads on the fuel assemblies. Section 4 of this report explains the methods used for the design evaluation of the fuel.

### **4.3 Control Assemblies**

The control assemblies have an outward appearance which is identical to the driver assemblies. The internals of the assemblies are slightly different for the primary (control) rods and the secondary (safety) rods assemblies. Figure 4.6 shows the control rod assembly. Figure 4.7 shows the safety rod assembly.

The two assemblies differ in the coupling mechanisms, and reactivity worth of the individual rods.

The temperature to which the assemblies and control elements are subjected during irradiation are significantly lower than the temperatures experienced by the driver fuel assemblies, and the phenomena affecting the assemblies are thermal and irradiation creep and their resulting strain, and deformations caused by differences in temperature and neutron flux across the faces of their ductwork.

The gap between the inner duct surrounding the absorber elements, and the outer duct of the control assembly is set at 4 mm to accommodate the expected deformations with significant margin.

The planned periodic measurement of pull-out forces for the driver assemblies is one means to anticipate and correct as necessary (by rotating the assemblies) core deformations which could result in difficulties during refueling or undesirable reactivity effect (as described in sections 5.4 and 7). The bowing of the external hexagonal duct of the control assemblies, and the measurement of its pull-out force, will not provide much information about the contact forces between it and the internal hexagonal duct. (Just as the measurement of pull-out forces for the driver assemblies do not provide information between the hexagonal duct and the internal pins).

Instead, for the control elements, data on the amount of current going to the control rod drive mechanism throughout the operation of the reactor will be used to inform the operator of any issues with rubbing between the control element external hexagonal duct and the internal hexagonal duct.







#### 4.4 Core Restraint System

The lower internals structure consisting of the core barrel, core grid, and the inlet plenum structure, provides the means for restraining the core. The entire assembly is supported on the core support structure as shown in Figure 4.8. The lower internals structure supports the reactor inlet plenum, the core assemblies, the fixed radial shielding, the core barrel, the redan, and various shields, brackets and baffles. It is designed to withstand seismic events with acceptable stresses and deflections. The lower internals structure contains the inlet coolant flow distribution system that controls the rate of flow to the core assemblies. This distribution system consists of a doughnut-shaped manifold, or torus, and associated ducts/piping, that encircles the inlet coolant plenum. Figure 4.8 shows the structure which supports the core, provides the inlet plenum for the coolant and the orifices to distribute flow to the various assemblies. The entire lower internal structure is supported by brackets near the bottom of the reactor vessel. These core restraint proper is shown by the yellow highlight and is described hereinafter.

**Figure 4.8**

The core restraint system consists of distributed passive hardware features which, acting together, must meet the following functional requirements:

- 1) Establish the positions of the individual core assemblies in the horizontal plane.

- 2) Control horizontal movements of core assemblies arising from thermal expansion effects, irradiation-induced swelling, and irradiation-enhanced creep, in such a way that reactivity effects are acceptable and control rod driveline alignments are maintained within specified tolerances.
- 3) Accommodate horizontal seismic motions within alignment and stress specifications; and
- 4) Maintain sufficient clearances in the horizontal plane to allow for fuel handling within specified vertical withdrawal and insertion force limits.
- 5) The design choices representing the major decisions in the design of a passive core restraint system are:
  - a) Length and stiffness of the core assembly lower adapters.
  - b) Lower Internals Structure interface with the core assembly lower adapters clearances, seals, and number of support points (1 or 2).
  - c) Number, location, configuration and height of the core assembly load pads.
  - d) Rigidity of the peripheral boundary - stiff radial shield assemblies or a rigid, shaped, core former ring attached to the core barrel.
  - e) Allowable vertical core assembly insertion and withdrawal loads.
- 6) The factors above contribute to an inherently negative temperature reactivity feedback.

The major challenge in core restraint design is to find the "design window" which contains sufficient clearance for fuel handling (even when core assemblies are bowed due to swelling and creep effects) and sufficient tightness or stiffness for adequate radial position control. The thermal contraction produced by the cooldown to refueling conditions is very important in creating this window of design feasibility. The tool used in core restraint design is the NUBOW-3D computer code. It calculates the elastic and inelastic effects on the shape of individual core assemblies in a three-dimensional representation of the whole core or typical sector thereof, the reactivity effects associated with short-or long-term movements from one set of equilibrium positions to another, and the side loads at all contact points. Under refueling conditions, the sum of these side loads, times the coefficient of friction yields the required initial withdrawal force over and above the dead weight.

The two separate strategies for core restraint system design are referred to as the "limited free bow" approach and the "free-flowering core." The first, used in FFTF and Clinch River Breeder Reactor (CRBR), employs a short lower adapter horizontally restrained in the lower internals structure (LIS) at one point (the lower end), and rigid core formers at the two elevations of core assembly load pads - one near the top end and one about 13.5 cm (5 in.) above the fueled zone. The second, used in EBR-II, Phenix and SuperPhenix, employs a long lower adapter horizontally restrained in the LIS at two points, and the "fence" of stiff and essentially isothermal radial shield assemblies constitutes the peripheral restraint.

The ARC-100 design borrows features from both approaches. The relatively long lower adapter fits into a cylindrical perforated sleeve in the inlet plenum. A ball-and-cone seat at the transition from the cylindrical lower adapter to the hexagonal duct provides the coolant seal, load support, and a positive horizontal restraint point. Close clearance between the bottom of the lower adapter and the lower internal structure sleeve provides limited-movement horizontal restraint.

A rigid core former ring at the elevation of the top load pads provides positive peripheral restraint. The ring has enough clearance, relative to a tight array of assemblies, to permit removal and replacement of both the planned cluster of seven assemblies and if necessary, of individual assemblies by the in-vessel transfer machine (IVTM) yet is tight enough so that the freedom of assemblies to move does not have adverse reactivity or alignment implications. The inner diameter of the ring is shaped so as to achieve flush contact with the outermost assemblies. The core former ring is welded to the inner diameter of the core barrel, to which the Upper Internals Structure is

attached during operation with a system of retractable keys, thus assuring control and safety rod drive-train alignments. Each core assembly is equipped with a second load pad centered 10cm. above the fueled zone of the reactor, but no peripheral core former ring is present at this elevation. Normally the core assemblies contact one another only at the two load pads, which completely circumscribe the hexagonal ducts. Figure 4.8 Illustrated the location of the core and assemblies' restraints. The duct is . across flats ( is the pad dimension) and the lattice pitch (also the hot across-flat dimension of the load pads) is 18 cm. The cm. clearance between ducts is provided to prevent general contact at end of life due to swelling, creep (rounding of the flats), and differential bowing, but the adequacy of this clearance needs to be confirmed by analysis.

## 4.5 Materials

The materials (permitted impurities are provide in section 4.7) for fuel fabrication are as follow:

Fuel slugs – U-10Zr

Cladding – HT9

Bond material – high purity sodium

Fuel assemblies- ductwork and upper/lower fittings – HT9

Control assembly's absorber material - Boron Carbide

Absorber material cladding - HT9

Bond material - Helium

Reflector assemblies' pins (rpds), ductwork, upper and lower fittings – HT9

Shield assemblies' pins- Boron Carbide

Shield assemblies cladding – HT9

Shield assemblies bond material - Helium

Shield assembly's ductwork, upper and lower fitting - HT9

## 4.6 Fuel System Design Basis

For completeness, the fuel system is complemented by reflector assemblies and shield assemblies.

The design basis for the driver fuel assemblies (99 assemblies per core) has been described in section 3.1 and 3.2. Deterministic analyses [7] establish the conditions the driver fuel (as well as all other assemblies experience during steady state power operation, anticipated operational occurrences design basis and beyond design bases events. The cladding material design basis is qualitatively set as a very low number (0.1% or pins) of pins failing during operation for 20 calendar years. In turn that is achieved by establishing the criteria on strains and cumulative damage functions, and eutectic formation listed in Table 3-1. For the structural elements, the design bases are predicated in stresses and strains that are set to prevent deformations which could affect core coolability or unacceptable reactivities feedback. Thos limits are given in section 3.2.

The fuel system (driver fuel control elements, reflector and shield assemblies) operates in the environment provided by the coolant within structural components, the behavior of which can affect the fuel behavior.

Deterministic safety analyses [7] conducted with a  $3\sigma$  uncertainty, verify the coolant margin to boiling to be always sufficient. The structural behavior of the components is verified by stress analysis utilizing ASME code allowables that vary depending on normal operation and AOOs (Levels A and B respectively), Design Basis Events (Level C) and Beyond Design Basis Events (Level D). Structural analyses are done for the various duty cycles to which the ARC 100 will be subjected during its refueling Interval. Appendix E summarizes the expected duty cycles.

Certain events have insufficient operational or experimental data to verify the likelihood of occurrence. One example is blockage of flow to an assembly or multiple ones. Simulation of such events is done on a best estimate basis. The specific case of an essentially full blockage of flow to an assembly has been investigated by reference [19]. The conclusion of the simulation is that the damage suffered by the affected assembly (boil-off of the sodium, melting of the fuel and local failure of the duct) does not propagate to adjacent assemblies to the extent that shoe assemblies would not be able to maintain the fuel cooled; and therefore, the flow blockage of an assembly would not cause loss of coolability of the remainder of the core.

## 4.7 Fuel Fabrication

The fabrication of the fuel slugs, the pins and the fuel assemblies are a critical activity affecting the fuel qualification. The fuel performance require that fabrication produce that very specific design used for the fuel performance assessment, within the tolerances considered in the analysis and design activities.

Fabrication starts with the procurement of the material which meet the materials requirements specified in the design within the specified tolerance in material chemical/mechanical composition and properties and continues through the fabrication methods that ensure the design dimension required properties are met. There are issues in each of these areas. Consequently, this section is divided into five subsections:

- An introductory section describing past experience in fabrication of similar fuel pins, the material requirements and a preliminary decision to proceed with a particular fabrication method.
- Material availability and procurement
- Proposed fabrication method and impact of ARC100 fuel pin dimensions on fabrication equipment design
- Improvement of fabrication operations for reduction of fabrication time and minimization of waste
- Description of the steps that will be taken to ensure the fuel fabrication will meet all of the requirements of its design during the commercial production of the assemblies.

### 4.7.1 U-10Zr metal fuel production

Several methods for turning metal fuel alloy feedstock into fuel slugs have been considered and used to varying extents. . The methods evaluated by ARC Clean Technology have included those most recently reviewed by the Versatile Test Reactor project and suggested by ARC Clean Technology personnel who actually fabricated fuel slugs at EBR II [57]. The method considered is summarized hereinafter.

- Extrusion pressing is appealing in that the method is reasonably simple in concept. Feedstock is placed in the extruder and the material is squeezed through a die at high pressure to form continuous fuel elements for plutonium production reactors that operated at the Hanford and Savannah River sites from the 1940s through the mid-1980s. Single-Pass Reactors (e.g., B-

Reactor, KE- and KW-Reactors, and N-Reactor at Hanford) used fuels co-extruded with either aluminum or zircaloy-2 fuel cladding. In the present day, INL has a small-scale extrusion press capable of extruding 1 to 2 kg batches of metal, and Pacific Northwest National Laboratory is developing extrusion methods to produce a Light Water Reactor fuel in collaboration with Lightbridge Corporation [58].

- Additive manufacturing techniques are only now being applied to nuclear reactor components, and the application to Pu-bearing fuel is years away, at best. Furthermore, there is no irradiation performance experience with fuel produced using additive manufacturing techniques [58].
- Continuous casting for metallic fuel production has been considered in smaller R&D projects since the 1990s. This technique offers some advantages; however, implementation details of the process to ensure proper alloying of the melt prior to casting remain; and as with extrusion pressing, the containment gloveboxes needed around continuous casting equipment are likely to be bulky and challenging to design. The technical readiness of such a method is low [58].
- Vacuum-injection casting. Over the life of EBR-II, more than 200,000 fuel slugs were produced using this manufacturing method [60]. The injection casting production process was successfully implemented at least seven times in separate facilities with separate equipment and spanned more than 40 years [59]. Fuel was also made for testing in FFTF[60]. This work has left a legacy of expertise in the manufacture of metallic fast reactor fuels at INL. Utilizing this expertise and experience base in production of ARC-100 fuel is deemed to reduce technical and schedule risk associated with the establishment of a new production line. The method is a batch casting process, with reasonable production throughput (~20 kg casting batches) and a high-quality product.

Other fuel production methods have been tried in the past and were dismissed due to a host of technical difficulties (e.g., powder metallurgy, swaging and drawing, centrifugal casting). [58] The significant experience gained with the vacuum injection casting, combined with availability of ARC Clean Technology personnel who actually operated the equipment and made the slug, is the reason why at present this is the technology of choice for the ARC-100 fuel slug manufacturing.

**4.7.2 Material supply and procurement**

The ARC 100 utilizes High Assy Low Enrichment Uranium (HALEU) for its fuel assemblies. The fuel in the core has an average enrichment of \_\_\_\_\_ with three zones of enrichment. The total weight of the U-10Zr required of the core is \_\_\_\_\_ tons, of which the HALEU is 23.8 tons. Procurement of HALEU continues to be a critical problem with no domestic source. However, during the past year DOE has initiated a program to develop a domestic source. Other SMR programs face the same difficulty.

ARC Clean Technology and ANL have explored ways in which the quantity of HALEU could be reduced and have identified core configurations different from the present one, that could reduce the amount of HALEU to as little as 4-5 tons of 19.95% enriched uranium, with the remainder of the uranium being 9.95% LEU, which presumably could be made available in the reasonably near term. That quantity of HALEU, enriched to 19.95 %, would then be down blended to create the fuel HALEU needed for the revised core.

A core with only LEU 9.95% LEU is impractical as it would require almost \_\_\_\_\_ tons of that material and be very large.

Another critical component is the HT-9 cladding and duct steel material. Carpenter Technology was the source of HT-9 for the EBR-II experimental program and FFTF reactor program. Carpenter Technology exists today under a different name. Recent attempts to acquire HT-9 were not

successful. However, efforts are ongoing in Canada to develop HT-material for the ARC 100, and once those effort are successful to establish a production line.

Zirconium used in EBR-II fuel is somewhat difficult to trace, however a procurement document from 1994 shows that zirconium “crystal bar” machine turnings were procured from A.D. Mackay, Inc. of Red Hook, New York. The specification for the purity of the zirconium is not referenced in the procurement document, however, the vendor provides a chemical analysis of the supplied material. ANL verified the purity upon receipt. ANL compared the supplied zirconium against the standard specification for zircaloy-3 as the requirement for acceptance. It should be noted that finding a modern supply of zirconium that does not have hafnium as a significant impurity can be troublesome. Global Nuclear Fuel, LLC (GNF) proposed the VTR project look at using zircaloy-2 or zircaloy-4 as a ready supply of zirconium that would have low hafnium (hafnium has a relatively high neutron cross-section that must be accounted for in reactor operations).

There are also procurements critical to the equipment needed for the manufacturing process. The presently preferred manufacturing process is that employed for manufacturing the fuel slugs and pins for EBRII and FFTF, as explained in section 4.7.1.

There exists a supply chain issue with the quartz tubing that can be obtained to serve as molds. Historically, to ensure round castings, precision bore tubing has been used for these molds. This labor-intensive forming process involves heating a quartz tube and drawing it over a precisely machined mandrel. Made this way, the resultant tube has a very precise inner diameter and straightness. Precision bore quartz tubing was readily available in large quantities from the 1950s into the 1990s. However, market conditions changed, and Corning Incorporated (formerly Corning Glass Works), the world’s largest supplier of precision-bore quartz, exited the glass tubing market and divested itself of the capability to manufacture these types of tubes. Fuel alloy “slugs,” cast in precision bore molds, helped ensure that the 75% smeared density specification was achieved. The tight-tolerance molds also ensured that the fuel slugs were as round as possible, thereby promoting uniform fuel swelling early in the fuel’s operation. Today, it may not be possible to obtain sufficient precision-bore tubing to support the needs of a modern fast reactor. When the VTR project solicited US vendors for a smaller number of molds, no positive responses were returned. If precision-bore tubing is not available, and lesser-quality molds must be used to produce the alloy fuel slugs, it is important to understand the mold’s impact on the variability of the cast metal. Commercially available quartz tubing typically does not have an inner-diameter tolerance specification. That specification must be derived from the outer-diameter and tubing wall-thickness tolerances; both of which can affect the cross-sectional shape of the tubing. Other dimensional variations (e.g., out-of-roundness, bow) have more influence on the straightness of the tubing and the ease with which a cast fuel slug slides into the fuel cladding. At the extremes of the outer-diameter and wall thickness tolerances for currently available quartz tubing, an oval- or elliptical-shaped quartz tube could be produced within applicable tolerances. Any fuel slug cast in such a tube would also be eccentric. It is possible to have a fuel slug that meets fissile-material loading requirements and provides smeared density despite its eccentricity or out-of-roundness. However, due to the difficulty in obtaining high quality, precision-bore tubing molds, there is value in considering the possibility of using fuel slugs with greater variability.

Analysis has shown that the dimensional variations possible for fuel slugs cast in common quartz tubing molds is not expected to impact overall fuel performance nor increase the probability of fuel cladding failure at early life [1]. It remains to be determined where several kilometers of tubing can be sourced and what company can make the molds from that tubing. However, it is encouraging that there is not a need for precision bore tubing to make the molds.

**4.7.3 Recommended fabrication method and impact of ARC100 fuel pin dimensions on fabrication equipment design**

The presently recommended fabrication method for the fuel slugs is injection casting, which was proven successful in the fabrication of the fuel slug at EBR II and FFTF, and which has also the method of choice for the planned fabrication of the Versatile Test Reactor (VTR) fuel slugs.

However, there are considerable differences in the dimensions of the fuel slug and the pins of the ARC 100 reactor from those of EBR II, FFTF and VTR, and those differences have an impact on the equipment required for their fabrication.

The differences in dimension are summarized in Table 4-3

**Table 4-3 Dimensions of Fuel Slugs and Pins of EBR II, FFTF, VTR and ARC-100**

All dimensions are in cm	Pin Length	Cladding OD	Cladding Wall Thickness	Slug Diameter.	Fuel Length
EBR-II	75	0.584	0.038	0.44	34.3
FFTF	238.1	0.686	0.056	0.498	91.44
VTR	~160	0.4547	0.05	0.4547	80
ARC-100					

The diameter of EBR-II and FFTF fuel slugs was smaller than that of the ARC-100, and the diameters of the VTR fuel slugs would also be smaller. Further, the length of the fuel slugs for EBR-II and FFTF were shorter as would be the VTR overall slugs' length. There is little experience casting slugs of the ARC-100 dimensions where, for three fuel slugs an ARC-100 fuel pin, the fuel slugs would be in length. It may be fuel slugs shorter than 50cm will be required for the ARC-100, which would increase the number of fuel slugs substantially.

However, casting 3 slugs for each of the pins of the ARC100 would require slugs. Making the slugs shorter would significantly increase that number, and the overall cost of manufacturing the slugs. Therefore, the equipment should be designed so that it is possible to cast long slugs. The comprehensive amount of information of the equipment used at the EBR II in section 2, is provided specifically to inform the changes deemed necessary in order to make slug with consistently high quality with minimum wasted material.

Once the slugs are produced, they are introduced in the cladding tube in which bond sodium is also added, to ensure good contact between the fuel and the cladding. For the present sodium bonded fuel is the fuel for which operational experience exists. Other forms of fuel pin have been studied, with limited ex-core testing, and is very likely the fuel that would be employed for the ARC 100. These fuels (annular fuel, fuels with specially shaped outside surfaces) lend themselves to fuel cladding coextrusion fabrication methods but would require a long time for qualification because of the lack of operational data. Nevertheless, they should be considered for longer term possible use, because the presence of bond sodium can complicate the ultimate disposal of the spent fuel.

Rod loading is the process of fabricating fuel rods. The following parts are brought together at the rod loading station:

- Cladding jackets with the bottom end fitting welded in place.
- Top end fittings

- Tag gas capsules (as needed for detection of an in-service fuel rod failure)
- Sodium metal slug
- of fuel slugs to possibly slugs).

The cladding jackets are inspected and cleaned, as needed prior to use. A specially constructed funnel is inserted into the open end of the cladding jacket. The assembly is tilted to an angle of about 30° to help the slugs slide to the bottom of the cladding jacket. Next, a sodium slug is chilled and straightened on a chill plate. The sodium slug is inserted in the cladding jacket. (An alternative to loading the sodium slugs is being evaluated. It has been proposed to procure the cladding jackets with the bottom end plug welded in place, and the sodium slug also loaded at a vendor location. Transporting those pre-loaded cladding jackets may be possible through the use of inerted shipping packages). Next, the fuel slugs are inserted. The funnel is removed, and the top end cap is inserted. The cladding jacket is rotated to the vertical position to ensure the parts have slid to the bottom of the jacket.

The end cap is welded in place using a pressure resistance welding technique. Since the rod loading station is contained within a radiological glovebox; the atmosphere is argon gas that contains a small amount of helium. Following welding, the rods are subjected to helium leak detection. After successful welding, the rods can be decontaminated and brought out of the rod loading station glovebox.

Any operations where the bond sodium is liquid requires the fuel pins remain in a vertical orientation. The next step in the fuel rod manufacturing process is rod settling and sodium bonding. The fuel slugs are settled in liquid sodium after which the top end fixture is welded. At this point the fuel pins are removed from the glovebox and subjected to bonding operations. The fuel rod is placed in a bonding machine that heats the fuel rod along the length of fuel and sodium slugs. The sodium is melted, and the rods are tapped on the top to impart a jarring impact to the fuel rod. This causes the fuel slugs to slowly sink into the liquid sodium (the settling process). The sodium is displaced upward, inside the fuel slug and cladding gap. The temperature is increased to allow the liquid sodium to wet the surfaces of the fuel and cladding. Then the fuel rods are agitated to remove any bond defects. After a predetermined time, the sodium should completely encapsulate the fuel slugs, with little or no bond defects. The heater is turned off and the sodium is allowed to solidify. The bonding operations will melt the bond sodium. The operations require a large glovebox and bonding equipment for the fuel pins remain in a vertical orientation until the termination of the operation, allowing the bond sodium to solidify. Fabrication of the longer fuel pins for FFTF, briefly described in [60], may be useful for the design of the ARC-100 fabrication equipment.

Quality inspection of the sodium bond is performed using x-radiography to confirm the location of the upper sodium meniscus and look for any voids along the fuel-cladding gap. Eddy current inspection can be done to ensure the bond quality. If needed, the rod can be reheated and impacted to improve sodium wetting and reduce or eliminate any voids.

The ARC 100 fuel rods are similar to those of FFTF and will be wrapped with a spacer wire that is spiral wound around the fuel rod. The wire wrap is used to space the fuel rods from each other and allow the reactor’s flowing sodium coolant to extract heat from the fuel rods. The spiral pattern helps mix the sodium and cause turbulence in the flow to aid heat transfer. the wires will be attached in a manner like used for FFTF fuel. The first operation is to drill and chamfer the holes in the fuel rod end fittings. A drilling fixture will be used to ensure these holes are precisely aligned. Next, the fuel will be mounted in a wire wrap machine. A loose end of wire will be pulled through the hole in the lower end plug, and a bead weld-formed on the end of the wire. This prevents welding heat from affecting



the mechanical properties of the end cap alloy. The wire is then wound around the fuel rod at a predetermined pitch. The wire is clamped to the side of the fuel rod, and the upper loose end is pulled-through the hole in the upper end fitting. This wire end is clamped in a tension measuring fixture to ensure the wire is not too tight (to preclude fuel rod bending during irradiation). A bead is then weld-formed onto that wire to complete the attachment.

The reference ARC-100 fuel assembly is also similar (but not equal) to the FFTF and has relatively few parts beyond the 217 individual fuel rods. At the bottom is an inlet nose piece used to position the assembly into the designated position in the reactor core and regulate the amount of sodium coolant flowing into the assembly (through a fixed orifice and sized flow holes). That inlet nose piece in combination with the support sleeves between reactor core upper and lower support plate are designed to minimize the possibility of flow blockage to the assembly. Just inside the assembly, near the bottom, is a shield/reflector block (or blocks). Above and affixed to the lower shield/reflector block(s), the “T-bar grid assembly” locates and secures the fuel rods within the subassembly. The ARC 100 fuel as presently designed, unlike the FFTF fuel assembly, does not have an upper shield block(s) hanging from the upper handling socket, above the tops of the fuel rods. Protection of the upper core structure and in-vessel components (e.g., pumps and intermediate heat exchangers(IHXs)) from neutron-induced radiation damage is provided by distance (the gas plenum for the ARC 100 fuel is considerably longer than that of the FFTF pins) and shielding of the IHXs. The hexagonal “duct” encloses the fuel subassembly internal components, defines the subassembly’s coolant channel geometry, and provides the load bearing structure between the upper handling socket and lower nozzle. The upper handling socket (or upper adaptor) is attached to the top of the duct and is used to handle the assembly. The handling “socket” can also be used to locate the top of the assembly in the reactor core. While the design of the assembly has not been finalized, the design will be like that used in FFTF (shown in Figure 1.3). Fuel subassembly components will arrive at the assembly station in a clean and inspected condition, ready to be assembled.

#### **4.7.4 Improvement of fabrication operations for the reduction of manual operations and minimization of fissile material waste.**

Several of the fuel fabrication operations must be improved for creditable commercial operations. The need for improvement was recognized in past practice but the fast reactor programs were terminated before solutions could be initiated. On occasion a casting run could be rejected for the following reasons. The fuel slugs could contain defects such as excessive porosity or “hot tears” where the slugs would part. Also, the slugs could be too short. Another problem that would occur would be when the mold pallet was removed too soon from the melt some of the fuel material would fall back into the melt. To solve this problem the mold pallet would remain in the melt until the fuel began to solidify at which point the pallet would be removed from the melt. If the removal operation did not occur at the exact time, then the molds would be frozen in the melt. If this were the case, then the quartz molds would have to be broken from the heel. The result was a heel that had to be recovered by a later operation. The casting operation parameters such as melt temperature, pressure, and pressurization rate were all determined by trial and error. The casting parameters would need to be optimized to avoid these problems to increase the efficiency of the operation and reduce the waste.

The fuel slugs were removed from the quartz molds in a glovebox by breaking the quartz molds manually. This manual operation was slow and resulted in some of the fuel particles adhered to the

glass shards. Equipment was designed but was never utilized to break the quartz molds. Further, attempts were made to remove the fuel material from the quartz shards by magnetic separation. This technique was never fully developed, but it is still needed to reduce the amount of waste as quartz molds are used.

Several possible solutions that would replace the use of quartz molds were considered. Rather than quartz molds the molten fuel was cast directly into zirconium tubes. The zirconium tubes that contained the solidified fuel were put directly into the cladding with the sodium bond. The reason for this technique was, during irradiation of U-10Zr fuel much of the zirconium would diffuse to the periphery of the fuel. A small-scale experiment was successfully conducted with this technique but was never pursued on a large scale. If successful on a large scale this technique could also help reduce or eliminate some of the FCCI phenomena affecting the life of the fuel. In addition, a search was conducted for the possible use of reusable molds with no success. In addition, rather than injection casting a bottom pour technique was considered.

The heels from the casting operation represented 20% of the casting charge. These heels would be put back in future casting charges. These heels would be broken by the use of a hammer into manageable pieces. The heels would contain an increased concentration of carbon from the graphite crucibles and perhaps an increased concentration of silicon from quartz shards that may be stuck in the melt. The casting charge would be made up of some pieces of heel along with fresh feedstock. It was suggested that a separate furnace be used to incorporate the heel material into the fabrication line.

One of the issues associated with fuel alloy casting is the recycle of end trimmings off of the slugs, the residual casting “heels” that are left in the crucible, and slugs that result from molds that do not fill properly or have other defects that cause them to be rejected. Using the EBR-II alloying-in-crucible strategy requires the alloy be made up of virgin material and recycled material. Getting confirmation of the alloy composition and enrichment can become a time-consuming obstacle in the workflow. Casting a batch of alloy without the analysis can complicate material accountability and can result in an entire casting batch being rejected due to failure to meet the analytical specification. VTR concluded that a separate batching line would be beneficial to separate the fuel alloying and compositional analysis from the fuel alloy casting production schedule. A separate line can allow for more efficient use of recycled materials and can produce alloy in a form that can be readily weighed and remelted in the casting furnace. Residual casting dross from previous casting batches can be cleaned from the fuel alloy prior to remelting. Because of the size of the ARC-100 fuel slug, there may be a higher risk for silica contamination, and pre-batching the fuel alloy allows this potential impurity to be avoided.

Consideration of a separate line to clean and re-coat (using an airbrush) the crucibles that will be re-used is another possible way to reduce the time necessary to make the slugs.

Just as for the VTR, given the greater diameters of the slugs required for the ARC 100, optimization of the pallet holding the molds needs to be examined, in order to reduce the amount of waste caused by “bridging” between the molds

Given the material availability issue of HALEU, it is critical that a review of the past fabrication of U-Zr slugs be undertaken to verify the amount of fuel which had been considered “waste” and not used, and determine an approach by which such waste could be eliminated or significantly reduced. Using The presently available information is not directly usable because it addresses fuels that are

not only U-Zr , but U-Pu-Zr fuels, and the presence of Plutonium and accountability issues caused the products of the manufacturing to be considered as waste rather than re-use.

Specifically, as a result of the above, it is imperative to focus on means to minimize the amount of heels that cannot be recycled because of the presence of silica and silicon . Heels represent about 20% of the metal in a casting batch, and it is imperative that as much of the heels be recoverable.

Rod loading is another function that could benefit from the application of robotics. Like the other two robots, a simple arm robot equipped with machine vision will be to assist in the rod loading functions. The robot will be used to pick up fuel slugs, read bar codes, load the slugs into the cladding jackets, and handle completed fuel rods.

#### **4.7.5 Steps to ensure fuel fabrication will meet all requirements of its design during the commercial production**

This section describes the plan for fabricating a prototype fuel assembly and fabricating the core for the ARC 100.

##### **4.7.5.1 Manufacturing Specifications**

The first step in fuel reliability is repeatable and documented manufacturing techniques and technologies. Related manufacturing variables are measured, tracked, and modeled so that nuances of a fuel design or actual performance condition can be inspected against the actual database of fabrication variables. Fuel manufacturers, core designers, and reviewing agencies expect sufficient confidence that the models can be used to predict reliability and that the fuel is ultimately qualified for use in the ARC-100 fleet. This concept was used for both EBR-II and FFTF.

The factors related to ARC fuel manufacture in this section of the Fuel Qualification Program are:

- Develop the fuel specification to support the design and performance requirements of the ARC fuel and measure them. Because a source of HALEU has not been identified, the form the uranium will take cannot be specified. For EBR-II, uranium was procured from the Oak Ridge Y-12 plant in the form of “buttons.” The uranium enrichment and purity were specified in an ANL specific SPM-73-1. The total uranium content was required to be 99.8%, the sum of metallic impurities less than 2000 ppm, and the sum of nonmetallic impurities less than 1000 ppm. ARC Clean Technology expects that similar uranium content will be specified.
- For the zirconium for the EBR II ANL had specified zircalloy 3 as a requirement for acceptance. As stated in 3.2, finding a modern supply of zirconium that does not have hafnium as a significant impurity can be troublesome. Global Nuclear Fuel, LLC (GNF) proposed the VTR project look at using zircaloy-2 or zircaloy-4 as a ready supply of zirconium that would have low hafnium (hafnium has a relatively high neutron cross-section that must be accounted for in reactor operations).
- Track fabrication variables and the supply chain certification.
- Evaluate fuel slug grain structure as function of fabrication processes.

The specification prepared for the supply chain will have to address the tolerance/limits which are to be applied to the major components of the fuel rod (i.e., fuel slug, sodium bond, cladding, spacing wire, end fittings). The experience gained at EBR II and FFTF will be used to determine those tolerances and limits, with considerations that the dimension of the fuel rod for the ARC 100 are different from the corresponding dimension of the EBR II and FFTF fuel rods, and the present availability of precision-bored quartz tubing may cause the fuel slugs to be manufactured with less precision, and hence affect the fuel performance. AS an example, fuel slug ratcheting was never

observed in either EBR II or FFTF. Will that also be the case of the ARC 100 fuel slugs, if they are manufactured will greater variability in straightness , roundness, and end flatness? The material below provides a summary to the fabrication tolerances and limits applicable to the fabrication of the fuel pins for the ARC-100.

**4.7.5.1.1 Summary of Preliminary technical requirements applicable to the fabrication of fuel pins for the ARC 100 driver fuel assembly**

Cladding Requirements

The material is HT-9 but for prototyping a pin fabrication, only the ID and length matter and any steel material can be used.

The cladding external and internal surfaces are to be free of scratches, dents, scuffs or pitting that exceed 25 microns in depth (for prototyping only the internal surface matters)

Tolerance in diameter, length and thickness of the cladding tube shall be as follows:

- Outside diameter cm
- Inside diameters cm
- Thickness cm
- Length (before fittings ) cm
  - The bottom end fitting length (this fitting is used to line the pin in the bar where the spacing wire is welded . Its length is approximately  $11.0 \pm 0.5$  cm. This fitting shall be welded to the cladding tube before placement of the sodium bond and fuels slugs.
  - The top fitting is actually an additional length of tube where the seal weld is placed, with the additional length being not less than
- Variation in diameter over length:
- Straightness: $\pm 0.025$ mm(established for a fuel slug length of cm)

Cladding seal weld requirements (after placement of bond sodium and fuel slugs). The welding shall be performed by welders qualified to achieve the following requirements The discharge end of the plug end of the tube shall have a shape of approximately a hemisphere the diameter of which is the same as the OD of the cladding. The weld shall be free of cracks, undercuts, surface inclusions, and excessive surface oxidation, In addition the weld shall:

- Have 10% penetration of the cladding wall to plug end weld joint.
- A minimum weld thickness (root to surface distance less any porosity and inclusion) equal to or greater than 80% (0.4mm) of the cladding wall thickness and
- Be visually and radiographically inspected for defects (this may require a tighter specification, but for now this should do) and
- Be leak tested to verify leakage rate to be below  $10^{-9}$  cc/sec air.

Spacing Wire Requirements

Material HT-9 but for prototyping a pin fabrication, only the diameter and length matter and any steel material can be used.

Diameter mm

Length: (determined by pitch of wrapping)

Sodium bond Requirements

The bond sodium shall have impurities not exceeding 2000 ppm, with Oxygen present in no more than 100 ppm and the following impurities , in ppm, being limited to:

B-25; Cl-10, C-30, Cr-30, Li-5, K-1000, S-10

The quantity of sodium to be inserted in the cladding shall be sufficient to fill the space between the as fabricated fuel slugs, the diameter of which is \_\_\_\_\_ and create a sodium filled space in the gas plenum above the fuel slugs which is not less than \_\_\_\_\_ cm. Typically this would be \_\_\_\_\_

The 0.5cm can be either the space about the fuel or a combination of gaps between the slugs which are filled with sodium.

Insertion of sodium in the tube shall be via an appurtenance consistent with the method of insertion, e.g., a funnel or similar, to prevent contamination of the top of the cladding tube, which would jeopardize the quality of the seal weld performed after the slugs are inserted .

The presence of sodium in the specified amount shall be verified by weighting.

The plenum sodium shall be verified by radiography, with the pin resting on its tip.

The sodium bonding throughout the length of the fuel slugs shall by verified by radiography or eddy current testing to be void free to the extent that a gaseous pockets, shrinkage areas or non-wetting of the cladding and the fuel so not exceed 180° of the circumferential direction.

Insertion of sodium and slugs requirements

Insertion of the sodium shall be done in an inert atmosphere, by whatever means the fabricator decides upon.

The bonding of the d sodium to the cladding and fuel shall be done by heating the sodium to not more than \_\_\_\_\_ , in order to reduce voids in the bond sodium. Consideration should be given to vibrating the pins as the bonding takes place.

Fuel Slug

The fuel slug shall be an alloy of Uranium and Zirconium with the following composition:

90% U ±1.0%; 10% Zr ±1.0%; ( average over all samples, but any individual sample can have a variability of ±1.5%);. Impurities materials present in the slug cannot exceed 2000 ppm, with the impurity levels of the following elements being reported: C, Fe, N, Si, O, Y, Ta+Nb.

Physical dimension of the fuel slugs is to be as follows:

Length : \_\_\_\_\_ cm

Diameter : Average over length \_\_\_\_\_ cm; Local diameter \_\_\_\_\_ cm

Straightness: \_\_\_\_\_ cm

Porosity : \_\_\_\_\_ mm

The isotopic composition of the Uranium in the slugs shall correspond to the three different enrichment region and is summarized below.

**Table 4-4 Isotopic Composition of Uranium in Core Enrichment Regions**

Enrichment	Isotope	Weight % of Total U
A	U-235	maximum
	U-234 + U-236 + U-238	
	U-234 + U-236	
B	U-235	maximum
	U-234 + U-236 + U-238	
	U-234 + U-236	
C	U-235	maximum
	U-234 + U-236 + U-238	
	U-234 + U-236	

#### 4.7.5.2 Present status and schedule forward

The schedule for the ARC 100 facility designed under the ARC 20 DOE program (DE-NE0009223) is significantly longer than the more immediate need for a fuel prototype designed for an ARC100 reactor that would be built in Canada. Consequently, the ARC100 for which this fuel qualification program has been developed can take advantage of the separate Canadian program, which uses the same fuel. A request for a proposal for the Canadian Nuclear Laboratory (CNL) to fabricate the prototype fuel assembly for the Canadian ARC-100 has been prepared and is summarized below. Key to the proceeding with the work in four separate phases is the design and procurement of the equipment and supplies needed to fabricate the pins and then the entire assembly, and the location of that equipment in a suitable area at the CNL. To facilitate the design and procurement of the two furnaces (a casting furnace for fuel slug fabrication and a pin fabrication furnace, in which the fuel slugs are inserted, the bond sodium added while vibrating the pin, and the pin welded with appropriate upper and lower fitting,), help has been solicited from the Idaho National Laboratory (INL).

INL has a large number of documents on the design and operation of the furnaces, which can then be used by CNL to scale up the furnaces as required for the dimensions of the ARC-100 fuel slugs and pins. Reference [3.3] summarizes the information, with the stated documents providing significantly more details. A suitable number of slugs and pins to assure reliably repeatable manufacturing with training of operators etc., ARC Clean Technology will also have to establish a supply chain for the materials of fabrication. When fabricating the assemblies for the core, a source of suitably enriched uranium will also have to be available. The possible sources of HALEU are being currently explored. ARC 100 needs enrichments between 10 and 16% and at present two options of HALEU supplies are considered: purchase HALEU at 19.95% and LEU at 9.95% and down blend the two to achieve the desired enrichments, or purchase LEU at 9.95% and contract with URENCO to use the 9.95% LEU and enrich to the higher levels.

The four phases of the CNL fuel fabrication are summarized hereinafter.

#### 4.7.6 Phase 1 - Preparatory work that is necessary to proceed to the subsequent phases.

The first phase concentrates on the learning from INL, designing the equipment needed for only the pin fabrication (not the fittings), and locating it within a facility. ARC Clean Technology has had interactions with the Canadian National Laboratory (as part of its Canadian reactor effort) as well as GNF for the US ARC 100 in regard to a prototype pin fabrication. The CNL effort has proceeded farther than the US effort. If at CNL, amending CNL's license with CNSC is necessary to do the work. This phase is in progress. The casting furnace is a critical piece of equipment, which is rather complicated electrically, mechanically (vacuum) and thermally. We have contacted INL to obtain the fabrication and installation drawings, which could be made immediately available directly to CNL if they do not require an export license. These drawings are summarized in Reference [3.3] and are part of the set of documents we have received from INL. Detailed specification for the EBR II fuel slugs, and the training manuals are also available from INL, and the detailed specification will be used to update the preliminary one prepared for CNL (and GNF). Many of the requested documents (all those not requiring export license have already been made available to us, and the permit to send them to Canada has been obtained).

#### **4.7.7 Phase 2 - Procurement, installation, and testing of the equipment and the training of the CNL (or GNF) personnel in its use (Establishment of pin fabrication line).**

This phase will proceed based on the scaling (if necessary) of the drawings for the casting furnace and pin fabrications furnace. While the furnaces are procured and installed per the “scaled, if necessary” drawings, the training manuals and fuel specification will become available, which will then allow testing of the equipment and training of the personnel in its use. This will be followed by the production of pins with enough pins (300-400) produced to ensure the process is reproducible and the pins are of the right quality. The “quality” of the slug (reproducibility of slug within specification, i.e., consistency of chemical and physical composition of U-10 Zr, and dimensions of slugs within tolerances) is one of the keys to proper qualification of the fuel. The other is the control of imperfections in the cladding material and the control of the bonding of sodium to the slug so that there be no gaps between the slug and the inner surface of the cladding exceeding a specified dimension and spacing between gaps.

*Phase 3 – Establishment of fabrication line for the fuel assembly fittings.*

Assembly fitting (Upper and lower fittings, grid plate, orifice plate, hexagonal can) fabrication which involves a lot of complex machining within the capabilities of existing industry. This fabrication line work could proceed in parallel and be subcontracted to industry as it is basically a precision machining effort.

The advantage of a separate fuel assembly fittings fabrication line, not at the CNL, is that it allows CNL to focus on the pin fabrication line, which is by far the most difficult and prone to requiring several trials, and is also the one requiring new equipment, training personnel and possibly requiring addressing complex issues. That would not be the case if work is done at GNF.

*Phase 4 – Fabrication and testing of prototype assembly (Assembly fabrication line).*

This line is for assembling the fittings, the hex can, and the pins together in a fuel assembly then subjecting the assembly to a variety of tests. This fabrication line (overall assembly) would then be done back either at CNL, or under CNL’s direction, as measurements on bow and straightness, flow through the assembly, flow induced vibrations (etc.), would have to be done. Alternatively, this line could be located at another industrial fabrication facility, which has the facilities to conduct the necessary hydraulic tests. This fourth phase will not proceed until results from Phases 2 and 3 are satisfactory.

*Phase 5 - Fabrication of fuel , reflector, and shield assemblies for the ARC 100 core.*

This phase will proceed after successful completion of the tests on the prototype assembly and will take place at the fabrication facilities of a qualified, after the technology learned in the first 4 phases has been successfully transferred to a suitable, nuclear qualified vendor. ARC has been in contact with Canadian companies that have the necessary qualification.

It is noted that although for the prototype assembly the equipment may be sized specifically to produce a single assembly, when transferring the technology, the equipment must be scaled for the ARC required throughput, which basically asks that a total of 100 driver assemblies plus the reflector, shield and control assemblies be fabricated in about 4 years.

This means that for the ARC-100 the process of developing a prototype fuel assembly should start no later than early 2030.

## 5 FUEL SYSTEM DESIGN EVALUATION

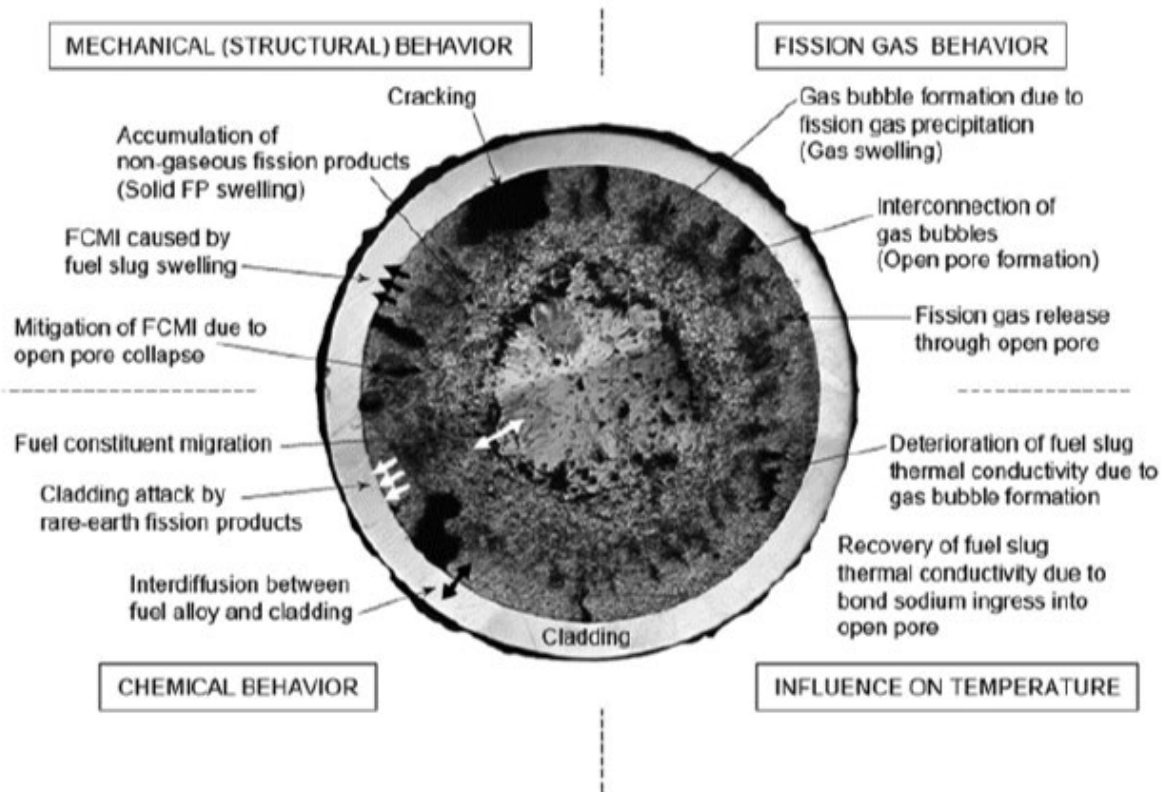
### 5.1 Important Phenomena

Figure 5.1 illustrates the phenomena which affect the performance of metal fuels, such as the U-10Zr fuel, which is the fuel type that will be used in the ARC-100. The metal fuel designs in operating reactors since that time, and presently being proposed, employ an appropriately sized gas plenum. Vented fuel pins (in lieu of the gas plenum) have also been proposed but have not found much acceptance because of the lack of operational experience. The ARC-100 fuel pin has a gas plenum which is 1.5 times the volume of the fuel slug volume.

#### 5.1.1 Formation of fission gas bubbles as function of burnup

In the early stage of irradiation (<1 at% burnup), most of the gas atoms generated by fission stay in the fuel slug and form gas bubbles. This leads to a gradual swelling of the fuel slug, driven by growth of fission product gas bubbles which continue to grow as the irradiation progresses. As stated in Section 3.2.2, high burnups in metal fuel are achievable by allowing the swelling of the fuel to not be constrained by the cladding. This is achieved by allowing an approximate 30-35% radial growth of the fuel, and by allowing fission product gases to escape into a gas volume designed so as to limit the hoop stress generated by the resulting gas pressure to a tolerable level, which for the type of cladding employed is below 150 MPa. The radial expansion is allowed by designing the diameter of the fabricated slug such that the “smear density” of the fuel is or less. The smear density is defined as the areal density of as-fabricated fuel inside the as-fabricated inner wall of the cladding. It is expressed as a percentage determined by the following:  $100 \times (\% \text{ of theoretical density}) \times (\text{square of fuel outer diameter}) / (\text{square of the cladding inner diameter})$ . A smear density of is important to allow radial expansion of the fuel slug during irradiation so that the resulting fuel to clad mechanical interaction (FMCI) load on the clad is quite small when compared to the load created by the generated fission gas pressure. In the low smear density ( fuel pin similar to that used in the ARC-100, where about 30 vol.% or larger swelling is allowed, further irradiation increases the population and volume of the bubbles and causes coalescence among them.





**Figure 5.1 Phenomena Involved in Metal Fuel Irradiation [61]**

The choice of the smear density is made in consideration that sufficient swelling of the fuel can occur (a when the fuel has expanded approximately 25 % volume ) so that gas release by interlinkage of porosity due to gas bubble occurs before the fuel pin contacts the cladding. Following contact with the cladding, the continuous release of gas to the fission gas plenum has been established, and this reduces the potential for fuel cladding mechanical interaction (FCMI). At high burnups, the additional accumulation of solid fission products creates the potential for FCMI with increasing burnup.

As the fuel expands its thermal conductivity deteriorates due to gas bubble formation, but as the bubbles interconnect, and the gas escapes to the gas plenum, the bond sodium ingresses into the pores and the thermal conductivity are partially recovered. The recovery continues as solid fission products build in the fuel slugs. The change in thermal conductivity over time is accounted for in the deterministic safety analyses.

### 5.1.2 Radial and axial expansion of the fuel matrix.

The fuel expansion (swelling is driven primarily by the internal pressure of fission gas bubbles, and reference [62] provided a theory, confirmed by later experiments, that once the fuel swells about 30 % in volume, the fission gas bubbles interconnect and provide passage for fission gas to be released to a plenum located about the fuel rod. By adequately sizing the plenum to contain fission gases released through the interconnected porosity, the fuel swelling can be easily constrained by the cladding and a high burnup can be achieved. The porosity is also available to accommodate the swelling from accumulation of solid fission products as irradiation proceeds. The fuel swells both radially, until it contacts the cladding, and axially.

The fuel swelling has been found to be anisotropic [27]. In particular, the axial swelling is consistently lower than the radial swelling. Figure 4.4 presents irradiation test data of fuel slug axial elongation. After rapid swelling in the early stage ( $\sim 2$  at.%), the elongation levels off at an asymptotic value of 2–10%, depending on the plutonium content. The possible dependency on fuel slug diameter is less clear. Figure 4.4 shows that the dependency on diameter of the slug, if any, is minor. The indicates a leveling off of the axial elongation, which is due to restraint by the cladding after contact of the swollen fuel slug with the inside of the cladding [45]. In a fuel pin of Smear Density (SD) (%), radial deformation of the fuel slug causes contact with the cladding; for example, in a fuel pin of 72–75% smear density, slug radial deformation at contact is 15–18%. Therefore, the test data in Figures 4.4 means that the fuel deforms more in the radial direction than in the axial direction. This anisotropic deformation may be attributed to the stress state of a whole fuel slug, which is similar to that of a thin cylindrical shell subjected to internal pressure [45]; the radial-to-axial stress ratio in the shell is about 2:1. This idea is based on the assumption that the central hotter part of the slug swells at a higher rate than the peripheral colder part, where the creep rate of the slug is small [45]. In fact, extrusion of the slug's inner part into the radial crack in the peripheral region was observed in an irradiated metal fuel cross section [45]. This suggests that the inner part of the slug swells at a higher rate than the peripheral part. Other factors that cause anisotropic deformation may be grain boundary tearing, cavitation void swelling, and/or cracking in the peripheral region. This trend can be attributed to cracking and irradiation growth in the peripheral region explained by Hofman et al [52] as shown in Figure 5.2 Fuel slugs of higher plutonium content ( $\sim 8$ -26 wt%) are brittle so that radial cracking occurs in the early stage of irradiation; radial cracking accelerates the time of slug-cladding contact, thereby suppressing the axial elongation. A proposed model correlates the anisotropic deformation with the plutonium content and the radial temperature gradient of the fuel slug [63].

Furthermore, this anisotropy increases with increasing plutonium content of the metallic fuel alloy. The primary reason for this phenomenon is due to the difference in swelling behavior (the radial temperature distribution in the fuel slug has a hotter central zone with cooler peripheral zone). In the central zone, the  $\gamma$ -phase of uranium dominates, while on the outer periphery the  $\alpha$ -phase of uranium dominates. These phases have different swelling characteristics, which leads to anisotropic behavior. This behavior is shown in Figure 4.4. It is seen that the alloys with no plutonium (maximum uranium content) have the largest axial growth, while those with the higher plutonium (minimum uranium content) content have lower axial growth. There is no noticeable dependency on fuel slug diameter, with the fuels of smaller diameters, whether without or with plutonium, experiencing a percentage axial elongation quite similar to that of greater diameters.

The radial expansion of the fuel slug is limited by the inner diameter of the cladding, and since the ARC-100 fuel, pin is designed to have a smear density of the radial expansion is limited to approximately of the fabricated fuel slug diameter.

Because of the scatter in the data pertaining to the axial expansion, ARC had to make a choice for the value to assume in the deterministic safety analyses. At the beginning of life, low burnups, the axial expansion is limited to values of 5% or less, but above a few at% burnup the axial expansion is significantly higher. ARC could have assumed the lowest axial expansion for burnups in excess of 4 at% (from Figure 4.4), which for U-10Zr is about 5 %) could have resulted in an underestimation of the needed fissile content of the core, with the consequence of the core not being able to go critical at a full axial growth, which is much greater than 5%. Therefore, ARC chose to use the most likely value of at low burnups and will continue to use this value in the deterministic analyses. The

deterministic safety analyses at the beginning of life, therefore, are run under two assumptions. One is the fuel has not yet expanded, and the other it has fully expanded. ARC will find out during the startup physics tests how deeply the control rods will have to be inserted prior to achieving 1.5 to 2 atom% burnup. If the actual axial expansion turns out to be less than the assumed the difference will be accommodated by deeper insertion of control rods. The deterministic analyses will be rerun for the actual value of the axial expansion, since the deeper rod location affects the TOP transients at BOL, an easier problem to deal with than having to increase enrichment and remanufacture of the assemblies and reload of the core, if the initial fissile content is underestimated. The ARC-100 peak burnup is approximately at% at core discharge. For lower burnups the assumed axial expansion will either be % or a value dictated by a periodic PRD measurement. Measurement of the Power Reactive Decrement during start up and periodically during operation will indicate whether the assumption of % regarding the axial expansion is correct.

### 5.1.3 Potential fuel Slug Ratcheting

In the early days of metal fuel development, ratcheting of the fuel slug within the pin was considered an issue and specific design features were employed to prevent or minimize its occurrence. For instance, at the EBR II reactor, the early fuel pins were designed with a restrainer (dimples) located at the top of the fuel slugs to prevent the fuel slug from somehow ratcheting up in the cladding and later dropping down to add unexpected reactivity. Unfortunately, the presence of such restraint caused cladding “failures” at its location.

Many experiments were conducted in EBR-II that ultimately demonstrated that a restrainer was not needed, because ratcheting did not occur [59]. At the EBR II, with single slugs within their pins, ratcheting was specifically looked for, but never observed. Then, later on for FFTF with 2 or 3 slugs, ratcheting was watched for again and was again not observed. It is notable that no ratcheting was observed for short slugs as well as longer slugs, with lengths approaching the slug length of the ARC-100 fuel ( ). FFTF slug lengths varied from approximately 35 cm to 45 cm.

Is upward ratcheting of the ARC fuel slugs a possibility? It is not unimaginable that the three cast fuel slugs inside the clad would separate axially during the initial and subsequent heat-ups, then at a later time, for some unexplained reason, drop back down—adding reactivity. Therefore, in principle, the possibility of ratcheting cannot be dismissed, even though it has not been observed in sodium bonded metal fuels. It is possible to visualize that it could occur during period of heating and cooling due to friction/imperfections between the fuel and the cladding which prevent a fuel slug from returning (for a time) to its original position during cooling. Assuming it occurs, first the slug (or multiple slugs) has to ratchet up, and that motion is accompanied by a detectable loss of reactivity. Thus, it is possible to calculate what would happen if indeed for whatever reason the slug drops back down in terms of a positive reactivity insertion, with the positive reactivity added being equal to the negative reactivity loss that was experienced as a result of the ratcheting, and determine whether it would or would not have a damaging safety effect since at worst, this would have the same effect as an unprotected reactivity insertion.

How such a determination would be made is explained in the following. First it is not realistic to perfectly predict (by calculation) the manufactured core reactivity. Therefore, the core designer must ensure that at the beginning of life, the core fissile mass and geometry (as cold critical) is such that, accounting for manufacturing uncertainty of actual fissile loading in the cast slugs (vs specification) and calculation uncertainties, the core can go critical at the end of life. Second, as the core goes hot critical, the Power Reactivity Decrements are measured (which determines how deeply the control rods have to be inserted at full power with zero burnup) and compared to the calculated one. Any mismatch will

be due to a combination of effects that account for the discrepancy. We will not know which effect has caused the discrepancy but we do know is that it isn't fission gas driven axial fuel growth that is responsible because no gas is yet generated}, and we can reasonably POSTULATE that it is unlikely to be due to axial ratcheting of the fuel slugs because the OD of the slugs is < the ID of the clad, so they don't yet scrape against each other. Third, as the core approaches 1.5 to 2 % burnup, where the gas driven expansion drives the fuel OD out to touch the cladding ID, the PRD is periodically measured. The expectation is that it will go down in amplitude due to gas driven elongation of fuel slug and it is possible to approximately calculate by how much. If the PRD decrease in amplitude exceeds the expected by a significant margin (e.g., exceeds 30- 35 cents}, the reasons for the discrepancy are investigated. At this point it is not possible to categorically determine that if it is not gas driven (i.e., the decrement is in excess of what could be accounted by gas driven expansion only) then it must be due to ratcheting, because it may be due to a combination of both, and other reasons. However, the reactivity effect is now determined and if it is within the limits than meet the single most reactive rod withdrawal without scram (~ \$), the reactor will have inherent safety characteristics. However, if the reactivity decrement is greater than the limit, core changes can be made, e.g., reflector assemblies can be removed, so that the control rods need less depth of insertion.

The response of the ARC-100 to unprotected reactivity insertion has been determined to have no adverse consequences on safety, provide it is limited to insertions of less than cents [7,8]. The ability of the ARC-100 to withstand unprotected reactivity insertions without damage can be confirmed at any time during its operation by means measuring the three coefficients of the quasi-static reactivity balance equation (see Appendix E)

The possibility that ratcheting could introduce a large enough amount of positive reactivity to offset the reactor's capability to self-adjust, and not be noticed as a reactivity loss vs the expected reactivity, is very small. The core has a total of over pins, and a significant fraction of them would have to ratchet to cause such effect, and then the effect would have to be missed.

To verify the above, an estimate has been made of how "bad" the ratcheting could be. It is assumed (ratcheting was never observed in EBR II or FFTF) that unexpected ratcheting of some fuel slugs occurs. The assumed ratcheting considers that the fuel expands axially during irradiation, and that changes the PRD from what it would be if no axial expansion takes place are not noted by the operator. The fuel also expands and contracts thermally during cycles of heat up and cooldown. Upon cooldown down, the fuel contracts, but hangs up in the top portion, therefore not returning as much fuel into the center part of the core as expected (as the worst example of ratcheting). Based on the thermal expansion coefficients provided in the Metals Fuels Handbook, it is calculated that conservatively one could estimate the possibility of pin ratcheting to a height which is cm above the top of the original fuel top location, when it is heated from an initial temperature of 200C to a temperature of about (3σ peak fuel centerline -depending on whether it is during BOL or EOL.)

From knowledge of the worth of the fuel, based on the input to SAS for fuel worth for reactivity calculation, it is calculated that the movement of cm of fuel from a single assembly (assuming all of the pins in that assembly ratcheted the same amount, which is extremely conservative) would corresponds to 4-4.5 cents of reactivity. ANL with a similar assumption determined the worth to be cents. Analysis of an unprotected reactivity insertion has shown the reactor being inherently safety with an insertion of 47 cents. Therefore, the reactor will take care of itself even if ratcheting occurred in 10 or so assemblies, which is rather incredible. Most importantly, however, is the fact that such a large change of reactivity would be immediately picked up by the PRD, and action would be taken.

While this analysis is only an approximate one, made on the basis of the fuel worth being estimated to be uniform axially (at the top the fuel is actually worth less), and moreover based on a worth per mass

of fuel which is correct for small changes in density, whereas the motion of cm out of may be considered more than a small change; one can have high confidence that an accurate neutronics analysis would confirm the worth of possible ratcheting would be a few cents per assembly, and were it to occur the reactor would self-adjust to the addition of reactivity that the fall back of the assembly in the core would have.

#### 5.1.4 Fuel Constituents Redistribution

Constituent redistribution in a metallic U-Zr/U-Pu-Zr alloy fuel is a commonly observed irradiation phenomenon. As shown in Figures 5.2 and 5.3, the microstructure of the irradiated fuels exhibits three distinct concentric zones. They are a Zr-enriched central zone, a Zr-depleted and U-enriched intermediate zone and a slightly Zr-enriched zone on the outer periphery. The presence of Pu in amount greater than 8% enhances the redistribution of U and Zr. For the ARC 100 % Pu is the maximum amount generated in the peak burnup fuel, at the end of life and therefore the Pu content is always less than %.

Figure 5.3 shows the temperature dependence of the redistribution, where a wider redistribution middle ring is formed at the top of the fuel (where the fuel is hotter) compared to the lower part. The annular zone structure is also characterized by differences in porosity.

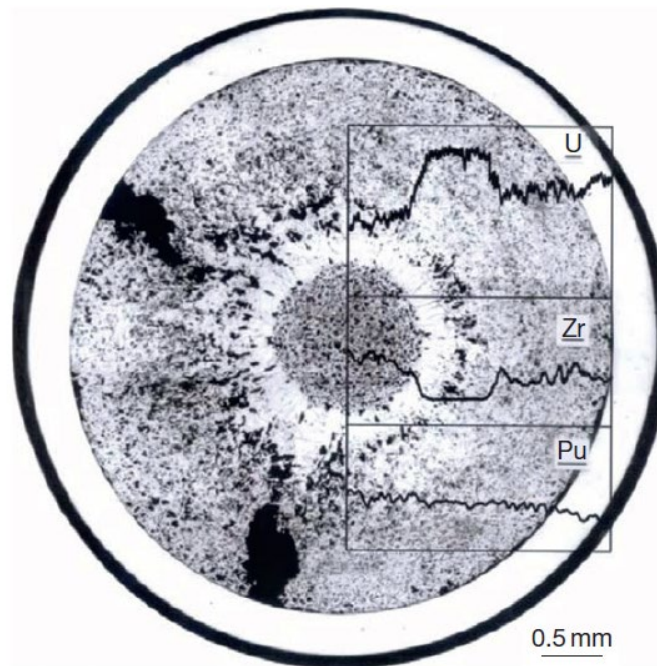


**Figure 5.2. Optical micrography and measured constituent redistributions of U–19 wt% Pu–10 wt% Zr fuel at 1.9 at.% burnup. Reproduced from Ref. [65]**

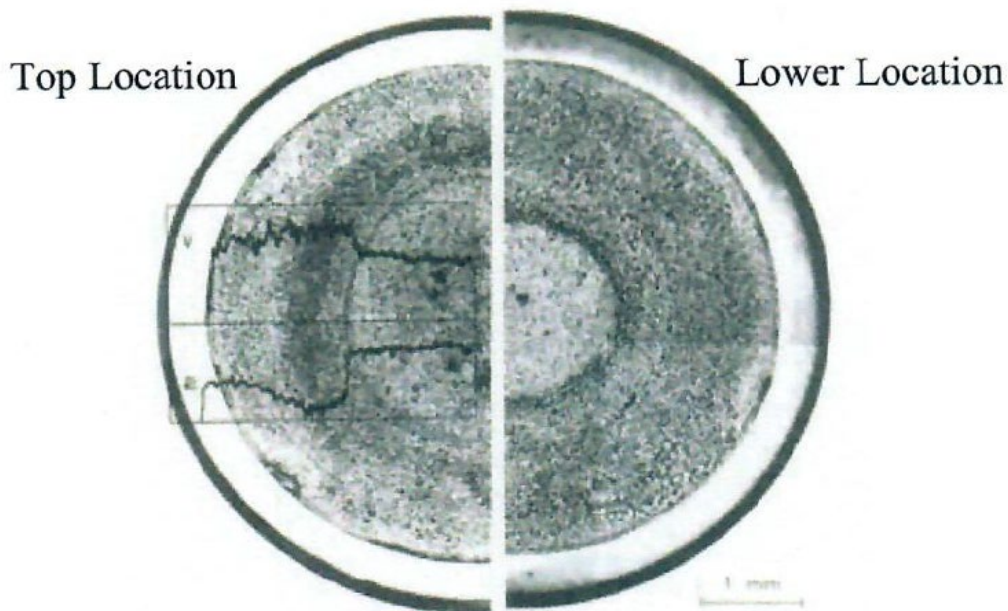


**Figure 5.3 U-10Zr at 10at% burnup (DP-11 from X447 at different axial locations. Reproduced from reference [66])**

There are a number of performance degrading issues associated with this phenomenon. The reduction of Zr fraction in areas within the fuel reduces the fuel melting point (solidus) during accident sequences (and this reduction is taken into account by the SASS-4A/SASSYS-1 code used to analyze the accident sequence). During normal operation, the temperature drops across of the ARC-100 fuel is normally less than  $8-60^{\circ}\text{C}$  (nominal and with a  $3\sigma$  uncertainty), and the temperature drop across the fuel/cladding gap is negligible because of the sodium bond. [2] This leads to peak fuel temperatures (nominal  $604, 670^{\circ}\text{C}$  with  $3\sigma$  uncertainty) that are dictated by the limit on the HT9 cladding peak temperature. The latter is a steady state temperature below  $600^{\circ}\text{C}$ . Thus the peak fuel temperatures are far from the melting point even in regions where the Zr is depleted (for the ARC-100 the peak temperature has a margin to boiling of about  $380^{\circ}\text{C}$  with a  $3\sigma$  uncertainty).

A more significant effect of redistribution is its impact on the fuel swelling rates and axial fuel growth. The multiphase regimes across the fuel radius, due to the redistribution phenomena, have different growth rates that play a part in observed metal fuel anisotropic growth. For the U-10Zr fuel used in the ARC-100 the data presented in Figures 4.4 indicates that the absence of Pu allows the fuel to grow more axially. The axial swelling occurs as rapidly as the radial swelling and effectively ceases once the contact with the clad is reached. Isotropic swelling would be expected to produce a growth of approximately 15% in the axial direction. That growth is not achieved because of the anisotropy caused by the redistribution and possibly by the lock up effect due to friction once the fuel comes in contact with the clad. For design purposes, it occurs early-in-life and sufficient data exist to conservatively estimate the amount of axial growth. From Figure 4.4, ARC has chosen to conservatively assume a zero-axial elongation at low burnups and an 8% axial growth at burnups exceeding 4 at%. These figures used data from EBR II only, because there was only one post

irradiation examination of U-10Zr pins in the IFR experiments in FFTF. The PIE showed axial growth to be slightly less than that of the experiments in EBRII, but still of the order of %.

Although PIE was not performed for other full length FFTF pins, measurement of the assemblies' outlet flow temperature during the first several weeks of irradiation provides an indication of the extent of the axial growth in the assemblies. The drop in temperature shown in Figure A.1 5.1 of Reference [2] cannot be explained by fuel depletion effect but was the result of axial growth of the fuel out of the active core region. The observed decrease in coolant temperature change through the assembly exceeded 3% which can be correlated to about 7% axial growth [64].

### 5.1.5 Fuel Cladding Chemical Interaction

Fuel-cladding chemical interaction is shown schematically in Figure 5.4 which shows two possible cladding wastage mechanisms. One is the formation of a low melting point phase (a eutectic formation) at the interface of the fuel and the cladding, which can occur during transients in which the cladding temperature exceed 650°C (actually closer to 715°C). The other is the creation of a ferritic layer which can weaken the cladding. Prior accumulation of lanthanides fission products at the fuel cladding interface (due to fission product migration), is characterized by the ferritic layer formation which could be the result of decarburization of the martensitic cladding, as shown in Figure 5.5. The eutectic formation is discussed in the next section and Appendix B.

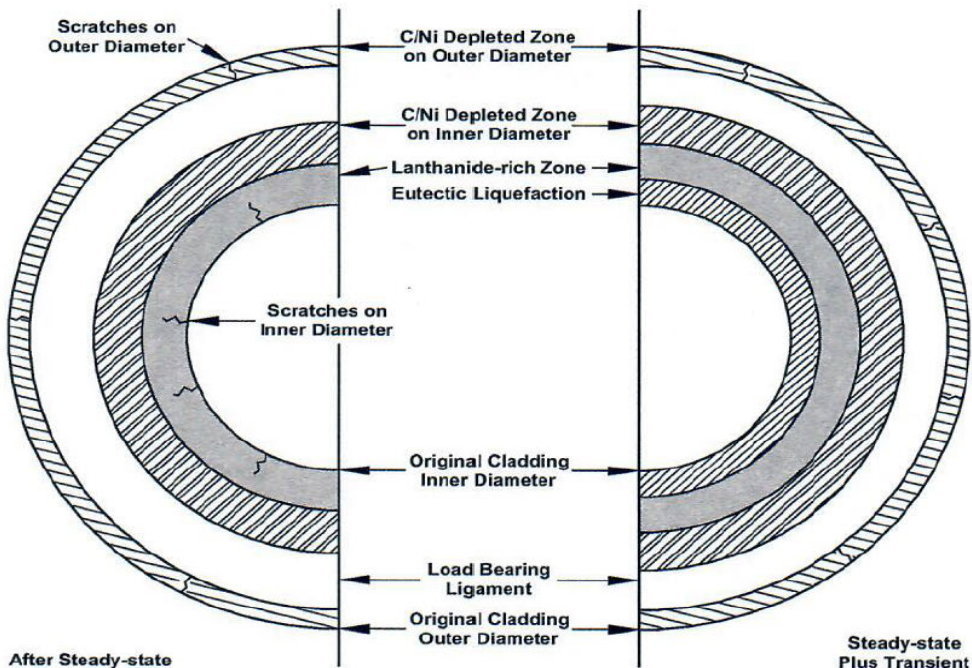


Figure 5.4 Cladding Wastage Mechanisms

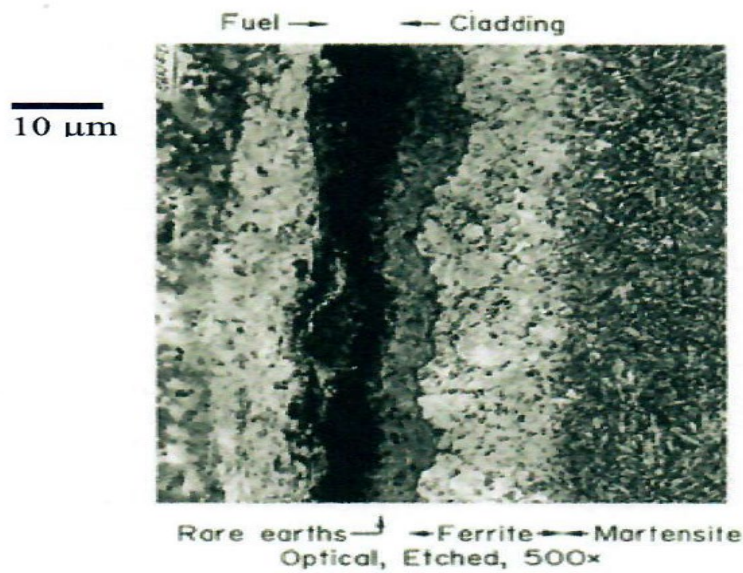


Figure 5.5 Fuel-Cladding Interdiffusion of U-10Zr and HT9 , in Pile, after ~6 at burnup at ~620°C [66]

#### 5.1.5.1 Eutectic formation for planned fuel as function of temperature, and fuel composition

The source of the eutectic liquefaction at the interface of the fuel and the cladding is the metallurgical interaction of metallic U-Zr fuel, with or without fission products, with the iron base cladding to form a low melting point phase. In equilibrium, the liquid eutectic phase has been observed at a temperature as low as 726 °C for an alloy that is 89% uranium. This liquefied region at the fuel/cladding interface is formed only if the fuel slug is in contact with the cladding, the contact temperature is sufficient to cause eutectic alloy formation, and the temperature remains elevated long enough to sustain the eutectic liquid formation. The primary importance of the eutectic liquid formation is the thinning of the cladding, reducing its ability to contain the internal pin pressure from the accumulated fission gas. Although a very slow process at low temperatures, eutectic liquid formation can lead to accelerated cladding failure at elevated temperatures [33].

Appendix F provides the correlations (equations) used to predict the formation and extent of eutectics as a function of time and temperature. These correlations are employed in the deterministic safety analysis[7] of the ARC 100 reactor and in the codes [12,13] used to determine fuel performance.

#### 5.1.5.2 Fission products (*Lanthanides*) migration as a function of temperature and concentration gradients

The other phenomenon that produces a fuel clad chemical interaction detrimental to the performance of the fuel is fission products migration, specifically the lanthanides, to the fuel/clad interface. Lanthanide fission products accumulate at the fuel slug cladding interface. As the concentration of lanthanide elements increases, by diffusing down the temperature gradient, at the cladding surface metallic compounds including eutectic compositions can form. These products result in cladding thinning. Clad thinning depends primarily on the peak temperature of the fuel, the



peak temperature of the inner diameter of the cladding, and the peak power in the pins, where the lanthanides are in the greatest concentration. So, this FCCI formation is clearly dependent upon burnup and temperature. For eutectic liquefaction, solely dependent on temperature and time at temperature of the fuel/clad interface, correlations have been established which are reliably applicable to steady state and transient conditions. The FCCI caused by fission product migration, however, is a complex phenomenon, which while reasonably well understood, can be estimated by correlations the prediction accuracy of which may be limited to the range of operational/experimental temperatures, burnup and times at temperature from which those correlations were developed. The ARC 100 burnup and temperatures fall within the experimental range, but the time at temperature is considerably longer.

Empirical relationships for this FCCI have been developed from a reasonably large body of data collected from in-pile (EBR-II), some from FFTF, and out-of-pile experiments. These relationships (correlations) may be questionable in predicting FCCI outside the range of experimental data. However, for the past several years, advances have been made on mechanistic modeling. As opposed to heavily empirical models that have been used to model FCCI in the past, mechanistic models embodied in the computer code BISON at the INL and the MFUEL module of SAS4A/SASSYS-1 codes, both of which is founded on the fundamental physics that drive inter-diffusion, allows the models to capture the behavior of diffusion couples, irradiated pins, and the advanced fuel/cladding combinations. BISON is the principal code used by ARC to predict fuel performance. The degree to which BISON has been able to capture the behavior of the FCCI is documented in Reference [12].

The method for capturing FCCI inter-diffusion, and predicting how it can happen over time, can take several different forms. The simplest implementation may be formulating empirical diffusion coefficients based on the diffusion-couple experiments. By changing the activation energy and pre-factor in an Arrhenius diffusivity relationship it may be possible to capture the behavior of the reaction zone as a function of alloying constituents (U, Pu, Zr, Fe, Ni, Cr) and impurities (lanthanides, oxygen, nitrogen). This is the approach followed by a group of Japanese scientists [20], and their results are discussed in this section, together with a modified approach which accounts for the proper presence of the lanthanide within the fuel alloy. Unfortunately, these models will still be heavily empirically based. Therefore, when determining the effect of FCCI on the cladding, at present the best approach is to compare the results obtained by both the empirically based models and the more physically based methods for capturing FCCI, such a use of the BISON [12] code and the MFUEL module of SAS4A/SASSYS-1 [13].

Fortunately, both empirically based modeling as well as physically based approaches indicate that the reaction rates are slow, and an incubation period prior to FCCI formation has been noted to approximately 2 at % burnup prior to observing an interaction [68]. **For the ARC-100, a 2 at% burnup corresponds to at least three years of initial operation. ARC plans to utilize this period during which this FCCI is known to NOT have an adverse effect on the facility safety and performance, to prepare for the subsequent fuel surveillance program which will verify FCCI data specifically for its fuel, by extracting periodically an assembly from the core, and conducting both non-destructive and destructive examination of the fuel.**

Since growth of the FCCI layer, which reduces the strength of the cladding is slow, the extraction of an assembly to determine actual condition of the fuel pins, can be delayed until such time that the growth is significant, but well below an amount which would challenge the integrity of the cladding. Cladding integrity can become challenged when the overall FCCI growth approaches 50  $\mu\text{m}$ . Prediction of the growth of the layer by the equation 5.2 (equation 5.1 from Reference [20] modified to account for the percentage of lanthanides present in the fuel ), show that at the temperatures in

which the fuel/cladding interface would operate (uncertainty for the ARC 100 fuel), such thickness would require about 14 years in the peak burnup pins where the lanthanides would be approximately 2-3% of the fission products. This is the reason why it is proposed to extract the first assembly initially after year 4, when the early phenomena will be manifest, and then to be nondestructively and destructively tested not sooner than year 12 of operation (possibly year 14) as shown in Appendix A.

The use of equation 5.2 to predict the possible lanthanide induced layer is justified only to the extent that it provides guidance on how soon the layer might build to an extent that it could cause significant weakening of the cladding, and suggesting an appropriate time when pins should be extracted for the core to demonstrate actual fuel performance. It is not suitable to determine actual fuel performance, since the overall performance involves other phenomena. It is, however, suitable as a check for the layer thickness computed by the fuel performance codes.

Reference[20] developed a correlation which as stated would help predict the extent (thickness) of the FCCI zone (portion of which acts as wastage in the cladding and some of which will be within the fuel). The thickness of the FCCI layer is given by :

$$\delta = K^{0.5} * t^{0.5} \tag{Eq. 5.1}$$

where  $\delta$  = thickness (m);  $K = 4.35E5 \times \text{EXP}(-38800/T)$ ; T is the temperature (K); and t = time (sec).

When comparing the layer thicknesses calculated by equation 5.1 the limitation of the equation becomes obvious. X477 irradiated the pins to 4.7 at % during a period of 284 EFPD and the test was then interrupted. Examination of the pins showed all elements to be intact and in good shape. The testing was then resumed for another 335 EFPD, until burnups of about 10 at% were reached. Failure of two pins occurred as previously reported in Table 4-2. The equation significantly overpredicts the depth of the layer (as shown by the yellow circles in Figure 5.6). The equation implicitly assumes the buildup of the layer begins immediately, while in reality it cannot begin until the slug contacts the cladding, which typically occurs at 2 to 3at% burnup. Even when a correction is made to define time zero as the time when the fuel has radially contacted the cladding, the predictions of equation 5.1 are still very conservative (shown as the red circled yellow dots in Figure 5.6). One of the reasons for the conservatism of the equation is its development relied on the data obtained by reacting a mix of pure lanthanides (denoted as RE5) with the cladding. The actual percentage of lanthanides present in the fuel of the experiments of Table 5-1 varied, but at the burnup achieved by those fuels' pins, it is determined to be approximately 2.3%. Table 5-2 shows the quantity of lanthanides in the ARC 100 core at the End (EOL) and Middle (MOL) of life.

**Table 5-1 Quantity of Lanthanides in ARC 100 core at End (EOL) and Middle of Life (MOL)**

	La	Ce	Pr	Nd	Sm	Total Lanthanides	Total Fuel	Lanthanides as % of Fuel
EOL (kg)	69.8	131.0	65.9	202.0	51.5	500.2		
EOL (%)	13.41	25.21	12.65	38.83	9.9	100		
MOL (kg)	39.4	76.1	37.0	125.0	25.9	302.4		
MOL (%)	12.98	25.04	12.19	41.27	8.53	100		
RE5 (%)	13	24	12	39	12	100	None	N/A

The relative percentages of the ARC 100 fuel at MOL and EOL are comparable to those of the RE5 mix used by Reference[20]. The burnup achieved by the ARC 100 fuel at EOL is comparable to the burnups experienced by X447 and MFF3. Therefore, it is expected that the percentage of lanthanides in X447 and MFF3/5 is close to the ARC 100 percentage at EOL. Examination of the data provided in Table 5-2 indicates that fuel centerline temperature and temperature gradient have an indirect effect on the buildup of the layer, i.e., they drive the cladding temperature, which seem to be the dominant effect on the layer. For instance, MFF3 behavior was not that similar to that of MFF5. The temperature gradients at which FCCI was noted were 166° C/cm at a location where the burnup was 5.7at%, and 185 °C/cm at a location where the burnup was 8.1 at%. Intuitively one would have expected the FCCI to be greater in the second location or at least for the two depths to be similar, but in fact the reverse was true. The first location had a depth of 152 and the second of only 76 . What was identical behavior is that at a third location where the burnup was 12.4at% (highest concentration gradient) , but the cladding temperature was only 550°C, even though the temperature gradient was greater 561°C/cm) NO FCCI was noted. . The cladding temperature must have a dominant effect on the extent of FCCI. This tentative conclusion seems confirmed by other data from Table 5-3.

MFF5 had a centerline temperature of 709-736 C and corresponding cladding inner diameter temperatures of 635°C and 612°C. The one with the lesser temperature gradient (709-635)/0.574=129 °C/cm, had less FCCI because at that location the burnup was only 4.8 % i.e., the gap between the fuel and the clad might not have been closed for very long and had lesser temperature and concentration gradients driving it. The other which had a greater temperature gradient (736-612)/0.574=216°C/cm also had a greater burnup of 8.1 at%. Not surprisingly the one with the greater burnup and gradients also had the greater FCCI thickness. However, at a location where the burnup was actually higher (9.8at%)r, and the temperature gradient (712-556)/0.574)=175 °C/cm quite comparable to that of the other location, but where the temperature of the cladding inner surface was much lower than at the other locations, no FCCI was seen. The same is also noted in the EBR II data discussed below. This might mean there is a threshold temperature at the inner cladding diameter below which the FCCI either does not occur or occurs in much more limited amount.

X447 inner diameter is only 82% of the FFTF diameter. Because this experiment was intentionally a high temperature experiment, the temperature gradients are higher than those in FFTF .

Pin DP69 had gradients of about 174°C/cm and very low burnups (2.4-2.7 at%) where the greatest depth of FCCI were noted. In regions of higher burnup (4.8-4.9) and similar gradients, no FCCI was noted, but in those regions the cladding inner surface temperature was below 552.

DP04 had universally high fuel centerline temperatures with all locations around 693-705 (it was one of the two which failed!)and burnups high enough to ensure contact between the clad and the fuel. FCCI was seen at all locations, but it was less at the lowest clad temperature (606°C).

The same can be said for pins DP 70 and 75. All locations have sufficiently high burnup to ensure contact between the fuel and the cladding. The location of the greater FCCI layer depth were not at the locations of the higher temperature or concentration gradients, but at the location of the higher cladding temperatures, with no FCCI noted at temperatures of the cladding below 533°C.

The conservatism of equation 5-1 and the conclusion that cladding temperature dominates the FCCI layer build-up, justifies an adjustment of equation 5-1 by multiplying it by the percentage of lanthanides in the fuel and applying it strictly to the cladding temperature.

$$\delta = (\%L) K^{0.5} * t^{0.5} \quad (\text{Eq. 5.2})$$

where %<sub>L</sub> is the absolute percentage of lanthanides in the fuel matrix in contact with the cladding.

Table 5-2 compares the measured FCCI layers to those predicted by equation 5.2 predicted FCCI layers, when the predictions are corrected for time of irradiation, differences in temperatures and percentage of lanthanides. Two values are given for Reference [20]. One value is from equation 5.2, developed for the interaction of the RE5 with different cladding material, including HT9, and the greater values are taken directly from the single test conducted with HT9. The predicted values, when corrected for the percentage of lanthanides, agree reasonably well with the measured ones. Their range is also plotted in Figure 5.6.

Keiser [68] provides summaries of the element trace analyses performed on a variety of metallic fuel and cladding combinations irradiated in the EBR-II and reported that the fuel side of the interface, Fe and Ni are both found to diffuse into the fuel. On the cladding side, fission products (Ce, Nd, and Sm) diffuse the deepest into the cladding region. The conclusions from reference [69] are summarized below:

- The lanthanide fission products penetrate deepest into cladding, forming phases with Fe and Ni.
- For binary, U-Zr fuel (like the ARC-100 fuel), uranium penetrates the cladding.
- Of the steel cladding constituents, Fe and Ni diffuse in the fuel and form phases with U and Zr. Cr becomes enriched at the cladding interface but does not penetrate into, nor react with the fuel.
- Near the fuel-cladding interface, light and dark contrast (high Z and low Z) phases can be observed on the fuel side of the interface that contain lanthanide fission products and Pd. Precipitate particles containing Zr, Mo, Tc, Ru, Rh, and Pd are observed in the fuel near the cladding.
- The Zr ring typically found on the outer surface of the as-fabricated zirconium alloyed fuel slugs made using injection casting methods, is a barrier to interaction and remains intact at lower fuel temperatures and lower power during operation, but later breaks up.
- Maximum fuel-cladding interaction occurs at the combined high power and high temperature region of a fuel pin.

This latter observation is important because it reflects the differences in this FCCI between short fuel elements used in experimental reactors and the much longer ones that will be used in the ARC-100.

The data obtained for EBR II reflects fuel pins of 74.9 cm total length, with a fuel slug length of 34.3 cm, reached cladding peak temperatures and high power at nearly the same location near the top of the fuel region where the significant FCCI occurred.

In FFTF, pins (MFF5 pin I95011 and MFF3 pin I93045) that had nearly the same burnup, temperatures and power as those irradiated in EBR II (X447X447A pins DP04, DP-11, DP-70 and DP5), were substantially longer (total pin length 238.1 cm, fuel slug length-91.44 cm, cladding diameter-6.86mm and clad thickness -0.533-0.559mm), attained peak linear power at nearly the midpoint of the pin, while the peak temperature occurred still near the top of the fuel. Consequently, the FCCI manifested itself at the location where the two combined were highest. That point is approximately 1/3 from the top of the fuel region. Results for the ARC-100 fuel are expected to be similar to those of FFTF. Table 5-2 from reference [67] summarizes the results of these tests.

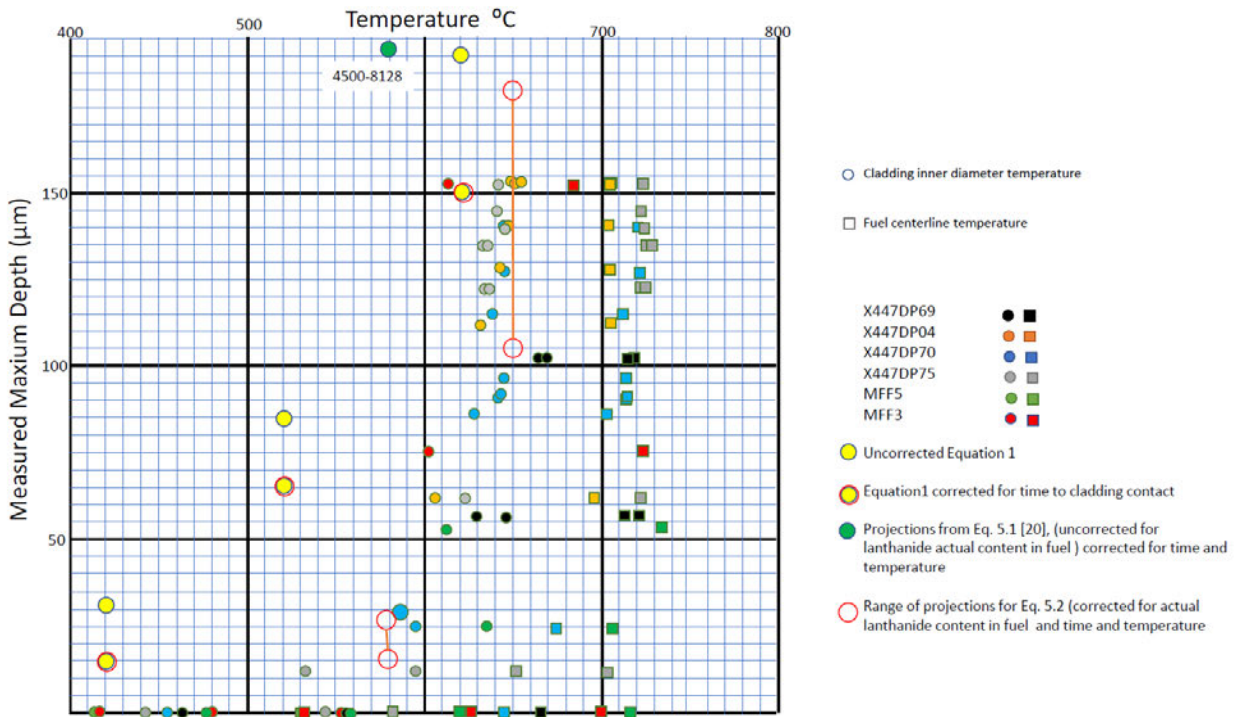


Figure 5.6 Data from Table 5-2 and projections with equation 5.2

Table 5-2

SA	X/L0	Burnup (at%)	Fission Density (fusion/m <sup>3</sup> )	Height from BOP (cm)	Measured Max Depth (cm)	Time Avg. Fuel Centerline Temperature (°C)	Time Avg. Chalking Inner Temperature (°C)
X447 D069	0.19	4.8	1.70E+21	7	0	574	463
	0.46	4.9	1.73E+21	17.1	0	661	552
	0.74	4.1	1.45E+21	25.4	50.8	713	626
	0.85	3.45	1.23E+21	29.2	50.8	720	648
	0.95	2.7	9.54E+20	32.985	101.6	720	664
	1	2.43	8.99E+20		34.3	101.6	718
X447 D004	0.69	9.2	3.27E+21	24.8	63.5	693	606
	0.86	7.5	2.65E+21	30.7	114.3	704	634
	0.94	6.4	2.36E+21	34.5	127	705	644
	0.95	5.9	2.09E+21	34.3	152.4	704	649
	0.97	5.8	2.05E+21	34.9	152.4	703	649
	0.98	5.6	1.98E+21	35.6	139.7	703	650
1	5.3	1.87E+21		36.2	152.4	701	652
X447 D090	0.18	10.2	3.61E+21	7	0	563	457
	0.49	10.6	3.75E+21	17.1	0	648	543
	0.62	9.9	3.50E+21	22.9	27.94	677	582
	0.71	9.3	3.29E+21	25.4	25.4	688	599
	0.84	7.7	2.72E+21	30.7	86.36	700	628
	0.92	6.8	2.40E+21	33.7	116.84	702	639
	0.94	6.5	2.30E+21	34.3	96.52	702	641
	0.95	6.3	2.23E+21	34.9	91.44	702	643
	0.97	6.1	2.16E+21	35.6	127	701	644
	0.98	5.9	2.09E+21	36.2	139.7	701	645
1	5.7	2.01E+21		36.8	88.9	700	647
X447 D095	0.19	10.2	3.61E+21	7	0	581	457
	0.44	10.7	3.78E+21	17.1	12.7	659	533
	0.68	9.5	3.36E+21	25.4	12.7	707	596
	0.81	8.2	2.90E+21	30.5	63.5	721	622
	0.9	7.3	2.58E+21	33.7	127	724	635
	0.91	7	2.47E+21	34.3	127	724	637
	0.93	6.8	2.40E+21	34.9	133.35	725	640
	0.94	6.5	2.30E+21	35.6	139.7	724	642
	0.96	6.3	2.23E+21	36.1	146.05	724	644
	0.98	5.9	2.09E+21	36.8	152.4	724	646
MFF5 198011	0.03	6.7	2.37E+21	2.54	0	532	414
	0.24	8.9	3.15E+21	22.9	0	628	480
	0.48	9.8	3.46E+21	45.72	0	712	556
	0.72	8.1	2.86E+21	68.6	50.8	736	612
	0.96	4.8	1.70E+21	91.4	25.4	709	635
MFF3 193045	0.03	8.4	2.97E+21	2.54	0	527	413
	0.25	11.3	3.99E+21	22.9	0	619	475
	0.49	12.4	4.38E+21	45.7	0	700	550
	0.74	9.1	3.22E+21	68.5	76.2	712	604
	0.98	5.7	2.01E+21	91.44	152.4	682	615

<sup>a</sup> – Calculated temperatures are EFPD averaged over the irradiation cycle histories.

### 5.1.6 Other Phenomena

Strictly speaking, thermal expansion and resulting strain and irradiation swelling and creep and resulting strain are not phenomena, but consequences of phenomena. Because they can be life limiting, they must also be addressed. Operational experience has shown that limiting the peak thermal strain to 1% and the irradiation creep to 2% will provide margin to fuel failure. Therefore, those same limits are used by ARC. Exceeding those limits does not mean that the fuel will in fact fail, but the margins of failure are reduced.

Since the correlations developed for the thermal creep strains and the irradiation creep strains [ have been developed from operational data from reactors and out of core testing for time durations significantly shorter than those of the ARC 100, and also for total fluences that are less than  $4 \times 10^{23}$  n/cm<sup>2</sup>, whereas the ARC 10 will experience fluences in excess of n/cm<sup>2</sup>, the use of such correlation should be accompanied by a good dose of conservatism.

While the release of fission product gas to the gas plenum has a major influence on fuel qualification, the phenomena that affect the transport of fission gas and other fission products from the fuel to the bond provide a summary list of the operating experience at the EBR II and that acquired during operation of FFTF with HT9 clad metal fuel sodium to the coolant to the cover gas do not directly affect the qualification of the fuel, but have consequences in term of what is released to the functional containment, and ultimately to the environment. They can also influence how best to monitor for failed fuel (this is addressed in section 6.0).

## 5.2 Operating Experience

Operating experience of metal, HT9 clad fuel has been excellent, with rare fuel failures. Appendix C provides a summary list of the operating experience at the EBR II and the more limited one acquired during operation of FFTF with HT9 clad metal fuel. In summary. It is possible to conclude that in general the metal fuel behaved better than had been expected from analysis.

## 5.3 Analytical predictions

The performance of the ARC 100 fuel has been predicted by using the BISON code. Bison has undergone extensive verification and validation [12]. The predictions of BISON have been checked by using the MFUEL module[13] of SAS4A/SASSYS-1 code, which has also been extensively verified and validated. The prediction has also been confirmed by using simplified correlation an example of which is provide by equation 5.2 of section 5.1 The analysis of the behavior of the peak burnup fuel pin having the highest cladding temperatures with  $2\sigma$  is reported in the next subsection.

### 5.3.1 BISON Predictions

100 reference fuel design and steady state operating conditions. ARC-100 fuel pin dimensions and operating conditions are significantly different from the pins tested in EBR-2 and FFTF. While ARC-100 peak burnup of 14% is within the range of EBR-2 FFTF experience, the irradiation time of 18 years is unprecedented in the field of any commercial nuclear fuels. Furthermore, the ARC-100 projected fast neutron cladding dose of 250 dpa is greater than the dose of 205 dpa observed in the EBR-2 and FFTF tests.

The intent of this work is to compare key fuel performance metrics CDF, peak fuel temperature, peak cladding inner temperature, peak cladding thermal hoop strain, peak cladding hoop stress from gas pressure to the limits postulated in Mark V safety case.

The additional focus of the report is on understanding and explaining predicted trends in thermal and deformation behavior of the fuel and cladding.

**Table 5-3. Reference fuel pin design, operating parameters and BISON nodalization**

Input	Value	Number of nodes in BISON mesh
Fuel length, cm		200
Cladding length, cm		200
Sodium fill length, cm		
Plenum length, cm		
Fuel diameter, cm		20
Radial gap, cm		
Cladding inner diameter, cm		
Cladding outer diameter, cm		
Cladding thickness, cm		4
Initial He fill gas pressure, Pa	1	
Fuel composition	U10Zr	
Fuel density, g/cm <sup>3</sup>		
Cladding material	HT9	
Coolant inlet temperature, C		
Coolant pressure, Pa		
Coolant flow rate, kg/m <sup>2</sup> -sec		
Fuel rod pitch, cm		
Subchannel geometry		
Irradiation time, years	18	
Peak linear heat generation rate, W/cm		
Peak fast flux, n/cm <sup>2</sup> /s		

**Table 5-4. Axial power profile normalized to the length of the fuel slug**

Z/L	
0.0	0.54
0.1	0.87
0.2	1.11



0.3	1.29
0.4	1.38
0.5	1.39
0.6	1.33
0.7	1.19
0.8	0.96
0.9	0.66
1.0	0.29

The ARC-100 fuel pin is designed so that statistically the number of fuel pin breaches during normal and off normal reactor operation (including unlikely events) is limited to a percentage of the pins which would not challenge the safe operations and performance goals of the ARC-100. The design requirement is to ensure that no more than 21 pins in 21,433 driver pins will fail during one core loading. This reliability is to be demonstrated first through an analytical performance assessment, followed by a fuel surveillance program. The analytical performance acceptance criteria (i.e., what limits the calculations must meet) are shown in Table 5.6. The allowable CDF of 0.05 during steady-state operation of the ARC-100 fuel pins with HT9 cladding is based on the HT9 out-of-reactor stress-rupture data and LIFE-METAL code calculations for fuel pins with HT9 cladding that have been irradiated in EBR-II. With regard to the time-to-rupture correlation used in the CDF formulation, it is fit to the unirradiated stress-rupture data for pressurized HT9 tubes. A statistical analysis referred to in ANL-NSE-1 (Mark V Safety Case) of these data shows the logarithm (base 10) of the CDF at failure is distributed normally. With 95% confidence, the mean and standard deviation of the probability distribution are -0.0354 and 0.1885, respectively. Thus, the failure probability will be less than 21 in 21,433 if the logarithm of the CDF is less than -0.61905, or the CDF is less than 0.24. The allowable value of the steady-state CDF of 0.05 that is used in the current safety case is considerably smaller than this value and corresponds to a failure of 1 pin in 1e11 pins. The additional conservatism is based on the precedent set by CRBR and PRISM reactor analyses, engineering judgment, and the desire to select a suitably low value of the steady-state CDF so that it can be argued that the transient performance of the cladding is not significantly degraded by the steady-state operation.

The significance of cladding thermal creep strain limit, peak fuel and cladding temperature and hoop stress is explained in the ARC-100 fuel Qualification Program Document and in section 3.1.

**Table 5-5. ARC-100 design criteria for steady state fuel service**

Parameter	Criterion
Thermal component of cladding hoop creep strain, %	1
Cumulative Damage Fraction	0.05
Peak fuel temperature (no U10Zr melting), C	1250
Peak cladding temperature (no eutectic), C	650
Hoop stress from gas pressure, MPa	150

Results from BISON calculation of the end-of-life design criteria characteristics for ARC-100 peak fuel pin are shown in Table 4. When compared to the design criteria listed in Table 3, these results suggest that ARC-100 fuel pin design meets the design criteria for steady state fuel service. For a CDF of  $7.04e-4$  a 10 base logarithm is -3.13 which corresponds to a failure of 1 pin in one million. Therefore, BISON calculations predict essentially zero pin failures during steady state fuel service.

**Table 5-6. End-of-life design criteria characteristics for ARC-100 peak fuel pin**

Time, years	CDF	Peak fuel temperature, C	Peak cladding inner temperature, C	Peak cladding thermal hoop strain	Peak cladding hoop stress, MPa	Peak cladding hoop stress from gas pressure, MPa
18	$7.04e-4$	574	537	$1.8e-4$	173	40.3

Fuel centerline temperature as a function of the elevation is shown in Figure 5.7. Fundamentally, fuel centerline temperature is proportional to LHGR and inversely proportional to fuel thermal conductivity. For example, at the mid-plane elevation of the fuel slug corresponding to a peak LHGR of 155 W/cm and a thermal conductivity of 20 W/cm/s, a radial temperature rise in the fuel would be only 62C and a radially averaged temperature gradient would be 152 C/cm. For the top portion of the fuel slug having LHGR of 73 W/cm and thermal conductivity of 20 W/cm/s a radial temperature rise in the fuel would be 30C and a radially averaged temperature gradient would be 74 C/cm. For comparison, a typical EBR-2 pin would feature a peak LHGR of 350 W/cm yielding a temperature rise of 140C and a radially average temperature gradient of 490 C/cm. Low LHGR of ARC-100 fuel pins results in a low radial temperature rise in the fuel and a low radial temperature gradient. These features are expected to suppress such undesirable fuel behavior phenomena as zirconium redistribution and lanthanide fission product migration characteristic for metallic fuels operating at higher LHGR and featuring smaller slug diameter.

**Figure 5.7.**

As shown in Figure 5.9 axial burnup profile follows axial power profile provided in Table 5.5. As evident from Figure 5.9 peak axial burnup of % is located at the elevation of cm. Maximum fission product generation is expected at the location of the peak burnup. The lowest burnup of % is observed at the top of the fuel slug. Local burnup is an important input to the fuel cladding chemical interaction (FCCI) layer thickness calculation. Low burnup values at the top of the fuel slug are expected to yield minimal FCCI layer growth.

Like burnup, axial fast neutron fluence profile also follows the axial power profile. As shown in Figure 5.10 peak fast neutron fluence n/m<sup>2</sup> is observed at an elevation of cm.

**Figure 5.8.**

**Figure 5.9.**

**Figure 5.10.**

The axial distribution of the predicted FCCI thickness layer is shown in Figure 5.11. Peak FCCI layer thickness of 25 micrometers is observed at the elevation of 130cm. The rise of FCCI with the increase of the elevation from the bottom of the slug to 130 cm is explained by the increase of cladding temperature. The rapid decrease of the FCCI layer thickness at the elevations between 130 cm and the fuel slug top is explained by a decrease of the local burnup.

**Figure 5.11**

Figure 5.12 indicates that cladding hoop stress peaks at the bottom of the fuel slug reaching 170 MPa at the EOL (End of Life). The location of peak cladding hoop stress is characterized by low burnup and low temperature of both fuel and cladding. It appears that low temperatures at the bottom section of the fuel slug resulted in a reduction of both cladding and fuel creep rates which impeded stress relaxation resulting in elevated cladding stress. It is also possible that fuel slug slumping under its own weight led to some fuel relocation toward the bottom of the fuel pin. The magnitude of the

cladding hoop stress in the plenum region is 40 MPa and is driven by the fission gas pressure and temperature. Cladding hoop stress in the plenum region is well below the limit of 150MPa.

**Figure 5.12.**

Cladding thermal creep strain as a function of elevation is shown in Figure 5.13. The maximum value of cladding thermal creep strain is                      and is well below the limit of 0.01. Cladding thermal creep strain increases with the increase of cladding hoop stress and temperature. Examination of axial cladding hoop stress and temperature distribution indicates that cladding thermal creep strain is suppressed in the lower portion of the fuel pin due to low temperature in that location. As the cladding temperature increases so does cladding thermal creep strain. The axial location of the peak cladding thermal creep strain coincides with the location of the maximum cladding temperature at the top of the fuel slug. In the plenum region cladding thermal creep strain is lower due to lack of the fuel-cladding mechanical interaction and cladding hoop stress associated with it. Fission gas pressure is the sole source of cladding hoop stress in the plenum region.

Total cladding strain which is a sum of irradiation and thermal creep strains, cladding swelling and elastic and thermal expansion strains is plotted as a function of elevation in Figure 5.14. As evident from Figure 5.14, total cladding strain peaks at                      at an axial elevation of                      cm. This elevation is characterized by the highest burnup and highest fast neutron flux. Therefore, the axial cladding strain distribution is driven by fuel cladding mechanical interaction which in turn is a result of fuel swelling. Peak total cladding strain of                      at a local burnup of 1 % predicted by BISON for ARC-100 appears higher than cladding strain observed for EBR-2 and FFTF experiments featuring similar burnup. For example, maximum cladding strain of the MFF-3-193045 pin reached 0.013 while peak burnup reached 13.8 %. Initial explanation for this observation is that in an ARC-100 pin the peak burnup location is characterized by a low temperature of                      which is approximately 200C lower than MFF-3-193045. It is theorized that the fuel creep is suppressed at a lower temperature which results in increased fuel cladding mechanical interaction.

**Figure 5.13**

**Figure 5.14.**

Detailed examination of BISON results indicated that throughout the irradiation, the cladding hoop stress and fast neutron flux remain nearly constant at the axial elevation of cm where peak cladding strain is observed. Therefore, irradiation creep rate of the cladding, being a function of neutron flux and cladding stress remains nearly constant as well. Since the EOL cladding strain is calculated by multiplying creep rate by time, large EOL ARC-100 cladding strain is the result of the very long irradiation time of 18 years. In contrast, MFF-3-193045 fuel pin reached the same burnup as ARC-100 in 726.2 days which explains why cladding strain is so much lower in MFF-3-193045.

As stated in the Mark V safety case, based on a very extensive database for Type 316 Stainless Steel, large swelling strains can be tolerated without imposing a failure ductility limit on the material. Also, at low temperature and stress, where thermal creep is negligible, the material can deform without any observable limit due to irradiation enhanced creep. Thus, the in-reactor ductility of a pressurized

tube is often associated with the thermal creep strain component. For HT9 cladding, there is a smaller data base for failure strain consisting of out-of-reactor and in-reactor pressurized tube tests. The lowest observed failure strain is 2.1%. Thus, the 1% limit is conservative. Also, based on the temperature to cause failure, whether the test was performed in-reactor or out-of-reactor. This observation supports the concept that it is the thermal creep component that is damaging for HT9 cladding, as is the case for 316SS.

To investigate factors contributing to cladding strain, a hypothetical case featuring zero solid fission product swelling in the fuel was modeled. Results from this simulation are shown in Figure 5.15. Examination of Figure 5.15 indicates that approximately 60% of the cladding strain occurred due to solid fission product swelling.

**Figure 5.15.**

As cladding deformation occurs due to thermal and irradiation creep, it is of interest to understand the impact of each creep mechanism on the EOL cladding strain. Figure 5.16 shows results of a hypothetical case in which irradiation creep rate of the cladding was set to zero while cladding creep remained active. As a result, a nearly 4-fold drop of the EOL cladding strain was observed. Further examination of the results revealed that lack of irradiation creep of the cladding resulted in an increased compressive force on the fuel which in turn caused fuel densification. Therefore, in metallic fuel the EOL cladding strain is a result of a balance between cladding creep and fuel densification. Furthermore, as fuel densification model is based on the fuel creep equations, it can be concluded that the EOL cladding strain is a result of two competing phenomena: creep of the cladding and creep of the fuel. Low fuel temperature and low volumetric fission rate are hallmark features of the ARC-100 design. In current BISON models fuel creep rate decreases with a decrease of both of these parameters which impedes ability of the fuel to densify resulting in a significant EOL cladding strain.

**Figure 5.16.**

To understand the impact of FCCI on cladding deformation in ARC-100 fuel pin a two-sigma case featuring accelerated FCCI layer growth was modeled. In the two-sigma case the EOL FCCI reached 100 micrometers. As shown in Figure 5.17, accelerated FCCI promoted cladding deformation near the upper portion of the fuel slug which resulted in a characteristic “double-peak” shape of the plot. This prediction is consistent with cladding profilometry results performed on the MFF pins irradiated in FFTF. Profilometry analysis of MFF-3-193045 pin irradiated to a peak burnup of 13.8 % and featuring a double-peak is shown in Figure 5.18. EOL maximum FCCI in the MFF-3-193045 fuel pin reached 152 micrometers.

Recognizing that fuel porosity is an important metric of the fuel microstructure during irradiation and to highlight a connection between fuel microstructure, cladding stress and strain, axial distribution of the fuel porosity at the slug centerline is shown in Figure 5.19. Fuel swelling model in BISON limits the maximum attainable fuel porosity at 33% based on the assumption that porosity interconnection results in cessation of any porosity growth above 33%. Porosity interconnection occurs at the beginning of irradiation. Examination of Figure 5.19 indicates that reduction of the porosity at the mid-section of the fuel slug occurred due to fuel densification caused by compression of highly porous fuel by stresses generated during fuel-cladding mechanical interaction. Higher porosity observed at the top and bottom of the fuel pin is explained by lower temperature and lower local fuel burnup. Lower temperature results in the reduction of the fuel creep rate, and lower burnup results in delayed fuel cladding mechanical interaction which is necessary to generate compressive stresses on the fuel leading to fuel densification.



Figure 5.17.

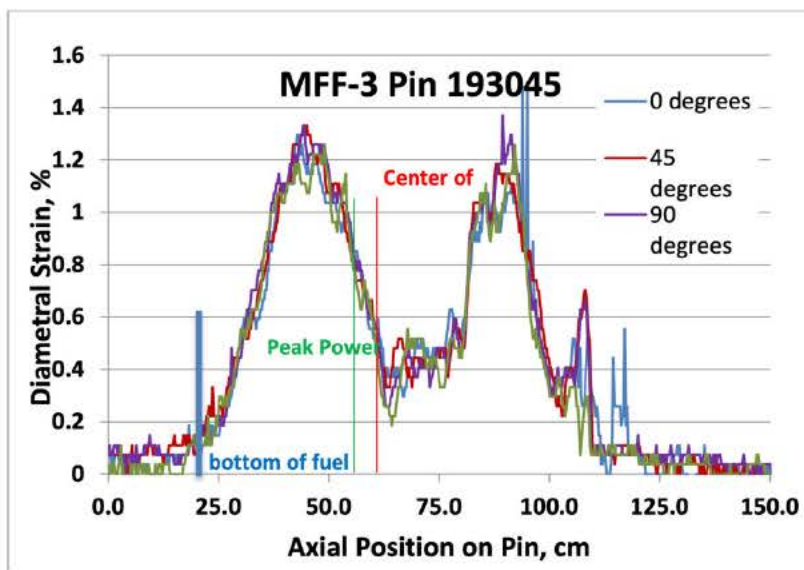


Figure 5.18. Profilometry analysis of MFF-3-193045 pin.

**Figure 5.19.**

Axial distribution of the cumulative damage fraction is shown in Figure 5.20. The CDF is extremely low and corresponds to essentially zero failure probability for the given operating conditions. Comparison of Figure 5.13 and Figure 5.20 indicates that cladding thermal creep strain is a main driver for the CDF. The peak of the CDF observed near the top of the fuel slug is explained by the cladding temperature peaking at the same location and the cladding hoop stress due to fuel cladding mechanical interaction.

**Figure 5.20.**

Fuel performance results calculated with two sigma uncertainty are shown in Table 5-7. It was determined that when accounting for a two-sigma uncertainty cladding thermal creep strain and

cumulative damage fraction exceed design limits if the fuel is irradiated for 18 years to a peak burnup of %. Table 5-7 also includes results for a reduced irradiation time of 16 calendar years (14.4 Equivalent Full Power Years-(EFPY) years) and peak burnup of %. As evident from Table 5-7 fuel performance parameters are within the design limits for a reduced irradiation time.

**Table 5-7 Fuel performance results with a two sigma uncertainty**

Parameter	6570 days	5256 days	Proposed Design Limits
Fission gas release, %			
Fuel axial elongation, %			
Plenum pressure, MPa			
Clad hoop stress, MPa			Clad yield strength
Peak clad total strain, %			2% based CEA findings
Peak clad thermal creep strain, %			1% - Widely used in Fast Reactor designs. It is for both steady-state and transients.
Peak clad void swelling strain,%			2% based on CEA findings
Peak clad CDF			0.05 for the steady state
Peak clad inner wastage, micrometers			
Peak clad outer wastage, micrometers			
Peak clad total wastage, micrometers			Steady state: 25% of the initial cladding
Peak clad inner temperature (°C)			650
Burnup, %			

Steady state fuel performance calculations have been carried out using BISON fuel performance code for the ARC-100 reference pin design and operating conditions. Performance results were compared to the EBR-2 Mark-V fuel performance limits where appropriate. The results obtained indicate ARC-100 design is compliant with EBR-2 Mark-V safety limits during steady state operation. It was noted that EOL cladding strain values approach due to irradiation creep of the cladding driven by fuel cladding mechanical interaction. While EBR-2 Mark-V safety limits do not apply to the total cladding strain, but only the thermal creep component of cladding strain, it is important that fuel assembly design accommodates EOL cladding strain at the peak power elevation.

BISON analysis indicates EOL FCCI values of 10 micrometers at the upper region of the fuel pin. For the steady state service FCCI does not appear to be a life limiting phenomenon.

ARC-100 fuel performance was also evaluated to account for a two-sigma uncertainty. It was determined that when accounting for a two-sigma uncertainty cladding thermal creep strain and

cumulative damage fraction exceed design limits if the fuel is irradiated for 18 years to a peak burnup of %. Table 5 also includes results for a reduced irradiation time of 14.4 years and peak burnup of %. As evident from Table 5 fuel performance parameters are within the design limits for a reduced irradiation time.

Based on the findings above, the proposed fuel surveillance program could focus on monitoring evolution of cladding strain during reactor operation. It would be of interest to explore non-destructive methods for cladding strain monitoring by possibly measuring hydraulic resistance of the assemblies.

For the steady state fuel service, future fuel modeling work will focus on the uncertainty analysis, sensitivity studies, code validation against the relevant legacy data, understanding BISON ability to extrapolate existing data to long irradiation times and updating the analysis as new fuel performance models are developed by DOE NEAMS program. The scope of the transient fuel performance analysis will be developed and executed in consultation with ARC reactor safety analysis team.

**5.3.2 SAS4A/SASSYS-1 MFUEL Module Predictions (Confirmations)**

The analyses done with the BISON code have been checked with the MFUEL module of SAS4A/SASSYS-1 the results are shown in Tables 5-8 and 5-9.

**Table 5-8 MFUEL Simulation results at 5256 and 6570 equivalent full power days (16 and 20 calendar years at 90% capacity factor - 2σ temperatures)**

Parameter	6570 days	5256 days	Proposed Design Limits
Fission gas release (%)			-
Fuel Axial Elongation (%)			-
Plenum Pressure (MPa)		4	-
Clad Hoop Stress (MPa) Peak Axial Node/Top Axial Node			Cladding Yield Strength
Peak Clad Total Permanent Strain (%)			2% based CEA findings
Peak Clad Thermal Creep Strain (%)			1% - Widely used in Fast Reactor designs. It is for both steady-state and transients.
Peak Clad Irradiation Creep Strain (%)			2% based on CEA findings
Peak Clad Void Swelling Strain (%)			2% based on CEA findings
Peak Clad CDF			0.05 for the steady state, 0.1 for transients
Peak Clad Inner Wastage (microns)			25% of cladding thickness
Peak Clad Outer Wastage (microns)			
Peak Clad Total Wastage (microns)			Steady state: 28% of the initial cladding
Peak Clad Inner Temperature (°C)			650
Burnup (at%)/cladding dose (dpa)			Dose limit: 250 dpa

**Table 5-9 Comparison between BISON and MFUEL Results**

	BISON Nominal	BISON 2 $\sigma$	MFUEL 2 $\sigma$	BISON 2 $\sigma$	MFUEL 2 $\sigma$	
Parameter	6570 days			5256 days		Proposed Design Limits
Fission gas release (%)						-
Fuel Axial Elongation (%)						-
Plenum Pressure (MPa)						-
Clad Hoop Stress (MPa)						Cladding Yield Strength
Peak Axial Node/Top Axial Node						
Peak Clad Total Permanent Strain (%)						2% based CEA findings
Peak Clad Thermal Creep Strain (%)						1% - Widely used in Fast Reactor designs. It is for both steady-state and transients.
Peak Clad Irradiation Creep Strain (%)						2% based on CEA findings
Peak Clad Void Swelling Strain (%)						2% based on CEA findings
Peak Clad CDF						0.05 for the steady state, 0.1 for transients
Peak Clad Inner Wastage (microns)						25% of cladding thickness
Peak Clad Outer Wastage (microns)						
Peak Clad Total Wastage (microns)						Steady state: 28% of the initial cladding
Peak Clad Inner Temperature ( $^{\circ}$ C)						650
Burnup (at%)/cladding dose (dpa)						Dose limit: 250 dpa

**5.3.3 SAS4A/SASSYS-1 Deterministic Analyses Predictions**

The preceding section addressed the predictions of the fuel behavior, using the conditions the fuel would experience as predicted by the core neutronic and thermohydraulic analysis under steady

state and postulated transients. Those analyses provide the inputs necessary to address fuel performance. This section summarizes the results of the deterministic safety analyses which provide those inputs. The analyses for steady state and design basis events have been done with  $2\sigma$  (for the detailed fuel performance assessment) and  $3\sigma$  uncertainties. For beyond design basis events the analysis has been performed using the best estimate methods.

These analyses establish limiting conditions (power, temperature and burnup) for operation of the fuel. The analysis must consider operational necessity as well as material limitation.

The ARC100 fuel, when operated at the extreme operational limit, will meet all safety-related design requirements. The analysis, then, is the basis for the Safety Limits, the Limiting Conditions for Operation, and the Limiting Safety System Settings that will be specified in an ARC-100 Technical Safety Requirements document.

The calculational sequence used for the analysis is as follows.

First, the assembly powers, flows, flux levels, and other quantities are calculated for the core rows using the methods described in Reference [78]. The key results are steady-state power, flow, and coolant bulk temperature rise for each assembly. These results allow identification of the hottest assembly in each row and provide powers and flows for detailed analysis of these limiting subassemblies. Detailed steady-state temperature calculations of the hottest assembly in each row are calculated with SE2-ANL [79] in order to define the maximum pin conditions for mechanical analysis. A by-product of the SE2-ANL analysis is the peaking factor, defined as the ratio between the hottest subchannel sodium temperature rise and the average bulk sodium assembly temperature rise. The identified highest power and temperature fuel pins are then analyzed by the fuel pin performance codes BISON [12] and/or MFUEL module of SAS4A/SASSYS-1 [13] to describe the expected behavior of fuel pins in the ARC 100 core loadings. Such calculations are described in sections 5.3.1 and 5.3.2 above.

At this point in the analysis the measures of fuel pin performance (i.e., temperatures; cladding stress, strain, and wastage; and cladding damage) at the maximum conditions of the core loadings have been calculated and shown to meet (or not) the appropriate design criteria. This analysis corresponds to a design or reference analysis but does not define limits upon burnup or irradiation temperature that steady-state fuel pin performance issues impose.

The burnup and irradiation temperature limits are then defined by a separate parametric analysis (sensitivity study), once again using BISON (and/or MFUEL) Initial conditions for transient thermal analysis are determined based upon the results of these calculations. Uncertainty factors are used (for N.O, AOOs and DBEs) in a SAS4A/SASSYS-1 [17] thermal hydraulic analysis to derive the assembly subchannel temperatures which become the Technical Specification limits actually imposed, together with a burnup limit. SASSYS is then utilized to perform a full transient thermal-hydraulic and BISO the fuel pin mechanical analysis, and the burnup and irradiation temperature limits confirmed, or modified, if necessary, based upon the criteria described in Section 3.1 The results of the BISON and SAS4A/SASSYS-1 analyses are then used to verify that all design criteria of section 3.1 are satisfied.

The SAS4A/SASSYS-1 calculations are performed using a combination of worst-case conditions to bound the actual pin condition for all the time in reactor.

This selection of conditions ensures that the conclusions drawn from the SAS4A/SASSYS-1 analysis will apply to all irradiation conditions anticipated for ARC-100 fueled assemblies.

A number of different limits are applied. First there are Safety Limits which are limits that protect the integrity of barriers to uncontrolled radiation release. In this case the barrier in question is the fuel pin

cladding. The next type of limit is the Limiting Safety System Setting (LS<sup>3</sup>), which gives the settings for automatic protective devices that monitor variables having significant safety functions. The LS<sup>3</sup> is at present established at the 15% overpower, 12% underflow, 15% over temperature rise, and 17s period trip settings, and ultimately, they will be defined in the Technical Specifications. These must be independent of the fuel type because any of the approved driver fuel could, in principle, be in any core position at any time. Finally, there are Limiting Conditions for Operation (LCO), which are conditions on equipment and technical characteristics of the plant required to ensure safe facility operation. Figure 5.21 shows the region defining the presently estimated LCOs for the ARC 100.

If a safety limit is exceeded, it must be demonstrated that a plant can still be brought to a safe and stable condition and maintained in that condition. Safety limits do not necessarily provide values against which monitored process parameters can be evaluated during operation; LS<sup>3</sup> and LCO's serve that function.

The fuel design criteria evaluate cladding damage using a cumulative damage methodology which explicitly accounts for the effect of time dependence of eutectic penetration and strain. The design criteria are predicated upon one fuel failure per core, which requires restricting the cumulative damage function (CDF) to 5% during normal operation and 10% accumulated over all anticipated design basis events plus the single most damaging unlikely event (see Sec. 3.1). To be consistent with the fuel design methodology, the fuel safety limit should also be expressed as a limit on the CDF. The limit which has been selected is that the CDF shall not exceed 1.0 for the limiting driver fuel pins.

A limit of CDF of 1.0 assures that the core is coolable and thus it can be demonstrated that the plant can be brought to a safe and stable condition. Assurance of core coolability at a CDF of 1.0 is indicated by the following argument. A CDF of 1.0 on the limiting fuel pins indicates a failure probability for these pins of 50%. Prior analyses for similar fuel assemblies have indicated that the pins most likely to fail are those on the outer rows, as a result of overcooling, and those in the inner rows as a result of power and flow variations within the inner rows. Therefore, the number of pins which operate at limiting conditions are less than 25% of the pins in the limiting assemblies. At a CDF of 1.0, only half of these pins, or about 10% of the pins of an assembly, will fail and these failures will be in the inner rows of pins of the subassembly. Since experience, (see section metallic fuel cladding breaches are of the pinhole type, they are benign with respect to blockage formation (see Secs. 1.1.2 and specifically the section on run beyond breach Table 1-5), and so neither pin-to-pin failure propagation within a subassembly nor failure propagation between subassemblies is indicated. Therefore, even in the highly improbable case of reaching a CDF of 1.0 in the limiting fuel pins, core coolability would still be maintained and uncontrolled radiation release would be avoided.

Of course, with the limits established for cumulative damage factor it is highly unlikely that any pin will fail.

The ARC-100 fuel temperature and power limits are determined row by row by evaluation of the design criteria provided in Section 3.1 for both steady-state and transient operation of the plant, including off-normal events. In the analysis, potential values for the Technical Specification (T.S) limiting temperatures and powers are first determined by the steady-state analysis. The steady state limiting values are determined by the condition that the fuel should be able to operate to its burnup limit at the boundary of normal operation (105% of normal power). These tentative limiting conditions of operation are then used to predict thermal transient behavior as well as fuel performance for off-normal conditions including parametric study at the bounds of the inlet temperature Limiting Condition of Operation. If

the design criteria cannot be satisfied for the proposed T.S. limiting temperatures and powers during off-normal transients, then the T.S. limiting values are adjusted. This approach is also used to develop LCO's for the safety and control rod assemblies which are consistent with the design criteria.

### Steady State Thermal Analysis

The steady-state core thermal/hydraulic performance was evaluated using the sub-channel analysis code SE2-ANL, which is a modified version of the SUPERENERGY-2 code. The SUPERENERGY-2 code is a multi-assembly, steady-state sub-channel analysis code designed specifically to perform efficient calculations of the detailed coolant temperature profiles in sodium cooled fast reactor core geometries. Reactor hot spot analysis method as well as pin-wise fuel heating rate distribution model have been added to the SUPERENERGY-2 code. Thus, the SE2-ANL code can calculate the detailed coolant, cladding, and fuel temperature distributions in assemblies, including double ducted control assemblies, at the conditions with or without hot channel factors. In this work, the hot channel factors were proposed conservatively by reviewing the hot channel factors developed in the previous SFR projects (see section 1.2.2.5). The hot channel factors consist of direct (non-statistical) and statistical hot channel factors, and both  $2\sigma$  and  $3\sigma$  statistical uncertainties are counted in the peak temperature calculations with the inlet and bulk outlet temperatures of  $355^{\circ}\text{C}$  and  $510^{\circ}\text{C}$ , respectively.

Coolant orifice zoning and flow allocation were determined through a series of neutron/gamma transport calculations and the steady-state thermal-hydraulic analyses. First, the heating distribution in the ARC-100 core was evaluated from the coupled neutron and gamma heating calculations using the ANL computation code suite for the fast reactor analysis. Region-dependent 33-group neutron and gamma cross sections and KERMA factors were generated by the MC<sup>2</sup>-3 code; the neutron and gamma fluxes were calculated using the triangular-z finite difference option of the DIF3D code and the GAMSOR code; and the heating distribution was determined by multiplying the neutron and gamma fluxes by the KERMA factors.

The thermal conductivity of the metallic fuel degrades by irradiation because of porosity build-up by gaseous fission products. In a U-Zr binary fuel, the porosity grows by %, but decreases gradually by filling bond sodium. However, the porosity in the metallic fuel is not fully filled by the bond sodium and remaining porosity is about 13% even though the fuel is irradiated for long time [70]. In this work, no porosity was assumed at BOL, while 13% porosity was assumed at EOL, and the SE2-ANL code adjusted the fuel thermal conductivity using the correlations described in the metal fuel handbook [70].

The goals of the analysis are:

- To show that, during normal operation at the beginning of life, the temperatures of fuel, safety and control rods are acceptable.
- To determine a row-by-row coolant peaking factor.
- To provide a benchmark for thermal/Mechanical analysis using BISON

### Transient Analysis

Analysis of off-normal events begins with determining the steady-state conditions which limit peak assembly power and power to flow ratio. Power/flow ratio is directly proportional to the coolant temperature difference axially across the assembly. For a given core inlet temperature, the limit on power/flow ratio can be a technical Specification limiting the coolant outlet temperature. For a given assembly flow and flow distribution radially across the assembly, the limiting power is determined based on the limits on fuel temperatures, steady state cladding temperature and transient cladding damage. So, the power and power/flow establish a local coolant temperature Limiting Condition for Operation (LCO).



The LCO in turn must be such that at steady state the fuel temperature is lower than the solidus temperature and the peak inner cladding temperature is limited to 650C. However, the behavior has to be evaluated and compared to the design criteria of section 3.1. In the transient analysis values of physical quantities, such as wastage are part of the initial conditions, together with the burnup at which they occur. These physical quantities are applied to the transient analysis irrespective of burnup, to ensure a bounding treatment of relevant phenomena for transient analysis.

For the ARC-100 the power of the inner row assemblies is generally higher than that in outer row assemblies [78], while power/flow is higher in the outer row assemblies; therefore, for the ARC100 fuel the steady state temperatures are limited by the low solidus temperature in the fuel intermediate zone (due to Zr redistribution), while the outer row assembly temperatures are limited by the fuel cladding eutectic liquefaction temperature.

The limit set for the ARC-100 fuel for FCCI at steady state is 600°C and is lower than the eutectic formation limit of 650°C and it is reached at a lower coolant ΔT than is the fuel solidus temperature. So that the steady-state temperature of assemblies in both the inner and outer rows is limited by the steady state cladding temperature limit.

Because the factors which limit temperature vary from row to row, assemblies’ temperature limits must be derived on a row-by-row basis.

The temperature limits for steady state operations have been determined using the SAS4A/SASSYS-1 code with a reactor inlet temperature of C

The same code has been used to determine the temperatures resulting from a limited number of transients. Results for the transients analyzed to date are documented in reference [7] and summarized in Tables 5.10a through 5.10 i.

As the design progresses, the rest of the transients will also be analyzed.

**Table 5.10 a:**

Analysis Types	Nominal peak channels (°C)			2σ peak channels (°C)			3σ peak channels (°C)		
	BOL	MOL	EOL	BOL	MOL	EOL	BOL	MOL	EOL
Core Conditions									
Peak fuel temperature									
Fuel melting margin									
Peak cladding temperature									
Margin to Service Limit B									
Peak coolant temperature									
Sodium boiling margin									
Peak hot pool temperature				NA	NA	NA	NA	NA	NA
Margin to service limit B				NA	NA	NA	NA	NA	NA

**Table 5.10 b:**

Core Conditions	BOL	MO L	EOL
Peak fuel temperature			
Fuel melting margin			
Peak cladding temperature			
Margin to SL B			
Peak coolant temperature			
Sodium boiling margin			
Peak hot pool temperature			
Margin to Service Level D			

**Table 5.10 c:**

Analysis Types	Nominal peak channels (°C)			2σ peak channels (°C)			3σ peak channels (°C)		
	BOL	MOL	EOL	BOL	MOL	EOL	BOL	MOL	EOL
Core Conditions									
Peak fuel temperature									NA
Fuel melting margin									NA
Peak cladding temperature									NA
Margin to SL B									NA
Peak coolant temperature									NA
Sodium boiling margin									NA
Peak hot pool temperature			NA	NA	NA	NA	NA	NA	NA
Margin to service limit B			NA	NA	NA	NA	NA	NA	NA

**Table 5.10 d:**

Core Conditions	BOL	MO L	BOL With unexpanded fresh fuel
Peak fuel temperature			
Fuel melting margin			
Peak cladding temperature			
Max. clad penetration			
Peak coolant temperature			
Sodium boiling margin			
Peak hot pool temperature			
Margin to service limit D			

**Table 5.10 e:**

Analysis Types	Nominal peak channels(°C)			2σ peak channels (°C)			3σ peak channels (°C)		
	BOL	MOL	EOL	BOL	MOL	EOL	BOL	MOL	EOL
Core Conditions									
Peak fuel temperature									
Fuel melting margin									
Peak cladding temperature									
Margin to service limit B									
Peak coolant temperature									
Sodium boiling margin									
Peak hot pool temperature				NA	NA	NA	NA	NA	NA
Margin to service limit B				NA	NA	NA	NA	NA	NA

**Table 5.10 f:**

Core Conditions	BOL	MO L	EOL
Peak fuel temperature			
Fuel melting margin			
Peak cladding temperature			
Max. clad penetration			
Peak coolant temperature			
Sodium boiling margin			
Peak hot pool temperature			
Margin to Service Level D			

**Table 5.10.g:**

Temperatures	Protected 3σ	Unprotected -
Peak fuel temperature		
Peak cladding temperature		
Peak coolant temperature		
Peak hot pool temperature		

**Table 5.10.h:**

Temperatures	Protected 3σ	Unprotected
Peak fuel temperature		
Peak cladding temperature		
Peak coolant temperature		
Peak hot pool temperature		

**Table 5.10 i:**

Steady State 3σ Peak Temperatures and Minimum Margins				S.S. Peak Temperatures and Minimum Margins		
LOF include SBO Loss of one and two primary pumps	LOF TOP and LOHS		LOHS LOF	LOF TOP and LOHS		LOF-LOHS
	BOL	MOL	EOL	BOL	MOL	EOL
Peak Fuel Temp.						
Fuel Melting Margin						
Peak Cladding Temp.						
Margin to Service Level B or D						
Peak Sodium Temp.						
Sodium Boiling Margin						

Since not all steady state and transients' events have yet been analyzed, it is germane to ask what the consequence might be for those the analyses for which will be done later. From the standpoint of fuel and cladding temperature limits (and possible damage, a qualitative assessment can be made for a lower of greater than normal inlet temperature.

The effect will be dependent on the trip setpoint of the reactor protection system., Events that scram the reactor on high power or flow trips, will scram at the same time regardless of inlet temperature, therefore lower than normal inlet temperature will lower both the fuel and cladding temperature thereby increasing the margin to fuel melting or cladding damage. For events for which the trip occurs on high outlet temperature, the lower inlet temperature will delay the scram, will so the outlet temperature will increase from its established set point (which does not change) Therefore decreases the margin to fuel melting and cladding damage. Such an event can only occur if a drift in the inlet temperature goes unnoticed by the operator, or the inlet temperature is intentionally reduced, without changing the outlet temperature set point to be consistent with that reduction. Thus, it is important that future analyses focus on such potential events.

For higher inlet temperatures scram times for transients which scram on power or flow, trips will still be independent of inlet temperature, but now the higher inlet temperature produces higher peak fuel and cladding temperatures, so the fuel melting margin decrease, and cladding damage is increased. Conversely the initial coolant outlet temperature now moves closer to the first set point, so the transient terminates earlier and lowers the peak fuel and cladding temperatures, thereby increasing margin to fuel melting and decreasing cladding damage.

On the other hand, analyses have been conducted assuming scram fails to act, and the results indicate that the margin to fuel melt and cladding damage are generally maintained. maintained

Another area that deserves attention is the transient overpower at low power during startup, which again has not yet been analyzed. At lower power levels of reactor startup, the reactivity feedback is not significant, and the rate of power rise during the transient overpower event (TOP) increases rapidly. A short period is therefore reached quickly. Therefore, the greatest margin of protective action is given by the period trip. The transient UTOP has been selected for analysis for precisely this reason. As power increases the maximum possible rate of power rise for a given rate of reactivity insertion decreases due to increased reactivity feedback, and the period trip becomes ineffective, and the reactor is protected only by the power level and the outlet temperature level However unlikely such transient can be used to demonstrate the importance of the period trip, since the reactivity increase in this case is fast enough [almost twice the rate assumed in the unprotected reactivity insertion caused by the accidental withdrawal of the most reactive rod (0.47 at 0.02\$/sec) analyzed as the limiting unprotected accident-see Table 5.10g].,so the period trip is effective over a significant power range.

Another safety aspect is the duct dilation of control and safety assemblies (see section 3.2.2) as well as the bowing of those assemblies. This has not yet been analyzed and it is a concern because of

- Interference between the control/safety assembly outer duct and the inner duct containing the absorbers.
- Duct dilation is larger than the diametral clearance between the duct and the storage position.

Dilation of the ducts is caused by irradiation/creep induced deformations, and irradiation-induced swelling; and bowing is primarily caused by temperature and fluence differences between opposite flats of the duct. Dilation and bowing outside limits established by the clearances created by the design can interfere with the ability to shut down the reactor.

## 5.4 Design Gaps

From the PIRT (Reported in reference [2]) and the various sections of this report, a number of gaps have been identified for the design of the fuel system. This section summarizes the gaps, and how the Fuel Qualification Program will resolve them.

#### 5.4.1 Swelling data for HT-9

The projected 20-year residence time for the ARC-100 core is a factor of five to ten times longer than that of FFTF and EBR-II; however, it should be noted that the neutron flux will be less in the ARC-100 core. After 20 years of residence time, the fast neutron average displacements-per-atom (dpa) on the cladding and fuel assembly duct is calculated with some uncertainty to be between (calculated by MFUEL [13] and (calculated with the method of Reference [91]) 208 dpa for the ARC-100, as compared to a maximum 200 dpa for the EBR-II and FFTF test samples. The database for the HT-9 used in both ARC-100 cladding and duct material ends at 208 dpa. Thus, the ARC-100 core design is either within or marginally outside the operation and experimental data. At 200 dpa the growth with irradiation (dpa) is “flat”, and even with a 6-7% extension it is not anticipated to see a ‘breakaway’ leading to a step change swelling or creep. However, the calculation of the conversion factor between fluence and dpa is subject to uncertainties because it is dependent on the spectra of the neutron flux (ARC 100 has a somewhat softer than FFTF which had a softer spectrum than EBR II), and the actual composition and treatment of the HT9, so a different behavior could occur. To resolve this gap there are few possible approaches: The first is to investigate the possibility of testing samples of the HT 9 material (and the fuel) utilizing heavy ions (dual ion) irradiation. Whether it is possible to simulate neutron irradiation by using heavy ions has been a controversial subject. The University of Michigan has produced remarkable results, which indicate the possibility to accelerate induced damage by a factor of 1000 ( ) over the damage that was being caused by fast neutron irradiation of the material at BOR 60 ( ). The BOR 60 testing for Terrapower has been terminated, before the desired results at high dpas could be obtained, so that possibility is no longer available. Results of the University of Michigan indicate that ion irradiation can be extended and compared to the results of theory predictions to much higher dpa, and it is possible to obtain swelling data beyond 200 and up to 250 dpa on HT 9 in matter of months instead of a decade long program of neutron irradiation [ $7-8 \times 10^{-4}$  dpa/sec vs  $8 \times 10^{-7}$  dpas/sec at BOR-60] However, to date, comparison to neutron irradiation has only been done to a relatively low dpa, with excellent results.. Moreover, heavy ions do not penetrate deeply in the material so there is the question whether the result obtained do in fact provide information applicable to the bulk of the material. Therefore, data obtained for ion irradiation to 250 or higher levels will continue to validate the theory which predicts the expected damage level (by ion irradiation), but in effect will extrapolate the conclusion that the effects of ion irradiation are the same as those from neutron irradiation at these higher levels of damage. A second alternative is to introduce a specially designed Fuel Surveillance Test Assembly (STA) in the core to produce some of the expected materials behavior three years prior to the ARC-100 driver fuel reaching fluence levels near 200 dpa. HT9 material coupons inserted in the central presently empty core position would of course provide useful information, but not in time to predict what swelling the HT would experience when approaching or exceeding 200 dpa. In order to produce the fluence necessary to achieve the 200 dpa a few years earlier than when the core fuel will experience it, it would be necessary to use a Special Test Assembly (STA). The feasibility of such STA has been scoped, but the STA has not yet been designed. The reason is that whereas the neutron fluence needed to achieve dpa above 200 can be generated in the STA, other material behaviors (FCCI) which are driven by temperature and fission product concentration gradients over time, are not as easily accelerated, and a program using actual assemblies from the ARC-100 operation (as a First of a Kind) is considered a better alternative to produce the results of all phenomena acting on the fuel simultaneously. That is the program proposed by ARC. Should that program reveal swelling breakaway behavior or FCCI layer depth trending to unacceptable levels, the refueling period of 20 years will be reduced.

#### **5.4.2 Flow caused phenomena.**

The likelihood of flow induced vibrations which may cause fretting of the spacer wire, the clad and the duct has been assessed by calculating the Strouhal number, and the result indicated that flow induced vibrations should not be a problem. Nevertheless the complexity of the fuel bundle and the flow within the duct require that this be demonstrated by testing. ARC plans to qualify the fuel assembly and bundle by conducting full scale testing of mockup assembly in water (because the fluid characteristics of sodium and water are very similar) This test will also provide information on the intra-assembly flow distribution, addressing one of the uncertainties that must be accounted for in the safety analyses and design of the assembly.

The test can also be used to validate the pressure drop and orificing uncertainty assumed in the analytical thermo-hydraulic simulation of steady state and transient behavior of the core.

A second issue related to flow is the possible flow reduction caused by diametral strain of the cladding which can occur as a result of the phenomena addressed in this white paper. A diametral strain of 2% corresponds a local restriction of the nominal gap between pins (provided by the mm thick spacing wire) of 0.1 mm, if symmetrical, or as much as 0.2 mm if asymmetrical, which can cause an 80-90% reduction of the nominal flow rate in the channel between pins. For fuel qualification, based on past practices, the cladding peak temperatures have been determined with a  $2\sigma$  uncertainty. That uncertainty, estimated with the use of hot channel factors, includes direct as well as statistical uncertainties in flow maldistribution. Those uncertainties may not be sufficient to account for the increase in local temperature due to the local decrease in flow. Past reactor operations have not shown this to be a problem. ARC plans to have both flow and temperature sensors placed in very close proximity of the exit of each driver fuel assembly (similar arrangement as was employed in FFTF). Significant differences in the flow and/or temperature between adjacent assemblies would provide an indication of partial obstruction that might become unacceptable if not corrected.

#### **5.4.3 Seismic design**

The reliance of only an analytical prediction of the behavior of the fuel assembly and the core to an external load like a seismic event can fall in the same category as the above, because of the complexity of modeling the various elements that would be excited by the motion. Therefore, ARC is considering qualification of the fuel assembly and the core not only by design, but by conducting shake table tests simulating the earthquake.

#### **5.4.4 Cladding wastage due to solid state interdiffusion**

The mechanisms that produce the wastage are slow and depend on temperature and concentration of fission products. The temperature and concentration gradients in the ARC-100 are not dissimilar from those that were present in the specimens from which the data on the depth of solid state interdiffusion were developed. However, diffusion phenomena are time dependent and the time over which they can occur in ARC-100 is significantly longer than the time in which they were measured in the various experiments and operations. Consequently, the adequacy of the correlations used by the fuel performance computer codes over such a long time can be questioned. Should the ARC 100 be its First of a Kind, the resolution proposed is to use, after an initial period, periodic extraction of an assembly, or preferably removable pins, from the core for destructive testing to measure the depth of penetration. In the initial period, verification of the fuel performance will be done by extracting an assembly (or pins) after four to five years during which burnup should be sufficient to confirm the fuel expansion and gas evolution phenomena and detect some wastage

(if any). During the first year or two the temperature in the fuel and cladding could also be maintained below the limits at which no wastage has been observed by operating at a reduced power. Bounding steady state analysis would have to be done to determine that power level, but from analyses performed to date and as well as bounding transient analyses, there is indication that the power would be about %.

#### 5.4.5 Eutectic formation/Liquefaction.

The formation of eutectic at the interface between the fuel and the cladding can significantly weaken the clad and cause it to fail. Its formation can be avoided by maintaining the temperature at the interface below 650°C. In normal operation this is the case for the ARC-100. For transients this is also the case except for very unlikely events in which incidents in which the reactor protection system fails to scram the reactor. These cases have been analyzed and the results, reported in reference [8], show temperature exceeding °C for only a relative short time of several minutes, with inconsequential limited penetration (less than 1%) by eutectic formation. 715°C is considered the threshold the temperature at which accelerated eutectic formation in a transient would commence. The data supporting these temperature limits was primarily developed from tests which are independent of fuel composition, aspect ratios diameter and length of the fuel/clad, burnup or irradiation, given that the results from irradiated pins or specimens are consistent with the results obtained from dipping test, as explained in Appendix B. Nevertheless, the difference between the ARC-100 fuels dimensions, and the time of its irradiation could be seen as a concern. The resolution of this is similar to that outlined in (4) above, but with one significant difference. During the initial period of operation, if for whatever reason the interface temperature in a particular pin (or set of pins) were to exceed the limits, or the limits are not appropriate for the ARC-100 fuel and eutectic formation occurs at lower temperatures, eutectic liquefaction could result in (a) motion of the melt within the pin(s), assuming the cladding has not failed, with consequent redistribution of the fuel matrix which causes a change in reactivity; and (b) a breach of the pin (s) with subsequent freezing of the melt in the colder coolant, which also changes the reactivity. During this initial period periodic measurements will be taken of the Power Reactivity Decrement, which is very sensitive to even minor changes in configuration of the core, and which is briefly described in Appendix E. A Research and Development program is being conducted by ARC Clean Technology to pre-calculate the PRD shape resulting from assumed core configuration changes [18]. Changes of the PRD from the expected shape and value (as calculated or measured from the prior measured PRD) are indicative that something is not quite correct, and an investigation would be conducted. The PRD measurements will continue for the life of the core, but in addition, after the initial period, the periodic extraction of individual assemblies might indicate whether there may have been formation of eutectic.

#### 5.4.6 Reactivity feedback and Ratcheting

Reactivity feedback that is different from what is expected could stem from a variety of sources. Examples include enrichment errors, errors in modeling the core with the neutronics suite of codes, unexpected deformations in the core, ratcheting of the fuel slugs, etc. For those occurrences, like enrichment errors, the measurement of the power coefficient during the initial startup will reveal the differences in the power coefficients and corrections will be made. For the changes in reactivity that can unexpectedly occur during operation, the periodic measurement of the PRD (as discussed above) will reveal a problem which can then be investigated and addressed. From the nuclear safety standpoint in addition to the PRD measurement, the coefficients of the quasi-static reactivity balance equation can also be measured, as explained in Appendix F and compared to the limits which ensure that the reactor will inherently adjust to a controlled stable state.



#### 5.4.7 Blockages

Flow blockages are not directly relevant to the ARC-100 fuel qualification. If the coolant flow to an assembly is completely blocked, the assembly will suffer considerable damage, i.e., the fuel will melt, and very likely the resulting eutectic interaction with the cladding will result in the cladding being breached. The gap in knowledge for such a situation is whether the damage remains localized or spreads to adjacent assemblies. The obvious resolution is to design the inlet (and outlet) of the assemblies in such a way as to render blockage virtually impossible (which is what the ARC-100 has done). Nevertheless, were it to occur, the spread of damage to adjacent assemblies is presently outside the capability of the SAS4A/SASSYS suite of codes, because the code assumes no failure of the hexagonal duct. If the hexagonal duct does not fail the flow in the adjacent assemblies is more than sufficient to limit the damage to the blocked assembly and to remove the additional power generated in the blocked assemblies and overall core by the positive reactivity cause by the voiding of the blocked assembly.

As part of the ARC Clean Technology contract with the DOE, a development program is in progress to simulate the effect of one assembly blockage on adjacent assemblies, and the results to date are very encouraging, showing that the damage to the blocked assembly does not propagate to adjacent assemblies to an extent that those assemblies would be unacceptably damaged [19]. . When completed this effort can be used to modify the SAS4A/SASSYS-1 code to predict the possible spread of damage. However, the issue with such modification is the availability of a facility to simulate the transient event so that the code modification can be validated as producing correct results. With no nuclear facility presently available, a non-nuclear test rig would have to be designed to simulate the blocked assembly behavior (fuel melting, hexagonal duct breaching) and adjacent simulated assemblies continuing normal flow. The heat source in the blocked and adjacent assemblies would have to be set up to mimic the initial increase in power (to simulate the positive reactivity feedback by the voiding of the blocked assembly following by a gradual decrease to mimic the negative feedback caused the fuel melting. Alternatively, it might be possible to validate the code modification against the only test that was conducted specifically to address the question of the possible spread of damage. In the late 1970s and early 1980s a series of tests were conducted in the Sodium Loop Safety Facility of the Engineering Test Reactor in Idaho, as part of the LMFBR Safety Program Plan to demonstrate coolability of local faults and local fault accommodation by inherent mechanisms. Experiment P4 was conducted in the Engineering Test Reactor to investigate the behavior of a "worse-than-worst-case" local fault configuration. Objectives were to eject molten fuel into the 37-pin bundle of full-length Fast Test Reactor-type fuel pins from one or more of the three heat-generating fuel canisters, to characterize the severity of any molten fuel-coolant interaction, and to demonstrate that any resulting blockage could either be tolerated during continued power operation or detected by global monitors in time to prevent significant fuel failure propagation. The results showed no propagation (from pin to pin), but that might have been because the blockage was only partial, and the fuel was oxide not metal.

#### 5.4.8 Loss of heat transfer (gas blanketing)

The issue of the possible adverse effect that the release of gas from a breached pin may have on the heat transfer coefficient, like the issue above, represents a gap in knowledge, but is not directly related to the fuel qualification. Pin failures have occurred, in every instance the failure was confined to the failed pin and did not extend to adjacent ones. Experiment P4 (mentioned above) corroborates this experience but for oxide fuel only. No analysis has been done specifically for the ARC-100 pin configuration, and no definitive or even preliminary conclusion can be drawn from the evidence seen

in the failed pins. The pressure in the gas plena of the failed experimental pins were similar to those that the ARC-100 will experience, but with the much smaller volumes of their gas plena (27-37 times smaller than the ARC-100 gas plenum volume), the jets that could blanket the adjacent pins and reduce the heat transfer would last a very short time and the coolant flow would quickly re-establish. The ARC-100 gas plenum volume is such that depending on the shape of the breach the emanating jet could last much longer and possibly have an adverse effect. A specific analysis will be done to ascertain what the possible effect will be by modeling the jet, its duration until the coolant flow is reestablished.

#### **5.4.9 Fission product transport**

The behavior of fission products in the fuel, the sodium and the cover gas region have been the object of considerable research worldwide. Their behavior once released to the sodium pool is not related to the fuel qualification. However, the amount that is released depends on the fuel matrix. One of the major advantages of sodium cooled metal fuel is that with the exception of the fission product gases, a small fraction of the halogens, and a relatively small fraction of alkali metals and few specific isotopes, the fission products are retained in the fuel. Table 6-1 shows the quantities that are presently considered to be bound. The resolution of these issue, of course, rests on prevention of fuel clad failures during all operations, transients and accidents, including Beyond Design basis Events (BDBEs), which is addressed in the Fuel Qualification Program designed so as to accomplish such prevention. Nevertheless, the safety case for the fission product transport is predicated on the assumption that severe damage to the core will occur, fission products will be transported to the containment and released to the environment. Reference [15] provides a description of the consequences of this event and concludes that no unacceptable doses would result outside the site boundary, as shown in Figure 6.3. Section 6.1 provides a summary of the analyses which demonstrate that even an event causing failure of all of the pins in the core would not result in unacceptable doses at the site boundary of the facility.

### **5.5 Testing and Inspection**

This section discusses only those tests and inspections which would be performed during operation to support the continued fuel qualification. Preoperational and start up testing are not included, nor are those tests which will be performed during the fabrication of the assemblies, e.g., flow tests to determine pressure drops, flow induced vibrations; structural tests to determine the structural response of assemblies and pin bundles.

Appendix A shows a notional schedule for the fuel qualification program assuming the ARC20 fuel performance program reactor to be the FOAK.

The result of the analytical predictions of fuel performance given in section 5.3 identify a concern that limited pin failures may occur as the irradiation reaches approximately 16 equivalent full power years. In addition, they identify strains in the cladding which could challenge the reactivity feedback and potentially the local coolability of the assemblies. The long irradiation period of the ARC 100 fuel (20 calendar years or 18 equivalent full power years) introduces an uncertainty in the results of the analytical predictions, because those predictions are partly underpinned by correlations developed from experimental and operational data that did not include such long period of irradiation, e.g. the swelling and creep behavior of HT9 beyond 200 dpa is not well known, nor is the effect of such irradiation on the thermal creep behavior of the cladding (the analytical prediction assume the two to be independent from one another).

Consequently, it is very important that the behavior of the fuel system be confirmed by a testing and surveillance program designed to provide information on the actual behavior of the fuel system as the period of irradiation approaches the 16 EFPY , and then continues for the remainder of the time until refueling.

The testing and inspection program consists of two complementary parts: a testing program which relies on the periodic extraction of pins from the core, and an inspection program of deformation as they occur in the core. Each is described herein after.

For the testing program, one fuel assembly would be removed from the core at the end of the fourth year of operation, and then again after the 12th and/or 14th, 16th, and 18th year of operation. The assemblies and pins would be subjected to nondestructive and destructive testing to verify their behavior. The first tested assembly at the end of calendar year four will be able to show how the early phenomena have manifested themselves and provide the first confirmation of expected behavior of the fuel. The time interval, taking into consideration an initial limitation in power level, is sufficient for the burnup to have resulted in measurable fission gas evolution and fuel expansion against the cladding will have occurred. However, the fuel chemical interaction phenomena and swelling (deformation) are expected to be negligible and barely observable. After the end of the 11<sup>th</sup> year of operation, the latter would manifest itself, and the subsequent fuel assemblies testing can follow its growth and be used to confirm or change the analytical prediction of the fuel behavior. The plan would extract assemblies, but if the inspection program indicates that assemblies' deformations are not a concern, only pins designed to be removable without removing the assembly, would be extracted and tested.

The inspection program relies on indirect observation/examination of the fuel assemblies extracted during outages necessary to perform in service inspection, and see measurement of the pull-out force measured by the In-Vessel Transfer Machine (IVTM) as an indication of the deformation of the assembly. Comparisons of the forces in measurement conducted in subsequent outage, provide indication of acceptability of the deformation and trends toward possible unacceptable deformation if left uncorrected. The pull-out force measurement is also part of the fuel surveillance program.

Extraction of an assembly for nondestructive and destructive testing during the early years of operation (shown at the end of year 4 is for the purpose of confirming that the behavior of the fuel is as predicted. The most appropriate timing will be informed by the core monitoring systems and provision discussed hereinafter, but 4 years will produce burnups sufficient to show the effects of the early phenomena: fuel swelling (radial and axial growth), fission gas release, Fuel Cladding Mechanical Interaction (FCMI), fuel coolant compatibility. Some indication will be provided on the fuel constituents distribution. However, those phenomena most likely to affect the lifetime of the core (as explained in section 5.1) take significantly longer time to fully manifest .

The reason for delaying the extraction of additional fuel assemblies for purposes of nondestructive and destructive test is that the phenomena that can cause failure of the cladding take a long time to manifest themselves. In the range of operating temperatures, the ARC 100 will experience eutectic formation will not occur, unless the reactor experience unprotected transients. Therefore, fission product and constituents' depletion, the combined effect of which is addressed in section 5.1 are the limiting factors in the ability of the cladding to withstand applied loads. Reduction in thicknesses of the order of 60-70 $\mu$ m begin to approach the levels at which the integrity of the cladding is challenged (about 100  $\mu$ m). This in combination with the protective measures established to monitor the behavior of individual assemblies and the core as a whole (PRD, reactivity meter, pull out force measurements and real time measurements of temperatures and flow at the exit of the individual

assemblies, justify delaying the extraction a test assembly until year 12 or later of operation, at which time the cladding could have experienced an effective thickness reduction of 60 or so  $\mu\text{m}$ .

Of course, if during the 12-year period the monitoring of the core indicates anomalies, the testing of the fuel can be accelerated.

It is noted that for every assembly which is extracted, a total of three to four years is assumed to be required for completing the test, from the moment the assembly to be withdrawn is identified, through the shutdown necessary for its removal and replacement, to its initial nondestructive dimensional measurements, to disassembly of the fittings in preparation for shipment of the fuel bundle to an appropriate Laboratory, to the comprehensive nondestructive and destructive tests conducted in that Laboratory, the data reduction and preparation of the final report. This period is considered conservative, and initial reports should be available by the middle of the period, so that a decision on extracting the next test assembly can be made with information from the preceding one.

## 6 FUEL SYSTEM MONITORING FOR FUEL PIN FAILURES

### 6.1 Radionuclide Release Limit

Radionuclide releases are limited by the ability of the fuel to retain many of the radionuclides generated by the fission process within the fuel matrix itself. and to retain within the cladding those which can escape from fuel matrix into the coolant, from the coolant to the cover gas, and from the coolant and cover gas to plant spaces and the environment. For normal operation and anticipated operational occurrences the extent to which cladding failures can be expected is set by the fuel performance envelop defined by the neutronics and thermohydraulic analyses which establish limits on power, power to flow, and temperatures within which the reactor is normally expected to perform. Those limits are shown in the radar chart of Figure 6.1.

For normal operation and anticipated occurrences, no cladding failures are expected to occur assuming the behavior of HT9 beyond the 200 dpa irradiation remain linear. Nevertheless, stochastically some failures might occur as a result of fabrication defects, or localized conditions that might be beyond those considered in the uncertainties included in the analysis of the pin behavior. The possible failures of the fuel for the ARC 100 has been established at 0.1 % (or pins) during one refueling interval.

This value is determined by examination of the failures experienced at the EBR II and FFTF facilities, both of which operated with considerably higher power densities, liner power, and similar but higher fuel and cladding temperature. So, one could expect either not much difference or possibly a higher number of failed fuel pins in those facilities than in the ARC 100.

Figure 6.1 ARC-

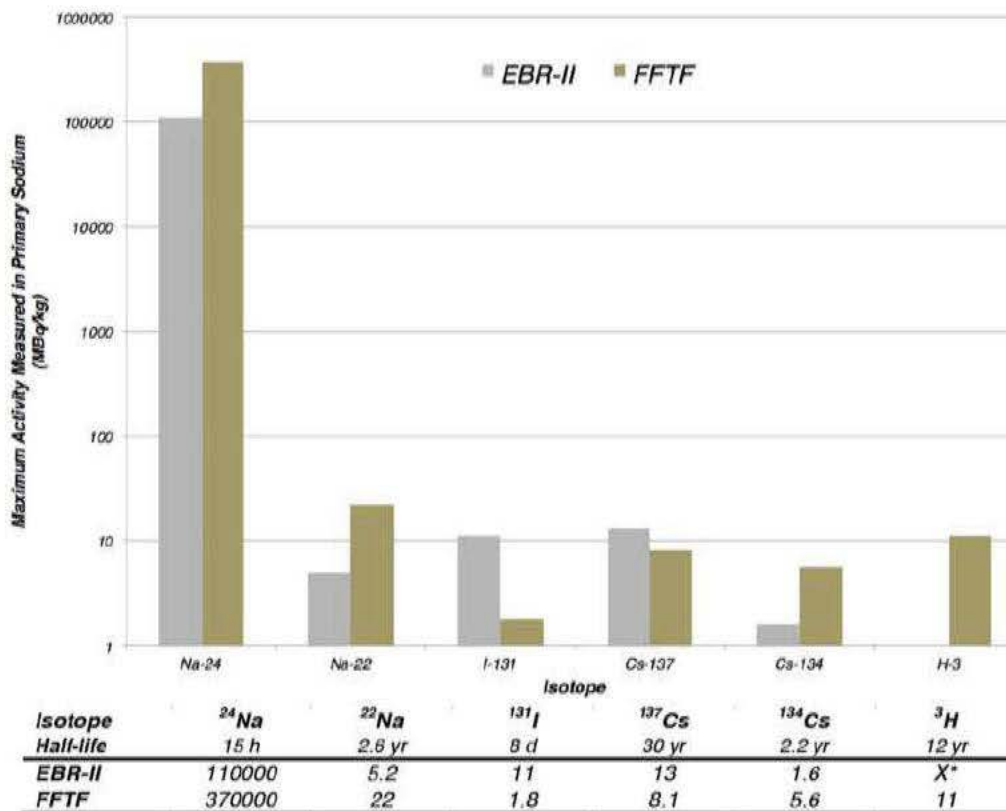


Figure 6.2 Maximum Activity Levels (MBq/kg) Measured in Primary Sodium

Fission products and fuel are found in the primary sodium if the reactor is operated with failed fuel pins. Figure 6.2 illustrates the amount of the fission products present in the primary sodium for EBR-II and FFTF, which is dependent upon the percentage of failed pins and is indicative of the amount with which ARC-100 could expect in operation. Figure 6.2 is used to calculate the range of pin failures experienced at the EBR-II. For the iodine, due to the relatively short half-life of I-131, the amount in the fuel during the time in-core (~1 year) would have reached equilibrium, and hence the amount of iodine present in the EBR-II fuel can be approximated by the amount in the ARC-100 fuel when adjusted for difference in power levels. and is about 290 Ci /pin. The number of pins in EBR-II varied somewhat but it is assumed that the number of 4823 is the most representative of the various cores. The ARC 100 core content of I-131 is 66.2 gms [71], so the EBR II content is assumed to have been close to 14.5 gms. Each pin of EBR II is calculated to have an average of 0.003 gms of I-131, which equates to 371 Ci.

From the amount found in EBR-II coolant (11 MBq/kg), assuming that the equilibrium amount of I-131 is directly proportional to the thermal power, the amount of I-131 in the coolant of EBR-II (~300,000 kg) corresponds to 89 Ci. If 10% of the I-131 leaked out, this means that 2 or at most 3 pins would have failed out of 4823., or about 0.05%

The fraction of iodine that actually migrated to the coolant, given the relatively high temperature at which EBR-II operated could have been 10% , but was probably less, hence amount of I-131 activity found in the coolant of EBR-II could have been caused by a failure of only two pins or more pins, if less iodine leaked out.

Experience at EBR-II indicates that the facility could continue operation with a number of failed pins, with negligible (almost non-existent) personnel exposures, and it is assumed that ARC-100 could operate with a maximum of 0.1 % fuel pin failures. There are assemblies of pins each; therefore, 0.1 % of failed pins would amount to pins.

A statistical analysis of the time to rupture developed by fitting unirradiated stress -rupture data for pressurized HT9 tubes, showed that the logarithm (base 10) of the cumulative damage factor is distributed normally with a mean of -0.0354 and a standard deviation of 0.1885.[See Annex A] Assuming the irradiation does not change the time to rupture, the failure of 0.1% corresponds to the mean + 3.4 standard deviations, or -0.6763, and  $\log_{10}(\text{CDF}) = -0.6763$  CDF = 0.21 Since the allowable CDF is 0.05, there can be good assurance that the failure of the pins will not exceed the 0.1 %

Therefore, to the fuel performance envelope presented in Figure 6.1, it is necessary to add a limit of 0.1% failed fuel as the expected range within which the ARC 100 will operate.

The small amount of failed pin is justified when considering that the operating temperatures of the fuel/cladding interface for normal operation and anticipated occurrence are at a level for which no eutectic formation has ever been observed, and for which the growth of fission product migration induced layers over the entire refueling period would result in layer thicknesses that would not challenge the integrity of the cladding. ARC Clean Technology determined the layer thickness after irradiation for 18 Equivalent Full Power Years (EFPY-20 year refueling at 90% capacity factor) At the nominal temperatures that the cladding experiences during normal operation and anticipated operational occurrence, calculations performed using a simple Arrhenius equation which depends only on the cladding temperature and time at temperature, and analysis using the BISON code, indicate the layer depth would be only  $\mu\text{m}$  thick , and for  $2\sigma$  temperatures a thickness of  $\mu\text{m}$  might result. BISON detailed analysis resulted in  $\sim \mu\text{m}$ . This thickness would be insufficient to weaken the cladding to the point of failure, even when added other wastage caused by manufacturing defects.

In addition to the fission product radionuclide, activated coolant isotopes and activated corrosion product are considered. when determining the potential releases of radioactivity to the plant and the environment. However these radionuclides are not from the fuel, and the amount of ternary fission tritium in the fuel negligible compared to the amount created of in the control rods.

For the limits established for fuel failures, normal operation and anticipated occurrences result in concentrations of fission products in the coolant and its connected system (primary sodium purification system and cover gas processing system) that when appropriately shielded results in very low exposures to radiation by operating and maintenance personnel (as has been the case in both EBR II and FFTF). Accidental releases of the coolant or the fission product gases, depend on the extent of the release, but to the environment are going to be a small fraction of what would result if all of the pins were to fail.

Data regarding the migration of radionuclides within the fuel pin and subsequent release during fuel pin failure (as described in more detail in ANL-ART-38 [72]), is not sufficient to more detailed calculations beyond using bounding radionuclide release fractions from failed fuel pins, which per reference [72] are shown in Table 6-1.

**Table 6-1: Migration Fraction for Radionuclide Groups as Function of Burnup**

Radionuclide Groups	Burnup %				Notes
	2	5	10	16.5	
Noble Gases (Kr, Xe)	30	70	75	100	Noble gases approach an asymptote of 85 as burnup increases
Halogens (I, Br)	10	10	10	10	Data above 10% burnup shows 10 % iodine in plenum and 90% in fuel. Most iodine remains in fuel until temperature ~1300°C
Alkali Metals (Cs, Rb)	15	40	50	55	Cesium approaches an asymptote of 60% as burnup increases
Tellurium Group (Te, Sb, Se)	1	1	1	1	
Barium	5	10	15	15	
Strontium	5	25	50	55	Strontium and Europium seem to behave as Cesium
Noble Metals (Ru,Rh, Pd, Mo, Tc, Co)	0.1	0.1	0.1	0.1	
Lanthanides (La, Zr, Nd, Nb, Pm, Pr, Y, Lm, Am)	0.1	0.1	0.1	0.1	
Europium	15	40	50	55	Strontium and Europium seem to behave as Cesium
Cerium	5	5	5	5	
Pu, Np, U	0.1	0.1	0.1	0.1	

As a bounding assessment of the characteristics of the fuel matrix and the cladding which limit releases of radioactivity, ARC Clean Technology has analyzed a postulated case in which all fuel pins were forced to fail, by assuming incapacitation of both diverse passive heat removal system. After nearly 67 hours all pins failed and the high temperatures of the fuel caused a maximum amount of the radionuclides contained in the matrix to be released to the coolant, then the cover gas and then the reactor building spaces and ultimately the environment.

The analysis of this hypothetical event is reported in Reference [15]. The Analysis was conducted by using the SAS4A/SASSYS-1 code [17] to analyze the conditions in the fuel and the reactor hot and cold pools and the cover gas region, and the SRT code [73,74] which is a mechanistic source term analysis code developed by Argonne to assist in the potential radionuclide release associated with fuel damage events in pool-type SFRs.

At  $^{\circ}\text{C}$ , the cladding eutectic penetration rate is approximately  $\mu\text{m}/\text{sec}$ , which would require approximately 7 hours for complete penetration of the  $\text{cm}$  cladding. However, complete cladding penetration is not necessary for fuel pin failure due to the internal pressure of the fuel pin. As cladding degradation would likely start to occur around  $725^{\circ}\text{C}$ , which occurs at 66.5 hours in the current analysis, fuel pin failures were conservatively assumed to occur between 67.5 and 68 hours.

The values utilized to assess radionuclide migration within the fuel pin and subsequent release from failed fuel pins was derived from ref [2.7]. The magnitude of radionuclide aerosol creation within noble gas bubbles in the sodium pool was treated as an uncertainty, as were the properties of the associated aerosols. Similarly, the presence and quantity of cesium vapor within the fuel pin at the time of pin failure was also considered an uncertainty. Many other uncertainties were also considered in the analysis.

The deposition of aerosols within the cover gas region and containment was assessed utilizing the Henry Fauske correlation [75], with associated uncertainties. All non-noble gas vapors were assumed to become condensed aerosols upon entering the colder containment volume. The potential dissociation of aerosolized NaI into gaseous I<sub>2</sub> once in the presence of an oxygen environment within containment was treated as an uncertainty based on the findings of ref [76]. A reactor head leakage rate of 5 vol %/day was assumed, along with a containment leakage rate of 1 vol %/day. The larger reactor head leakage rate was assumed based on the increased temperature of the primary sodium during the transient, which could result in increased leakage from the head seals.

Offsite dispersion was assessed utilizing a  $\chi/Q$  value of  $3.5\text{E-}3 \text{ sec}/\text{m}^3$  and a breathing rate of  $3.5\text{E-}4 \text{ m}^3/\text{sec}$ . The  $\chi/Q$  value was selected based on Department of Energy (DOE) guidance for a distance of 100m from the release site [77].

The SRT analysis assessed a release period of seven days. However, since the release of radionuclides to the environment is a result of reactor system leakage (such as the continued release of radioactive noble gases contained in the reactor vessel cover gas region and containment), the resulting offsite dose is dependent on the assumed release period. The current results represent a scenario where leakage rates are assumed to be minimized after seven days, possibly as the result of human actions.

Results of this “bounding” analysis are presented in Figure 6.3, which also shows results of calculation that utilized scaling of results from similar analyses conducted for higher power pool type sodium cooled reactor and reported in Reference [16]

The bounding analysis shows the combination of the metal fuel ability to retain radionuclides within its matrix, even when the cladding fails, combined with the scrubbing action of the pools and the deposition of sodium aerosols on colder surfaces result in doses at an ARC 100 boundary



located meters from the reactor, which meet regulatory limits. In actuality, even for beyond design basis events the deterministic safety analyses indicate that very limited, if any cladding failures would occur. This shows that the fuel design is that has the fuel performance envelope defined by Figure 6.1, has a high likelihood of meeting all the requirements of NUREG 2246.

**Figure 6.3 Offsite Dose (TEDE) from failure of all the pins in the ARC-100 Core**

## 6.2 Detection Methods

Detection of pin failures is accomplished by monitoring the cover gas. Radioisotopes released in the coolant from pin failure are transported to the cover gas, and detected in the cover gas treatment system, which is continuously monitored for radioactivity. A multichannel analyzer is used to identify

the radioisotopes that are fission products. This measurement of course will only provide information that fuel has failed, but not the assembly with the failed pin(s).

A more accurate method to specifically identify in which assembly pin(s) failure has occurred is the tagging of each pin in an assembly with a unique combination of Xe-Kr isotopes. This method has been used in both the EBR II and FFTF reactors. The latter introduced the tag gas as a capsule in the gas plenum and uses a laser to rupture the capsule when seal welding the pin. A gas chromatograph is used to detect the specific isotopes which uniquely identify the fuel assembly that has experienced pin failure.

Other reactors have utilized delayed neutrons as a means to identify fuel failures. ARC is considering whether such a system should also be employed. Feedback from operations in reactor where the system was used, however, has indicated that its reliability is questionable.

Figure 6.4

## 7 FUEL SURVEILLANCE

The fuel surveillance during operation, relies on:

- (1) periodic measurement of the pull-out forces.
- (2) real time determination of the coefficients A, B, and C of the quasistatic reactivity balance equation. Coefficient B provides direct information on the effect of deformation on the reactivity feedback of the reactor. Alternatively, the comparison of measured Power Reactivity Decrement shapes compared to the shapes per-calculated for assumed deformations in the core, will be used as indications of potentially unacceptable strains/deformations if left uncorrected. The reactivity meter that will be provided in the control room will assist in this work.
- (3) Monitoring fuel failures, as described in section 6.2.

Of course, measurement of pull-out forces cannot provide information on the internal conditions of the pin bundle, nor information on the internal conditions of the control assemblies. For the latter measurement of the current provided to the control rod drive mechanism will provide an indication of the force necessary to move the absorber. The pull-out force measurements will be supplemented running a tuned version of NUBOW (or perhaps a newer code) to predict the withdrawal forces of all of the core assemblies and then shutdown before the withdrawal forces exceed the IVTM fuel handling capacity. This process was used at the FFTF. Just like FFTF (and EBR II), when the reactor is operating, it can be decided to rotate some of the core assemblies, in order to allow for continued core operations with the existing core. The rotation would cause deformations in a specific direction to be reversed.

## 8 CONCLUSION

The conclusion of the information presented in this white paper is that the ARC100 fuel cannot be completely qualified by design. This is because there is insufficient knowledge of the behavior of the HT9 material and the fuel matrix itself after the irradiation over its long refueling interval of 20 years, which introduces uncertainties in the material properties and correlations used in the design. Those uncertainties mean that, when the irradiation period approaches and exceeds 16 EFPY, analytical results may not be sufficient to provide high confidence that the fuel will not experience failure. Consequently, a testing program utilizing the reactor operation as its own test bed is necessary to provide that confidence.

The testing program will be accompanied by a complementary program which provides real time information on the condition of the fuel and can be used to stop operation at the moment its indication is that the behavior of the fuel may not be as expected.

If a test reactor or similar reactors become available worldwide in time to fill some or all of the present design gaps, the need for the ARC 100 to be operated as its own test bed may be eliminated. Until then the combined qualification by design and testing with compensatory measure provides assurance that the ARC 100 can be operated safely with minimal fuel failures.

What are the design gaps which should be eliminated in the future?

NUREG 2246 and NUREG/CR 7305 have identified the major ones. This white paper lists those having the most immediate effect on the proposed fuel qualification program.

- The computer codes used to predict fuel performance have made significant progress in modeling the phenomena using the first principles. However, they still depend on correlations for a number of them, and the validity of the correlations when applied to irradiation times beyond those in the experiments and operations from which the correlation was developed is questionable.
- The conservatism of the acceptance criteria established for stresses and strains is only partly known and should be better quantified.
- The physical/thermal properties of the fuel when the porosity changes with time from the fission product gas interlinking and the filling of the pores with solid fission products and how the creep behavior of the fuel is affected.
- The material properties and behavior of the HT9 cladding material at radiation doses exceeding 208 dpa is unknown.

## 9 REFERENCES

- [1] S.C. Marschman, "Review of EBR 2 fuel fabrication process as a basis for conceptual design of ARC-100: INL/RPT-22-70433 Rev 0, December 2022
- [2] ARC Clean Technology, "ARC-100 Small Modular Reactor, Fuel Qualification Program Summary Report, Rev D", ARC20-F-002, February 2023
- [3] A. M. Yacout, et al. "FIPD: EBR-II Fuels Irradiation & Physics Database." In: Argonne National Laboratory ANL-ART-124 (2017).
- [4] W.J. Carmack, H.M. Chichester, D. L. Porter, D.W Wootan, "Metallography and fuel cladding chemical interaction in fast flux test facility irradiated metallic U-10Zr MFF-3 and MFF-5 fuel pins" journal of Nuclear Materials, 473 (2016), 167-177.
- [5] J.M. Kramer, "Design Criterion for the Allowable CDF During normal operation of Mark-V Fuel," ANL Intra-Laboratory Memo, February 10, 1992
- [6] N.S. Cannon, F.H Huang, and M.L Hamilton, "Simulated Transient Behavior of HT9 Cladding", WHC-SA-0127-FP
- [7] Argonne National Laboratory, "286 MWth Core ARC-100 Safety Analysis," ANL/NE-ARC/ARC20-05, Rev. 2, August 31, 2023.
- [8] T. Sumner, A. Moisseytsev, R. Ramey and N. Stauff, "Analyses of ARC-100 Unprotected Transient Overpower Event at Different power levels, ANL/NSE-ARC-11, June 30, 2023
- [9] T. Sumner, "Simulation of PTOPT Perturbation to support ARC-100 Probabilistic Risk Assessment", January 24, 2023
- [10] T. Sumner, "ARC-100 Ticket 75- BOL PTOPT with, degraded RVACS and DRACS" Private Communication, April 21, 2023
- [11] T. Sumner, "Assessment of how Long Power Must Be Supplied to the Primary pumps While Coasting Down", ANL/NE-ARC/XX, October 21, 2022
- [12] <https://mooseframework.inl.gov/bison/assessment/index>.
- [13] Aydin Karahan, Taeil Kim, Thomas Fanning Dan O'Grady, "Validation of MFUEL Metal Fuels Performance Models of SAS4A/SASSYS-1," ANL/NSE-23/11, June 1, 2023
- [14] L.L.Briggs et al, "Safety Analysis and Technical Basis for Establishing an Interim Burnup Limit for Mark-V and Mark VA Fueled Subassemblies in EBR II", ANL-NSE-1. May 23, 2018
- [15] D. Grabaskas, T. Starkus, T. Sumner, "ARC-100 Bounding Accident Source Term Analysis", ANL/NSE-ARC/ARC20-12, Oct. 2022
- [16] ANL-ART 49, "Regulatory Technology Development plan, Sodium Fast Technology, Vols 1 and 2 Mechanistic Source Terms- Trial Calculations", Feb 2016.
- [17] T. H. Fanning, A. J. Brunett and T. Sumner, "The SAS4A/SASSYS-1 Safety Analysis Code System," ANL/NE-16/19, Nuclear Engineering Division, Argonne National Laboratory, March 31, 2017.
- [18] N. Stauff, K. Ramey, M.A. Smith, T. Sumner, and T.K. Kim, "Interim Report on Predictive Analysis of PRD as Function of Deformations", ANL/NSE-ARC/ARC20 -19, June 30, 2023
- [19] A. Tentner and Taeil Kim, "Simulation of a Severe Assembly Blockage Accident in a Sodium Fast Reactor with the SAS4A Safety Analysis Code" 2023, ANL winter meeting,

- [20] K. Inagaki, K. Nakamura, T. Ogata, and T. UWA A, "Chemical Interaction in Metal Fuel for F R", Vol2, No 2, p 149-157, (2013, Doi:10.3327/taesj.J12.007
- [21] G.L. Hofman et al, "Metallic Fuels Handbook", sections D.2 and E.2, ANL-NSE-3, April 2019
- [22] ARC Clean Technology, "Overall Plant Design Description", October 2022.
- [23] U.S. NRC, NUREG 2246, "Fuel Qualification of Advanced Reactors- Final", March 2022
- [24] U.S. NRC, NUREG/CR-7305, "Metal Fuel Qualification- Fuel Assessment Using NRC NUREG-2246 "Fuel Qualification for Advanced Reactors", August 2023
- [25] Nuclear Systems Materials Handbook, Vol. 1 Design data, Oak Ridge National Laboratory Report TID 26666, Oct 1991.
- [26] C. Martinez and R.J. Puigh, "Interim Report on Pressurized Tube Data from MOTA01E (Cycle 9), Westinghouse Hanford Co, Report WHC-SP0277 Jan 1988
- [27] R.G.Pahl, C.E. Lahm and S.L. Hayes. "Performance of HT 9 clad metallic fuel at high temperature", Journal of Nuclear Materials, **204**, pp 141-147, 1993
- [28] D.C.Jacobs, "The Development and Application of a Cumulative Mechanical Damage Factor for Fuel Pin Failure Analysis in LMFBR System, ' Clinch River Reactor Plant Report CRBR-ARD-0115, Aug 1976
- [29] J.F. Koenig et al, "Irradiation of Mark IA Fuel Elements with Bond Sodium Defects ," Argonne National Laboratory Progress Report, ANL-RDP-30, 1.10 July 1974
- [30] J.F. Koenig et al, "Irradiation of Mark IA Fuel Elements with Bond Sodium Defects ," Argonne National Laboratory Progress Report, ANL-RDP-45, 1.14, November 1975
- [31] G.D. Johnson and C.W. Hunter, "Mechanical Behavior of fast Reactor Fuel Pin Cladding Subjected to Simulated Overpower Transients," Hanford Engineering Development Laboratory Report HEDL-TME 78-13, June 1978
- [32] N.L Hamilton and N.S. Cannon, "HT9 Transient Data Base and Failure Correlations, " Hanford Engineering Development Laboratory Report HEDL-TC-2681, March 1985
- [33] T. Sofu, "A Review of Inherent Safety Characteristics of Metal Alloy Sodium Cooled Fast Reactors Against Postulated Accidents" Nuclear Engineering and Technology, Vol 47, pp.228-239, 2015.
- [34] T. H. Bauer, C. R. Fenske, and J. M. Kramer, "Cladding Failure Margins for Metallic Fuel in the Integral Fast Reactor," Proc. 9th Int. Conf. Structural Mechanics in Reactor Technology, Lausanne, Switzerland, August 17-21, 1987, p. C-31, International Atomic Energy Agency (1987).
- [35] T.G. Bauer, A. E. Wright, W. R. Robinson, J. W. Holland, and E. A. E Rhodes., "Behavior of Modern Metallic Fuel in TREA Transient Overpower Tests", Nuclear Technology, Vol. 92. pp. 325-352
- [36] O. Derollepot, "Statistical Analysis of HT9 Transient Failure Data," ANL Intra Laboratory Memo, September 17, 1991.
- [37] R.G. Pahl et al., "The Characterization and Monitoring of Metallic Fuel Breaches in EBR II" 1991 International Conference on fast Reactor and Its Fuel Cycles, Oct 29-Nov 1, 1991, Kyoto, Japan
- [38] G.L. Batte and G.L. Hofman, "Run-Beyond-Cladding-Breach (RBCB) Test Results for the Integral Fast Reactor (IFR) Metallic Fuels Program", Proceedings in International Fast Reactor Safety Meeting, 1990, Snowbird Utah: American Nuclear Society, La Grange Park, IL
- [39] "Structural Design Guidelines for FBR Core Components- Guidelines for Analysis" RDT, Draft F9-8, August 1978

- [40] “Structural Design Guidelines for FBR Core Components- Structural Design Criteria” RDT, Draft F9-7, August 1978
- [41] E.A. Little, “Fracture Mechanics Evaluation of Neutron Irradiated Type 312 Austenitic Steel,” J. Nucl. Mater., Vol 139, pp261-279, 1986
- [42] Huang, F. and M. L. Hamilton, “The fracture toughness database of ferritic alloys irradiated to very high neutron exposure”, J. Nucl. Mater. 187 (1992) 278
- [43] Byun, T.S, D.Ds. Lewis, M. B. Toloczko, S. A. Maloy, “Impact Properties of irradiated HT9 from the Fuel Duct of FFTF,” J.Nucl. Mater., 421, (2012),pp104-111
- [44] ASME Boiler and Pressure Vessel Code, ,Section III, Div. 5 Class 1 Components in Elevated Temperatures Service.
- [45] R.G. Pahl, D.L. Porter, D.C. Crawford, and L.C. Walters, “Irradiation Behavior of Metallic Fast Reactor Fuels”, J. Nucl. Mat. 188, pp3-9 (1992).
- [46] A. M. Yacout, et al. “FIPD: EBR-II Fuels Irradiation & Physics Database.” In: Argonne National Laboratory ANL-ART-124 (2017).<https://fidp.ne.anl.gov/>
- [47] Douglas C. Crawford, Douglas L. Porter, Steven L. Hayes, “Fuels for sodium-cooled fast reactors: US perspective”, Journal of Nuclear Materials, (2007) 202–231
- [48] B.R. Seidel et al,” A Decade of Advances in Metallic Fuel in LMR: A Decade of LMR Progress and Promise” Nov 11-15, 1990 Washington DC : American Nuclear Society, La Grange Pek, IL
- [49] G.L. Batte and G.L. Hofman, “Run-Beyond-Cladding-Breach (RBCB) Test Results for the Integral Fast Reactor (IFR) Metallic Fuels Program” , Proceedings in International Fast Reactor Safety Meeting, 1990, Snowbird Utah: American Nuclear Society, La Grange Pek, IL
- [50] G.L. G Hofman, L.C. Walters and T. H. Bauer, “Metallic Fuel Elements for Fast Breeder Reactors, Progress in Nuclear Energy, **31**,No1/2 (1997 pp83-110
- [51] Pahl, R. G.; Wisner, R. S.; Billone, M. C.; Hofman, G. L., Proceedings of the International Fast Reactor Safety Meeting, Snowbird, UT, 12–16 Aug 1990; Vol. IV. p 129.
- [52] Hofman, G.L.; Pahl, R.G.; Lahm, C.E.; Porter, D.L., Metall, Trans. 1990, 21A, 517
- [53] Crawford, D. C.; Hayes, S. L.; Pahl, R. G. Trans. Am. Nucl. Soc. 1994, 71, 178.
- [54] E. Pauline Alexanderson, “Fermi 1, New Age for Nuclear Power, American Nuclear Society, 55 N. Kensington Ave. La Grange, Ill., 1979.
- [55] P. Medvedev, “Summary of INL’s fuel design and analysis work to date”
- [56] G..D. Hudman, D.D. Keiser, and D.L. Porter, “Ex-Reactor Testing for loss of HT9 cladding in metal fuel”, ANL-IFR-70, June 1987
- [57] Walters, L.C., Kittel, J. H., Development and Performance of Metal Fuel Elements for Fast Breeder Reactors, Nucl. Technol., **48** (1980) 273–280.
- [58] S.C. Marschman et al., “Fabricating Fuel for the Versatile Test Reactor”, INL/XXX-XX-xxxxx, Rev 0, September 2022
- [59] Douglas E. Burkes et.al. (2009) “A US perspective on fast reactor fuel fabrication technology and experience part I: metal fuels and assembly design”, Journal Nuclear Materials, **389** pp. pp. 458-469 (2009).

- [60] A.L. Pitner, and R.B. Baker, "Metal fuel test program in the FFTF", *Journal of Nuclear Materials*, 204 , 1993 page 124-130, paragraph 2.3
- [61] T. Ogata, Chapter 3.01 Metal Fuel Central Research Institute of Electric Power Industry, Tokyo, Komae, Japan, 2012 Elsevier Ltd
- [62] R.S. Barnes, "A theory of Swelling and Gas Release for Reactor Materials", *Jour. Nucl. Tech.*, **11**, pp135-148, 1964.
- [63] T. Ogata, T. Yokoo, " Development and validation of ALFUS: Irradiation Behavior Analysis Code for Metallic Fast Reactor Fuels", *Nuclear Technology*, **128** Vol 1, pp113-123, October 1999.
- [64] A.L. Pitner, and R.B. Baker, "Metal Fuel Test Program in GGTG" , *Journal of Nuclear Materials*, **204**, p 124-130 (1993).
- [65] Kim, Y. S.; Hofman, G. L.; Hayes, S. L.; Sohn, Y. H. J. Nucl. Mater. 2004, **327**, 27.
- [66] A. B. Yacout "Long –Life Metallic Fuel for the Super Safe. Small, and Simple Reactor, Toshiba Corp. and CRIEPI, June 2008.
- [67] William J. Carmack " Temperature and Burnup Correlated FCCI IN U-10ZR Metallic Fuel" INL/EXT-12 2555, May 2012
- [68] Keiser, D.D., "The Development of FCCI Zones in Irradiated U-Zr and U-Pu-Zr Fuel Elements with Stainless Steel Cladding." *Nuclear Reactors, Nuclear Fusion and Fusion Engineering*," A. Aasen and P. Olsson eds. ISBN: 978-1-606.92-508-9, 2009.
- [69] Keiser, D. D. "Fuel-cladding Interaction Layers in Irradiated U-Zr and U-Pu-Zr Fuel Elements." Argonne National Laboratory Report # ANL-NT-240. Jan. 2006.
- [70] G.L. Hoffman et al,: *Metallic Fuels Handbook*, " ANL-NSE-3. April 10, 2019, Section E2.21.1
- [71] T.K. Kim "Decay Heat of 286 MWW ARC Core Fuel Assembly (Rev 00)", Nuclear Science and Engineering Division, Argonne National Laboratory, August 23, 2021.
- [72] D. Grabaskas, M. Bucknor, and J. Jerden, "Regulatory Technology Development Plan -Sodium Fast Reactor: Mechanistic Source Term - Metal Fuel Radionuclide Release, "ANL- ART-38, 2016.
- [73] Argonne National Laboratory, "Simplified Radionuclide Transport (SRT) Code: User’s Manual," ANL-SRT-4, 2020.
- [74] D. Grabaskas, "Development of the Simplified Radionuclide Transport (SRT) Code Version 2.0 for Versatile Test Reactor (VTR) Mechanistic Source Term Calculation," *Proceedings of the 2022 International Conference on Fast Reactors and Related Fuel Cycles (FR21)*, 2022.
- [75] Fauske & Associates LLC, "IDCOR Technical Report 11.7: FAI Aerosol Correlation," 1985.
- [76] M. Naritomi, M. Murata, and Y. Yoshida, "Monitoring Technique for Radioiodine in Sodium Aerosol," *Proceedings of the 3rd International Conference on Radiation Protection*, vol. 2:388, 1974.
- [77a] U.S. Department of Energy, "Technical Report for Calculations of Atmospheric Dispersion at Onsite Locations for Department of Energy Nuclear Facilities," NSRD-2015-TD01, 2015.
- [77b] U.S. Environmental Protection Agency, "Limiting Value of Radionuclide Intake and Air Concentration and Dose Conversion Factors for Inhalation, Submersion, and Ingestion," EPA-520/1-88-020, Federal Guidance Report No. 11, 1988.
- [77c] U.S. Environmental Protection Agency, "External Exposure to Radionuclides in Air, Water, and Soil," EPA-402-R-93-081, Federal Guidance Report No. 12, 1993

- [78] E.A.. Hoffman, T. Fei and T.K. Kim, "286MWth ARC-100 Core Design Report, (Rev 06)", June 22, 2023
- [79] W. S. Yang, "Fortran 77 Version of SE2-ANL," Intra-Laboratory Memo, Argonne National Laboratory, March 3, 1993.
- [80] A. Yacout, M. Billne, K. Mo, A. Oaks, C.. Tomchik, " Progress Report on SFR Metallic Fuel Data Qualification", ANL/CFTF-22/30, Rev 0, September, 2022
- [81] NRC-SER-ML200541929 :Safety Evaluation for Argonne National Laboratory Quality Assurance Program Plan for Sodium Fast Reactors Fuel Data Qualification, Letter dated March 3,2020
- [82] L. Ibarra et al, "Verification and Validation for Qualification of SAS4A/SASSYS-1 for Licensing of Sodium Cooled Fast Reactors", 19<sup>th</sup> International Topical Meeting on Nuclear Reactor Thermal Hydraulics (NURETH 19), Brussels, Belgium, March 1-March 11, 2022.
- [83] T. Sumner, T.H. Fanning, and A. J. Brunett, " Validation and Verification Test Suite: (a ) definitions and Analytical Solutions: (b) Simulation Results and Comparison with Analytical solutions; Dec 2014; (c)Control System Cases, Oct 15, 2018, and (d) A.J. Brunett, L. Bullerwell, A. Dix and T. Sumner "Test Regression Cases: Pin Nodalization", March 22, 2019
- [84] D. O'Grady and A.J. Brunett, " Validation Test Cases: Reactor Vessel Auxiliary Cooling System", (RVACS), Ticket 198, Argonne National Laboratory, February 13, 2020
- [85] M.A. Smith, G Aliberti and F. Heidet, " Argonne Reactor Code Software Verification and Validation Plan for the Versatile Test Reactor", ANL-VTR-10, Dec 15, 2018
- [86] J.M. Kramer, T.H . Hughes and E. E. Gruber, "Validation Models for the Analysis of the Transient Behavior of Metallic Fast Reactor Fuel, " Argonne National Laboratory Report ANL IFR-66 (April 1987)
- [87] IAEA TECDOC-1819, " Benchmark Analysis of EBR II Shutdown Tests, International Atomic Agency, Vienna, 2017
- [88] Hans Ludewig and Michael Todosow, " Assessment of the Adequacy of Metallic Fuel Qualification to Support Licensing of Small Modular Sodium Cooled Fast Spectrum Reactors, (4S, ARC-100, PRISM)" BNL-NUREG-2102, (April 2012)
- [89] A. Karahan, "ARC fuel optimization\_ANL\_08072023R.docx", shared via email by Dr. Christopher Grandy, 08/08/2023.
- [90] A. Karahan, "ARC\_fuel\_2-sigma\_simulations\_MFUEL.docx", shared via email by Dr. Aydin Karahan, 08/16/2023.
- [91] U.S. Nuclear Regulatory Commission, RG 1.206 Section C.I.4, "Reactor"
- [92] U.S. Nuclear Regulatory Commission, NUREG 0800, , Section 4.2, "Fuel System Design"
- [93] U.S. Nuclear Regulatory Commission, RG 1.232, "Guidance for Developing Principal Design Criteria for Non-Light-Water Reactors."
- [94] F. A. Garner, L.R. Greenwood and A.M. Ermi "Calculation of Displacement Levels for Pure Elements and Most Multicomponent Alloys Irradiated i n FFTF MOTA-IF", Fusion Reactor Material Semiannual Report, DOE/R-0313/12, March 1992, pp 54-58.
- [95] C. Tomchik, A. Wright, "Benchmark Specifications for TREAR TestsM5, M6, and M7," ANL-ART-174 Rev 1, Argonne Nat'l Laboratory (2023)



[96] D.L. Porter and D.D. Crawford, “Fuel Performance Design basis for the Versatile Test Reactor”, Nuclear Science and Engineering, Vol 00, XXX, Nov 2021

## 10 APPENDICES

### A Appendix A.

|





## B Appendix B Correlations for determination of Eutectic formation as function of temperature, and fuel composition

Above the threshold for the onset of eutectic liquid formation ( $\sim 715^\circ$  or  $\sim 1000^\circ\text{K}$ ), the rate of cladding penetration is strongly temperature dependent but shows little dependence on particular fuel or cladding type. In the models used in deterministic safety analyses, the cladding thickness is assumed to be reduced at a temperature dependent rate correlated from laboratory measurements of iron dipped into melts of high uranium content, shown in Figure B.1[34,35].

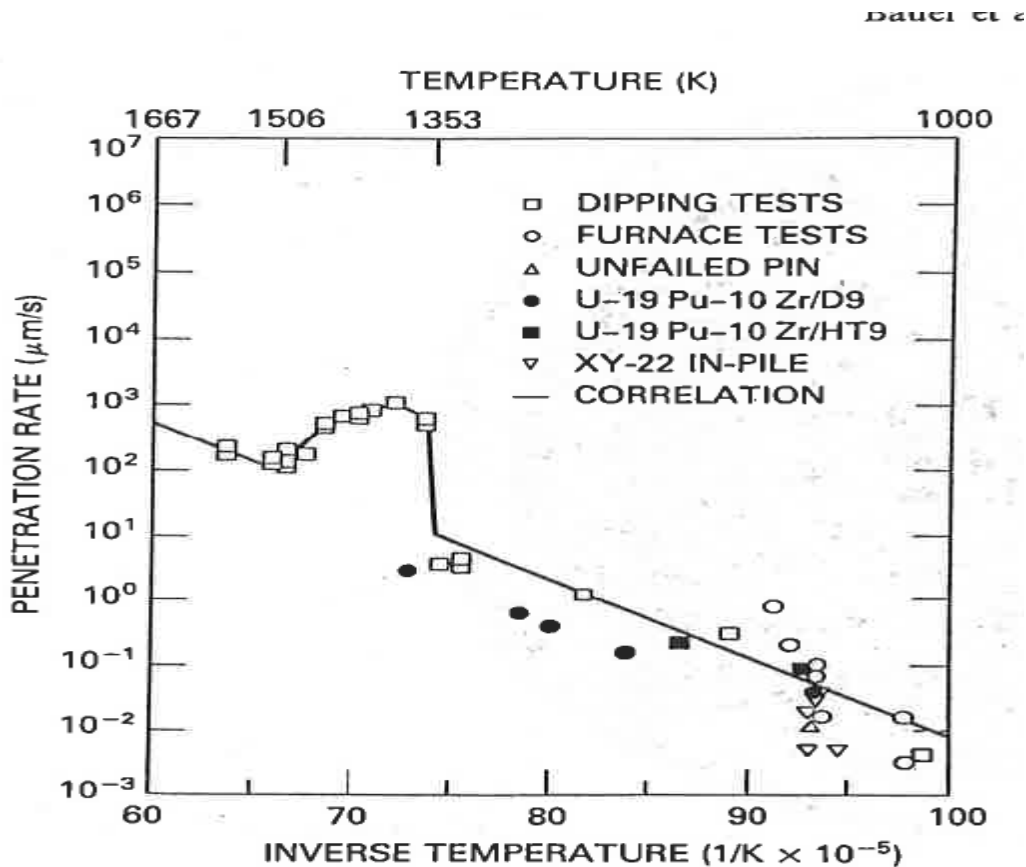


Figure B.1 Rates of cladding penetration by uranium-based melts as compiled from various sources. The correlation shown is a fit to laboratory measurements of iron dipped into melts and supported by data from a wide range of actual fuel pins [35].

It is evident from Figure B.1 that at temperatures below  $650^\circ\text{C}$  ( $923^\circ\text{K}$ ) there is effectively no eutectic liquefaction- and none has ever been observed at this temperature or lower ones.

Except for the temperature range between  $1080^\circ\text{C}$  ( $1353^\circ\text{K}$ ) and  $1233^\circ\text{C}$  ( $1506^\circ\text{K}$ ), the penetration of the cladding due to eutectic formation can be determined by the following Arrhenius correlation, which is the best fit to Figure B.1. This correlation is used in the SAS4A/SASSYS-1 code employed for the deterministic safety transient analysis.

$$\dot{r} = \exp(22.847 - 27624/T), \text{ where } \dot{r} \text{ is the penetration depth in } \mu\text{m/s}, \quad (\text{Eq. B.1})$$

Below about 715°C the melting rate is zero because liquid phases do not form. In the 1080°-1233°C the eutectic penetration increases, and the rate can be expressed by a different correlation [34].

$$\dot{r} = 922 + 2.9765 (T-1388) - 0.21522 (T-1388)^2 + 0.0011338 (T-1388)^3. \quad (\text{Eq. B.2})$$

The accelerated penetration in the 1080°-1233°C temperature regime has been attributed to the breakdown of a protective UFe<sub>2</sub> layer that forms between the liquid and the cladding [34].

There have been a limited number of tests where failures of different cladding resulted from eutectic formation, and these are reported in reference [35] Only one test was done with U-10Zr and HT9. This test was carried out in TREAT, and the cladding did not fail as the correlation would have predicted. Reference [35] attributed the survival of the U-10Zr/HT9 cladding (tested to over 4.8 times nominal power and reaching temperature far exceeding those where rapid eutectic formation is expected) to the higher solidus temperature of the U-10Zr fuel (~1225°C). This resulted in a significant amount of fuel near the cladding never melting and being at a temperature above that which results in rapid melting.

## C Appendix C. Experimental and Operational Data (EBR II/FFTF)

Table C-1 Metal Fuel Irradiation Experiments in EBR-II and FFTF

Experiment Number	Fuel Composition	Cladding Material	No. of Rods in Assembly	Smear Density (%)	Cladding OD (cm)	Wall thickness(cm)	Plenum/Fuel vol. ratio	Peak Power (kW/m) (beginning of life)	Peak Cladding temp (°C) (beginning of life)	Peak Burnup (at.%)	Fast Fluence x10 <sup>22</sup> n/cm <sup>2</sup> (E>0.1MeV)	Breached Rod Information
X397 Advance Metal Blanket	U				12.9					~1.0		
X419 Prototype & fuel behavior	U-10Zr, U-8Pu-10Zr, U-19Pu-10Zr	D9	61	75	0.584	0.038	1	39.4	560	11.9	12	
X420 Prototype, fuel behavior, failure mode, RBCB	U-10Zr, U-8Pu-10Zr, U-19Pu-10Zr	D9	61	75	0.584	0.038	1	36.1	590	18.4	18.5	1 breach @ 16.4 at.% burnup; 530 C at breach
X421 Prototype,fuel behavior, failure mode	U-10Zr, U-8Pu-10Zr, U-19Pu-10Zr	D9	61	75	0.584	0.038	1	39.4	560	17.1	19.6	
X423 Fuel swelling & restructuring	U-10Zr, U-3Pu-10Zr, U-8Pu-10Zr, U-19Pu- 10Zr, U-22Pu- 10Zr, U-26Pu-10Zr	316	37	75	0.737		1	42.7	522	4.9	8.07	
X425 (X425A/B/C) Lead IFR	U-10Zr, U-8Pu-10Zr, U-19Pu-10Zr	HT9	61	75	0.584	0.038	1	48.2	590	3,11,16.2, 19.3	20.6	
X427 Run beyond eutectic		316SS			0.44						11.5	
X429 (X429A/B) Fabrication variables & strain prediction	U-10Zr, U-8Pu-10Zr, U-19Pu-10Zr	HT9, 316SS	61	75	0.584	0.038	1	42.7	600	7.7,10.6, 14.4	13.8	1 breach ea. @ 6.5 & 10 at.% burnup
X430 (X430A/B) HT9, peak cladding temp., large diameter, compatibility	U-10Zr, U-19Pu- 10Zr, U-22Pu- 10Zr, U-26Pu-10Zr	HT9	37	75	0.737	0.041	1.4	49.2	540	11.5	20.6	
X431 (X431A) Blanket safety	U-2Zr, U-6Zr, U-10Zr	HT9	19	85	0.940	0.038- 0.051	1.8	39.4	507	3.9	15.4	

**ARC20-FQ-003 White Paper on ARC-100 Fuel Qualification Program**

X432 (X432A) Blanket safety	U-2Zr, U-6Zr, U-10Zr	HT9	19	85	0.940	0.038-0.051	1.8	39.4	507	4.5	16.6	
X435 (X435A) Mk-III qual	U-10Zr	D9	61	75	0.584	0.038	1.4	49.2	591	19.8	22.8	
X436 Mk-III qual	U-10Zr	D9	61	75	0.584	0.038	1.4	34.4	596		8.45	
X437 Mk-III qual	U-10Zr	D9	61	75	0.584	0.038	1.4	37.7	597		10	
X438 Mk-III qual	U-10Zr	D9	61	75	0.584	0.038	1.4	32.8	623		9.45	
X441 (X441A) FCMI test & LIFE-METAL benchmark	U-19Pu-6Zr, U-19Pu-10Zr, U-19Pu-12Zr	HT9&D9	61	70-85	0.584	0.038	1.1-2.1	45.9	600	12.7	10.1	
X447 (X447A) U-Zr high-temp.	U-10Zr	HT9	49	75	0.584	0.046	1.4	36.1	660	10	9.17	2 breach @ 9.5 at.% burnup; 630°C at breach
X448 (X448A) Mk-IV qual.	U-10Zr	HT9	61	75	0.584	0.046	1.4	45.9	552	14.6	14.9	
X449 Mk-IV qual.	U-10Zr	HT9	61	75	0.584	0.046	1.4	29.5	578	11.3	17.7	
X450 Mk-IV qual.		HT9	61	75	0.584	0.046	1.4	36.1	576	10.2	13.1	
X451 (X451A) Mk-IV qual.	U-10Zr	HT9	61	75	0.584	0.046	1.4	32.8	623	13.7	13.7	
X452 Fuel Impurities	U-10Zr	D9	61	75	0.584	0.038		34.4	596	6.1	5.38	
X453 Fuel impurities	U-10Zr	D9	61	75	0.584	0.038		34.4	596	8.5	8.45	
X454 Fuel impurities	U-10Zr	D9	61	75	0.584	0.038		49.2	547	8.3	9.12	
X455 Fuel impurities	U-10Zr	D9	61	75	0.584	0.038		49.2	547	10.3	9.16	
X481 Mk-III design with Pu	U-19Pu-10Zr	D9	61	75	0.584	0.038	1.4	49.2	579	10	11.3	
X483 (X483A) Mk-III, reference 316SS qual.	U-10Zr	316	61	75	0.584	0.038	1.4	49.9	552	14.8	15.7	
X484 Mk-III, reference 316SS qual.	U-10Zr	316	61	75	0.584	0.038	1.4	36.1	576	11.7	11.9	
X485 Mk-III, reference 316SS qual.	U-10Zr	316	61	75	0.584	0.038	1.4	39.7	576	10.5	10.7	
X486 Mk-III, reference 316SS qual.	U-10Zr	316	61	75	0.584	0.038	1.4	37.1	623	13.9	13.9	
X489 High-Pu for PRISM design	U-19Pu-10Zr, U-28Pu-10Zr	HT9, HT9M	61	75	0.584	0.046	1.4	36.1	606	5.4	4.83	



**ARC20-FQ-003 White Paper on ARC-100 Fuel Qualification Program**

X492 (X492A/B) Zr-sheathed fuel	U-3Zr, U-20.5Pu-3Zr	HT9, HT9M	61	75	0.584	0.038	1.4	41.0	551	10.5	11.1	
X496 Long lifetime	U-10Zr	HT9	37	59	0.686	0.056	3	63.3	536	8.3	6.9	
X501 Minor- actinide- bearing fuel	U-20.2Pu- 10Zr-1.3Np- 1.2Am, U-10Zr	HT9	2+59	75	0.584	0.046	1.4	44.9	≤540	7.6	14.2	
X510	0/22.2 PU	HT9			0.584					1.9		
X521 Synthetic LWR fuel	?	HT9			0.584					1.9		
FFTF												
IFR-1 Fuel column length effects	U-10Zr, U-8Pu-10Zr, U-19Pu-10Zr	D9	169	75	0.686	0.056	1.2	49.2	615(604)	94 Gwd/MTHM	15.4	
MFF1A FFTF Lead Metal Fuel Test	U-10Zr	HT9	8	75	0.686	0.056	1.2	42.7	577	38 Gwd/MTHM	5.6	
MFF-1 FFTF Lead Metal Fuel Test	U-10Zr	HT9	5	75	0.686	0.056	1.2	43.0	577	95 Gwd/MTHM	17.3	
MFF-2 FFTF Metal Prototype	U-10Zr	HT9	169	75	0.686	0.056	1.3	54.1	618	143 Gwd/MTHM	19.9	
MFF-3 FFTF Metal Prototype	U-10Zr	HT9	169	75	0.686	0.056	1.3	59.1	643	138 Gwd/MTHM	19.2	
MFF-4 FFTF Series III.b qualification	U-10Zr	HT9	169	75	0.686	0.056	1.5	56.8	618	135 Gwd/MTHM	19	
MFF-5 FFTF Series III.b qualification	U-10Zr	HT9	169	75	0.686	0.056	1.5	55.8	651	101 Gwd/MTHM	14	
MFF-6 FFTF Series III.b qualification	U-10Zr	HT9	169	75	0.686	0.056	1.5	55.8	588	141 Gwd/MTHM	12.8	

For completeness Table C-2 provides the data from the tests conducted at the EBR-II to determine the possible consequences of continuing operation with failed pins, the so-called Run-Beyond-Cladding Breach (RBCB) tests. Even though EBR-II ran tests with both oxide and metal fuel, for the ARC-100 the metal fuel results are the relevant ones, and are the only ones reported here. These results indicated that failure in one pin did not propagate to adjacent ones. There were few failures of pins, not associated with these specific tests. Those failures are reported in Table 4-1 (Tests X429 and X447). The latter are particularly relevant since they occurred in pin clad in HT9 at temperatures significantly higher than the temperatures at which other pins were tested and because the two failed pins were next to one another and showed significant fuel chemical interaction caused wastage of the pins cladding thickness. Reference [27] provides an exhaustive description of the failures and of the reasons why the failures occurred... It is noted that although adjacent to one another, the failures of the two pins were independent (they did not face each other) but occurred in the narrowest region of the coolant channel.

Table C.3 provides the results of the TREAT tests conducted with metal fuel. TREAT ran analogous tests with oxide fuel but only the metal ones are reported as being those relevant to the behavior of the ARC 100 fuel.

Table C-2 Summary of Run-Beyond-Cladding Breach Tests with Metal Fuel at the EBR II

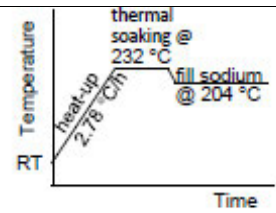
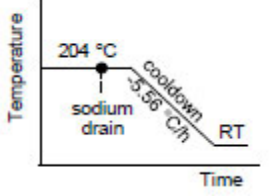
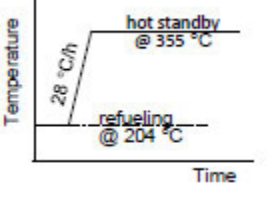
Test Designation	Test Type	No. Rods	Fuel Composition	Cladding Type	Cladding OD(cm)	Pitch-to-Diameter Ratio	Linear Power <sup>e</sup> (kW/m)	Cladding Temp. (°C)	Burnup <sup>f</sup> (at. %)	No.Rods Breached	Days Irr'd after Breach
Metal Fuel RBCB Tests (taken from Seidel, et al. [48], Hofman, et al. [50], and Batte and Hofman [49])											
XY-21	BFTF <sup>a</sup>	1,60 <sup>b</sup>	U-5Fs	316SS	0.44	1.38	24	573	7.9	0	N/A
XY-21A	BFTF	1,60 <sup>b</sup>	U-5Fs	316SS	0.44	1.38	25	593	9.3	1	54
XY-24	FPTF <sup>c</sup>	2,59 <sup>b</sup>	U-19Pu-10Zr	316SS	0.44	1.38	21	541	7.6	1	233
XY-27	BFTF	2,59 <sup>b</sup>	U-8Pu-10Zr	316SS	0.44	1.38	23	520	~6.0	2	131
X482	Open Core	1,60 <sup>b</sup>	U-19Pu-10Zr	O9	0.58	1.24	39	600	14.4	1	168
X482A	Open Core	1,60 <sup>b</sup>	U-10Zr	D9	0.58	1.24	36	600	13.5	1	100
X482B	Open Core	1,60 <sup>b</sup>	U-19Pu-10Zr	HT9	0.58	1.24	36	600	~14	1	150
X420B	Natural Breach	61	U-19Pu-10Zr	D9	0.58	1.24	.	.	~17	1	34

- BFTF: Breached Fuel Test Facility in EBR II which provided separate delayed neutron signal monitoring for the experiment and an above-core sampler for collection of released fuel and contamination.
- First number indicates the number of pre-defected (thinned) rods, and the second number indicates the remaining number of rods in the assembly. Note that the XY-series tests used instrumented assemblies that contained 61 Mark-II size EBR II rods, which would typically fill a 91 pin EBR II driver assembly.
- FPTF: Fission Product Test Facility in EBR-II with provision for monitoring fission products released from a breached fuel rod.
- With 15% overpower transient.
- Linear power values for metal fuel tests are pre-test predictions.
- Burnup values for metal fuel tests are burnup at end of test

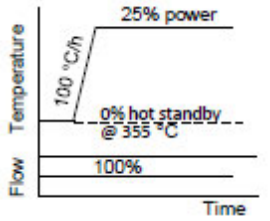
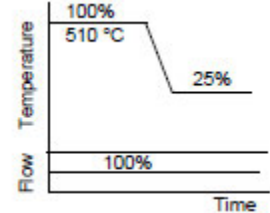
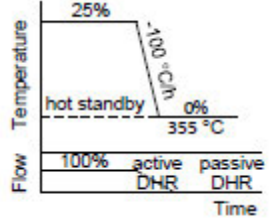
Table C-3 Summary of Selected TREAT Experiments (From Table 3 of Reference [41])

Test	Fuel/Cladding	Burnup (at.%)	Transient Rate (Period)	Overpower In Test (P/ Po)	Calculated Breach Threshold	Comments
Metal Fuel TREAT Tests (taken from Bauer, et al. [11.8])						
M2	U-5Fs/316SS; Mark-II design	0.3	8-sec	4.1	4.7	16% max. axial expansion; fueldamaged but intact
	U-5Fs/3 16SS; Mark-II design	4.4	8-sec	4.2	4.5	cladding breached
	U-5Fs/316SS; Mark-II design	7.9	8-sec	4.1	3.6-4.0	3% max. axial expansion; cladding breached
M3	U-5Fs/3 16SS; Mark-II design	0.3	8-sec	4.1	4.8	18% max. axial expansion; fueldamaged but intact
	U-5Fs/3 16SS; Mark-II design	4.4	8-sec	4.0	4.4	4% max. axial expansion; fueldamaged but intact
	U-5Fs/316SS; Mark-II design	7.9	8-sec	3.4	3.6-4.0	4% max. axial expansion; fuel damaged but intact
M4	U-5Fs/316SS; Mark-II design	0.0	8-sec	3.8	4.3	4% max. axial expansion; fueldamaged but intact
	U-5Fs/316SS; Mark-II design	2.4	8-sec	4.1	4.4	7% max. axial expansion; claddingbreached
	U-5Fs/316SS; Mark-II design	4.4	8-sec	3.8	4.3	4% max. axial expansion; fueldamaged but intact
M5	U-19 Pu- 10Zr/D9; X4 19,420,421 design	0.8	8-sec	4.3	5.1	1% max. axial expansion; fuel damaged but intact
	U-19 Pu-10Zr/D9; X419,420,421 design	1.9	8-sec	4.3	5.1	2% max. axial expansion; fuel damaged but intact
M6	U-19Pu-10Zr/D9; X419,420,421 design	1.9	8-sec	4.4	4.6	2 to 3% max. axial expansion; fuel damaged but intact
	U-19Pu-10Zr/D9; X419,420,421 design	5.3	8-sec	4.4	4.5	3% max. axial expansion; claddingbreached
M7	U-19Pu-10Zr/D9; X419,420,421 design	9.8	8-sec	4.0	4.4	3% max. axial expansion; cladding breached
	U- 10Zr/D9; X425 design	2.9	8-sec	4.8	4.4	2 to 4% max. axial expansion; fueldamaged but intact

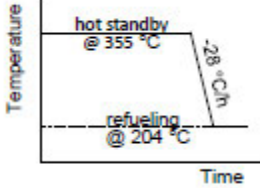
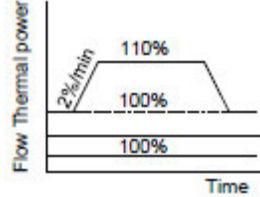
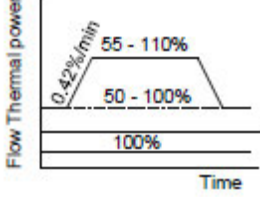
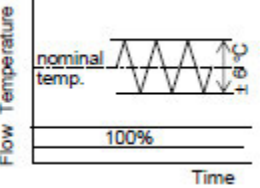
## D Appendix D: Duty Cycle Events for the ARC 100 Fuel (and Reactor Internals)

Events	Occurrences	Design Frequency	Description	Event Sequences
<i>Level A Normal and anticipated occurrences</i>				
1a	Dry system heats up Sodium Fill, Heat up to Refueling Temperature	1	Heat up the outer surfaces from room to 232 °C at 2.78°C/hr. Hold at 232°C for thermal soaking and allow cooling to 204°C then fill with Sodium. If the heat up schedule is not sufficient, then structural analysis should identify slower heat up rates.	
1b	Cooldown from refueling temperature, Sodium drain, and dry system cooldown	1	Sodium is drained. Cooldown from 204°C to room temperature at 5.56°C/hr. If the cooldown schedule is not sufficient, then structural analysis should identify slower cooldown rates.	
2a	Startup from Refueling Temperature to Hot Standby Conditions	3 for NOAK 12 for FOAK	<p>For ARC-100 60-year plan lifetime and 20-year refueling interval, this is 3 events (initial + 2 for control element replacement coincident with ISI, but if the ARC 100 is a FOAK, the PRD measurement will require 4 such events in the first 4 years, then fuel surveillance specimen's extraction will require this occurrence in years 4, 12, 14 16 and 19.</p> <p>Maximum heat transport system heatup/cooldown rate between refueling at 204°C and 355°C shall not exceed 28°C/hr.</p> <p>The maximum rate of change of primary system heat transport hot leg shall not exceed an average of 100°C/hr. between hot</p>	

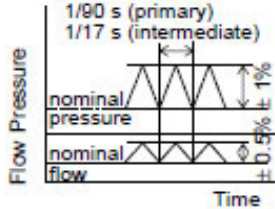
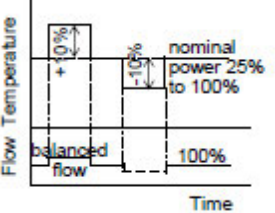
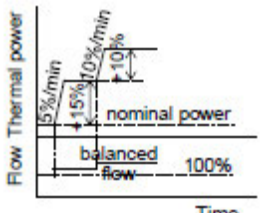
**ARC20-FQ-003 White Paper on ARC-100 Fuel Qualification Program**

			standby and 25% thermal power at which the superheated cycle is started.  Heatup rate is achieved with combination of sodium pumps at 100% flow, Brayton cycle normal shutdown heat removal system, and fission power	
2b	Manual or automatic startup from Hot standby conditions to 25% power	40 NOAK 80 FOAK	The transient returns reactor from hot standby temperature of 355°C to conditions at 25% thermal power at which it is assumed the Brayton cycle is started.  Reactor power is increased such that primary and intermediate sodium temperatures increase at maximum average rate of 1.67°C/min with sodium pumps at 100% flow.  Assuming 2 trips of Brayton cycle per year for NOAK, and 4 trips for FOAK	
2c				
3a	Shutdown from operating conditions to 25% power	1 for NOAK 6 for FOAK	Neutronically reducing power from the core and cooling down of primary coolant system. In 3a the Brayton cycle is operating, and the pumps are at 100% flow.	
3b	Shutdown from 25% power to hot standby conditions	40 for NOAK 80 for FOAK	Cooldown to hot standby temperature of 355°C. Reverse of occurrence A-2b. Heat removal is by the normal shutdown heat removal system utilizing the shutdown cooling system of the Brayton cycle initially and the DRACs/RVACS thereafter.	

**ARC20-FQ-003 White Paper on ARC-100 Fuel Qualification Program**

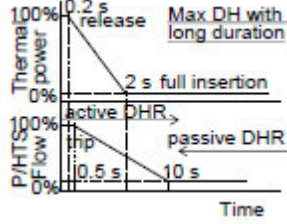
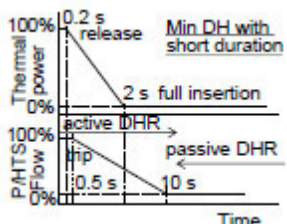
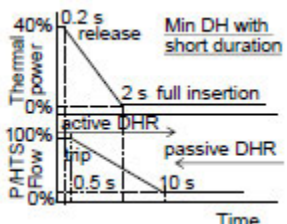
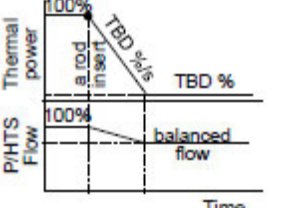
3c	Shutdown from hot standby to Refueling temperature	3for NOAK 9 for FOAK	Reverse of A-2a	
4	Weekly loading and unloading	1040 loading, 1040 unloading	Assume about one event per week, resulting in 2880 loading and 2880 unloading. Power changes consist of incremental changes of up to 10% of nominal power at 2%/minute. Load changes are accomplished by varying power with constant sodium flow rates and Brayton cycle automatic control.	
5	Daily loading and unloading	7300	Assume one event each day or 20 x 365 = 7300. Power change from 50 and 100% at an average rate of 0.42%/min. Power changes consist of incremental changes of up to 10% of nominal power at 2%/minute. Load changes are accomplished by varying power with constant sodium flow rates and Brayton cycle automatic control.	
6	Temperature fluctuations	10 <sup>7</sup>	Considers sodium temperature variations produced by power fluctuations within the plant control system dead bands (TBD). Fluctuations are ±6°C (from EBR II experience) for both primary and intermediate sodium systems	

**ARC20-FQ-003 White Paper on ARC-100 Fuel Qualification Program**

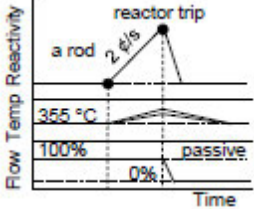
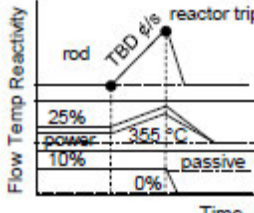
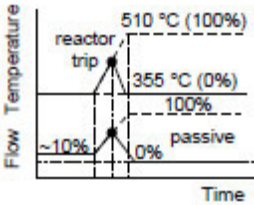
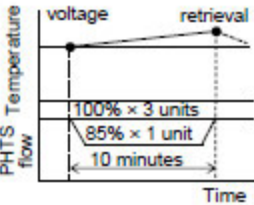
7	Steady State Flow Induced Vibrations	Continuous	Vibrations induced by fluctuations in pressure from sodium pumps. EM pumps may be subject to double supply frequency pulsations occurring at twice the supply frequency. For ARC-100 the driving frequencies for the primary and intermediate EM sodium pumps are 90 and 17 Hz respectively. The electromagnetic pressure and the amplitude of the resulting flow pulsation is taken to be 0.5% of the nominal flowrate. The amplitude of the pressure pulsation is taken to be 1%.	
8	Step Load Increase or Decrease of 10% of rated power	500 step increase 500 step decrease	Increase assumed to occur 25 times per year, and similarly decrease assumed to occur 25 times per year; hence roughly one step load per week. Plant control system is designed to maintain plant operating conditions without reactor trip following a ±10% (fast) step load change between 25% and 100% load. Brayton Cycle automatic control attempts to match heat removal from intermediate sodium to load.	
9	Fast Ramp Load changes of 25% rate power	10 increasing 10 decreasing	Reflect reliability of power grid and assumed to occur every two years. Consist of a power ramp of 10% nominal power at 10%/minute followed by an additional power ramp of 15% nominal power in the same direction of 5% nominal power/minute	
<b>Level B Upset conditions</b> (Note: All trips are assumed to begin at 100% nominal power and end at hot standby conditions)				

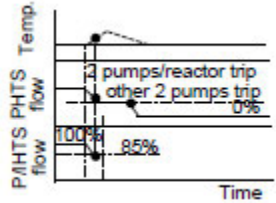
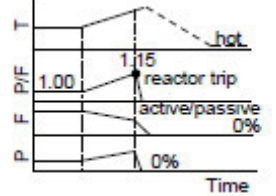
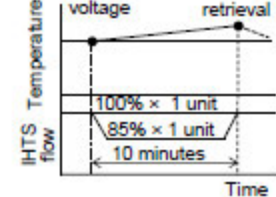
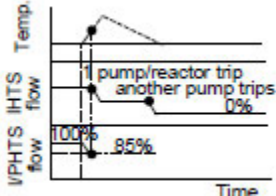


ARC20-FQ-003 White Paper on ARC-100 Fuel Qualification Program

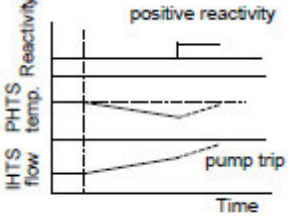
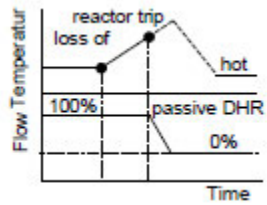
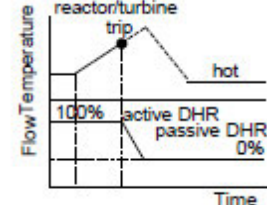
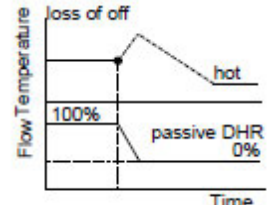
1a	Reactor trip from full power to max. decay heat	40	Assumed twice per year. Following trip signal the control rods are released at 0.2 sec, with full insertion at 2 seconds. The Plant protection system trips the primary and intermediate sodium pumps at 0.5 seconds. The primary Sodium pumps coast down to zero flow with a halving time of 10 seconds. The secondary pumps stop essentially instantaneously. Heat is initially removed from the intermediate sodium by the Brayton Cycle and then by the DRACS/RVACS.	
1b	Reactor trip from full power to min. decay heat	40	Same as above, but with decay heat corresponding to a core which has been in operation for only a short duration.	
1c	Reactor trip from partial power to corresponding minimum decay heat	40	Same as above, but from a power level of about 40% of nominal power to a decay heat corresponding to operations at 40% nominal power	
2a	Uncontrolled single rod insertion	5	Every 4 years controller malfunction inserts a rod causing a TBD% per second reduction in thermal power from 100%. This is not the gravity fall resulting from unlatching the rod, but an RC&IS insertion.	

ARC20-FQ-003 White Paper on ARC-100 Fuel Qualification Program

2b	Uncontrolled single rod withdrawal with automatic trip	1	Once during refueling interval. Initial condition is hot standby, with minimal decay heat. All pumps at 100% flow. Uncontrolled withdrawal at 2¢/sec. Trip is initiated by “over flux” measurement. Heat is initially removed from the intermediate sodium by Brayton Cycle and then by the DRACS/RVACS	
2c	Reactor loading at maximum rod withdrawal rate	1	Once during core life. Initial condition is 25 thermal power and load and 10% sodium flow. Mechanical malfunction upon load increase request causes maximum rod withdrawal speed, so that power increases from 25% at a rate determined by the reactivity addition of TBD ¢/sec. Plant control system trip is initiated by “over flux” measurement.	
2d	Protected reactivity insertion during startup		Reactor is scrammed by the power period trip.	
3a	Partial loss of primary pump flow	1	Once per pump during refueling interval. Primary flow in one pump is assumed to decrease to 85% due to a ramp decrease in pump voltage. Other pumps are unaffected. No action is taken, or action is taken to terminate the event after 10 minutes. This transient envelopes control malfunctions and operator errors causing mismatches in primary pump flows. Transient results in increased outlet temperature and a redistribution of temperatures in the IHXs.	

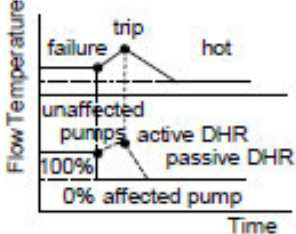
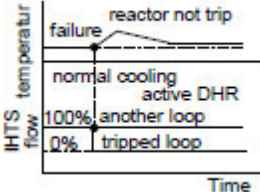
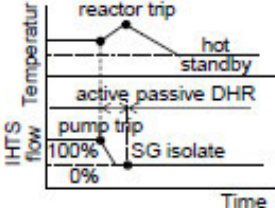
3b	Loss of power to two (one Train) Primary Pumps	1	Other pumps are unaffected. Intermediate sodium pump flow remains at the initial value until a reactor/ pump trip is initiated when the ratio of primary to intermediate pump flow is less than (85% or TBD). Following trip, the rest of the pumps and BOP respond as for occurrence B-1a. This transient envelops those occurrences that would cause the pump to trip or those resulting from control failures more severe than in occurrence B-3a or from significant operator errors. In this transient the mechanism to enhance pump coast down is effective.	
3d	Slow power to flow ratio increase	1	Power to flow ratio increase due to a drift upwards in power and a drift downwards in flow. Manual trip or automatic when P/F = 1.15	
4a	Partial loss of intermediate pump	1	Once per pump during refueling interval. Intermediate flow in one pump is assumed to decrease to 85% due to a ramp decrease in pump voltage. Other pumps are unaffected. No action is taken, or action is taken to terminate the event after 10 minutes. Intermediate cold leg and primary hot leg temperatures increase	
4b	Loss of Power to B-3b) Intermediate Pump (Note loss of one train is covered by B-3b)	1	Other pumps are unaffected. Primary sodium pump flow remains at the initial value until a reactor/ pump trip is initiated when the ratio of primary to intermediate pump flow is less than (85% or TBD). Following trip the rest of the pumps are treated as for a normal reactor trip (B-1a). mechanism to enhance pump coast down is effective.	

ARC20-FQ-003 White Paper on ARC-100 Fuel Qualification Program

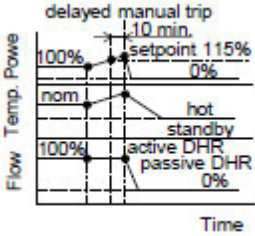
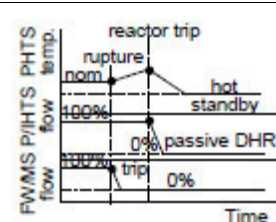
5	Overcooling event due to intermediate pump malfunction	1	Intermediate pump flow exceeds normal, resulting in overcooling of primary system with corresponding reactivity insertion	
6	Loss of normal heat sink (loss of balance of plant)	2	Reactor is manually scrammed or automatically tripped on high temperature	
7	Brayton cycle trip with Reactor Trip	480	8 per year. The reactor is tripped. Heat is initially removed from the intermediate sodium by the Supercritical CO2 Brayton Cycle and then by the normal shutdown cooling system within the Brayton cycle cooling circuit. Later decay heat can be removed by the DRACS.	
8	Loss of Off-site Power	3	0.133/year based on grid reliability. ARC-100 does not need offsite power for decay heat removal, but temperature of system rises until it matches removal by DRACS and/or RVACS. Mechanism to extend pump coast-down (TBD) does not rely on offsite power. Reactor trip would occur on "over temperature", or "power/flow" measurements.	
9	Plant shutdown in response to small H2O to Sodium Leak Indication	1	Small leak, however, may be dealt with by sodium purification system, which would remove reaction products, and therefore it may not be necessary to include this as an occurrence.	

**Level C – Emergency Conditions** (Note: All emergency events resulting in a reactor trip are considered to result in a transient followed by cooldown to refueling conditions. The number of occurrences is specified as a design basis (based on judgment). Each plant component is designed to accommodate 4

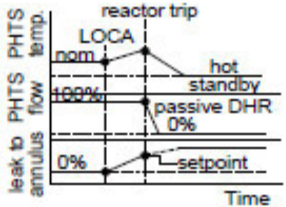
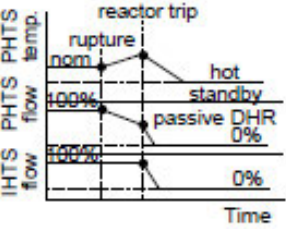
*cycles of the most severe emergency event. (If transient occurrences of any two like or unlike emergency events produce a more severe effect than the four isolated occurrences, then the design must for a few seconds accommodate this more severe sequence.)*

1	Protected Primary Pump Electrical Failure (Short negates flywheel coast down)	1	Primary sodium flow through the affected pump decreases to zero instantaneously (assumes that mechanism for extended coast down is useless on the affected pump) and reverses as the unaffected pumps run out on the head/flow curves. Event causes power to flow ratio in excess of trip set point so, the reactor is tripped. In case it is manually tripped or automatically tripped by high temperature or power/flow signal, the transient for the intermediate heat transport systems and BOP are the same as for those in case of a reactor trip. Heat is initially removed from the intermediate sodium by the Supercritical CO <sub>2</sub> Brayton Cycle and then by the RVACS. Event analyzed and reported in reference [12.19]	
2	Intermediate Pump Electrical Failure		Same as above for one intermediate pump, while the pump on the other loop continues to function. Event causes high outlet temperature. Reactor may not be tripped. In case it is manually tripped or automatically tripped by high temperature or power/flow signal, the transient for the intermediate heat transport systems and BOP are the same as for those in case of a reactor trip. Heat is initially removed from the intermediate sodium by the Superheated Rankine Cycle and then by the normal shutdown cooling system within the Rankine cooling circuit.	
3	Rupture disk failure in IHTS sodium-H <sub>2</sub> O reaction protection system	1	Flow of intermediate sodium or cover gas through the failed rupture disk. Pressure sensor downstream of rupture disk trips the intermediate pumps, and if more than one steam generator, the affected one is automatically isolated. Reactor outlet temperature rises and reactor may trip on "over temperature" signal. Alternatively, it may either ride through the transient or be manually tripped. Heat is initially removed from the intermediate sodium by the Supercritical CO <sub>2</sub> Brayton Cycle and then by the normal shutdown cooling system within the Brayton cooling circuit.	

**ARC20-FQ-003 White Paper on ARC-100 Fuel Qualification Program**

4a	Protected uncontrolled rod withdrawal from 100% power	1	An uncontrolled withdrawal of the single most reactive control rod causes the reactor power to increase above 100%. Power increase is terminated below trip setting (see Appendix F- power rises to 123% as calculated by the quasi-static equilibrium equation, and to 115% by actual analysis). A manual trip may occur after 10 minutes. Transient results in temperatures that are similar to a normal trip but start from a higher initial value and higher temperature.	
4b	Uncontrolled Rod Withdrawal from Startup Trip Point with delayed Manual Trip	1	Covered by the above	
5	Design Basis Na to Steam Generator leak	1	Must be defined, but likely we would want to continue operation, with the plant shutdown in the normal mode as for maintenance or refueling.	
<b>Level D – Faulted Conditions</b> <i>Note: Faulted events are assumed to occur one time for each event)</i>				
1	Brayton Cycle High Pressure Line Rupture between Na-CO2 Heat Exchanger and Turbines	1	Large pipe breaks are initiators in the Brayton cycle. The cycle systems and components (other than the one that is the initiator), are to be designed so that both the Sodium and the CO2 boundaries maintain their structural integrity. The Brayton cycle is tripped (not a safety system), but the reactor need not be automatically tripped, unless there is an over temperature or over flux signal (which may occur since the normal heat removal system is not available once the Brayton cycle is tripped). The manual trip will be at the discretion of the operator. Since the break can occur at a location such that the normal shutdown heat removal is not possible, the DRACS and RVACS will remove the decay heat. It is assumed that one of the three DRACS is not available, and/or the RVACS is not available.	

**ARC20-FQ-003 White Paper on ARC-100 Fuel Qualification Program**

3	Reactor Primary Vessel Leak to Guard Vessel	1	Sudden decrease of Sodium levels inside the reactor vessel as Sodium fills the gap between the primary and guard vessels. The reactor is scrammed manually upon detection of Sodium in the annulus. The Guard vessel fills with Sodium, while the sodium level in the primary vessel decreases. The geometry is such that the inlets to the IHXs are not uncovered with a significant margin. The Brayton Cycle is tripped. Heat is removed from the IHTS by the normal shutdown heat removal system initially and then by DRACS.	
4	Rupture in High Pressure Primary Circuit	1	This occurrence assumes a rupture in any of the components connecting the discharge from a primary pump to the core inlet plenum. Failure results in a reduction in the flow delivered to the reactor core, and a surge in the cold pool level. Two general possibilities: (1) guillotine rupture of a primary piping segment leading to a reduction in flow delivered to the inlet plenum, and backflow through the broken leg; and (2) failure resulting in leakage from the inlet plenum, resulting in shunting a portion of the core coolant to either the hot plenum or the cold plenum depending on the location of failure.	
5	Flow Blockage to one or more assemblies	1	A subset of (D-4(2)) above can also be a broken piece(s) lodging in the inlet orifice of a core assembly (or few orifices of few assemblies) interrupting flow to the affected assembly(ies)	Same sequence as above
6	Unprotected Station Black Out (USBO)		These four transients have been analyzed and are reported in reference [12.19]	
	Unprotected reactivity Insertion of most reactive rod (UTOP)			
	Unprotected Instantaneous loss of One primary Pump			
	Unprotected loss Once electrical train			
<b>External Events –Earthquakes, Aircraft Impact, etc.</b>				

**ARC20-FQ-003 White Paper on ARC-100 Fuel Qualification Program**

1	Operating Base Earthquake (OBE)	2	Depends on site, but for now assume once every 10 years. All structure, systems, and components important to safety shall be capable of withstanding the effects of the OBE without loss of capability to remain functional	
2	Safe Shutdown Earthquake (SSE)	1	All structure, systems, and components important to safety shall be capable of withstanding the effects of the SSE without loss of capability to perform their safety function	
3	Beyond Design Basis Earthquake – Design Extension Earthquake (DEE)	1	All structure, systems, and components important to safety shall be evaluated for the effects that the DEE would have on their capability to perform their safety function and the ensuing effect on off-site consequences (of site dose)	
4	Design basis aircraft impact	1		
5	Wind and turbine generated missiles	1		



## E Appendix E – Procedure for measuring the values of the quasi-static reactivity balance equation coefficients A, B, and C

The three reactivity feedback parameters {A, B and C} in the Quasi-static Reactivity Balance Equation are each an amalgam of numerous individual physical effects which produce a change in reactivity in response to a change in coolant and fuel temperatures in the operating reactor. When relying on these reactivity feedbacks for passive safety response to upsets and for passive load following, it is essential to have accurately measured determinations of their values on the reactor itself and not to rely on calculated values. Presented in this Appendix is one of several alternative procedures that could be used to make the measurements under the mandate of Technical Specifications for periodic confirmation that the parameters have values lying in the range required to produce the desired passive response.

$$\Delta\rho = (P - 1) A + (P/F - 1) B + \Delta T_{in} C + \Delta\rho_{TOP} \quad (\text{Eqn E.1})$$

Conditions for passive response, with  $\Delta\rho_{TOP}$  being the worth of the single highest worth rod are.

$$A, B \text{ and } C \text{ are all negative; } A/B < 1; \quad 1 < C \Delta T_{in}/B < 2; \quad \frac{\Delta\rho_{TOP}}{\dots |B|} \leq 1$$

The sufficient conditions are in terms of ratios of the parameters. That makes them independent of reactivity scale (i.e., we can do the measurements in \$, %Δk, in-hours, or cm of control rod motion. For ARC-100 this is useful, because the value of beta changes significantly over the burn cycle.

Individual reactivity feedback usually contributes to the value of all three parameters. Therefore, the sufficient conditions benefit from partial cancellation of uncertainties since the same effect is in the numerator and denominator of the ratio.

The PRD (which can be measured) equals the value of A+B.

We can measure C by holding primary flow rate unchanged and holding control rods fixed, then reducing flow rates in both intermediate loops by 10% and adjusting the Rankine cycle to 90% full heat demand. After letting the transients die away, the core inlet temperature should rise (by about 60 °C)

Confirm via heat balances that the power is ~90% full power and the temperature of core inlet is measured using the thermocouples on the discharge pipe of each primary pump. [May have to take average of 4 signals, or weighted average if pump flows differ].

The quasi-static reactivity balance is  $A (0.9 - 1) + B (0.9/1.0 - 1) + C \Delta T_{in} = 0$  and  $C = \{0.1(A + B)\}/\Delta T_{in}$

With measured values for (A + B) and C calculated as above, A [the reactivity vested in the fuel temperature increment above the coolant temperature] is measured in a way that retains the primary coolant temperature field unchanged.

Starting at full power conditions in both reactor and Rankine cycle, the same rod(s) used for the PRD measurement is (are) inserted to achieve ~90% of full power in the reactor as indicated by the fission chamber. The primary flow is adjusted until the reactor P/F is 1.0 as indicated by attaining a 510 deg-C reading on thermocouples at the intake of the IHXs. The intermediate loop flow rates are adjusted to 90% flow and the Rankine cycle is adjusted to 90% heat demand. After allowing the transient to decay, and verifying by heat balance the power levels are correct, the quasi-static reactivity balance is:

$$A (0.9 - 1) + B (1 - 1) + C \times 0 + \Delta\rho_{TOP} = 0, \text{ and } A = - \Delta\rho_{TOP}/(-0.1)$$

The values of A, B and C are now known.

## F Appendix F Verification and Validation

### F.1 Legacy Data Qualification (Verification and Validation)

The results of all of the experiments/tests conducted on metallic fuels in reactors (EBR-II, FFTF, and TREAT), as well as tests and examinations out of pile (i.e., in hot cells/furnaces using both irradiated and un-irradiated, chopped and full pins) has been organized for online access, by PNNL and ANL. This effort has been ongoing for a number of years, and includes:

- EBR-II Metallic Fuel Irradiation Testing Databases (ANL)
  - PIE reports, digitized micrographs, profilometry measurements, gamma scans, porosity and cladding strain measurements, and scans for other microstructural characteristics to support fuel qualification and code validation.
  - Pin-by-pin fuel fabrication and core load information for each EBR-II operating cycle (operating parameters, temperature, fluence, and burnup predictions as input to fuels performance codes).
- EBR-II passive and inherent safety tests (ANL)
  - Approximately 80 integral experiments from comprehensive shutdown heat removal, BOP, and inherent plant control testing program during the 1984-87 period, including several unprotected (without scram) LOF and LOHS tests.
- TREAT M-series tests (ANL)
  - Rapid transient over-power tests to examine margin to cladding failure, fuel melting and relocation, with whole irradiated EBR-II pins in flowing Na loops. And U-5Fs/SS, U-10Zr/HT9, U-19Pu-10Zr/D9 fuel types.
- TREAT Experiments Relational Database (TREXR) (ANL)
  - Searchable collection of information on reactor transient tests conducted in TREAT (1959-1994) consisting of approximately 900 tests and categories with parametric information (e.g., fuel, transient info, results), documented in approximately 6000 searchable PDFs with links to referenced tests.
  - Metallic Fuel Transient Overpower Tests Experiment specifications, test plans, and digital data.
- Transient furnace tests in hot cells (PNNL)
  - Chopped irradiated pin segments in Fuel Pin Test Apparatus (FBTA)
  - Full length irradiated pins in Whole Pin Furnace (WPF)
  - Simulated reactor accidents, varying ramp rates and peak temperatures
    - U-(0-26) Pu-10Zr pins in D9, HT9, 316SS clad with burnup: 2-3 a/o in WPF, 6-12 a/o in FBTA.
      - Fuel compatibility tests on clad fuel segments
      - Fission gas retention examinations
      - Measurements for cladding penetration depth
      - Metallurgical examination of the tested materials

- Fission product release measurements

All of the data above is being assembled in two major searchable databases:

- Metal Fuel Irradiation and Physics Analyses databases (FIPD) at ANL (<https://fipd.ne.anl.gov/>), and
- FFTF Metallic Fuel Irradiation Testing Database at PNNL.

Verification and validation of the legacy data has been in progress [80] under a Quality Assurance Program endorsed by the NRC [81].

## F.2 Main Codes verification and Validation

The two main computer codes used for the evaluation of the fuel performance are the BISON code (Idaho national Laboratory) and the SAS4A/SASSYS-1 code (Argonne National Laboratory). Both codes have been extensively verified and validated against the available operational and experimental data (legacy data).

SAS4A/SASSYS-1 [ 17] is used to perform the deterministic safety analyses that establish the conditions to which the fuel is subjected under normal operation (NO), Anticipated Operations Occurrences (AOOs), Design Basis (DBE) and Beyond Design Basis Events (BDBE). The code has been verified and validated with documentation provided by references [82] through [86]. It is noted that SAS4A/SASSYS-1 has been also validated in a four-year IAEA coordinated research project (CRP), benchmark analyses were performed for two landmark EBR-II shutdown heat removal tests (SHRT) [. This was the largest fast reactor CRP ever conducted by the IAEA, with nineteen participating organizations representing eleven countries. The primary objective of the CRP was to improve state-of-the-art sodium-cooled fast reactor (SFR) codes by extending code validation to include comparisons against whole-plant data recorded during the SHRT transients .A module of this code, MFUEL, is used to check the prediction of BISON, and its verification/validation is documented in reference [13].

BISON. The code is well documented and conforms to ASME NQA-1 guidelines. Its verification has been done against simple problem with a known solution, but its validation for metal fuel has been relatively limited, as explained hereinafter.

BISON, to date, has been verified and validated against a significant number of experiments. An extensive summary of all of the validation to date can be found in the following interactive site: <https://mooseframework.inl.gov/bison/assessment/index.html> [12]

The interactive site also provides the theory behind BISON and the documentation, including the complete Code Manual and the software quality. It provides the models and the comparison with experimental results for fairly large number of LWR and TRISO fuel tests and operations, but far fewer cases for metallic fuel. For the latter only three experiments [X430 series, X 441 and X447] from EBR II, several experiments at FFTF (MFF and IFR-1) and one TREAT (M7) test have provided experimental data against which BISON has been validated.

The X441 experiment in EBR-II contained a series of fuel pin design changes to determine the effect of plenum/fuel volume ratio, fuel smear density, zirconium content, cladding material and cladding thickness. The fuel pins were examined at interim times to check for cladding deformation or breach. The cladding hoop strain at EOL was used to measure the effect of the fuel pin design changes tested in this experiment.

The X441 experiment consisted of a 61-pin bundle irradiated in EBR-II under steady-state conditions to a target burnup of ~10%. The main objective of the experiment was to determine a design envelope for ternary (U-Pu-Zr) fuel design in EBR-II. The fuel design parameters that were varied include the plenum/fuel volume ratio (1.1, 1.5 and 2.1), fuel smear density (70, 75 and 85% TD), Zr content (6, 10 and 14 wt. %), cladding thickness (0.015 and 0.018 in.) and cladding material (HT9 and D9). The results of the X-447 and MFF experiments (conducted with t HT9 cladding) are summarized in Table 5-3. Figure F.1 and F.2 show a comparison between the test results and BISON Predictions.

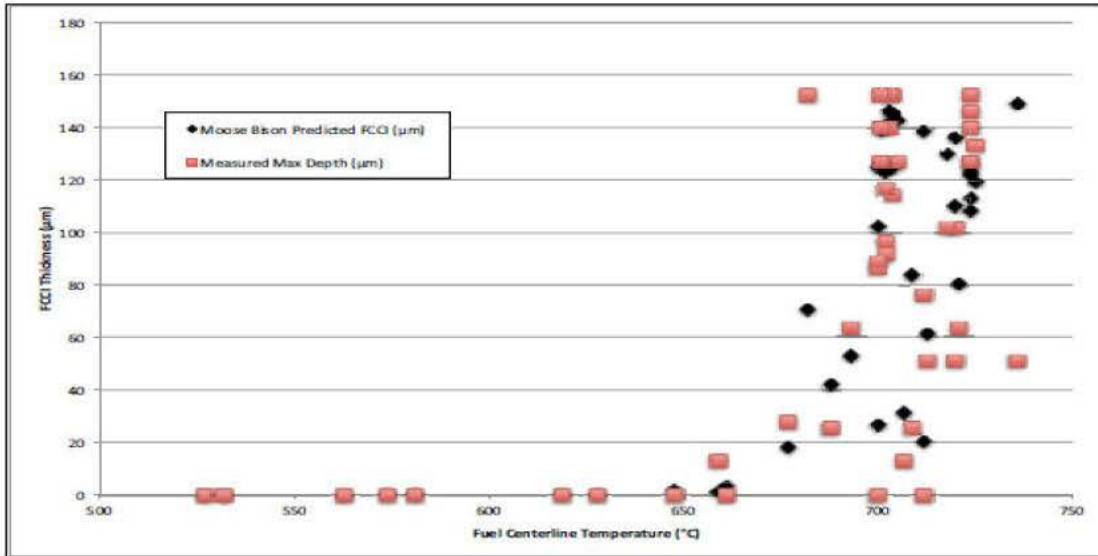


Figure F.1 Measured vs. BISON Predicted FCCI thickness versus Fuel Centerline Temperature [86]

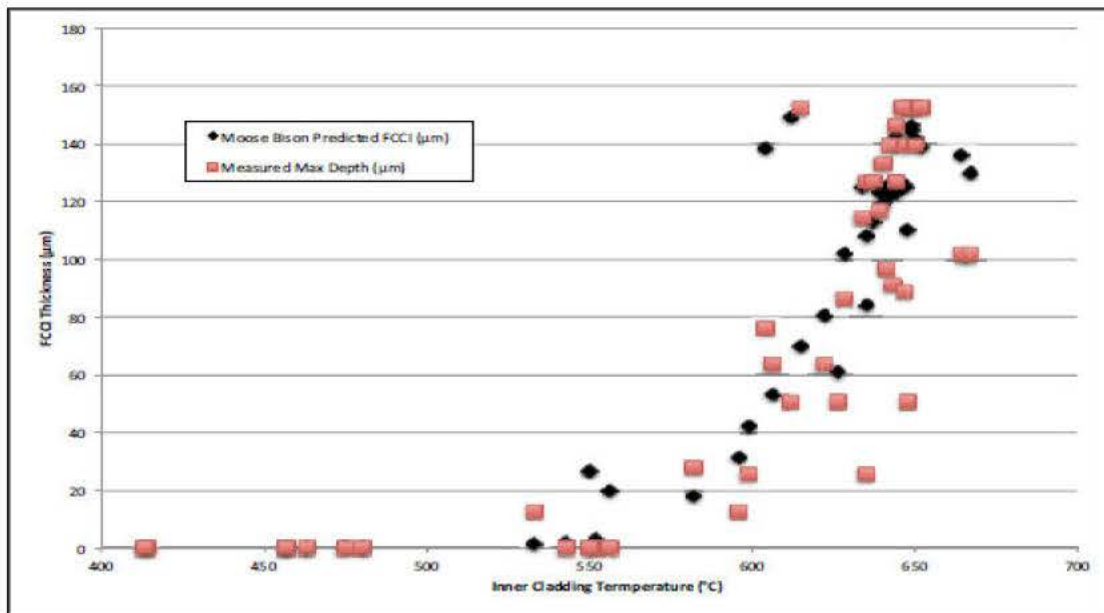
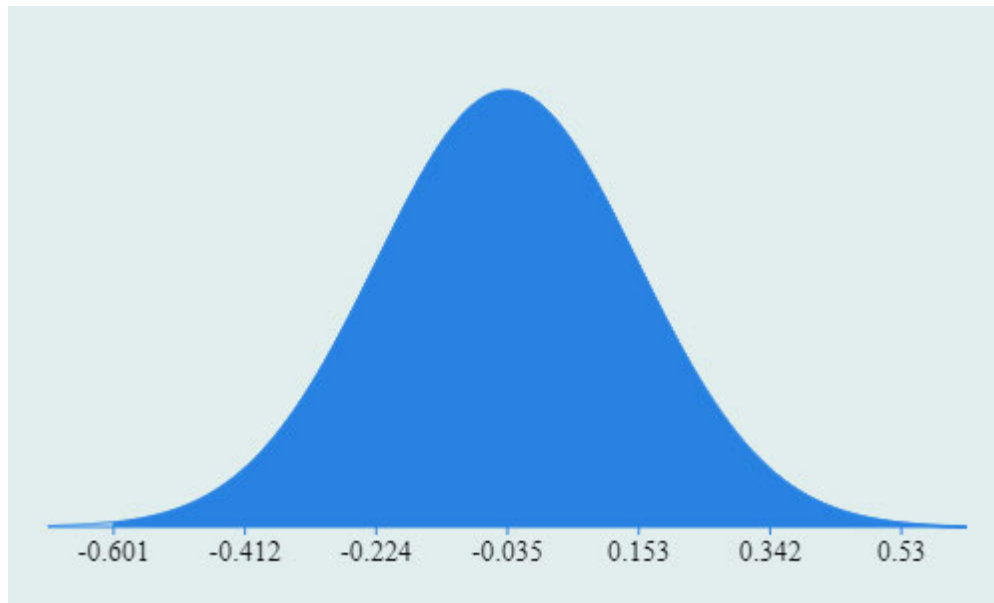


Figure F.2 Measured vs. BISON Predicted FCCI thickness vs. Inner Cladding Temperature [86]

## G Annex A Conservatism of Cumulative Damage Function (CDF)



**Figure An.1 Statistical Distribution of Log<sub>10</sub> CDF**

Statistical analysis of the data of time to rupture correlation used in the CDF formulation shows that the logarithm (base 10) of the CDF at failure is distributed normally as shown by the curve above. With 95% confidence the mean of the curve and its standard deviation are -0.0354 and 0.1885 respectively [5].

Our design approach is to keep the maximum number of failed pins at or below 0.1% (instead of the 1% used LWRs). This corresponds to the integral under the curve being 0.999, which requires the abscissa number to be -0.62. The  $\log_{10}$  CDF = -0.62 or CDF = 0.24.

The CDF used to date for steady state has been 0.05, so  $\log_{10}$  0.05 = -1.301, which equates to a probability of essentially no failure.

The ARC 100 has 21,483 total pins, and if we desire to have no more than 1 pins fail (1/21,483), the area under the curve would have to equal 0.999953, which requires the abscissa to be a bit less than -0.72. The CDF in this instance is  $\log_{10}$  CDF = -0.72, or CDF = 0.19.

One of the reasons that a CDF lower than the 0.24 or even 0.19 is recommended is that the correlation of time to rupture was developed for unirradiated HT9 tubes. The behavior might be different for irradiated ones.

In the case of HT9, however, there is data suggesting that stress and temperature at which the rupture occurs is relatively insensitive of whether the HT9 is or is not irradiated [6]. However, the time to rupture is longer for irradiated material as seen in Figure An.3 (from reference [13]) The data unfortunately is for transients and not long-term steady state, and that introduces uncertainty in its use. See for instance the figures below, taken from references 6 and 13 respectively. We are continuing to search for directly applicable data, but based on what we have so far, we feel that the use of 0.05 is overly conservative, since a value of 0.15 would correspond to a value of -0.8239 or a negligible failure probability.

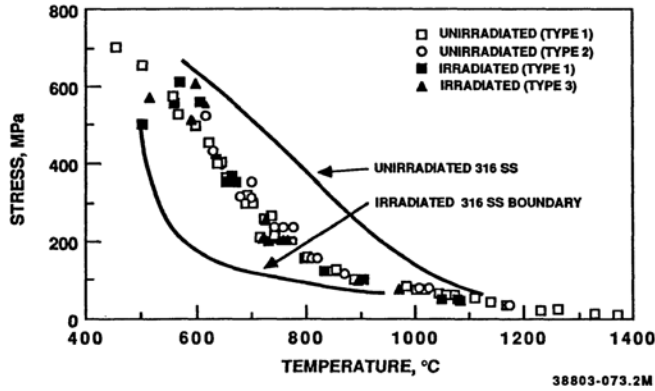


FIG. 2--HT9 5.6°C/s Transient Strength Results.

KHC-SA-0127-FP

Figure An.2 Temperature dependent Rupture Strength of HT9 (from Reference [6])

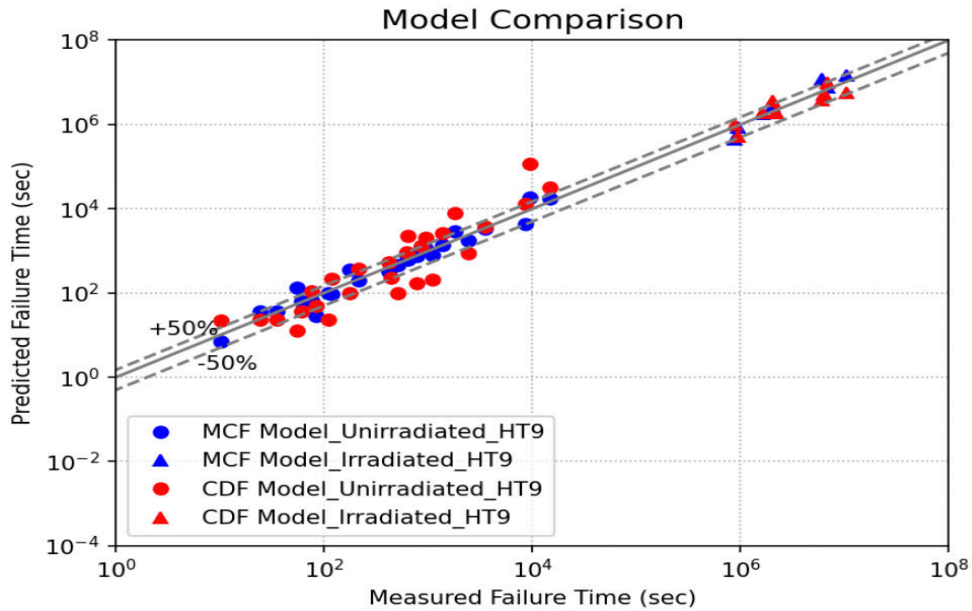


Figure An.3 Comparison of Predicted and Measured Time to Rupture for HT9 Tubes in Ramp-and-Hold tests. Blue and Red are MCF and CDF Predictions, respectively.